Naval Surface Warfare Center
Dahlgren Division

Technical Digest

1996

Expeditionary Warfare

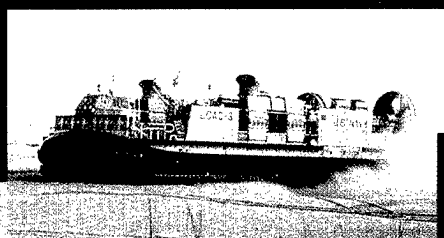

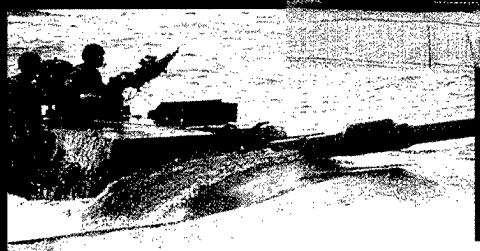

The Naval Surface Warfare Center Dahlgren Division Technical Digest presents unclassified articles, contributed primarily by Division scientists and engineers, on selected research and development programs. The Dahlgren Division, under the leadership of the Naval Surface Warfare Center, provides research, development, test and evaluation, engineering, and Fleet support for surface warfare systems, surface ship combat systems, ordnance, mines, amphibious warfare systems, mine countermeasures, special warfare systems, Marine Corps weaponry systems, and strategic systems. Please address any correspondence concerning the NSWCDD Technical Digest to: Dahlgren Division, Naval Surface Warfare Center, Technical Digest (Code B60), 17320 Dahlgren Road, Dahlgren, VA 22448-5100. Telephone (540) 653-8921.

About the cover: Naval Expeditionary Forces (NEFs) rely on a multitude of systems to control the battle space in a littoral environment. For these Marines (far left photo) to successfully "hit the beach," a well-coordinated effort must already be underway utilizing the latest technologies, as embodied in the group of four figures. Clockwise, from far right, the Vertical Launch System (VLS) provides fire support; an artist's rendering depicts the soon-to-be realized LPD-17 beside an air cushion landing craft (LCAC); an M1A1 tank churns towards shore; and an LCAC makes the beach during an amphibious assault.

NSWCDD/MP-96/96

DISCLAIMER NOTICE

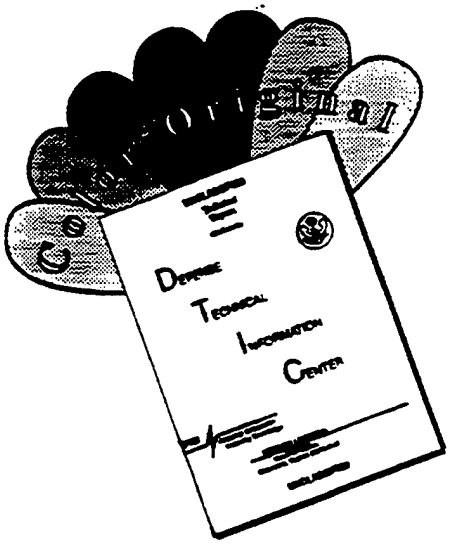

THIS DOCUMENT IS BEST QUALITY AVAILABLE. THE COPY FURNISHED TO DTIC CONTAINED A SIGNIFICANT NUMBER OF COLOR PAGES WHICH DO NOT REPRODUCE LEGIBLY ON BLACK AND WHITE MICROFICHE.

Naval Surface Warfare Center
Dahlgren Division

Technical Digest

1996 Issue

EW
EXPEDITIONARY
WARFARE

Guest Editors' Introduction

Robert L. Stiegler, Robert V. Gates, and Daniel E. Harris

In . . . From the Sea *and* Forward . . . From the Sea, *the Secretary of the Navy, The Chief of Naval Operations, and the Commandant of the Marine Corps set the strategic direction for Naval Services into the 21st century. The strategy places an unprecedented emphasis on the ability to operate in the littoral environment; that is, those regions relating to or existing on a shore or coastal region, within direct control of and vulnerable to the striking power of Naval Expeditionary Forces (NEFs). This strategy requires the development of new approaches to self-sustaining naval operations and future Navy/Marine Corps capabilities. This broad multifunction, joint, and complex concept is expeditionary warfare. This issue of the Naval Surface Warfare Center, Dahlgren Division (NSWCDD) Technical Digest focuses on expeditionary warfare and the enabling technologies that support that concept (Figure 1).*

EW
EXPEDITIONARY
WARFARE

Expeditionary Warfare

In the last several years, the Department of Defense (DoD) has placed more and more emphasis on preparing our forces to fight regional conflicts involving one or more third-world countries. There are at least two reasons for this change in emphasis, one being the dissolution of the former Soviet Union. The second reason is the proliferation of relatively inexpensive but highly effective weapons and weapons systems, giving third-world countries an unprecedented capability to arm themselves. As a result, interest has shifted to the development of strategies and tactics for joint-service warfare in littoral environments, a concept now known as expeditionary warfare. One of the major participants in such a force is the Marine Corps.

Expeditionary warfare has been tentatively defined by N85, Expeditionary Warfare Office, as military operations mounted (usually on short notice) in response to crises or potential crises, and conducted by forces with capabilities tailored to achieve a limited and clearly stated objective (or a specified range of objectives). The term "expeditionary warfare" conveys a sense of prompt and effective response; hence, in its initial stages, expeditionary warfare is best carried out by forces that are forward deployed or self-deploying, and which can sustain themselves in the objective area until a robust, logistic support system can be established.

Expeditionary Warfare Technologies

NSWCDD has become the focal point for superior, advanced technology solutions that nullify operational deficiencies and enable new approaches to self-sustaining naval operations and future Naval/Marine Corps capabilities. These efforts are focused on five imperative areas:

- Naval Fire Support (NFS)
- Command, Control, Communications, Computers, and Intelligence (C^4I)
- Survivability
- Battlefield Surveillance
- Mine Countermeasures (MCM)

This issue of the NSWCDD Technical Digest provides a sampling of Dahlgren Division's research and development in the technologies intrinsic within each of the imperative areas. As the primary focus is broad, so is the selection of topics for this publication. It will be noted that all the technologies presented have areas that interconnect in their applications to expeditionary warfare and to the support of Marine Corps' maneuver elements.

Naval Fire Support

Since the end of the cold war, the Navy has emphasized a strategy of littoral warfare. As part of this strategy, the Navy and the Marine Corps have been developing operational concepts for amphibious warfare that will rely heavily on an ability to launch and support amphibious assaults from ships up to 25 nautical miles from the enemy's shore. Successfully conducting amphibious operations requires all-weather fire support. If artillery and other ground-based fire support assets are not available, the Marine Corps' ground forces will need long-range, sea-based fire support from Navy ships, or from attack helicopters and fixed-wing aircraft.

The NFS mission is to:

- Provide supporting naval gunfire for amphibious operations
- Provide suppression and/or destruction of hostile antiship weapons and air defense systems.
- Provide supporting naval gunfire for the joint land battle

Currently, the Navy's cruisers and destroyers carry the 5-inch, 54-caliber gun, which can fire unguided projectiles to a maximum range of about 13 nautical miles. This short range, combined with threats to surface ships from mines and antiship missiles, currently precludes the Navy from adequately

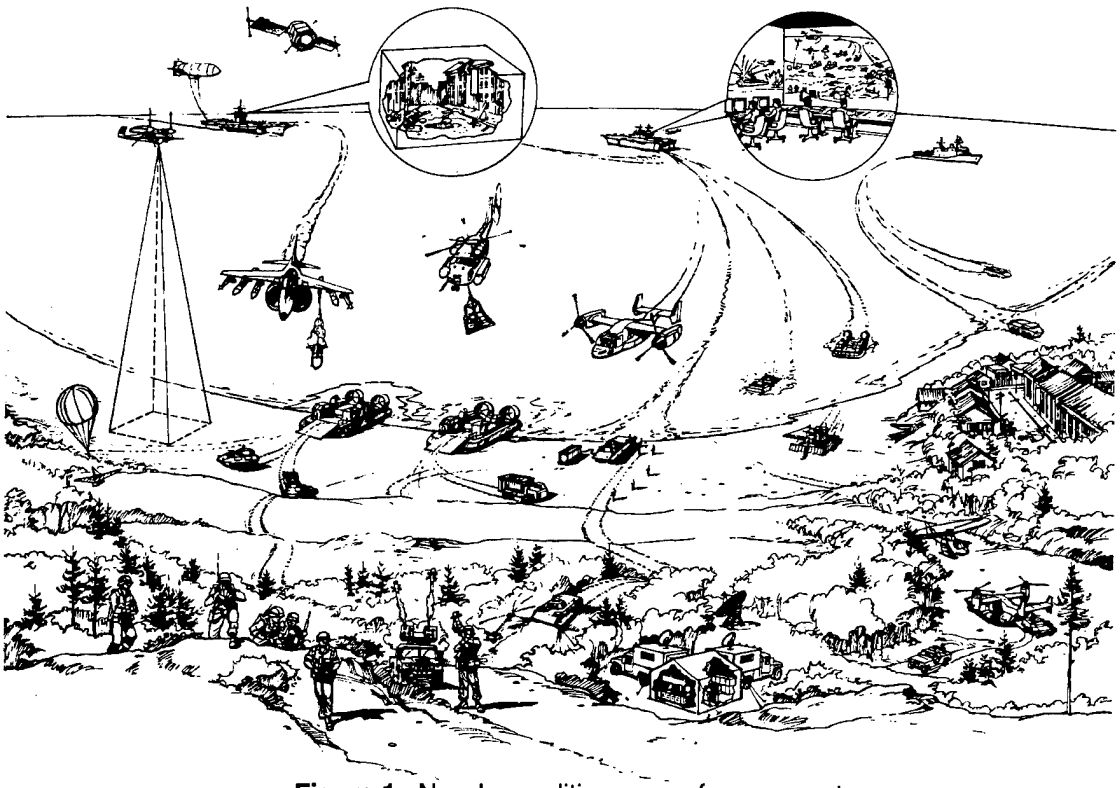

Figure 1. Naval expeditionary warfare concept

supporting the Marine Corps' amphibious operations or engaging other long-range targets.

The NFS program has three major thrusts:

- Improve near-term, surface-ship fire support capability by developing modifications to systems already in development or production
- Maximize the total theater-level fire support capability by integrating shipboard elements into existing and developing C^4I systems
- Develop advanced capabilities needed to keep pace with the evolution of expeditionary warfare systems by incorporating science and proven technologies

Some key elements of the investment in improved NFS capability by the year 2001 are discussed in this issue of the NSWCDD Technical Digest.

Command, Control, Communications, Computers, and Intelligence

Today's NEFs, including the maneuver elements they support, depend on modern and robust communications and computer systems throughout the battlefield environment. This requirement is due to the sophistication of weapons systems, the expanse of likely battlefields, the vast distances separating forces, and the speed at which strategic, theater, and tactical decisions must be made. "C^4" is the dissemination of information so that properly designated commanders can exercise authority and direct assigned forces to accomplish their mission. Commanders at all levels must have the right information, in the right place, at the right time. This requires the collection, fusion, assessment, and dissemination of information throughout the battlefield. Moreover, information must be accurate; and it must travel quickly, travel without unscheduled interruption and, most often, travel to many receivers simultaneously. Each of these aspects of C^4 plays key roles in attaining NEF objectives.

The NEF and maneuver element also require dynamic intelligence support, tailored to their specific mission requirements. Intelligence must be in time to enable informed decisions for the simultaneous application of focused combat power across the depth and breadth of areas of responsibility. The key to an ability to apply focused and synchronized combat power is a seamless intelligence "system of systems" that enables the use of all the capabilities of the intelligence community, including national agencies and theater assets to see the battlefield and accurately target high-payoff enemy targets.

The object is to create a seamless system of intelligence systems from NEF to maneuver battalion level. To meet the targeting challenges of the 21st century, key information and a common view of the battle space will be sent to all commanders immediately; graphic, rather than narrative, reporting will be emphasized. The intended battlefield will be visually portrayed throughout its width, depth, and height, with sensor input sufficiently accurate to permit precision targeting.

Mobility and Survivability

"The single most significant opportunity in power projection lies in the current revolution in littoral battlefield mobility."

Operational Maneuver From The Sea (OMFTS)

Investment in technologies improving ship-to-objective maneuverability is critical in neutralizing and defeating 21st century threats.

The Department of the Navy's recent white paper *Forward . . . From the Sea* recognizes the changes in the strategic landscape and marks an evolutionary shift away from Cold War thinking. Integral to this broad document is the Marine Corps' concept of OMFTS. Keys to OMFTS are the mobility of naval forces at sea, the rapid buildup and maneuver of combat power inland, and the early accomplishment of critical objectives. Although new systems are currently being developed (e.g., LPD-17, MV-22 *Osprey*, and the Advanced Amphibious Assault Vehicle (AAAV)), even newer, more technically advanced systems are required to project power over larger distances, more quickly, and in a seamless manner. The OMFTS concept faces

many challenges, such as joint operations, greater standoff distances, and sustainment. In addition, many threats such as shore-to-ship missiles, mines, and direct-fire weapons must be countered or avoided when operating in the littoral area. To overcome these hurdles and successfully execute OMFTS, new technologies must be developed, along with operationally feasible concepts, to meet the component- and system-level deficiencies that currently exist.

Investments in the technology that supports OMFTS must continue. The technological thrust of this task is to enhance or improve the mobility of all maneuver surface elements envisioned in future missions, such as joint littoral operations, amphibious assaults, political operations, sustainment, and combat support. Alternative concepts, platforms, and configurations need to be developed and evaluated using traditional test and evaluation methods, as well as advanced modeling and simulation tools. To improve the mobility of future systems, innovative components, subsystems, and platforms need to be continually assessed and developed. The expected payoffs will be new components and subsystems required for mid-term and future warfare platforms, and new system concepts to support the successful conduct of OMFTS.

Tactical deception and signature management are major factors with regard to the Marine Corps' need for an amphibious capability supporting OMFTS. In addition, future concepts may require small task forces to spread out on the battlefield. To enhance these operations, camouflage, concealment, and deception (CCD) technologies are required to minimize the vulnerability of vehicles and other systems to the myriad of sensing mechanisms used by the enemy. Signature management within the electromagnetic spectrum, tactical deception technologies, and reduction of dust generation are key areas to be explored to minimize the detectability of a vehicle by enemy sensors.

There is a continued proliferation of "smart" weapons throughout the world. These potential threat munitions incorporate sensor technology to assure greater probability-of-hit against enemy platforms. In addition, the penetrator technology available today is more lethal than when many platforms were fielded in the past 20 years. The Marine Corps has two unique problems related to their vehicles. First, the vehicle must operate on the open ocean and through the surf, which demands a very low weight. Second, particular care needs to be paid to corrosion because of the salt water environment.

Current Navy/Marine Corps amphibious assault capabilities bring valuable Navy assets close to the hostile beach. Projected amphibious assault tactics will involve the use of the AAAV to allow Navy ships to stand-off farther from the shore. However, both today's and tomorrow's tactics will require the use of technologies that reduce detectability and enhance tactical surprise. These technologies will enable tactical surprise to be integrated into shipboard and vehicle systems, in order to minimize the detectability of naval expeditionary warfare (NEW) and maneuver forces by the wide range of enemy devices. The payoff will be tactically superior and cost effective. The aim will be to produce a system that optimizes the interaction between ships' and vehicles' systems and applicable technology. Through the use of detection/avoidance technologies, the NEW and maneuver elements will reduce vulnerability to enemy sensors. Development of lightweight technologies that can survive the marine environment will provide the capability to maneuver in and out of the water, as well as the ability to quickly change a camouflage system from a water environment to an inland environment.

Battlefield Surveillance

The most significant constraint on the performance of future weapon systems, as they apply to NEF and maneuver units, is the performance of the targeting sensors that provide tactical real-time acquisition, accurate identification, and effective engagement. Faster and more lethal weapon systems require the supporting fire-control systems to rapidly acquire, track, recognize, identify, and engage

targets. Challenges on the battlefield, such as significantly increased engagement ranges, high operation tempo, obscuration, and terrain masking, must be effectively overcome. Disparate sensors operating in different media require sophisticated fusion in order to properly support the weapon system. The functional area of tactical targeting sensors is an increasingly dynamic growth area.

Technologies that fuse the capabilities of lightly armored stealthy vehicles, advanced sensors, and standoff weapons need to be developed and demonstrated. Using electro-optics and smart weapons, this technology will minimize the vulnerability of light forces by providing the capability to kill the enemy before closing to direct fire ranges.

Compact, lightweight, affordable, integrated multisensor systems need to be developed: systems capable of implantation behind enemy lines to provide day/night, adverse weather, unmanned surveillance, and targeting information. Data will be transmitted to friendly weapons platforms using smart data-compression techniques. The system may have integrated, low-cost imaging to include uncooled thermal imagers and television (TV) cameras, as well as acoustic and other target cueing and position/location sensors.

This technology will provide NEF and maneuver elements with accurate and timely "over-the-hill" reconnaissance, surveillance, and battle-damage assessment capability through the use of aerial sensors enhanced with aided target recognition and smart workstation technologies. A variety of imaging sensors may be used on a surrogate aerial platform, as well as a ground-based image exploitation workstation. Candidate sensors could include, forward-looking infrared (FLIR), infrared (IR) linescanner, day TV, and Moving Target Indicator (MTI) radar. The goal is to demonstrate a reduction in data time lines, from tasking to output of tactical information.

These enhancements would provide automated target transfer from forward sensors to weapons systems, with the capability to engage high-value targets beyond traditional direct and indirect fire ranges.

Mine Countermeasures

The threat posed by mines, especially in the pursuit of our interests in the littorals, is one that must not be allowed either to inhibit or deter us from our ability to execute our nation's taskings.

The strategic concept and direction of the naval service outlined in the 1992 paper . . . *From the Sea* and reaffirmed in the 1994 companion document *Forward . . . From the Sea* provide compelling requirements for effective and modern mine-warfare forces. We must be prepared to operate in distant waters in the early stages of regional hostilities to enable the flow of land-based air and ground forces into the theater of operations, as well as to protect vital follow-on sealift required for delivery of heavy equipment and sustainment of major forces.

Forward-deployed U.S. naval forces must be allowed unencumbered maneuver within the theater of operations. To acquire battle space dominance, in-theater force buildup is required. This buildup is possible only if we can sail safely across the sea lanes of communication and into littoral operating areas and ports of debarkation.

For the foreseeable future, we must anticipate increases in both the lethality of mines and the number of mines available for use by practically any adversary. Modern mine countermeasures skills and systems are thus pivotal if U.S. naval forces are to maintain a credible forward presence and, if required, to ensure battle space dominance and conduct power projection operations. The development of these skills and systems must be guided by a well-defined concept of operations and system architecture.

There are four general types of MCM operations that build on each other:

- Mapping, Survey and Intelligence Operations–includes bottom mapping, environmental survey and intelligence collection
- Surveillance Operations–includes national sensors, joint forces, special operations, and allied forces
- Organic MCM Operations–provides deployed naval forces the ability to locate and clear mines

• Dedicated MCM Operations–sustained focused MCM operations

There is no single solution to the mine threat. A combination of existing systems and capabilities, coordinated with technology development, is essential.

This issue of the NSWCDD Technical Digest includes articles concerning overall MCM approaches, as well as articles covering specific systems and technologies that address countering the mine threat.

Introduction To The Technical Presentations

Aspects of the NFS imperative are addressed by several of the articles in this issue of the NSWCDD Technical Digest. These articles focus on both the requirements for new or improved weapons systems and their coordination. Blosser addresses the development of conceptual approaches for NFS mission planning and coordination. A major consideration in this development is a requirement for operations in a joint warfare environment.

The Extended-Range Guided Munition (ERGM) is a key element in the upgrading of the Gun Weapon System, and is intended to provide the longer range needed to meet NFS requirements while maintaining the necessary terminal accuracy. Hagan discusses the systems engineering of future gun weapon systems with an emphasis on ERGM. He also presents some of the longer term possibilities provided by new and evolving technology.

A key to maintaining or improving the accuracy of both gun and missile systems lies with the capabilities of guidance and navigation from the Global Positioning System (GPS). Ohlmeyer and others discuss the development and use of a detailed computer simulation that supports future concept studies and systems design for systems such as ERGM, which will integrate GPS and an onboard inertial navigation system.

Weapon planning algorithms planned for the Advanced TOMAHAWK Weapons Control System will include algorithms for the construction of composite allowable launch areas and missile inflight avoidance areas. These regions can be constructed by calculating the unions and intersections of simple polygons that represent operating and defended areas. DiDonato describes a computationally efficient algorithm that computes the intersections and unions of planar polynomials, which can be used for this purpose. It should be noted that this algorithm has also been used to evaluate the potential of a conceptual long-range theater interceptor and, indeed, has many other potential applications.

The remainder of the articles address the ship-to-objective mission of expeditionary warfare, including the complete area of battle, C^{4}I, survivability of personnel and physical assets, battlefield surveillance to provide real-time situational knowledge, and the critical area of MCM.

Holland and others discuss the fundamental technologies of advanced processing and their application to all aspects of the imperative areas. Advanced targeting and communication concepts are described by Melton in his Forward Observer/Forward Air Controller article. Headley and others continue the discussion on surveillance and sensors in their technical article on Horizon Infrared Surveillance Systems. Surveillance technologies meld into survivability with Driscoll and LaMoy's description of imagery spectroscopy.

The technologies then shift to applications of mine detection with Tuovila and Nelson's presentation of the use of fractal features for mine detection in cluttered sonar images; high-resolution array processing by Wilbur and others; and Shepherd's Systematic Mine Countermeasures. The final two articles by Moritz and Floore provide a transition from technology development to the simulation of the expeditionary warfare environment and the application of technology to the fleet, as presented in the AN/KSQ-1 Amphibious Assault Direction System.

The Authors

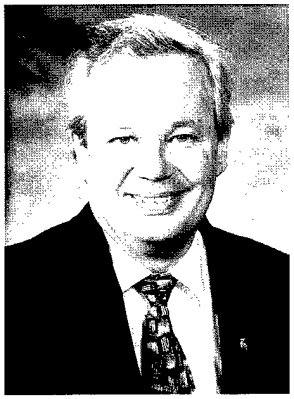

ROBERT L. STIEGLER, Program Manager for Maneuver Warfare Technology in Dahlgren Division's Weapon Systems Department, received a B.S. degree in electrical engineering from the University of Wisconsin; an M.B.A. from Roosevelt University - Chicago; and is currently working on a Ph.D. in public administration at Virginia Tech. After serving six and a half years in the U.S. Air Force, he began his civilian career as a radar technician on EC-121 Airborne Early Warning Aircraft. After two years as a quality assurance specialist on the MK-48 Torpedo Program, he joined the Naval Training Systems Center (NTSC) where, over a 15-year period, he established two training system support activities in support of shipboard, antisubmarine warfare (ASW), Aviation, and Marine Corps Training Devices. He was Head of NTSC's Aviation and Marine Corps Engineering Division from 1986 to1988, after which he served over two years as Science Advisor to the CG, FMFLANT, for which he received the Navy Superior Civilian Service Award. He joined NSWCDD in 1990 as Assistant Director of the Naval Science Assistance Program, subsequently as a branch head in the Strike Systems Department. Currently, Mr. Stiegler is the Program Manager for Maneuver Warfare Technology supporting U.S. Marine Corps (USMC) Science and Technology and Deputy of the NSWC Center of Excellence for Expeditionary Warfare Technology. Mr. Stiegler received the Technology to Sea Award in 1995 and was awarded the Navy Meritorious Civilian Service Award by the USMC in 1996.

Robert L. Stiegler

ROBERT V. GATES has a B.S. in physics from the Virginia Military Institute, an M. Eng. in engineering science from the Pennsylvania State University, an M.A. in political science from the Virginia Polytechnic Institute and State University, and has graduated with distinction from the Naval War College. He is currently Director of Strategic Planning for NSWCDD. His previous assignment was as a Principal Physicist in the Strategic and Space Systems Department of NSWCDD where he developed concepts for future Navy strategic systems, performed targeting analysis for the CNO staff, and led the Strategic and Strike Warfare Focus Team at NSWCDD. Employed at NSWCDD since 1970, he has provided technical support in the areas of stellar inertial guidance, accuracy modeling, and flight test support for the development of fire control and targeting software for TRIDENT I, TRIDENT II, and the United Kingdom POLARIS SLBM programs. He has also held a variety of management positions within the SLBM Research and Analysis Division at NSWCDD. He is a member of Pi Alpha Alpha, the national Public Administration Honor Society. Among his awards is the Navy Meritorious Civilian Service Award.

Robert V. Gates

DANIEL E. HARRIS earned a B.S. degree in mechanical engineering from the University of Maryland in 1984. After arriving at NSWCDD, White Oak in 1984, he worked on the MK50 Torpedo Warhead Program as a designer engineer. In 1990, he accepted an assignment in the NAVSEA Torpedo Program Office (PMS406) as the warhead engineer. Upon returning to NSWC, he continued his involvement in warhead design. He transferred to the Mine Division in 1994, where he managed several shallow-water MCM projects. Before relocating to NSWCDD's Coastal Systems Station (CSS) facility in 1995, he served in the Office of the Chief of Naval Operation's Mine Warfare Branch (CNO-N852). He is currently in the Mine Concepts and Evaluation Branch at CSS, where he manages various mine programs and performs systems engineering for mine warfare.

Daniel E. Harris

Naval Surface Fire Support—Mission Planning and Coordination

O. Kelly Blosser

EW
EXPEDITIONARY
WARFARE

Naval surface fire support (NSFS) is the use of gun-fired projectiles and missiles from surface combatants to support amphibious operations and the land battle. NSFS is one of three supporting arms (including tactical aviation and shore-based artillery) that have traditionally provided fire support to amphibious assault landings. New NSFS weapons are being developed, and it is generally recognized that improved NSFS mission planning and coordination will be necessary for the effective use of these weapons in the littoral battle space of the 21st century.

This article identifies required NSFS mission planning and coordination capabilities and explores alternatives for implementing these in surface combatants and amphibious command ships. The Navy must improve NSFS mission planning and coordination capabilities to be compatible with new joint-warfighting doctrine and to be interoperable with the landing force and forces operating ashore. The Army and Marine Corps have joint programs for automating fire-support coordination and effecting digital battlefield connectivity, and the Navy will be required to develop a system that will provide the targeting and fire coordination to make surface-launched fire-support weapons effective on the battlefield.

The approach suggested in this article would be to build a constructive interim capability in parallel with the development of the near-term, extended-range guided munition (ERGM). Further development will provide a fully capable system that will operate with the joint targeting and fire coordination systems of the 21st century.

Introduction

NSFS is the modern successor to traditional naval gunfire support (NGFS) from battleships, cruisers, and destroyers, providing supporting fires for Marine Corps and Army amphibious assault landings. In the battle space of the 21st century, NSFS may have an expanded role with tactical aviation to provide firepower from the sea: to support joint forces, to ensure dominance in littoral operations, and to support the land battle.

Fire support encompasses (in an organization and system) sensor, force-level command, fire coordination, and engagement elements. Many of the elements are not dedicated wholly to fire support, but each has an essential contribution. Sensor systems, including forward observer (FO) teams and

intermediate information processing or intelligence systems, locate targets and refine targeting information. An amphibious command ship or shore-based coordination center provides force-level planning and fire coordination, while NSFS ships and other supporting arms plan unit-level missions and engage assigned targets. A notional fire support system focused on NSFS ships as the engagement elements (i.e., a subset of the full supporting arms system) is shown in Figure 1. Although considered a system, current NSFS is assembled from existing equipments, operated by manual and man-intensive organizations, and held together by voice communications.

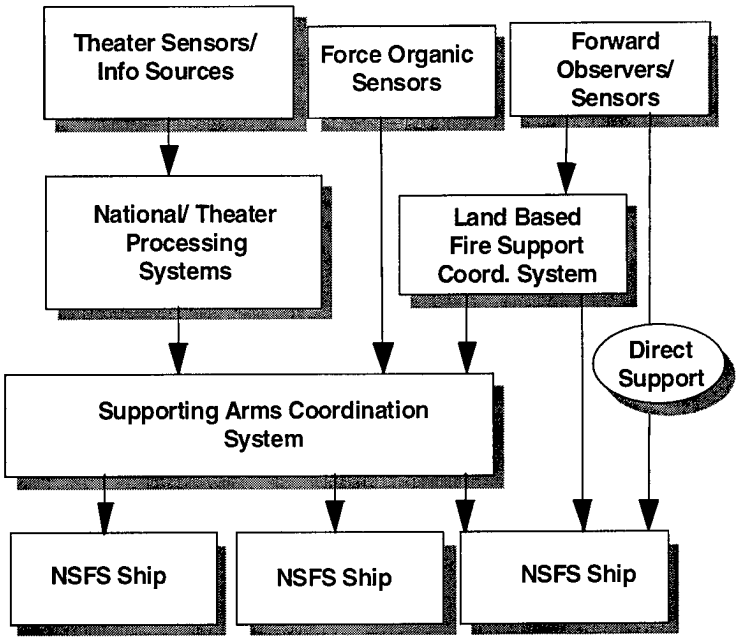

Figure 1. The notional NSFS system

In the future vision of the Navy expressed in . . . *From the Sea* and *Forward . . . From the Sea* the United States will conduct Naval Expeditionary Force (NEF), joint, and combined military operations in the littoral regions of the world; an essential requirement will be the capability of naval forces to project overwhelming firepower from the sea.[1] NSFS and the other supporting arms will be elements of a joint fire-support system providing fires "that assist land and amphibious forces to maneuver and control territory, populations, and key waters."[2]

The first step towards a modern NSFS system was taken in January 1995 when the Chief of Naval Operations (CNO) authorized the development of a naval weapon to meet Marine Corps near-term fire-support requirements. The goal was to introduce, by 2001, the ERGM EX-171 fired to a range of 63 NM by a modified 5"/62 Mk 45 gun mount. Missile concepts will also be evaluated as a supplement to the gun system and to provide an effective weapon against deep, high-value targets.[3]

Effective NSFS weapons are essential. The current emphasis on improving weapon capabilities is well placed. However, current NSFS mission planning and targeting capabilities will be inadequate to support the improved, near-term NSFS weapon and obsolete in the future battle space. A fully capable NSFS planning and targeting system evolved to support the family of NSFS weapons in the 21st century must be developed within the framework of:

- Evolving joint visions and concepts of littoral warfare
- Automation of Army and Marine Corps fires coordination systems
- New NSFS weapons
- Digitalization of the battle space
- Reduced military budgets for new developments

Background

While the tactic of moving a combat force by sea and landing it in the face of a shoreline defense dates back many centuries, modern amphibious warfare doctrine was developed by the U.S. Marine Corps in the 1920s and 1930s. Application of this doctrine required special landing craft and amphibious vehicles to speed the ship-to-shore maneuver and overwhelm beach

defenses before enemy reinforcements could arrive. Ships and aircraft supported the assault with surface gunfire and rockets and air-launched ordnance, which were joined by artillery emplaced ashore in the early phases of the assault.

Traditional amphibious assault operations consisted of several steps: prepare and move to the area, soften the area with bombardment, seize a beachhead, defend the beach, build up power ashore, and break out to extend the battle landward. Landings were predominantly "across the beach" using slow-moving landing craft, and because only about six percent of beaches were suitable for landings, the assaults were usually opposed by heavily fortified enemy defenses.[4] These amphibious concepts and equipments served the Navy, Marine Corps and the Army through World War II and Korea.

New doctrine, tactics, and organization for supporting arms were also crucial to the success of these amphibious operations. Supporting fires from all elements (a) prepared the landing beach, (b) interdicted enemy reinforcements and communications leading to the landing beach (in order to isolate the enemy force already in place), and (c) responded to calls from landing force elements on the way to the beach and ashore for fires to suppress and neutralize enemy troops and positions (Figure 2).

Current Capabilities

The backbone force for current amphibious operations is the forward-deployed Amphibious Ready Group (ARG) with an embarked Marine Expeditionary Unit (MEU), which has a Special Operations Capability (SOC). Amphibious operations will be conducted by task forces composed of multiple ready groups reenforced with other Navy and Marine elements.

This force will be equipped with Air Cushion Landing Craft (LCAC) and helicopters: The LCAC makes over 60 percent of all beaches accessible by amphibious landing, and helicopters can vertically lift assault forces well inland, behind beach defenses.

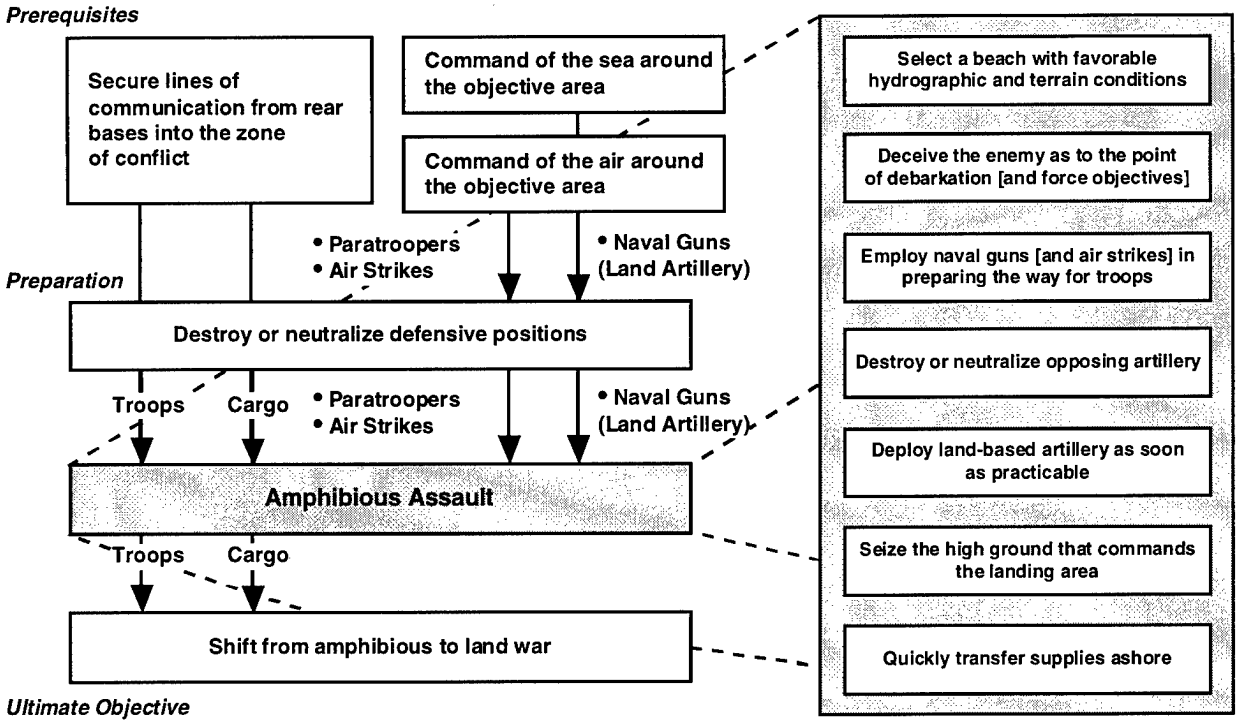

Figure 2. Traditional amphibious assault

The V-22 *Osprey*, now in development, will greatly increase the reach and momentum with which vertical assault elements can be moved ashore. The Advanced Amphibious Assault Vehicle (AAAV), also in development, will more than triple the speed with which over-water elements can move ashore. These advanced lift capabilities will enable amphibious operations to be launched from over the horizon, provide greater safety for amphibious forces, and keep the enemy confused about the location and timing of the landing. He will be forced to scatter his forces over a wider geographic area, thus weakening defenses of any single potential landing area, or he will tie up many more forces in the defense of his coastal areas. The naval gun system with ERGM will provide the range and accuracy needed to support the greatly extended range and tempo of operations of assault forces, and a fire support missile will be used against high-value deep targets. However, to fully exploit its potential, NSFS must be closely integrated with assault element planning and operations.

Fire support planning in the Amphibious Task Force is done by the combined landing-force operations staff, with intelligence support from the Joint Intelligence Center (JIC). In the operational plan (OPLAN), NSFS ships are identified and given prearranged targets to engage on schedule. When the operation commences, a Supporting Arms Coordination Center (SACC) in one amphibious command ship executes the plan and coordinates general support call-fire missions.

Surface combatants in a fire-support role are either in general support (GS) and respond to calls for fire from the SACC, or are in direct support (DS) of a landing force battalion ashore. DS ships respond to calls for fire from the battalion's fire-support element and FO teams to directly support maneuver elements. Missions assigned to NSFS ships during phases of a traditional assault are shown in Figure 3.

Once the combat force is ashore and the Commander of the Landing Force (CLF) assumes control, a Fire Support Coordination Center (FSCC) takes on the primary role for supporting-arms coordination. The fully developed NSFS organization is shown in Figure 4. This organization is very similar to that used during World War II and remains sound. It provides the logical framework for developing a Navy force-level, fire-support planning and coordination system for the future.

However, supporting-arms mission planning and coordination capabilities and

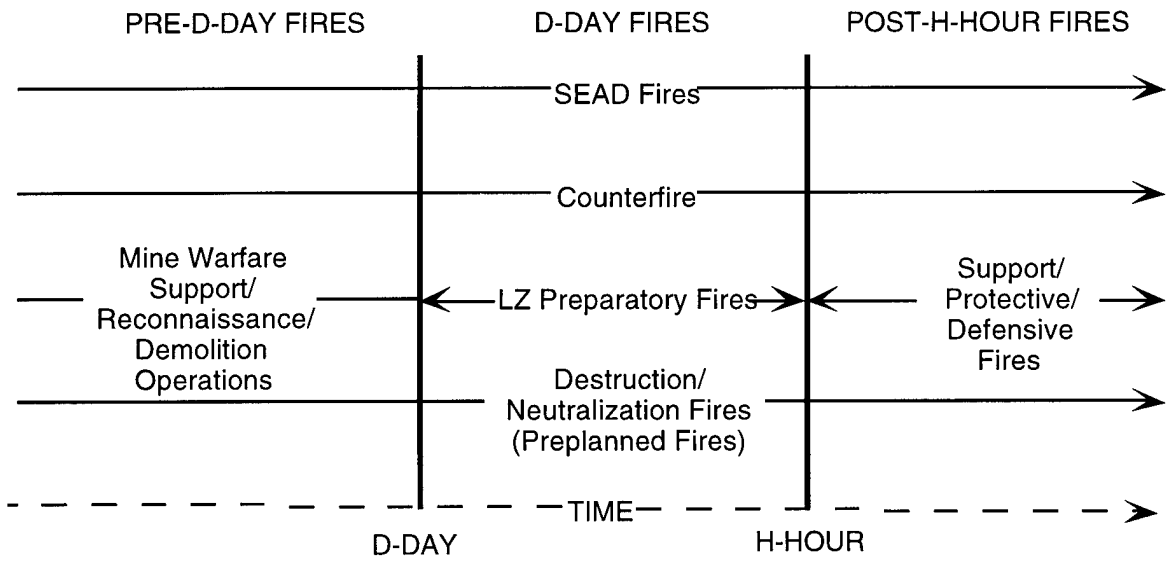

Figure 3. Phases of a traditional amphibious assault operation

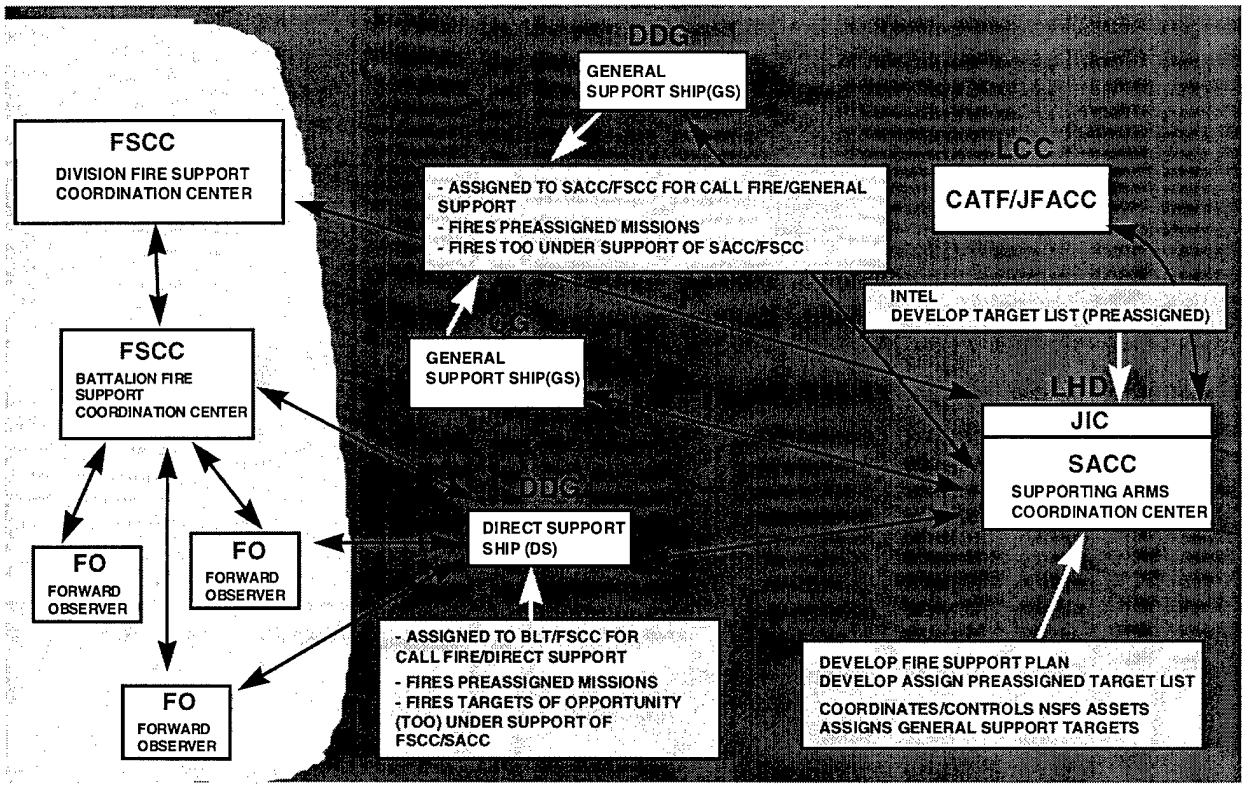

Figure 4. Elements of an NSFS fire coordination organization

supporting systems must be updated and automated to respond to future operational tempos. A SACC on the most modern amphibious command ships plans and conducts fire support very much as it was done in World War II; it is a manually intensive operation using charts, maps, overlays, and 3 by 5 file cards. Voice communications or naval-text-formatted teletype messages are the means connecting separate elements of the organization. Marine Corps elements have recently installed interim automation systems in the SACC and Landing Force Operations Center (LFOC) of several amphibious command ships, but these terminals are not integrated with the command ship's combat system.

Improvements in gun fire control have been made in surface combatants since World War II and Vietnam, but NSFS advances have not kept pace. The Mk 160 Gun Computer System (GCS) in *Arleigh Burke* class destroyers is a modern fire-control system, and the use of the Global Positioning System (GPS) enables these ships to get a precise fix on ownship's position, instead of using dead reckoning or navigation reference in inshore waters. However, a modern NSFS planning and coordination capability does not exist. In the Combat Information Center (CIC), a gunnery liaison officer (GLO), plot team, and fire-control system operator constitute the NSFS organization, and these personnel work a largely manual process. Sector geographic feature maps (e.g., 1 to 25000 or 50000 scale), overlays, and voice communications are their planning and coordination tools. Voice radio nets connect operators to the SACC or FSCC for general support missions, and to FO teams operating with battalion fire-support elements for direct support missions. A plot team at the Dead Reckoning Tracer (DRT) confirms the ship track, plots gun-to-target lines, and reviews fire missions against fire coordination lines and no-fire zones to ensure coordination and safety of fire. The GCS operator enters target locations, and when solutions generated by the plot team

and the GCS operator agree, firing commences. Grid spot conversion for adjustment of fire is done using a manual tool, and spots from the FO are called to the fire control operator to adjust fire.

In the future, the manual process will not work. The surface combatant has a fragmented and inadequate tactical picture of the battlefield, and the man-intensive process and voice communications connectivity severely limits the NSFS system's ability:

- To rapidly respond to calls for fire
- To handle multiple fire missions
- To rapidly replan targets
- To determine dynamic zones of fire and no-fire
- To coordinate operations with other surface and air combatants

Overloaded operators will be prone to make errors, and manual data entry will require an excessive response time.

The Future: A Rapidly Changing Scene

New warfighting concepts, movement towards joint services commonality, and progress in the other services in automation of fire-support coordination systems will exacerbate the existing problem in future NSFS operations. Several of these influences are described below.

Warfare Evolution: New Paradigms

As the United States approaches the 21st century, changing political and international relationships have altered national and military strategies of the United States and its military, respectively. We are committed to a littoral warfare doctrine that incorporates joint expeditionary warfare. Parenthetically, significant improvements in defense technologies available to potential adversaries could affect the ability of U.S. forces to project their power, unhindered, in the littoral regions of the world. The capability of the services to carry out joint expeditionary operations will be impaired in the face of enemy defenses, were the traditional doctrine, tactics, and equipments designed for World War II and the Cold War maintained. The Navy has defined its strategic concepts for the future in . . . *From the Sea* and *Forward . . . From the Sea*. The Marine Corps conceived Operational Maneuver From The Sea (OMFTS) as its goal for future amphibious doctrine and a series of experiments termed Sea Dragon to experiment with visions of warfare in the 21st century. The Army is developing the Force XXI concept. The current chairman of the Joint Chiefs of Staff, General Shalikashvili, has apparently melded these into his concept of a joint force exerting "full-spectrum dominance" over future battlefields.[5] OMFTS and Force XXI, in stressing joint operations and the extended and extensive use of firepower, will have a fundamental impact on the Navy requirement to provide fire support.

The Marine Corps' vision and experimental concepts for NEF operations emphasizes the Marine role as the "naval advanced guard." OMFTS stresses surprise, speed, information, decision support, and mobility to give an expeditionary force the ability to maneuver before landing force elements are landed, and to rapidly move these units to maintain a tempo of operations to foil enemy defenses and achieve our own force objectives.

The expeditionary force will operate on vital objectives without the traditional buildup of support forces ashore. The concept includes dispersing and concentrating forces in terms of breadth, depth, and time; and, in addition, "employs maneuver to engage by fires, and shapes the battle space in a nonlinear manner with forces capable of acting independently to achieve the commander's intent." It is "distributed and centrally coordinated but decentralized in execution on a more dispersed and opportunistic battlefield." Command and coordination "will usually remain sea-based." Sea Dragon concepts will integrate "both expeditionary and joint force elements"; therefore, fire-support coordination systems should be fully interoperable, if not identical, with Marine

and joint-force fire support coordination elements.[6] Sea Dragon experiments will exploit the use of OMFTS to its maximum extent.

Fires from a sea-based platform will be the primary means for engagement early in an operation. Further, the concept stresses "engagement coordination." FO teams and other sensor systems will directly or indirectly feed targets to the engagement systems. However, the new concept allows for operations in the more traditional hierarchical organization where required.

The command structure may feature a flatter configuration with fewer echelons of control and coordination between fires team and the Marine Air Ground Task Force (MAGTF). Response, accuracy, and lethality will be necessary attributes for all supporting arms, and dispersed fire systems will be coordinated against a target set over an expanded battlefield. All fire-support elements must have a common tactical picture and a common understanding of the commander's intent, and they must respond with common decision logic to the engagement requests from MAGTFs and subordinate echelons.

Force XXI is the Army's vision for "full-dimensional operations of the strategic Army in the early 21st century." War will require doctrinal flexibility and lighter, more lethal, and better-protected forces to operate over a larger and deeper battlefield. These forces will be modular, with flatter and less rigid hierarchical organizations.[7] Information sharing among systems will provide all command levels with a common tactical picture. Information sharing and distribution to all units will be an essential element for operations.

Fewer forces and smaller units will outperform and outpace the enemy's defenses through "simultaneous engagement of targets by a greater variety of joint warfighting systems." The maneuver forces will be supported and, in some cases, replaced by direct and indirect fires with extended range, greater accuracy, and greater lethality.

Deep operations and simultaneous attack may alter the current concepts of fires and maneuver: the operational commander will attempt to stun and quickly defeat the enemy throughout the battle space. Stress on early entry of Army components of a joint force is a dramatic change from the current, standard operational approach. Early entry will be required by the future strategic environment. Early-entry forces may have to fight their way into the theater and face an enemy who is attempting to retain control of the area.

Common elements of the OMFTS and Force XXI concepts that will have a significant influence on NSFS planning and coordination, as well as weapon requirements, are:

- "Flatter" command structure (central coordination of distributed assets)
- Information sharing at all levels
- Large battle space, including the deep and close battles
- Fire teams, and maneuver to support fires
- Overwhelming firepower from the sea

Digitization of the Battlefield

Digital data connectivity is an essential part of modern warfighting concepts, for the sharing of tactical data and for assured command control. A joint-services agreement on digitization of the battle space will lead to common digital-communications systems, protocols, and message standards.[8] Command systems that rely on manual operations and voice communications to connect with other commands must evolve to full, digital capabilities or they will be unsuitable for future joint-battlefield operations. The Army and Marine Corps are now fielding a common system for battlefield tactical communications, the single channel ground-to-air radio system (SINCGARS), which provides a secure, jam-resistant, very high frequency (VHF) communications medium. In Force XXI, the Army envisions a tactical internet incorporating SINCGARS, the Enhanced Position Location Reporting System (EPLRS), and mobile subscriber equipment (MSE) to electronically route digital data.

Ship-to-ship and ship-to-shore fire support coordination now rely on voice communications for operation, but as an interim measure, amphibious ships and NSFS ships will be fitted with SINCGARS to provide tactical voice and digital communications for command and coordination. However, SINCGARS has significant limitations in extended-range ship-to-shore communications since its radio frequency is line-of-sight, and man- and vehicle-portable radios are low powered. New solutions for reliable high-speed digital data exchange among surface ships and shore-based fire support elements must be developed as part of the Navy Joint Maritime Communications System (JMCOMS).

Fire Coordination System Automation

Computer-aided systems were introduced in the Navy in the 1950s for antiair and antisubmarine warfare but, as noted earlier, these capabilities have not been applied to maritime fire-support coordination. Since 1975, the Army and Marine Corps have moved from manual fire-direction centers to modern computer-aided systems for artillery fire direction. The first-generation Marine Corps systems providing significant automation for artillery support were the Tactical Fire Direction System (TACFIRE) and its replacement, the Interim Fire Support Automation System (IFSAS). IFSAS is implemented in field computers distributed among tactical command echelons and connected via combat net radio communications. Marine Corps units operating ashore employ IFSAS terminals, and IFSAS terminals are being installed in the LFOC and the SACC of modern amphibious command ships.[9]

The Army, with Marine Corps support, is developing the Advanced Field Artillery Tactical Data System (AFATDS), a distributed fire coordination system connected by a tactical radio communications system. Compared to IFSAS, AFATDS will have a greatly expanded capability to process and display tactical information and provide control information to all fire-support elements. It will provide a common tactical picture of the battlefield and tactical fire control and coordination for all fire-support elements. AFATDS capabilities will include coordination of all supporting arms (naval gunfire and tactical aircraft). It will be used at all echelons, from force-level to artillery battalion and Army Multiple-Launcher Rocket System (MLRS) battery level. AFATDS will be incorporated in MAGTF *command, control, communications, computers, and intelligence* (C^4I), for use ashore and afloat. AFATDS will be implemented as part of the Marine Corps technical architecture (TA) to ensure "interoperability of Marine Corps, joint, and combined Forces in a three-dimensional battle space."[10]

Digital communication devices and spotting devices will be used by FO teams and Air and Naval Gunfire Liaison Organizations (ANGLICO) operating with the maneuver elements. FO teams are now equipped with Digital Communications Terminals (DCTs) or Forward Entry Devices (FEDs) for exchanging digital fire-support messages with the fire coordination elements.

In the future, FO teams will have the Target Location Designation Handoff System (TLDHS), which is being developed for use by the Marine Corps. TLDHS is a device with a laser rangefinder, an azimuth measuring device, GPS, digital computer, and radio with digital-message capability. Using TLDHS, the observer spots the target to record the offset target position in GPS coordinates, enters amplifying target identification data, and sends the targeting data to close air-support aircraft, specified command elements, or a direct-support NSFS ship.

Required Capabilities

Based on (a) the current state of NSFS coordination capabilities, (b) the significant improvements being made by the other services in fire coordination, and (c) the bold visions of military operations in the early 21st century, it is clear that the Navy NSFS system must be a key part of a fully integrated

fire-support system: it must use the shared tactical battlefield picture, it must provide fires and fires coordination to meet Marine Corps OMFTS and Army Force XXI needs, and it must communicate with all fire-support elements using joint message standards over high-speed, digital data paths. These general capabilities imply modernization of not only the physical system, but nearly every aspect of NSFS organization, tactics, and procedures. The fully effective NSFS mission planning and coordination system for the 21st century must meet several basic requirements:

1. The NSFS system must support the use of NSFS weapons against assigned targets: prearranged and call-fires, in general support and direct support missions. The system must provide target information to accurately place NSFS ordnance within lethal radius for a variety of targets. In order to achieve this goal, the system must be provided with timely data from external targeting sources. The near-term need is to support initial operational use of the 5-inch ERGM round to its maximum range, with targeting accuracy sufficient to provide high, single-round damage to targets. The system must support the use of tactical missiles in fire support when these are introduced.

2. The NSFS system must operate with both digital and voice communications with joint forces on the battlefield. A communications support system, e.g., JMCOMS, must provide reliable tactical communications among all maritime components of the NSFS and the land-based elements. Ideally, one communications system would provide the capability for all supporting-arms components and coordination systems, afloat and ashore, to maintain reliable and high-speed information flow. Voice will be less important, but for the near future, voice must be retained as a parallel and backup capability.

3. The NSFS system must have the capability to fully interoperate with the force fire-support coordination system. The problems of the future battlefield include maintenance of a common relevant tactical picture, assignment of resources effectively, and deconfliction of aircraft, helicopters, missiles, and gun-fired ordnance over a dynamic battlefield. The system may be organized with multiple fire teams, a fires coordination center, and multiple NSFS ships, as illustrated in Figure 5.

System Candidates

NSFS system concepts are being explored to evolve specific system requirements and to identify candidate systems that could be incorporated in a full NSFS system. This process includes the identification of existing and developmental systems that could have a major role in fulfilling the above requirements and conducting demonstrations to provide a proof of concept.

Today, the requirements to develop a new system must be tempered with concern for cost and flexibility in the combat system. Reuse of systems, especially where this provides enhanced capabilities and interoperability, is a design goal that must be incorporated.

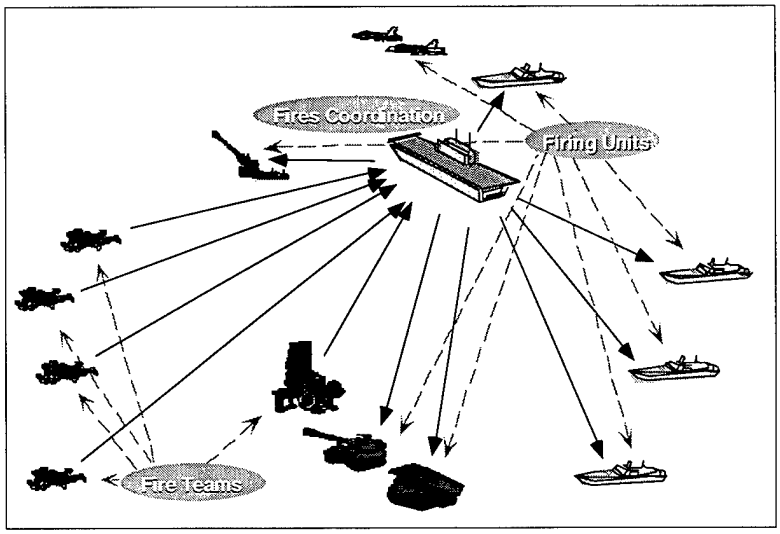

Figure 5. Notional fire support system of the future

New joint systems are being developed in a common operating environment under open-system architecture standards to operate in standard hardware. Future surface combatants will have fully integrated combat systems with a computing system backbone and common display terminals: mission-specific applications will run on the common system. In the interim, several candidates could be used as building blocks for an NSFS mission planning and coordination system. Features of these systems could be combined to provide a constructive step to development of a fully functional NSFS system.

AFATDS

A relevant, shared tactical picture and full interoperability with Marine Corps and Army fire-support coordination systems is a key required capability for NSFS. Reuse of applicable AFATDS software modules and displays may expedite the achievement of full Navy interoperability with the force fire-coordination system. AFATDS is the future Marine Corps system that will provide "fully automated fire support command and control."[11] In limited operation with Army combat units, AFATDS version 1 was implemented for field artillery coordination on standard Army Tactical Computer Units (TCUs). Version 2 will be the first fielded by the Marine Corps and, at the same time, AFATDS will be modified to operate in a common operating environment. It will also incorporate naval gunfire and tactical air-support functions. Close-air support messages are being implemented to integrate tactical air operations. NSFS messages are being implemented to permit AFATDS operators to assess NSFS ship resources and task NSFS ships to engage.

AFATDS will be installed on amphibious command ships as part of MAGTF C^4I, much as IFSAS terminals are being installed today. With AFATDS as the standard land and amphibious command-ship fire-coordination system, use of relevant AFATDS modules, databases, and displays in an NSFS system on surface combatant ships will give these elements an immediate interoperability with all force and land-based fire-coordination elements. Using the same algorithms, databases, and refresh rates, an NSFS ship will maintain a shared common tactical picture with afloat and shore-based coordination centers and operate as a node of the fire coordination system. Implementation of specific features of AFATDS on a standard Navy computer will provide shared situational awareness and a powerful set of tactical algorithms. Additional Navy requirements would be implemented in future builds of AFATDS software. A common application will require that only one program must be modified for all services each time a new version is fielded.

Advanced Tomahawk Weapon Control System (ATWCS)

ATWCS is the next-generation weapon control system for the family of Tomahawk Land Attack Missiles (TLAM). TLAM was designed as a strike weapon, but changes in the missile and weapon control system will give it a capability against time-critical targets. One variant of TLAM has been proposed as an effective interdiction weapon against massed enemy armor reinforcements.

ATWCS is being built on the common operating environment using standard Navy displays, a local area network, and both commercial and government off-the-shelf software. ATWCS will have interfaces with the ship's combat system, with the Joint Maritime Command Information System (JMCIS), and with standard Navy communications systems.[12] In the future, ATWCS could assume additional roles, including control of unmanned aerial vehicles (UAVs) and deep strike operations, and weapon control for a ship-based fast response NSFS missile.[13]

ATWCS could also assume NSFS functions; once AFATDS is converted to a common operating environment, appropriate modules of its software could be run as an application in the ATWCS system.

Mk 160 Gun Computer System

The current Mk 160 GCS in DDG-51 *Arleigh Burke* class destroyers is being modified with a new display, a local area network for data transfer, and computer programs operating in a common environment. With appropriate interface processing capability and software modifications, this system could also support a full, two-way digital-data transfer capability with an external fire-support source.

Computer Aided Dead Reckoning Tracer (CADRT)

As described above, in current NGFS operations, the plot team uses maps and manual procedures to plot ship's course, mark major features and tactical data on the battlefield, and plot gun-to-target lines to ensure accurate range and bearing and safety of fire. The CADRT is being introduced by the antisubmarine warfare community for tactical decision support and is proposed to replace the outmoded DRT in shipboard use.[14] CADRT is being developed in an open system with standard Navy TAC-X processors, a local area network, and a large horizontal display. CADRT as a component of the NSFS system could provide an improved plotting capability with fewer personnel. Interfaces with ship's systems would be effected through the local area network. AFATDS could also be implemented as an application on the CADRT, in order to fulfill the need to automate many current routines in CIC.

Demonstrations

Two demonstrations, completed in 1995 and 1996, respectively, showcase new concepts for NSFS planning and coordination.

The first, a digital interface between the Mk 160 GCS and an external Digital Communications Terminal (DCT), demonstrated the capability of an FO to input digital data on land targets to the gun system. The Remote Digital Data Link (RDDL) experiment required a desktop computer with interface cards. Two TACFIRE messages from the DCT were converted to Navy Tactical Data System (NTDS) low-level serial messages for processing in the Mk 160 GCS. Target data were then displayed on the Mk 160 console for operator action including target selection and adjustment of fire. RDDL provides the nucleus of a capability to use digital TACFIRE and the new variable message format (VMF) fire-support messages to streamline the sensor-to-shooter data path.

An NSFS demonstration, part of Combined Joint Task Force Exercise (CJTFEX) 96, was an ambitious attempt to showcase planning and coordination capabilities at force and NSFS ship levels. Mission planning, air-space coordination, general-support and direct-support fire missions with the gun system, and a notional engagement with a simulated shipboard Army Tactical Missile System, were demonstrated using AFATDS terminals installed in USS *Mt. Whitney* (LCC-21), USS *Saipan* (LHA-2), USS *Nassau* (LHA-4), and USS *Mitscher* (DDG-57).

Direct-support missions were simulated with a shore FO using the DCT to pass fire-support messages to the AFATDS terminal on USS *Mitscher*. An expanded RDDL device then converted these TACFIRE messages to NTDS format for display on the Mk 160 GCS console. SINCGARS radios and an extremely high frequency (EHF) satellite communications link were exercised to exchange tactical data and coordinate fire missions among the ships and land stations.

Interim System Approach

Development of a fully capable NSFS mission planning and targeting system is a long-term goal; however, steps should be taken to meet the near-term requirements of surface combatants to support the introduction of the improved, 5"/62 gun and the ERGM projectile.

Interim system requirements are clearly based on the requirements discussed earlier. The ship should interface with the force coordination system and FOs over digital and voice links to receive target data. A shared tactical picture is required to enhance

coordination with the force. Communications must be improved even though SINCGARS combat-net radios will be installed in fire-support ships to provide short-range digital communications with shore-based or ship-based force coordination systems. The Mk 160 GCS could be modified with an expanded RDDL interface card to receive and transmit TACFIRE and VMF messages. The DRT may be replaced by the CADRT in new destroyers; with appropriate software and displays, this system could support a small team to perform the same plotting function performed by today's large team. A notional interim system is shown in Figure 6.

Conclusions

A future NSFS system, with advanced weapons, a modern unit-level mission planning and targeting system, and interoperability with a modern, force-level, fire support coordination system, would be fully capable of supporting Marine Corps OMFTS and Army Force XXI operations in the 21st century. Moreover, the combatant would be a responsive member of the force fire-support coordination system. The concept would integrate sensor interfaces, force interfaces, unit-level planning and coordination, and weapons control and coordination into a coherent system, one that can respond to ship's command for operations and safety. A notional concept is shown in Figure 7.

This NSFS system would interface with theater and force targeting systems, be integrated into the joint fires coordination system, and function with many fewer operators than the current system. Integration of AFATDS capabilities into an existing shipboard system, probably ATWCS, would require additional software, training, and consoles to incorporate

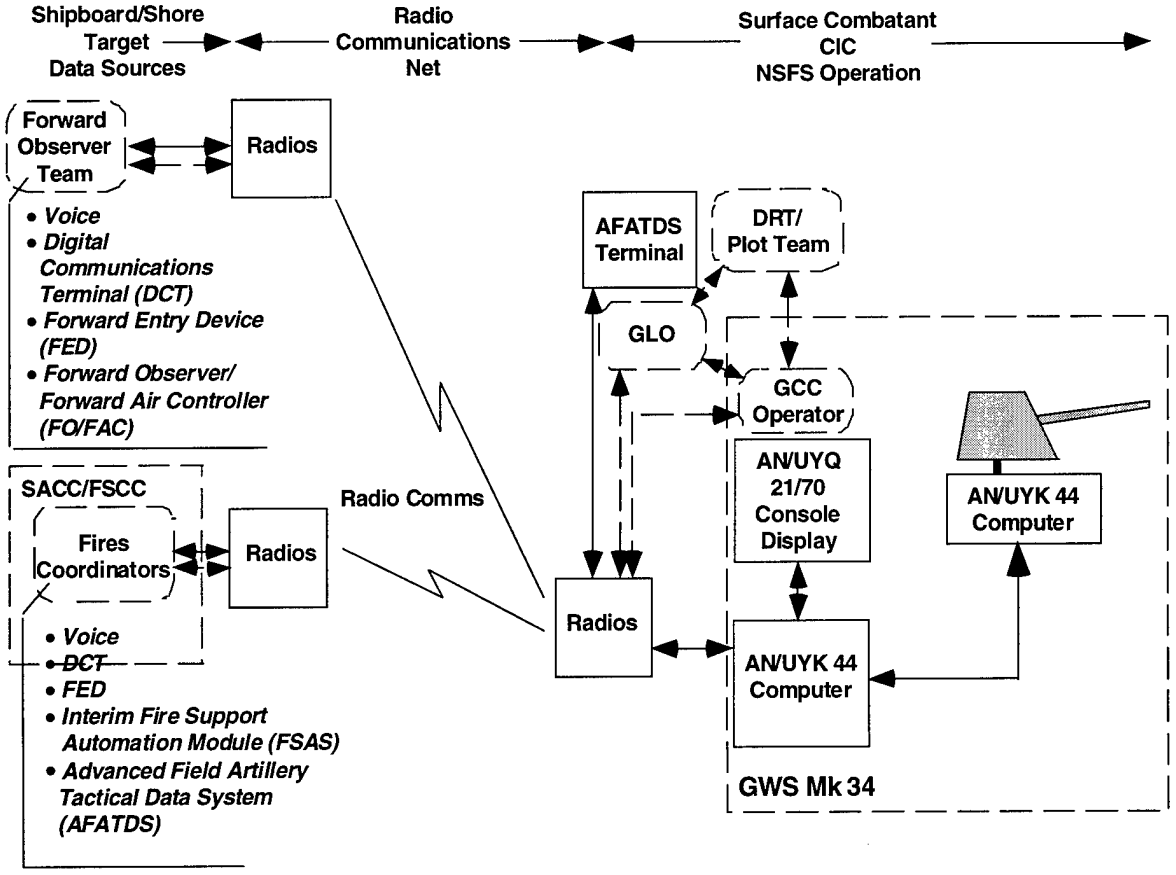

Figure 6. Near-term NSFS planning and coordination system

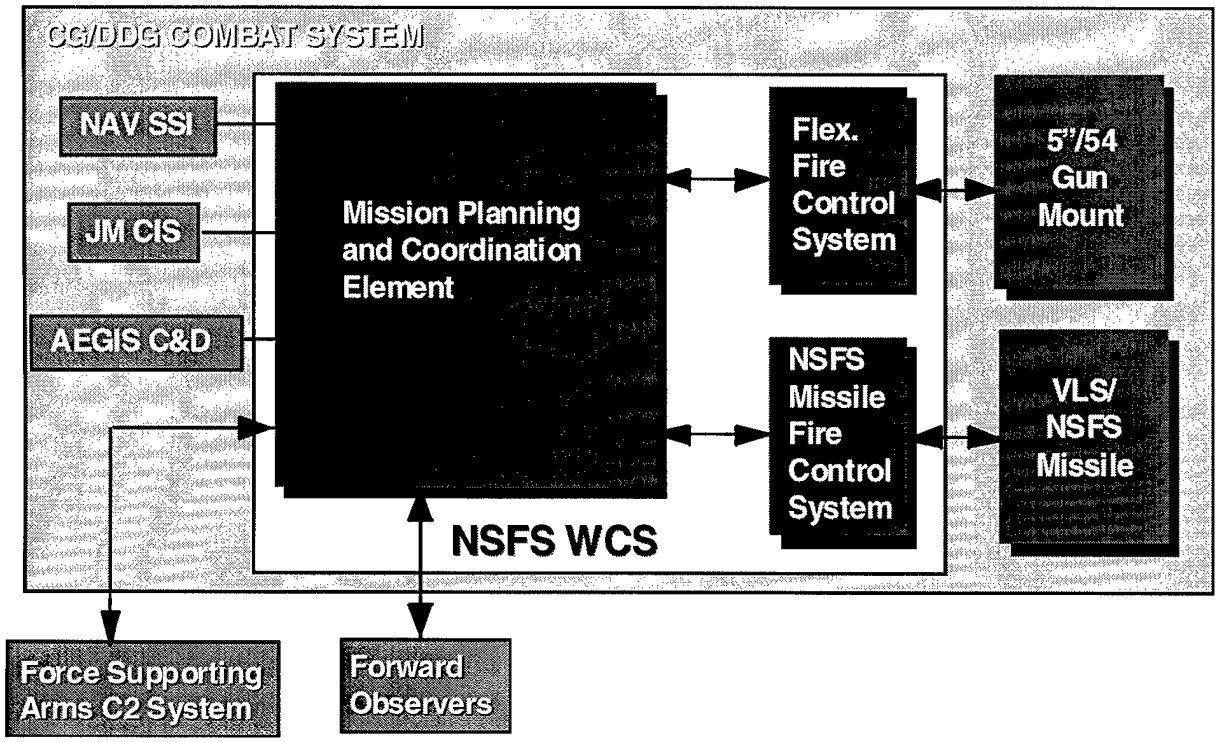

Figure 7. NSFS warfare control system architecture

all of the new functions. However, the advantages of this approach as compared to the development of a new system have been recounted above. In fact, in today's defense environment, with its stress on joint development, reuse of systems, and reduction of cost and risk, this may be the only way to go.

References

1. . . . *From the Sea—Preparing the Naval Service for the 21st Century*, Navy and Marine Corps White Paper, Sep 1992; and *Forward . . . From the Sea—The Strategic Concept for the Employment of NAVAL FORCES*, Navy White Paper, 19 Sep 1994.
2. *Doctrine for Joint Fire Support*, Joint Pub 3-09 (Third Draft), Joint Warfighting Center, Fort Monroe, VA, 11 Dec 1995, p. I-1.
3. CNO Memo, Ser N804/5U644700 Memo, Subj: CNO Executive Board (CEB) Briefing on 14 December 1994-Navy Surface Fire Support (NSFS) II- Action Memorandum (94-10), 3 Jan 1995.
4. Ferrebee, J.G. et al., *Naval Surface Fire Support Study*, Naval Surface Warfare Center, Dahlgren Division, Technical Report TR-92/667, Jul 1992.
5. Holzer, R., "U.S. Mulls Future Battlefield Vision," *Defense News*, Feb 5-11, 1996, p. 3 and 48.
6. "Commandant's Warfighting Laboratory Advanced Planning Briefing to Industry," U.S. Marine Corps, Commandant's Warfighting Laboratory, Quantico, VA, 19 Dec 1995.
7. *Force XXI Operations, a Concept for the Evolution of Full-Dimensional Operations for the Strategic Army of the Early Twenty-First Century*, U.S. Army Training and Doctrine Command (TRADOC) Pamphlet 525-5, U.S. Army TRADOC, Fort Levenworth, KS, 1 Aug 1994.
8. "Slatkin, Decker Sign Navy/Army Digitization Memorandum of Agreement," *Inside the Navy*, 6 Mar 1995, pp. 5-7.
9. NSWCDD A51/JSH Memo, Subj: Trip Report On Supporting Arms Coordination Center (SACC) Team Trainer Exercise, 1 May 1995.

10. *Marine Air Ground Task Force (MAGTF) Command Control Communications Computer and Intelligence (C^4I) Research, Development, and Acquisition Plan (RDAP)* FY 95-96, Marine Corps Systems Command, Nov 1994.
11. Boutelle, Col. S.W., Advanced Field Artillery Tactical Data Systems (Program Briefing), U.S. Army Systems Command, Field Artillery Tactical Data Systems Program Office (PM FATDS), Fort Monmouth, NJ, 5 Oct 1995.
12. Thomas, A.; Horne, A.; Sheehan, C.A.; and Tripp, W.A., "The Evolution Of Strike Weapon Control," *Naval Surface Warfare Center Dahlgren Division Technical Digest*, 1995.
13. "Coordinating NFS From the Sea," Supporting the Land Battle, Program Executive Office-Cruise Missiles, Arlington, VA, 30 Nov 1995.
14. "Computer-Aided Dead Reckoning Tracer," Naval Surface Warfare Center, Dahlgren Division (NSWCDD), Dahlgren, VA, brief, 19 Jan 1996.

The Author

O. Kelly Blosser

O. Kelly Blosser received a B.S. degree in mechanical engineering from the West Virginia University Institute of Technology in 1961 and an M.A. degree in public administration from the University of Oklahoma in 1970. In 1985 he was awarded a diploma with distinction for graduate-level studies at the United States Naval War College, Newport, Rhode Island.

Mr. Blosser has 36 years of experience at the Naval Surface Warfare Center, Dahlgren Division (NSWCDD), Dahlgren, Virginia. He was an ordnance engineer conducting safety and environmental testing of explosive ordnance, participated in an air and surface target vulnerability program and, subsequently, in a wide variety of studies on ship concepts, amphibious warfare fire support, force-level surface warfare requirements, and Soviet anticarrier warfare threat capabilities. He contributed to a number of ship combat system engineering programs: modernization of the DDG-2 *Adams*-class destroyers, concepts for a 3000-ton surface effects ship (SES), requirements development for the DDG-51 *Arleigh Burke*-class destroyers, and AEGIS strike and NSFS system engineering support.

Mr. Blosser is currently in the Warfare Analysis Department, where he is a lead analyst with a team evaluating NSFS and tactical land-attack system mission planning and targeting requirements and capabilities. The team completed a study of mission planning, coordination, and targeting requirements for a Navy variant of the Army Tactical Missile System (TACMS) missile, and is applying the same process to develop planning and targeting system capabilities for land-attack systems for future NSFS ships. Mr. Blosser also co-chairs a team evaluating strike and fire support options for the next generation Navy surface combatant, the 21st Century Surface Combatant.

Future Gun Weapon System Technology

J. Dennis Hagan

Effective naval surface fire support (NSFS) is a key element of expeditionary warfare. Among various systems which contribute to NSFS, a gun weapon system is a cost-effective system for those targets that fall within its range and payload capability. Recent studies have shown that a submunition payload is quite effective against a variety of tactical targets. Existing 5-inch naval guns in the fleet can be equipped to deliver such payloads to a range beyond 60 NM. This long-range capability requires a greater muzzle energy on the part of the gun, and a projectile airframe having rocket propulsion and aerodynamic lift to extend its range beyond the usual ballistic limit. The terminal accuracy of a projectile at this extended range is poor without some form of guidance and control, but the accuracy required for a submunition payload is only a few tens of meters. Guidance based upon the Global Positioning System (GPS) is compatible with these range and accuracy requirements. The Chief of Naval Operations (CNO) has directed that an acquisition program shall accomplish the "now" objectives of a more energetic Mk 45 5-inch gun and an extended-range guided munition, now designated as the EX 171. With regard for the future, the CNO directed that a "campaign plan" be developed to consider the next generation of naval gunnery. This could involve a larger caliber gun—using advanced forms of propulsion and guided munitions—installed in a new class of surface combatant.

EW
EXPEDITIONARY
WARFARE

Introduction

Expeditionary warfare is offensive by its very nature. It involves forcible entry into a foreign, and usually hostile, sovereign nation in pursuit of U.S. national interests. Opposition to such an invasion can be massive and lethal to expeditionary forces as they establish an enlodgement, then begin to advance toward military objectives. Preparatory and supporting fires from air and surface platforms are essential for both the minimization of own-force casualties and the successful attainment of military objectives. Supporting fires from surface platforms are generally referred to as NSFS. Naval gun fire, surface-to-surface guided missiles, and ballistic rockets are included within this category. This article will address the naval gun fire component of NSFS, with special emphasis upon the near- and far-term future technologies that will greatly improve this capability, so vital to expeditionary warfare.

The Role of Naval Gun Fire in Expeditionary Warfare

The recent Department of Navy policy document, *Forward . . . From the Sea*, has articulated the changing role of maritime forces from that of blue-water combatants to one of power projection ashore involving joint littoral operations.[1] The Marine Corps has developed its companion doctrine promulgated in a policy document entitled *Operational Maneuver From The Sea*.[2]

Turning these doctrinal ideas into warfighting concepts through the application of innovative technologies is the objective of an operational concept called *Sea Dragon*[3] from the Commandant's Warfighting Laboratory. One of the primary concepts within *Sea Dragon* is a paradigm shift away from supporting fires in-order-to-maneuver, to one using maneuver as a means to engage by fires. Fires are to become a primary means of engagement rather than simply supporting arms. The Navy is planning shipbuilding programs for two new classes of combatants: the SC-21 and the Arsenal Ship. The guiding documents for both of these ships cite power projection and fire support among their various mission areas.[4,5] A recent draft of a proposed doctrine for joint-service defense against air and missile threats cites naval gun fire as an effective means for offensive counterair operations, wherever enemy air and missile assets are within range.[6]

In all of these areas of current warfighting focus, naval gun fire plays an important role. Naval ships can carry a large loadout of ammunition, compared to what a mobile ground unit can carry. Ships can be replenished in relative safety, beyond the enemy's horizon. Ground artillery, when massed to deliver massed fires, creates a vital asset ashore that itself must be protected. Massive fires from surface ships can be provided with no additional protection other than that warranted for the amphibious task force itself. Ground-based artillery must "shoot and scoot" as a survival tactic. Naval guns just "shoot and shoot." It is important to note, however, that in order for naval guns to be truly effective in the face of these opportunities, they must have adequate range and lethality. These attributes are the principal objectives of future gun technology initiatives.

Performance Required from Guns for NSFS

Guns are versatile weapon systems, addressing a variety of warfighting needs. The principal gun in the fleet today is the Mk 45 5-inch, 54-caliber naval gun. It was designed during the mid-1960s, primarily as an antiair warfare (AAW) system, with secondary and tertiary roles for antisurface warfare (ASuW) and gun fire support, respectively. Throughout the years since then, these roles have changed as missiles assumed the primary role for AAW. The Mk 45 gun's primary role then became fire support, but its maximum range of ~13 NM limited its utility in this area. Accuracy at this maximum range, on the order of 400 m, circular error probable (CEP), further restricted the situations where naval gun fire could be used effectively without collateral damage. The most notable advantage of naval gun fire is the capability to deliver large quantities of ordnance within a short period of time, at an affordable cost, and from a relatively safe standoff distance. Improvements to the gun should seek to exploit this advantage, while increasing range and reducing CEP.

The Marine Corps is the principal expeditionary force of the U.S. armed forces. The Marine Corps is therefore the primary customer for NSFS. Established Marine Corps doctrine for amphibious operations has led to requirements for range and accuracy for NSFS. From ships operating beyond the horizon, at least 25 NM offshore, naval gun fire must reach 16 NM inland to prepare and secure the beachhead, and an additional 22 NM inland to suppress and/or neutralize enemy artillery seeking to defend that beachhead.[7] These requirements add up to 63 NM of range—almost a fivefold increase over present capability. Accuracy at this maximum range must be no worse than the present capability of Marine Corps artillery, which is 333 m, CEP, for the M549-A1 rocket-assisted projectile, fired to its maximum range of 16.3 NM. The attainment of such accuracy at the 63-NM maximum range required for NSFS calls for a guided munition; hence, the NSFS program will develop such a munition, presently designated as the EX 171 Extended-Range Guided Munition (ERGM).

The Near-Term Technology Program

In December 1994, the CNO directed that an immediate program be executed to develop and deploy a 5-inch gun with the capability described above.[8] Such an extraordinarily quick response is made possible by the availability of needed technology from a variety of sources. The attainment of NSFS performance objectives requires a more energetic gun with the ability to fire a massive guided projectile weighing up to 110 lb and with a muzzle energy of 18 MJ. Such a capability affects every aspect of a gun's design, from interior ballistics to recoil/counterrecoil system.

The Navy executed a Balanced Technology Initiative from FY90 through FY94 to develop a 60mm electrothermal gun. This effort was joined by the Defense Nuclear Agency, which developed the same technology in a 5-inch size gun. The objective was increased muzzle energy in the range of 18 to 25 MJ. These efforts provided much of the gun science needed to expand the capability of the Mk 45 gun for NSFS.

Muzzle energy alone is insufficient to project 5-inch ammunition to 63 NM. Additional range must come from the ERGM using rocket assistance, and an extended flight path accomplished by aerodynamic lift from a gliding airframe. The flight path must be altered beginning at apogee, thus requiring an onboard navigator and some means to steer the airframe for several minutes. The GPS offers an attractive basis for guidance and navigation. An earlier 5-inch guided projectile known as DEADEYE provides the design baseline for the airframe. Other needed technologies, developed under small business innovative research contracts and the strategic defense initiative, provide the means for adapting the DEADEYE airframe to fulfill NSFS perform-ance requirements. Examples of these technologies include a miniature, rugged steering actuator, a fast-acquisition military GPS receiver, long-life primary and reserve batteries, and micro-machined silicon inertial instruments.

Improving the Contribution of the Gun

The increased muzzle energy of the Mk 45 gun is the result of several design changes. The first and most simple change involves increasing the size of the propellant charge. Two primary constraints must be considered. First, the resulting peak pressures within the gun chamber and barrel cannot exceed safe operating levels, as determined by structural limits of the gun barrel, breech closure mechanism, and/or the projectile. Second, the impulse, equal to the momentum of the projectile as it leaves the muzzle, cannot exceed the limits of the braking force and recoil distance allowed by the recoil/counterrecoil system. The present Mk 45 gun is constrained by the latter when firing guided projectiles weighing in excess of 100 lb; thus, the propelling charge's operating pressure can be increased from present levels (around 45 ksi) to about 65 ksi without overstressing the gun, provided that the recoil/counter-recoil system is upgraded accordingly.[9]

The next design parameter to be considered is barrel length. The Mk 45 has a 54-cal barrel length (e.g., 54 times the barrel's inside diameter, or 270 inches). Lengthening the barrel allows the propellant pressure to act upon the projectile for a longer time, further increasing its velocity before it exits the muzzle. The primary constraint in this area is the added weight and moment of the barrel, which can cause the barrel to droop, and whip upon firing, in addition to placing an unacceptable load upon the train and elevation drives. With engineering consideration given to these design criteria, the Mk 45 was determined to be capable of supporting an 8-cal longer barrel.[10] This adds about 400 lb to the end of the existing barrel. The added weight helps the recoil problem by reducing the initial velocity of the recoiling parts for a given impulse at the muzzle. The total impulse developed at the muzzle is equal to the momentum of both the projectile and the propelling charge gasses as they leave the gun. An empirical formula for this total momentum is as follows:

$$M_t = (m_{proj} * IV) + (m_{prop} * 4700),$$

where M_t is the total momentum, m_{proj} is the mass of the projectile, IV is the initial velocity of the projectile at the muzzle, and m_{prop} is the mass of the propellant. With each of these expressed in English units, the factor of 4700 works out to the approximate speed of sound, in feet per second, for the high-temperature, high-density compressed propellant gasses pushing the projectile as it exits the muzzle. This total momentum divided by the mass of the recoiling parts yields the initial velocity of the recoiling parts. The product of this velocity squared, times the mass of the recoiling parts, times 0.5, yields the kinetic energy of these parts, the motion of which must be arrested by dissipating their energy in the form of work done on the recoil system. This work is the product of a so-called brake load acting over a recoil distance, or stroke. The present Mk 45 has a brake load capacity of 100,000 lbf and a stroke of 24 inches. The modified gun will be capable of 156,000 lbf and a stroke of 30 inches. The interrelationship of all of these parameters is shown in the nomograph of Figure 1.

The Capability of the ERGM

The ERGM comprises three basic subsystems. It has a solid-propellant rocket motor aft, ahead of which sits a payload bay containing submunitions. Ahead of the payload bay, at the front of the round, is a guidance and control subsystem, which performs two important tasks. It alters the ballistic flight path beyond apogee by controlling the total airframe to assume an angle of attack upward, thus developing lift to oppose gravity and enabling the airframe to glide along a shallow glide slope, greatly extending its range. Additionally, the guidance and control subsystem steers the airframe to the target and releases the submunition payload to fall upon it. The ERGM, after launch at an optimum quadrant elevation by the 18-MJ gun, proceeds along a ballistic trajectory. The rocket motor is burned at an optimum point in the upward climb toward apogee. This adds yet more energy to the trajectory to extend range. Depending upon

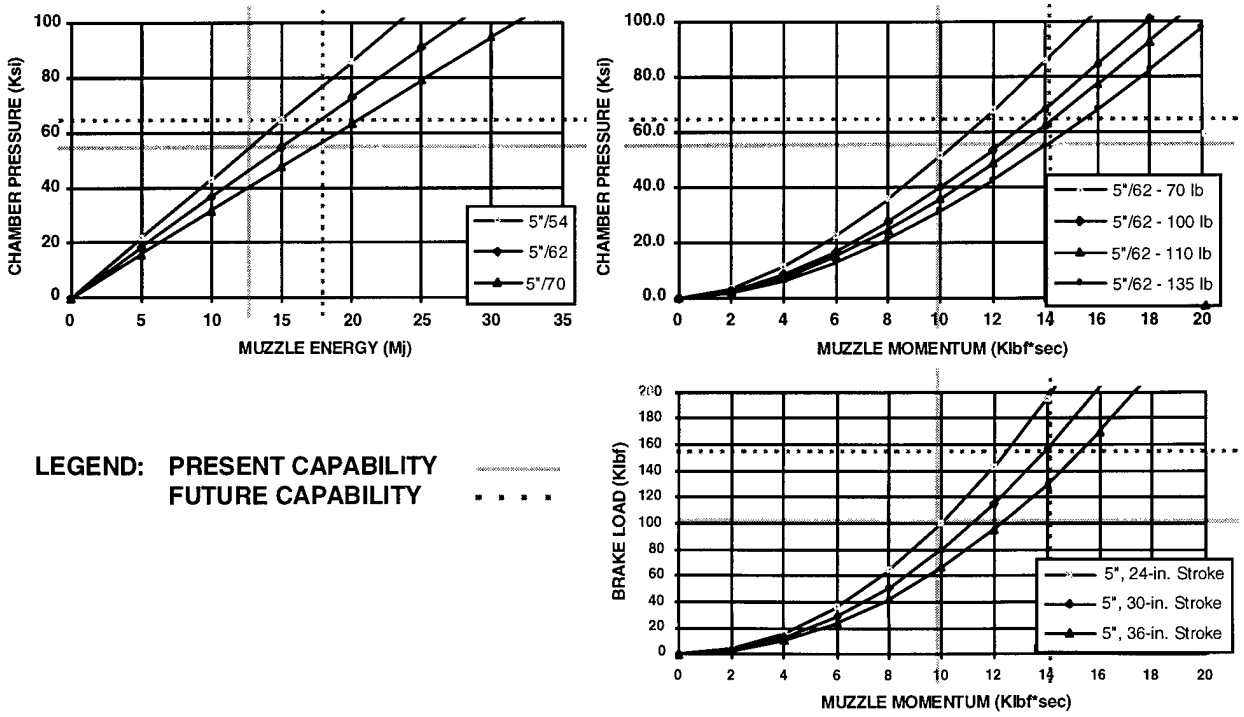

Figure 1. Nomograph showing relationships between chamber pressure, muzzle energy, muzzle momentum, and recoil parameters

its size and where in the trajectory it is burned, the rocket motor can contribute on the order of 10-MJ additional energy. The combined effect of the 18-MJ gun launch, the 10-MJ rocket motor impulse, and the gliding flight path can yield the sought-after range of 63+ NM.

The submunition payload was selected on the basis of a study done by the Marine Corps. This study considered different NSFS expeditionary scenarios and found that a majority of the targets to be taken under fire by naval surface units were most effectively engaged with dual-purpose submunitions (i.e., antipersonnel and antimateriel). The Army's XM-80 was chosen as the model for the ERGM payload. At least 70 of these submunitions can be carried by the ERGM. This payload is lethal to "soft" targets if dispensed in a pattern no larger than 100 m across. The required delivery accuracy then needs to be comparable to the pattern radius of 50 m, minus the target location error, which is typically around 20 m when based upon a GPS targeting system. The resulting 30-m CEP requires some type of terminal guidance, but not the "surgical" accuracy associated with terminal seekers. A GPS receiver tightly coupled to an inertial navigation system (INS) was chosen for the ERGM guidance system. Such a system is autonomous, small, rugged, affordable, and can operate in virtually any type of weather, day or night.

The GPS/INS Guidance System

Operationally, a GPS/INS guidance system in a gun-launched munition has several interesting characteristics. The inertial system cannot be aligned and initialized prior to launch, as can be done with a missile; therefore, the system is completely dependent upon the GPS subsystem for calibration during flight. Immediately after the launch, the GPS receiver must quickly acquire four GPS satellites to establish the position and velocity of the ERGM. The INS can aid this process by informing the GPS receiver of body angular rates and accelerations. Once GPS acquisition and track is established, the INS can be calibrated and aligned via a Kalman filter with inputs from the GPS receiver. The combined system is synergistic in this respect. The INS also provides feedback of body dynamics to the autopilot, which controls the flight of the round to the target. The primary need for the INS arises from the expectation that the GPS receiver will be jammed by enemy emitters as the ERGM approaches the target area. The INS then becomes the sole means of guidance for the terminal encounter.

The Gun-Launchable GPS Receiver

The GPS has a commercial signal known as the C/A-code, and a more accurate military signal known as the P(Y)-code. The latter is encrypted to protect it from enemy exploitation and use. It also involves a very long nonrepeating, pseudorandom sequence encoded at a 10.23-MHz "chipping" frequency. Military users must be able to acquire this code sequence directly, without first locking on to the much simpler C/A-code. This capability requires a very precise time and frequency reference onboard the projectile. For this purpose, a crystal oscillator must be energized and calibrated within the ERGM immediately before it is rammed and fired. This oscillator must continue to operate throughout gun launch, and maintain its prelaunch accuracy afterward, in order for the GPS receiver to directly acquire the P(Y)-code.

The Navy has conducted rather extensive tests of crystal oscillators to reduce the technical risk in this important area.[11] The Naval Air Warfare Center at Indianapolis, Indiana, acquired 10 samples of 9 different types of oscillators. Five of the samples for each type were subjected to a temperature and shock test program. The other five were given to the Army Research Laboratory for similar tests.

The Navy shock tests were carried out by a commercial laboratory, using a 4-ft square

steel plate, ½-inch thick, shocked by a coil of primer cord attached to one side. The resulting shock spectrum closely matched that of a 5-inch projectile fired from a Mk 45 gun at 10,000 and 16,000 g. The crystal oscillator was instrumented throughout the test. Two devices were damaged by the test. The rest survived and showed a shift in frequency averaging around 2.5 ppm.

The Army tested their samples in an air gun at 10,000 and 16,000 g. In their test, 38 percent of the devices were damaged, and the rest showed a frequency shift averaging about 4 ppm.

The Naval Surface Warfare Center, Dahlgren Division (NSWCDD), is preparing an all-up projectile to be fired at Yuma Proving Ground. This projectile will have a crystal oscillator running prior to, during, and after the gun-launch event. A telemeter onboard will monitor performance and relay it to a ground-based computer for analysis. This will be the first real-time test of an oscillator's performance in a gun-launched airframe.

GPS Jamming Must Be Considered

Previously, it was mentioned that the GPS is subject to jamming. This cannot be prevented in a practical sense, so the INS was added as an alternate means of terminal guidance. The INS must be small, rugged, and affordable; hence, it is not generally of high-quality, high-performance technology. A technical tradeoff must be made here between a highly capable GPS receiver that can closely approach a powerful jammer, and a highly capable INS that can deliver terminal accuracy from a long way out without an unacceptable growth in CEP. (An example of this analysis is described in the article by Ohlmeyer et al., which follows this one.) In general, the GPS receiving system, comprising the antenna subsystem and the receiver itself, should be able to acquire track in a broadband noise environment of 65-dB jammer-to-signal (J/S) ratio and maintain track in an 85-dB J/S noise environment. The INS should have gyros with startup drift no worse than 100 deg/hr and accelerometers with startup bias no worse than 100 milli-g. These are initial values that should be improved at least an order of magnitude by the Kalman filter, as it tightly couples the GPS receiver to the INS during flight.

GPS Accuracy

A final characteristic of GPS guidance is the accuracy it can deliver. To understand that which follows, a brief discussion of the GPS is helpful.[12] The GPS satellite orbits are at half geosynchronous altitude. Their orbital period is ~12 hr, so they do not change their apparent position in the sky very quickly. Because the orbits are so large (~20 E+6 m above the earth), they appear more or less the same to simultaneous users spread over distances of hundreds of kilometers. The position error experienced by users within hundreds of kilometers of each other is predominantly due to ionospheric effects, the relative geometry of the satellites in the sky, and the uncertainties with respect to reported time and position from the satellites themselves. These errors represent a bias in the position determined from the GPS and are seen the same by all users during any given period of time. Therefore, individual users are each subject to an "autonomous" error in determining their GPS position, and the magnitude of that error is on the order of 15 m. Whenever two cooperative users—say one locating a target and the other programming a weapon to navigate to that target—are both seeing the same error, then that error is common to both elements of a closed loop, so it ceases to matter. The effective position error in that case is the random noise component, which is quite small—on the order of a few meters.

One other way of reducing the error in the GPS is by means of a technique known as differential GPS, or DGPS. In this arrangement, a receiver located at a known geodetic survey point, in the vicinity of user clients, observes the error in the GPS on a

continuous basis. This information is then continuously broadcast to all user clients in the area so that they can subtract this error from their observed GPS locations. The resulting error from DGPS, operating on the military P(Y)-coded signal, is less than one meter! Thus, it can be seen that the accuracy of the GPS has a range of possibilities, depending upon the way in which it is being used.

The Far-Term Technology Program

As the CNO chartered the near-term program, he also directed that a "campaign plan" be developed to address the mid- and far-term needs of NSFS. Even with the modified Mk 45 gun and its ERGM, NSFS needs greater improvements in range and throw-weight, along with more diverse target engagement capabilities. In keeping with the high-volume characteristic of naval gun fire support, these new technologies must be developed in such a way as to keep them affordable. The campaign plan must also be consistent with future shipbuilding plans. Future needs must be considered when structuring initiatives for development within the Navy's RDT&E technology base. The ERGM acquisition program includes a preplanned product improvement (P^3I) phase following the initial operational capability. This P^3I phase provides a transition path for the emerging products of the technology base. The following paragraphs will describe those technologies with the most promise.

Far-Term Gun Technology

The most likely gun technology to supersede the modified Mk 45 would be a larger caliber gun—probably a 155mm. Past studies, including the recent NSFS cost and operational effectiveness analysis (COEA), have established this size gun as the optimum for NSFS. The volumetric ratio of a 155mm gun and ammunition, compared to a 5-inch gun and its ammunition is $(155\text{mm}/5\text{ inch})^3$, which is ~1.8. This means that an 18-MJ 5-inch gun scaled up to 155mm would have ~32 MJ of muzzle energy. The payload bay of the scaled-up 155mm projectile could carry 1.8 times the weight carried by the 5-inch projectile. The rocket motor could also contain 1.8 times more propellant. With the muzzle energy and rocket motor impulse scaled up from the 5-inch analog, in proportion to the overall weight increase of the 155mm projectile, the resulting range would be the same in a vacuum.

Naval guns are not fired in a vacuum, however. They are fired at sea level where the atmosphere is most dense. This fact brings into play a parameter known as the ballistic coefficient, $B = \frac{W}{C_D A}$, determined by the ratio of the weight of a projectile to its drag. The higher the ballistic coefficient, the better a projectile will penetrate the atmosphere, with a resulting increase in range. The weight of a projectile is proportional to its diameter cubed; its drag is proportional to cross-sectional area, or diameter squared. Forming the ratio of these two characteristics results in a linear dependence of the ballistic coefficient upon the body diameter; consequently, the ballistic coefficient of a 155mm projectile is ~1.2 higher than that of a 5-inch projectile (assuming the same drag coefficient for both rounds).

Thus it can be seen that a 155mm gun can project a 1.8-times heavier payload to a 1.2-times greater range. The entire gun mount tends to weigh 1.8 times as much as a 5-inch gun, and a magazine space of comparable volume will hold only about 1/1.8, or 56 percent, of the capacity for 5-inch rounds. These factors make the installation of a 155mm gun into the space currently occupied by an existing 5-inch gun highly impractical. For this reason, the near-term program could only proceed with an improved 5-inch gun. The development and deployment of a 155mm gun was deferred until a new and larger ship class, with an NSFS mission, emerges from one of the current ongoing studies.

Far-Term Projectile Technology

Innovative technology for the guided projectiles to be used for NSFS falls into two general programmatic categories: advanced technology demonstrations (ATDs) and P^3I of the ERGM.

Competent Munition for the 5-inch Gun ATD. This technology involves the development and testing of a miniature GPS/INS guidance system to be packaged within the nine-cubic-inch volume of the NATO-standard fuze for conventional spin-stabilized projectiles. The Charles Stark Draper Laboratory of Cambridge, Massachusetts, is the principal performer for this effort, which began in FY96. In addition to miniature GPS/INS components, this device will also include a steering actuator that is roll-decoupled from the spinning projectile by means of a bearing assembly. The nose can thus be aerodynamically controlled to stop it from spinning so it can be positioned and its canards deflected to steer the projectile. An electrical generator is also driven by this relative spin difference. This generator provides electrical power to supply the guidance system's needs, and it provides a reaction torque opposing the aerodynamics of the nose, thereby producing a torque balance that is controlled to position the nose. The NATO-standard fuze fits virtually all of the artillery ammunition of U.S. and NATO armed forces; thus, this ATD will find a wide range of applications and a correspondingly large production potential, which will drive down its cost. This ATD will enable a diverse family of competent munitions obtained from vast conventional stockpiles. It will not increase the range of this ammunition, but it will give it GPS accuracy. This device can also be used on the ERGM airframe. Its small volume will permit either a larger payload or a larger rocket motor, depending upon the need for either increased lethality or range. Here, it can deliver long range as well as accuracy by virtue of the ERGM airframe with its rocket motor and aerodynamic lift. This configuration is shown in Figure 2.

"Best Buy" ATD. This technology initiative seeks to circumvent the length constraint imposed upon the ERGM by the Mk 45 gun's autoloader. Presently, the overall length of the ERGM cannot exceed 61.195 inches. This limit on the payload and propulsion systems constrains both the lethality and the range. "Best Buy" will exploit technology under development by the Army, including composite structures and a joint between two separate sections of a single round of ammunition that can be joined within the gun barrel as the second section is rammed behind the first. At present, the gun must undergo two ramming cycles when firing ERGM. The first cycle places the ERGM in the gun, and the second places the propelling charge, which is only about 33 inches in length. Thus, an additional 28-inch section of the ERGM could be included with the second ram cycle, allowing a substantial increase in either the payload or propulsion system, again, depending upon need. The use of composite materials can help to maintain strength while reducing weight. The joint would likely involve a "snap-ring" forced upon a conical interface terminating in a locking groove. Such a round could approach the range and payload

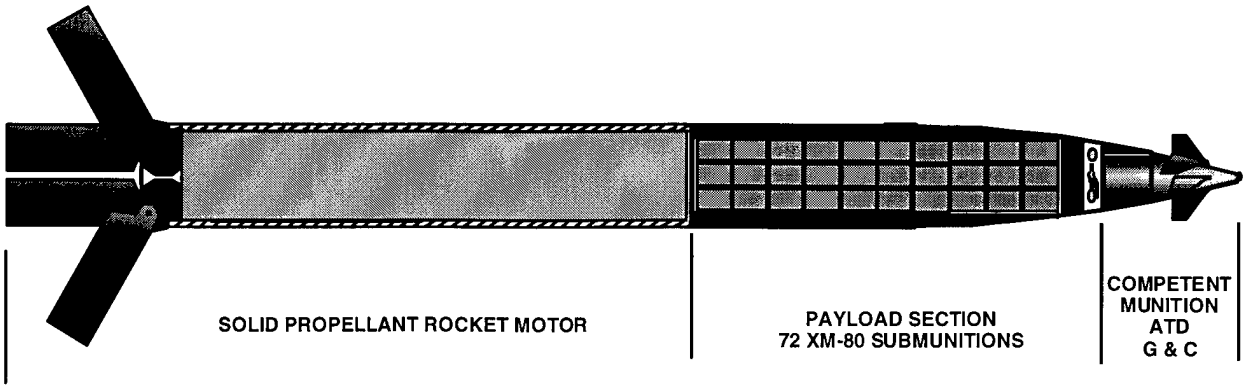

Figure 2. ERGM with Miniature GPS/INS Guidance System from the Competent Munition ATD

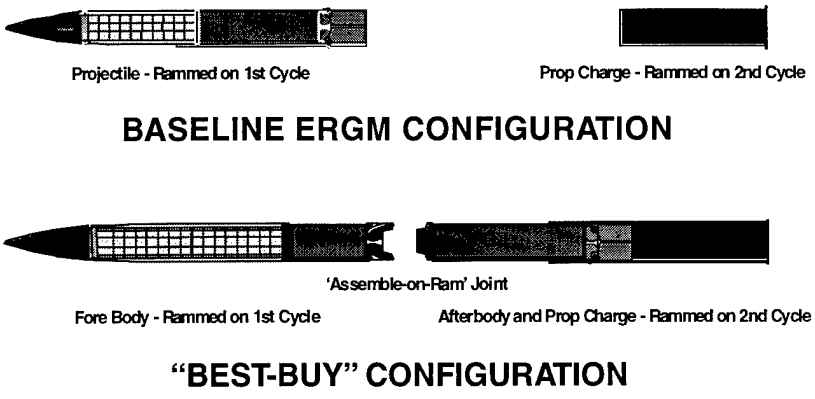

Figure 3. Comparison of ERGM and "Best-Buy" configurations

of a 155mm gun.[13] This ATD is scheduled to begin in FY97. A comparison of the ERGM and "Best-Buy" configurations is shown in Figure 3.

"Longlook" ATD. This concept involves the placement of an unmanned aerial vehicle (UAV) for reconnaissance and targeting by means of a gun-launched delivery vehicle. Such a method circumvents the problem of quickly getting a slow-flying UAV where it is needed. The UAV will have either a ram-air-inflatable fabric wing or a composite "swing-wing," an internal combustion engine, and an avionics package with a GPS receiver, attitude instruments, autopilot computer, video camera, and radio-frequency uplink and downlink. It can be placed 60 NH downrange within 10 min. Its loiter time will be 3 hr. It can indicate the location of an object of interest with respect to its own location determined by reference to the GPS. It can be commanded to move to a preferred position and point its camera in a preferred direction.[14] This concept has not been accepted for funding as of this writing—it is still being marketed. The "Longlook" concept is shown as Figure 4.

ERGM P³I. The Marine Corps study mentioned above, which established the

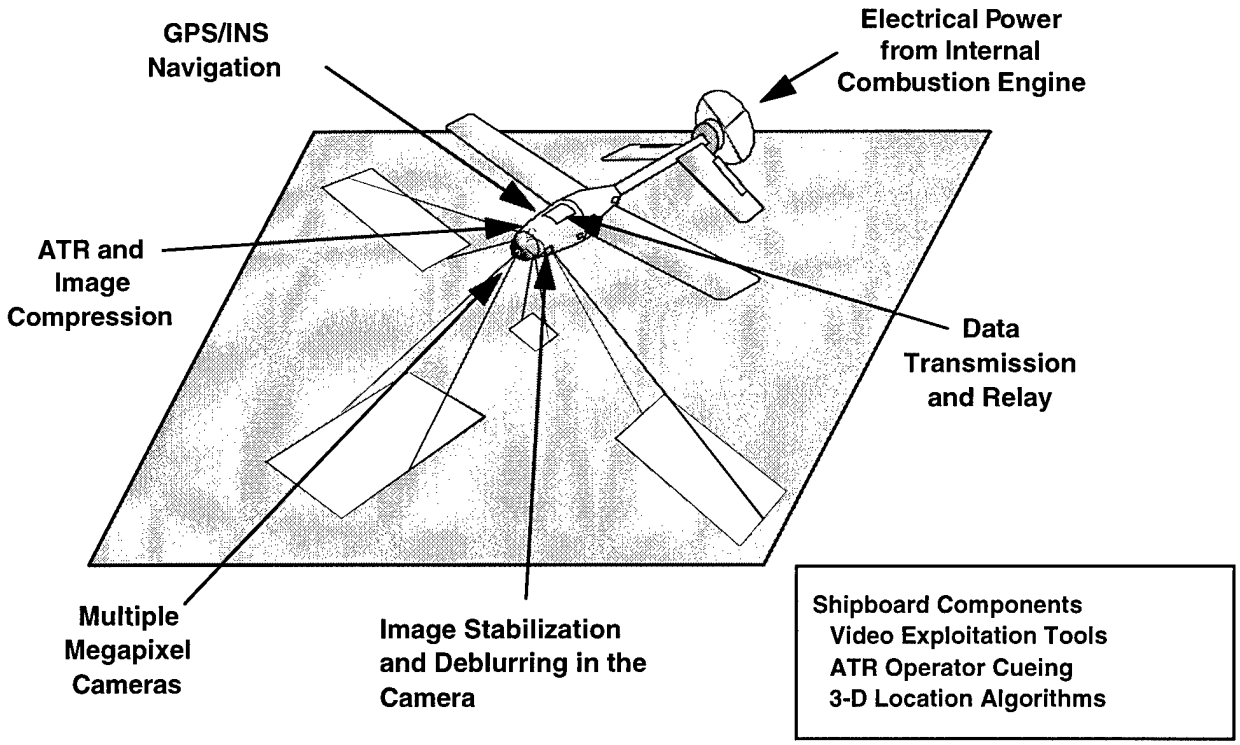

Figure 4. "Longlook" concept

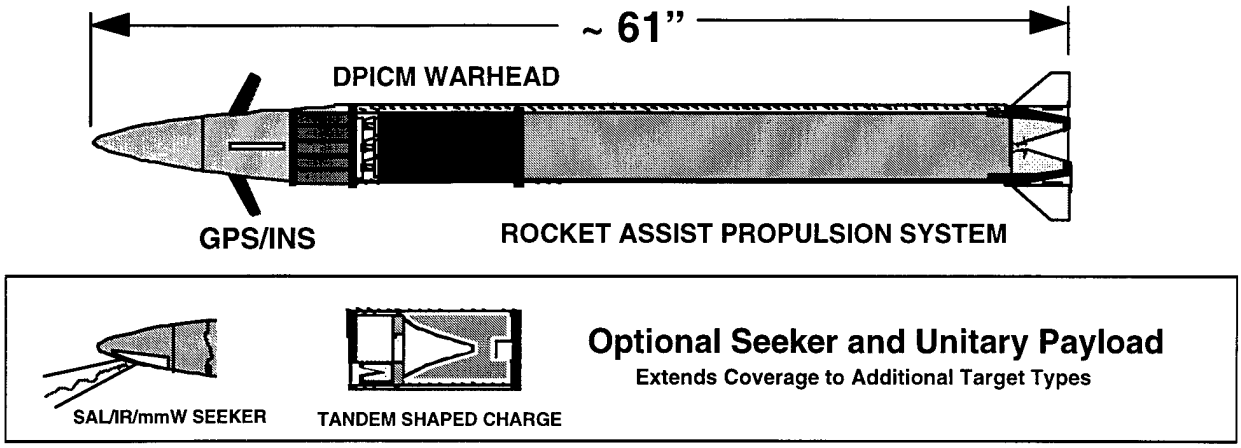

Figure 5. P³I ERGM

priority for a submunition payload for the 5-inch ERGM, also indicated that a large fraction of the NSFS target set required a terminal seeker and a large unitary warhead. These targets include moving vehicles and hardened targets such as armor and fighting bunkers. For that reason, the Operational Requirements Document for the ERGM calls for a future improvement in the form of a terminal seeker coupled with a unitary warhead.[15] The terminal seeker technology will be decided by a future study, but the obvious candidates include semiactive laser (SAL), imaging infrared (IR), low-light-level TV, and millimeter wave (mmW). These can be configured as body-fixed sensors, having no moving parts—made possible by installing them as an adjunct to the existing GPS/INS guidance. The inertial instruments of the INS will provide measurements of the rigid-body dynamics to determine the true target line-of-sight dynamics for terminal guidance. The GPS guidance system provides midcourse guidance to get into the vicinity of the target for the terminal seeker's acquisition and handover. The unitary warhead would likely be a tandem-shaped charge pair, designed to defeat reactive armor. The planning and funding for this P³I will be an issue for future years' defense plans. The P³I ERGM is shown in Figure 5.

Conclusion

Naval guns will play an important role in expeditionary and joint warfare. A far-reaching lethal gun, fired from a surface combatant within the littorals, is a vital element of modern warfighting concepts such as *Operational Maneuver From The Sea* and *Sea Dragon*. Technology affecting both the Navy's Mk 45 5-inch gun and its ammunition are advancing, as directed by the CNO. Emerging technologies at various stages of execution and planning are providing for an even greater benefit from naval guns in the future.

References

1. U.S. Department of Defense, Department of the Navy, *Forward ...From the Sea*, Washington, DC, Office of the Chief of Naval Operations, 1994.
2. U.S. Department of Defense, U.S. Marine Corps, *Operational Maneuver From The Sea*, Quantico, VA, Marine Corps Combat Development Command, 1994.
3. "Sea Dragon Experimental Concepts," *Inside the Navy*, Washington, DC, Inside Washington Publishers, 25 Dec 1995.
4. "Surface Combatant for the 21st Century Milestone I COEA Guidance," reprinted in *Inside the Navy*, Washington, DC, Inside Washington Publishers, 8 Jan 1996.

5. Portions of the Navy's Arsenal Ship Performance Specifications Draft, reprinted in *Inside the Navy*, Washington, DC, Inside Washington Publishers, 8 Dec 1996.
6. Excerpts from Joint Pub 3-01, *Inside the Navy*, Washington, DC, Inside Washington Publishers, 15 Jan 1996.
7. U.S. Department of Defense, U.S. Marine Corps, Position Paper, Subj: The Marine Corps Requirement for Naval Surface Fire Support, LTCOL Robert M. Carroll, Quantico, VA, Marine Corps Combat Development Command, 1994.
8. U.S. Department of Defense, Department of the Navy, Memorandum for Distribution, CNO Executive Board (CEB) Briefing on 14 Dec 1994 - Navy Surface Fire Support (NSFS) II - Action Memorandum (94-10), Washington, DC, Office of the Chief of Naval Operations, 1994.
9. U.S. Department of Defense, Department of the Navy, Requirements for Development, Engineering, Manufacture and Test of 5"/54 Caliber Gun Mount MK 45 MOD 2, WS-3783, rev B, Washington, DC, Naval Sea Systems Command, 1990.
10. Langerud, D.S.; Hummel, K.W.; and Panek, A.W., *MK 45 Train Bearing Analysis*, E. C. 1623, Contract N00024-92-C-5406, Fridley, MN, United Defense, L.P., 1994.
11. *Pyrotechnic Shock Test Results for Crystal Resonators and Oscillators*, Naval Air Warfare Center, Aircraft Division Indianapolis, Shipboard Electronics Project Office, Code 11XP16C, Indianapolis, IN, 1995.
12. Wells, D. et al., *Guide to GPS Positioning*, Fredericton, N. B. Canada, Canadian GPS Associates, 1986.
13. Fraysse, J.W., " 'Best Buy' Low Cost Capability Multiplication for 5-inch Fire Support Projectiles," presentation from Naval Surface Warfare Center, Dahlgren Division, Dahlgren, VA, 1996.
14. Fraysse, J.W., "The Longlook Concept—Organic Real-Time Target Location, Battle Damage Assessment and Communications Relay," presentation from Naval Surface Warfare Center, Dahlgren Division, Dahlgren, VA, 1996.
15. U.S. Department of Defense, Department of the Navy, *Operational Requirements Document, Serial Number 421-86-95, For Extended Range Guided Munition*, Washington, DC, Office of the Chief of Naval Operations, 1995.

The Author

J. DENNIS HAGAN is a principal weapon systems engineer in the Guns and Munitions Division at NSWCDD. He serves as the chief systems engineer for the NSFS program. He has made major contributions to various guided munition and guided missile RDT&E programs of the Navy and other agencies during his 25 years of government service. Examples include the infrared and semiactive laser guided projectiles, the Army's Copperhead guided projectile, Stinger, Standard Missile, the Rolling Airframe Missile, the Anti-Satellite Missile, upper and lower tier TBMD missiles and, most recently, the Extended-Range Guided Munition for NSFS. He received a B.S. degree in physics from Roanoke College in 1968, and an M.S. in systems engineering from Virginia Polytechnic Institute in 1995. In December of 1991, he received the Navy Meritorious Civil Service Award. He was the recipient of the Bernard Smith Award in 1995. He is also a licensed Professional Engineer in the Commonwealth of Virginia.

J. Dennis Hagan

Application of GPS/INS to Extended-Range Guided Munitions and Tactical Ballistic Missile Interceptors

Ernest J. Ohlmeyer, Thomas R. Pepitone, B. Larry Miller, D. Stephen Malyevac, John E. Bibel, and Alan G. Evans

EW
EXPEDITIONARY
WARFARE

The Global Positioning System (GPS) is finding increasing use as an effective means to improve the accuracy of inertial navigation systems (INS) in guided projectiles and missiles. Two areas that have provided strong motivation for using integrated GPS/INS are Naval Surface Fire Support (NSFS) and Tactical Ballistic Missile Defense (TBMD). This article presents an overview of various techniques for the integration of GPS and INS in a guided weapon system. The article describes a multipurpose GPS/INS simulation and analysis tool developed to support a variety of possible technology demonstrations and full-scale development programs involving GPS-aided guided weapons. The simulation includes detailed models of GPS satellites and receiver, jamming environment, navigation Kalman filter, INS with strapdown inertial measurement unit (IMU), six-degree-of-freedom (6-DOF) airframe, and guidance and control components. To illustrate capability, the navigation performance of a GPS-aided smart munition is analyzed in detail. The article also reviews some emerging technology trends and potential future applications for GPS/INS.

Introduction

A growing number of new weapon systems are relying on the GPS to provide accurate in-flight calibration of the onboard INS. This navigation system updating can achieve high terminal precision for surface attack and NSFS missions by greatly reducing the buildup of weapon flyout errors. As an example, the use of GPS allows guided projectiles and other precision guided munitions to navigate more accurately to the target area and deploy their payloads in a tightly controlled pattern. Weapons that employ terminal seekers for homing, such as the interceptor missile used for TBMD, can also be rendered more effective through the use of GPS. GPS navigation updates permit more accurate handover from midcourse guidance to terminal guidance by reducing heading and alignment errors in the navigation system. Smaller heading errors allow guidance systems with limited divert or maneuver capability to steer out the delivery errors before intercept. Reduction in alignment errors permits earlier target acquisition by narrow beam (small field-of-view) seekers without the need for an extended search pattern.

Because of the expanded use of GPS in a wide range of weapon system engineering applications, an effort was initiated to develop a general purpose

Overview of GPS

The GPS has three major operational segments:

Space Segment. The space segment consists of a constellation of satellites in semisynchronous orbits around the earth. The fully operational GPS space segment has 21 navigation satellites plus 3 active spares. The satellites are uniformly distributed in six orbital planes, providing four to seven visible satellites to a user anywhere on Earth. The satellites' orbital planes are inclined at 55-degrees with respect to the equatorial plane, the orbital altitude is 20,200 km, and the orbital period is 12 hr. The system measures range to a set of four or more satellites by timing the arrival of radio signals transmitted from the satellites at precisely known times. Each satellite transmits specially coded signals that allow individual satellites to be distinguished, and the range and range rate to the user to be measured. The satellites transmit their signals at two L-band frequencies: L_1 = 1575.42 MHz and L_2 = 1227.60 MHz. The transmitted signals are modulated with two pseudo-random codes: the P-code and the C/A code. The P-code denotes the precise code and provides the highest degree of GPS accuracy. An encrypted version of the P-code is termed the Y-code. Users of the P/Y-code must obtain authorization from the DoD. The C/A, or coarse/acquisition, code is open to civilian users.

Control Segment. The control segment consists of one master ground control station and several other monitor stations with tracking antennas at accurately known positions throughout the world. The function of the control segment is to accurately track the GPS satellites and periodically update the satellites with corrected data. At the main ground control station, the orbits for each satellite are fitted and predicted. Almanacs good for several weeks and ephemerides good for a few hours are computed and uploaded to the satellites. Satellite clock corrections and atmospheric data are also uploaded. Each satellite also broadcasts as part of its data message a subset of the ephemerides and almanacs for all the satellites.

User Segment. The user segment is composed of the various military and civilian end users with GPS receiving equipment. GPS user equipment consists of antenna, receiver, and associated electronics and displays. The objective of the user segment is to process information received from the GPS satellites to obtain position, velocity, and time.

GPS/INS digital simulation environment to support future concept studies and system design efforts. The intent was to make the simulation flexible enough to accommodate a variety of ongoing and planned weapon system development and demonstration programs. Strong motivation for the model's development was provided by the Extended-Range Guided Munition (ERGM) program and the Navy's Theater-Wide TBMD Program (designated "SM-X").

This article will review the application of GPS/INS to guided weapon systems and describe the design implementations and required levels of system modeling to analyze such systems. Various approaches are examined for the integration of GPS with INS for guided weapon navigation. The various subsystem models required for an integrated GPS/INS system model are also described.

An example of ERGM system performance is provided, along with simulation results that show the navigational accuracies that are achievable using a conceptual ERGM GPS/INS system. Also included are preliminary results that show the effects of jamming on ERGM terminal accuracy. Some anticipated future trends in the evolution of GPS/INS systems are then provided.

GPS/INS Integration With Weapon Systems

The GPS is a space-based radio navigation system managed by the U.S. Department of Defense (DoD). It provides accurate three-dimensional position, velocity, and time to authorized users. The system provides continuous, worldwide, all-weather coverage. Because GPS receivers are relatively low-cost, and have

small size, weight, and power requirements and fairly high reliability, GPS has many advantages for application to guided weapon navigation. Some useful general information on GPS is given in References 1 through 6.

The GPS's principle of operation is based on range triangulation. If the satellite position is known accurately via ephemeris data, the user can receive the satellite's transmitted signal and determine the signal propagation time. Since the signal travels at the speed of light, the user can calculate the measured range to the satellite. The actual measurement (called the "pseudorange") contains errors because of a bias in the user's clock relative to GPS reference time. Because atomic clocks are used in the satellites, their errors are much smaller than errors in the users' clocks. Thus, to determine three-dimensional position, and also to calculate the clock bias, a minimum of four satellites is needed to obtain a solution to the navigation problem. Velocity can be obtained by various methods, which amount to time differencing the pseudoranges over the measurement time interval. The resulting measurement is called the "delta-range."

Inertial navigation refers to the determination of a vehicle's position, velocity, and course with respect to the earth. The navigation solution is obtained by numerically solving Newton's equations of motion using meas-urements of vehicle specific forces and rotation rates, obtained from onboard instrumentation. The onboard sensing components consist of accelerometers and gyros which, together with other platform electronics, compose the IMU. The IMU and the computer software and hardware that implement the navigation solution make up the INS. A good discussion of GPS/INS integration topics is given in Reference 7.

The INS may be mechanized in either a gimbaled or strapdown configuration. In a gimbaled system, the accelerometers and gyros are mounted on a gimbaled platform to isolate the sensors from the rotations of the vehicle and to keep the measurements and navigation calculations in a stabilized coordinate frame. Some possible navigation frames include:

- Earth-centered inertial (ECI)
- Earth-centered, earth-fixed (ECEF)
- Locally level with axes in the directions of north, east, and down (NED)
- Locally level with a wander azimuth (LLWA)

In a strapdown system, the sensors are rigidly mounted to the vehicle airframe, and coordinate transformations ("electronic gimbals") are used along with the body-fixed acceleration and rate measurements to perform the navigation computations in the stabilized frame. Gimbaled systems can be more accurate and easier to calibrate than strapdown systems, but they tend to be larger, heavier, more expensive, and less reliable than strapdown systems. Strapdown systems can be subject to higher dynamic conditions (such as high turn-rate maneuvers) that can stress instrument performance. However, with the appearance of newer, high quality gyros and accelerometers, strapdown inertial systems are becoming the predominant mechanization because of their low cost and reliability.

There are numerous sources of error in the INS that must be considered in evaluating system accuracy and performance. For example, errors associated with the gyros and accelerometers typically include:

- Static and g-sensitive biases and drifts
- Scale factor errors
- Misalignment errors
- Random noise

Additional errors arise from calibration, initialization and transfer of alignment, computational inaccuracies, and approximations in the navigation solution. Without compensation, all INS errors will propagate in time; some errors (such as position) will typically diverge with time; others will be bounded and oscillate.[8,9] The accuracy of an INS is therefore highly dependent on sensor quality, navigation system mechanization, and the dynamics of the flight vehicle.

Inertial navigation systems, in principle, permit autonomous operation. Because of their error propagation characteristics,

however, most applications requiring high terminal accuracy utilize external aiding to reduce errors.

An aided INS uses data from some source (e.g., track radar, GPS, Terrain Contour Matching (TERCOM), star fix) in conjunction with a navigation Kalman filter to improve the accuracy of the navigation solution.[10-12] Figure 1 illustrates the inertial aiding concept. The residual formed by differencing the INS and external aiding data is sent to the Kalman filter. The filter contains an internal model of INS error dynamics and processes the measurements to estimate instantaneous values of INS errors. These error estimates are then used either to correct INS outputs or, alternatively, to correct (reset) navigation data within the INS itself. The former approach is called a feed-forward scheme, while the latter is called a feedback technique. The feedback technique is usually preferred for its greater robustness and will be described in more detail.

In the integration of GPS with INS, the short-term accuracy of the INS and the long-term stability and accuracy of the GPS directly complement each other. GPS is fairly accurate, but is available at slower data rates. INS data have low noise and are generated at high data rates, but are subject to biases and drifts that cause the errors to grow with time. This suggests an integration approach that utilizes the INS for accurate weapon navigation and guidance, with the GPS used to periodically calibrate the INS and keep its errors bounded. A Kalman filter[13,14] usually serves as the method for fusion of GPS and INS data, and provides a means of estimating the navigation errors for later correction. Thus, design of the navigation filter is crucial to the performance of the INS.

The integrated GPS/INS is usually configured in either a loosely coupled or a tightly coupled system. While variations exist across applications, typical examples of these systems are shown in Figure 2. In the loosely coupled system, the GPS receiver has its own internal Kalman filter to process the satellite-derived pseudorange and delta-range measurements. These measurements are used to calculate positions and velocities in the World Geodetic System 1984 (WGS-84)

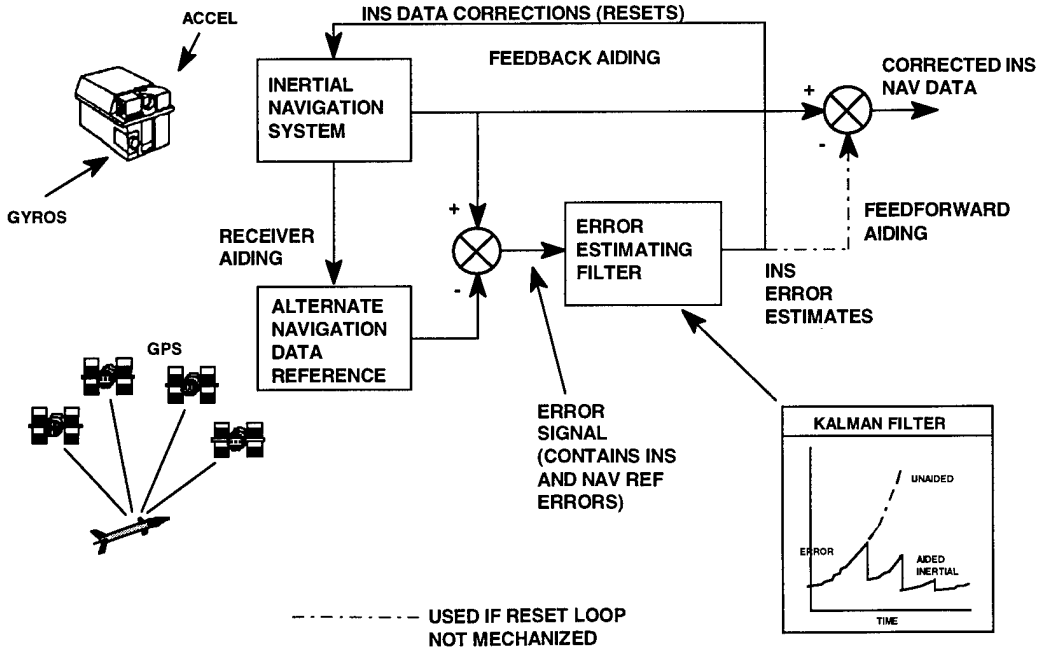

Figure 1. Inertial aiding concept

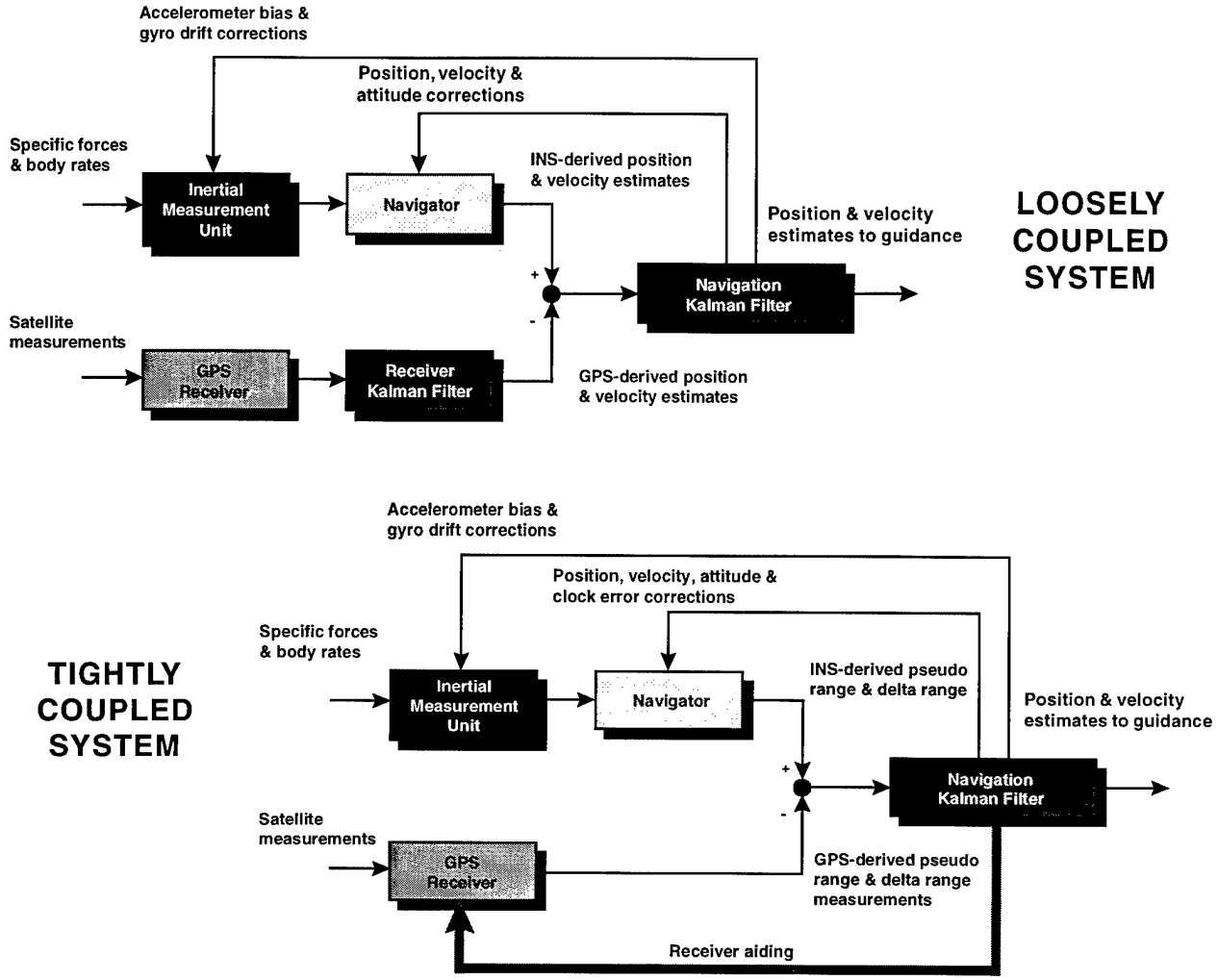

Figure 2. Comparison of loosely coupled vs. tightly coupled GPS/INS

ECEF coordinates. GPS-derived ECEF position and velocity are combined with INS estimates of the same states to form error residuals that are sent to the navigation Kalman filter. The navigation Kalman filter corrects the INS in a feedback manner to remove the effects of biases and drifts in the IMU and system alignment errors.

One disadvantage of the loosely coupled mechanization is that cascaded filter performance can be degraded by correlations in the data. Care must be taken to ensure that the time-correlated outputs of the GPS filter do not cause stability problems in the navigation filter.

Another disadvantage of the loosely coupled architecture is that the GPS filter can experience large errors in the presence of high receiver dynamics; this may necessitate aiding from the navigation filter, which can worsen the correlation problem.

An obvious advantage of the loosely coupled approach is that it allows maximum use of off-the-shelf hardware and software that can be easily assembled into a cascaded system without major new development.

In a tightly coupled system architecture, the separate Kalman filters for receiver and navigation processing are combined into a single integrated filter. This filter accepts GPS pseudorange and delta-range measurement residuals directly. The filter error states now include INS error states (position, velocity, attitude, gyro drift, and

accelerometer bias) as well as new states representing receiver clock bias and drift. The components of the filter state vector that represent INS errors are used to calibrate the INS; i.e., to correct its estimates of ECEF position and velocity and the direction cosine matrices (DCM) describing vehicle attitude. The filter estimates of clock bias and drift are used to correct GPS measurements. An INS-derived estimate of pseudorange and delta-range is formed using satellite ephemeris data, INS position and velocity data, and estimated receiver clock errors. These predicted pseudorange and delta-range data are combined with receiver output data to form residuals that drive the navigation filter. Outputs from the Kalman filter and INS are also used to aid the satellite tracking loops in the GPS receiver.

The tightly coupled architecture more effectively utilizes available measurements and *a priori* information to determine and correct for system errors in a highly integrated fashion. It can thus yield better performance than the loosely coupled system, providing accurate navigation estimates during periods of high vehicle dynamics or jamming.

GPS, due to its accuracy and availability, can be an effective aiding source for INS systems, with the ability to rapidly remove errors in navigated position and velocity at moderate update rates. GPS measurements can also drive rather large initial alignment and inertial sensor errors to small values over sufficiently long mission time lines. The achievable accuracy depends on IMU quality, GPS/INS integration architecture, presence or absence of countermeasures, and amount of kinematic activity over the trajectory, since the observability of some error states depends on vehicle motion histories.

Two examples illustrate the application of GPS/INS to current tactical weapon systems: ERGM and SM-X.

The ERGM[15,16,17] is an ongoing development program that will provide NSFS capability to a maximum range in excess of 60 NM. The program will use GPS, combined with an INS, to navigate and guide a gun-launched 5-inch projectile to a specified target location. Integral to the concept is the use of a miniaturized GPS receiver and IMU sensors that are adequately hardened to withstand the severe shock and vibration of the gun-launch environment, yet accurate enough to achieve the required navigation performance. A conceptual illustration of the ERGM vehicle is shown in Figure 3. A more extensive discussion will be given later in this article.

The SM-X missile, shown in Figure 4, is the Navy's primary interceptor for theater-wide TBMD. The ongoing program integrates a number of key existing technologies,

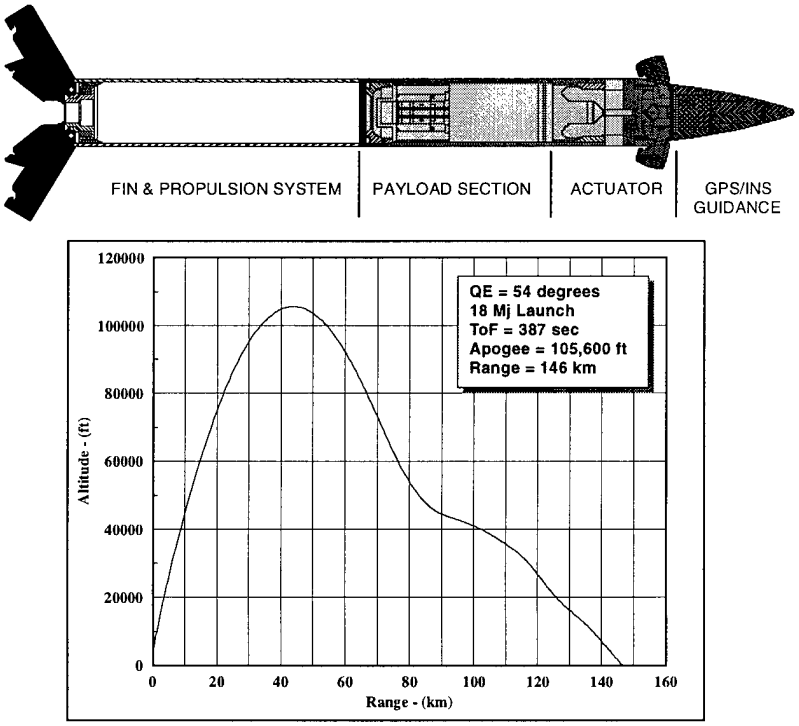

Figure 3. ERGM configuration and trajectory profile

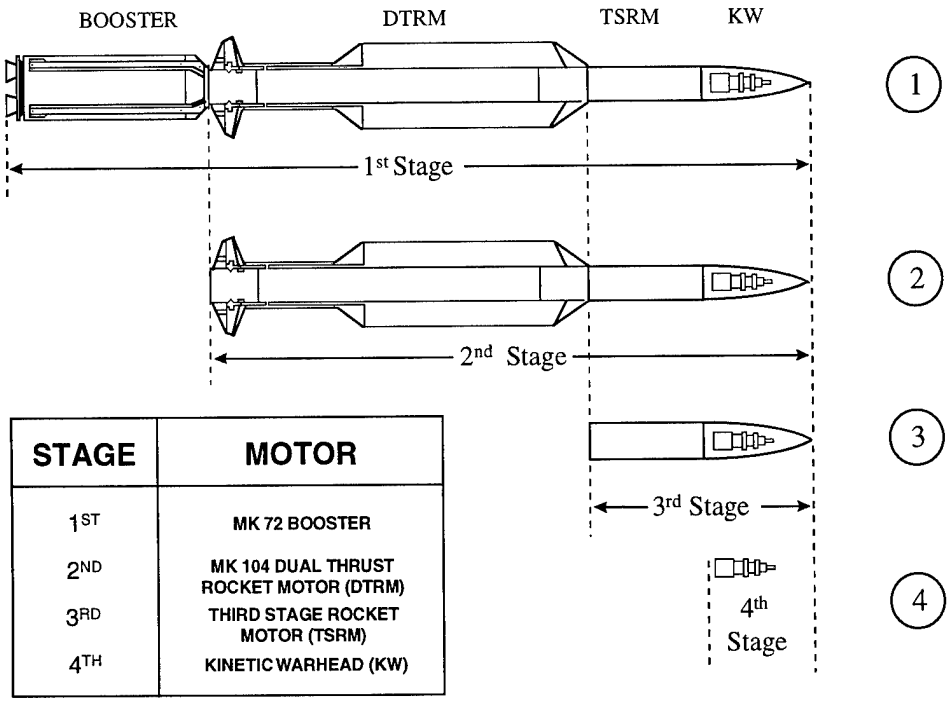

STAGE	MOTOR
1ST	MK 72 BOOSTER
2ND	MK 104 DUAL THRUST ROCKET MOTOR (DTRM)
3RD	THIRD STAGE ROCKET MOTOR (TSRM)
4TH	KINETIC WARHEAD (KW)

Figure 4. SM-X System components

including a kinetic warhead (KW), a dual-pulse rocket motor for the third stage, and the SM-2 Block IV missile. Main mission functions include:

- Boost and flyout by the SM
- Third stage separation
- Midcourse guidance using thrust vector control
- Nose cone removal
- Alignment and pointing of the KW at the target
- KW ejection and seeker acquisition
- KW divert to intercept

Essential to the successful operation of the SM-X is the use of an integrated GPS/radar/INS system on the third stage. In-flight updates are provided by both GPS and the SPY radar on AEGIS ships. The GPS and SPY complement each other and provide accurate missile state vector data to the guidance system. These data, in conjunction with radar uplinked target state data, allow an accurate intercept solution to be derived and continually updated. In addition, the mission scenarios and small KW seeker field-of-regard place demanding accuracy requirements on the third stage to deliver the KW into an acceptable acquisition basket. The GPS and SPY play a critical role by correcting the navigation system and reducing system alignment errors to values commensurate with KW seeker angle containment requirements.

Modeling of the GPS Receiver

A model of a GPS receiver with navigation software was developed to provide a tool for analyzing the performance of proposed GPS/INS configurations for guided projectiles or missiles. The receiver will track four or more GPS satellites during flight and compute an estimate of vehicle position and velocity. When an INS is available, these data can also be used to update the INS solution. The receiver model is designed so that it can (a) be incorporated into a full-scale, 6-DOF vehicle dynamics model, (b) be included in a covariance analysis model, or (c) be used in a stand-alone mode.

The receiver model selects an appropriate satellite set and calculates the pseudorange and delta-range to each satellite. These raw measurements are corrupted by various

hardware and environmental error sources and are sent to an internal Kalman filter at a nominal 1-Hz rate. This filter calculates the vehicle's position and velocity, which are sent to the external INS and navigation Kalman filter for further processing that executes the complete navigation solution.

GPS satellite system modeling includes the satellite constellation as a function of time, and characteristics of the satellite broadcast data. By knowing the position of the GPS satellites and the ranges to them, a receiver can determine its own position, velocity, and, clock bias. Several types of measurement data may be acquired, including:

- Pseudorange data
- Delta-range (or integrated Doppler) data
- Phase data
- Multiple antenna phase difference data
- Differential GPS data

To compute the position and velocity of a satellite, the receiver algorithms require ephemeris data. The current almanac or ephemeris for a satellite can be downloaded, converted, and used in the simulation.

The actual position and velocity of GPS satellites are computed using an orbital perturbation model. The orbits for each satellite are randomly modified for each component of radial, along-track, and cross-track error. For each error component, the amplitude of the error and the period of perturbation are randomly selected. GPS clock errors are estimated by the main ground station, and predicted corrections are included in the broadcast almanacs and ephemerides. Any error in this estimate is included in the model as a bias when measurement data are computed.

When the receiver is tracking a GPS satellite, it may lose lock on the signal because of such factors as:

- Blockage of the signal by the host vehicle (HV) or external objects
- Weak signal because of geometry or environment
- Signal jamming from an external transmitter
- The dynamics of flight (line-of-sight acceleration and jerk)

Acquisition of the signal is even more difficult under these conditions. The quality of the GPS track is very dependent on the make, model, and attributes of the particular receiver and the characteristics of the antenna. As a basic assumption, the following attributes are modeled: four or more satellite tracking channels, Y-code pseudorange and delta-range measurements, fast acquisition and reacquisition within dynamic limits, and a quartz oscillator.

The GPS receiver model computes tracking dynamics (range, range rate, acceleration, and jerk) between the receiver HV and each satellite vehicle (SV) being tracked (see Figure 5). Range rate, acceleration, and jerk are estimated by computing finite differences every 0.1 sec.

Whenever acceleration or jerk exceeds tolerance values, tracking lock on that satellite is lost. When tracking fails for an SV, a default reacquisition time is used to determine when data from that SV will again be available. For applications with high vehicle dynamics, the receiver will probably need aiding data from the INS to

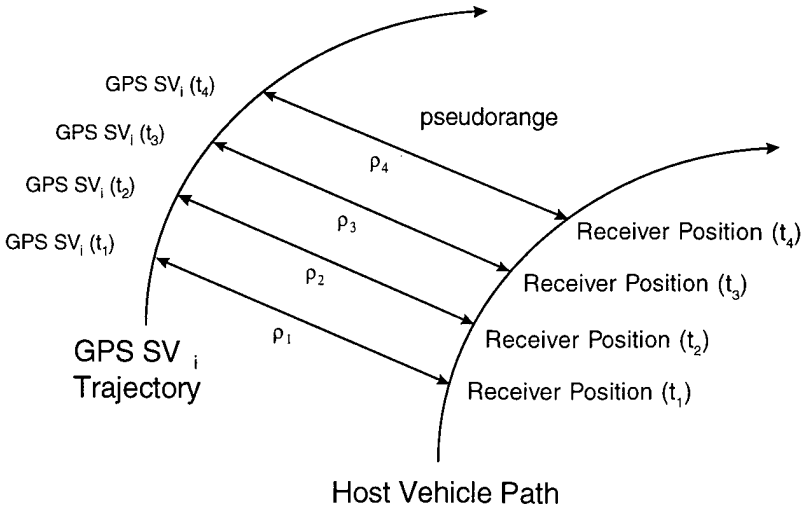

Figure 5. GPS receiver and satellite geometry

help it maintain tracking lock on the satellite signals. Navigation is very dependent on the accuracy of the receiver state propagation models and whether geometrically strong GPS data are available at each measurement update. When data from at least four satellites are used, and the dynamics are reasonable, accurate position and velocity can usually be obtained.

Several different options are available for GPS antennas. Some have fairly simple gain patterns, such as an isotropic hemisphere (possibly with cutout zones), which can track any satellite above the horizontal plane. Others use highly detailed digitized patterns. The model computes the line-of-sight vector from HV to SV and transforms to the body frame. Then the angle of incidence at the antenna is calculated to determine the antenna gain, which is used to decide if the satellite can be tracked.

In the absence of any tracking problems, the selection of which satellites to track is based on which set is geometrically the strongest (produces the most accurate solution). A satellite selection algorithm scans the constellation and determines the best geometry for the tracking scenario. To be feasible, a satellite's signal must (a) fall into the receiver's antenna pattern, (b) be unblocked and sufficiently above the earth's horizon, and (c) be of adequate signal strength. Satellites in some directions might be avoided because of possible jamming. The selection of which satellites to use is made by eliminating unfeasible candidates and using the best geometric dilution of precision (GDOP) to pick the preferred set. (GDOP is a measure of accuracy for a four-satellite solution.) For some applications, tracking the same satellites for the duration of the flight is desirable. At other times, dynamically choosing a set of four that minimizes the possibility of tracking loss during the flight might be the objective. Any application-specific constraints can easily be added to the selection criteria.

The receiver model contains an option for simulating the effects of jamming on GPS signal reception. An array of jammers defined by location, type, and effective radiating power is constructed and input to the model. The angle of incidence of each jammer signal on the GPS antenna gain pattern is calculated, and the attenuation at the receiver is determined. The model assumes the jammers will be primarily continuous wave (CW) at GPS frequencies (tone jammers). Constant GPS signal strengths at L1 (−163 dBW) and L2 (−166 dBW) are assumed. For analyzing the collective effect of the jammer array, it is assumed that the jammer signals add incoherently. The model computes the jammer-to-signal power (J/S) ratio for each transmitter/receiver pair. The J/S ratio[18] is a function of jammer radiating power, distance between the transmitter and receiver, GPS tracking frequency, and receiver antenna gain.

The effects of jamming on the GPS receiver extend from complete loss of data to reduced tracking performance and degraded navigational accuracy. In the current model, signal reception is treated in a simplified fashion: When J/S values exceed specified tolerance levels (45 dB for acquisition and 65 dB for tracking), the GPS receiver is denied the ability to acquire and/or track the satellites. Some effective ways to reduce jamming susceptibility include:

- Antenna null steering
- Antenna beam pointing
- Direct Y-code acquisition
- Using large numbers of correlators
- External aiding from the INS
- Signal processing enhancements
- Receiver countermeasures

GPS measurements are computed by adding bias and random errors to truth data for GPS satellites and HVs. Table 1 shows the components of the GPS measurement error model. The pseudorange errors include biases in the receiver and SV clocks, atmospheric propagation errors, and random noise. Errors in the delta-range are represented by a receiver clock drift error and random noise. The error model for the receiver clock assumes a quartz crystal

Table 1. GPS measurement error model

Pseudorange			ρ	=	$c\,\Delta T + b_r - b_s + d_i + d_t + \varepsilon_1$
Delta Range			δ	=	$c\,\Delta T - c\,\Delta T_{old} + b_d\,\Delta t + \varepsilon_2$
Clock Bias			T_b	=	$T_{bo} + T_{do}\,(t-t_o) + \frac{1}{2}\,T_{ao}\,(t-t_o)^2$
Δt	=	delta range measurement interval	d_t	=	tropospheric delay
ΔT	=	$t_r - t_t$ = signal time delay	b_d	=	bias due to receiver clock drift
t_r	=	time of reception	T_{bo}	=	clock bias
t_t	=	time of transmission	T_{do}	=	clock drift
c	=	speed of light	T_{ao}	=	clock aging
b_r	=	receiver clock bias error	t	=	current time
b_s	=	bias due to SV clock error	t_o	=	receiver turn-on time
d_i	=	ionospheric delay	$\varepsilon_1, \varepsilon_2$	=	random noise

oscillator, and includes bias, drift, and aging components.

Processing of raw GPS measurements to obtain HV position and velocity for navigation purposes is also performed in the receiver model. The receiver model contains an internal Kalman filter that processes GPS data to determine the best estimates of errors in the HV states. The filter model also includes states representing receiver clock bias and drift. In addition, a system state model is used to propagate HV states and clock errors dynamically in time. Outputs from the state model are used to form predictions of GPS measurements, and the difference between predicted and measured values (residuals) are sent to the Kalman filter. Error estimates from the filter are then used to correct the state estimates before they are passed to the navigation system.

The receiver's dynamic state model[19] consists of 11 states, representing 3 components each for position, velocity, and acceleration in the ECEF frame, and 2 components for receiver clock bias and drift. The gravitational model includes the J_2 term in the potential field and assumes the earth is an oblate spheroid conforming to the WGS-84 description.[20]

Unless external data are available from other sources, the model will use GPS measurement data to derive a best estimate of instantaneous vehicle acceleration. This works well except for periods of high dynamics (e.g., during thrusting or when stages are separated). When GPS data are plentiful and state dynamics are moderate, this process can yield a very accurate navigation solution with a low degree of dynamic modeling. If GPS data are sparse or if high dynamic conditions are encountered, then modeling errors will begin to show an effect. High dynamics may also cause tracking problems and a reduction in GPS observations. The preferred way to handle high dynamics is with a tightly coupled GPS/INS navigation filter. Such a system can provide improved navigation accuracy because the INS provides better dynamic modeling and aiding for the receiver, as well as stability during periods of satellite tracking loss.

The navigation filter is modeled as an 11-state extended Kalman filter simulating receivers with real-time capability. The filter uses UD matrix factorization with vectorized storage. Divergence control is implemented via residual ratios, fading memory, and data rejection; and measurements are processed sequentially. At each update, any combination of pseudorange and delta-range from any of the SVs under track may be processed. The filter, like the state model, assumes a low-order acceleration model, but has provisions for thrust flagging and utilizing feedback acceleration from the INS. Normally the filter will detect thrusting from its solution for acceleration and velocity.

However, a delay will be introduced, and the solution will be biased. If the filter receives a flag from the HV as thrusting begins, then filter process noise can be increased appropriately and the bias reduced. Unless a tightly coupled GPS/INS filter is used, periods of high thrusting will usually produce degraded navigation.

Modeling of the Navigation System

As with the receiver model, the navigation system model was developed to represent a general purpose INS architecture that could be adapted to a variety of actual flight hardware and software configurations. There are many possible forms of the inertial navigation and Kalman filter state equations that may be implemented depending on the specific application. The ECEF coordinate frame is a natural one for the receiver model because it is the frame in which GPS measurements are taken. For navigation purposes, however, a LLWA mechanization similar to that found in many commercial applications was utilized. Of course, in either case, appropriate coordinate transformations are necessary to convert data between the ECEF and LLWA frames.

The navigation system can be configured in either a loosely coupled or a tightly coupled implementation. Many current systems use the loosely coupled architecture because of the ease of assembly from off-the-shelf hardware and software. The current version of the INS model was constructed along these lines. However, it is expected that the trend for future systems will be increasingly toward the tightly coupled approach. Efforts are presently underway to extend the existing loosely coupled model to a tightly coupled version.

The navigation model was developed in two versions to support different analysis objectives:

1. The full implementation of the Monte Carlo 6-DOF model containing the receiver, INS, Kalman filter, and airframe subsystem models was intended for conducting complete system-level performance evaluations and providing flight test analysis support. This model represents the most accurate characterization of system performance. However, it can also be highly computer-intensive because of the high model fidelity, small computational intervals, and large number of Monte Carlo trials required.

2. A covariance version of the model was also developed, primarily to analyze navigation performance. In the GPS/INS Covariance Analysis Model (GCAM), statistical evaluations are done by propagating and updating covariance matrices representing the actual system (truth model) and a lower order approximate system carried on the flight vehicle. GCAM also includes simplified versions of the receiver and INS that allow the model to be exercised in a deterministic mode for comparisons with covariance results. The covariance analysis approach[8,10,12,14,21] can provide a more efficient tool for conducting specialized studies of INS performance and for determining sensitivities to parameter variations. It is intended to complement the higher fidelity, 6-DOF model where appropriate.

A description of the INS and Kalman filter formulations common to both of these models follows.

Inertial Navigation System

In the LLWA approach, the navigation frame remains tangent to the oblate earth's surface, and has zero angular velocity about the vertical axis with respect to earth, as shown in Figure 6. The missile's translational and rotational dynamics[8] may be written as shown in Table 2, and are in the form of differential equations for earth-relative velocity $\underline{v}$ and the direction cosine matrices C_b^n and C_n^e relating the body, navigation, and earth frames. In these equations, $\underline{\Omega}$ is earth rate, $\underline{\rho}$ is the vehicle transport rate, $\underline{\omega}^b$ and $\underline{a}^b$ are the IMU-measured body rates and specific forces, h is altitude, and $\underline{g}$ is gravity. $S(\underline{x})$ denotes the skew-symmetric matrix form of the vector $\underline{x}$.

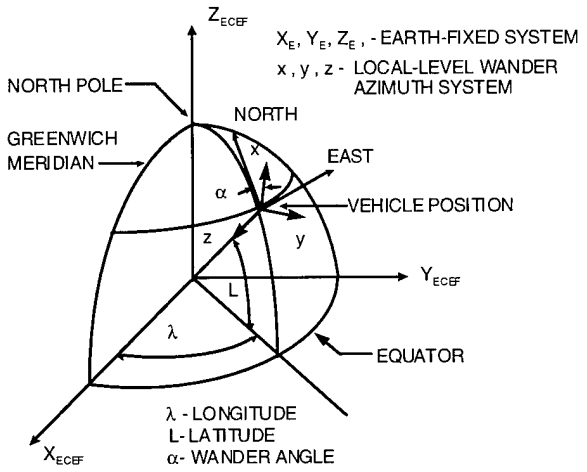

Figure 6. Local-level wander azimuth navigation frame

Inertial Measurement Unit

The strapdown inertial instrument error descriptions can be chosen to reflect a wide range of IMU types and quality. The IMU errors are treated as constants for a given mission, but may vary over an ensemble of possible instrument sets when Monte Carlo studies are conducted. To ensure a high degree of INS simulation accuracy, the IMU is typically sampled at data rates in the neighborhood of 500 to 1000 Hz. Table 3 provides the IMU error model description.

Navigation Kalman Filter

The loosely coupled navigation Kalman filter was patterned after actual flight software developed for missile demonstration and development programs,[12,22] and was derived independently prior to implementation. Navigation system error equations relating missile position, velocity, and attitude errors to inertial instrument errors were formulated assuming linear system dynamics and measurements.[8] These equations are shown in Table 4.

Normalized vehicle position errors, described by the vector $\underline{\theta}$, represent errors in the knowledge of the earth-to-navigation DCM, C_e^n. In a similar way, missile orientation errors are represented by the vector $\underline{\phi}$ that describes uncertainties in the body-to-navigation DCM, C_b^n. The growth of errors

Table 2. INS mechanization equations

$$\dot{\underline{v}} = C_b^n \underline{a}^b - (2\underline{\Omega}^n + \underline{\rho}^n) \times \underline{v}^n + \underline{g}^n$$

$$\dot{C}_b^n = C_b^n S(\underline{\omega}^b) - S(\underline{\Omega}^n + \underline{\rho}^n) C_b^n$$

$$\dot{C}_n^e = C_n^e S(\underline{\rho}^n) \qquad S(\underline{\omega}^b) = \begin{bmatrix} 0 & -\omega_z & \omega_y \\ \omega_z & 0 & -\omega_x \\ -\omega_y & \omega_x & 0 \end{bmatrix}$$

$$\dot{h} = -v_z^n$$

Table 3. IMU error model

Gyro Errors

$$\begin{pmatrix} \delta\omega_x \\ \delta\omega_y \\ \delta\omega_z \end{pmatrix} = \begin{bmatrix} S_x & M_{xy} & M_{xz} \\ M_{yx} & S_y & M_{yz} \\ M_{zx} & M_{zy} & S_z \end{bmatrix} \underline{\omega}^b + \begin{bmatrix} G_{xx} & G_{xy} & G_{xz} \\ G_{yx} & G_{yy} & G_{yz} \\ G_{zx} & G_{zy} & G_{zz} \end{bmatrix} \underline{a}^b + \begin{pmatrix} G_x^2 a_x a_z \\ G_y^2 a_y a_z \\ G_z^2 a_z a_y \end{pmatrix} + \begin{pmatrix} \varepsilon_x \\ \varepsilon_y \\ \varepsilon_z \end{pmatrix} + \begin{pmatrix} n_x \\ n_y \\ n_z \end{pmatrix}$$

S_i = scale factor errors
M_{ij} = misalignment errors
G_{ij} = g-sensitive drifts
G_i^2 = g^2-sensitive drifts
ε_i = gyro bias drifts
n_i = random walk errors

Accelerometer Errors

$$\begin{pmatrix} \delta a_x \\ \delta a_y \\ \delta a_z \end{pmatrix} = \begin{bmatrix} K_x & L_{xy} & L_{xz} \\ L_{yx} & K_y & L_{yz} \\ L_{zx} & L_{zy} & K_z \end{bmatrix} \underline{a}^b + \begin{pmatrix} \nabla_x \\ \nabla_y \\ \nabla_z \end{pmatrix}$$

K_i = scale factor errors
L_{ij} = misalignment errors
∇_i = accelerometer biases

in earth-relative velocity, $\delta\underline{v}^n$, is driven directly by the accelerometer bias $\underline{\nabla}$, and the growth of the attitude error $\underline{\phi}$ is directly influenced by the gyro drift $\underline{\varepsilon}$.

Errors in missile position are treated indirectly as errors in C_n^e, as opposed to direct perturbations in missile ECEF coordinates. This approach is better suited to the in-flight compensation scheme that is used to correct for IMU errors. The INS estimate $\hat{C}_n^e$ is related to the true DCM by

$$\hat{C}_n^{\,e} = C_n^{\,e} + \delta C_n^{\,e} \qquad \delta C_n^{\,e} = C_n^{\,e}\Theta \quad (1)$$

The small angle perturbation matrix Θ is the skew symmetric form of the position perturbation vector $\underline{\theta} = (\theta_x, \theta_y, \theta_z)^T$

$$\Theta = \begin{bmatrix} 0 & -\theta_z & \theta_y \\ \theta_z & 0 & -\theta_x \\ -\theta_y & \theta_x & 0 \end{bmatrix} \quad (2)$$

Missile attitude errors are modeled as an uncertainty in C_b^n and represented as:

$$\hat{C}_b^{\,n} = C_b^{\,n} + \delta C_b^{\,n} \qquad \delta C_b^{\,n} = -\Phi C_b^{\,n} \quad (3)$$

where Φ is the skew symmetric form of the attitude error vector $\underline{\phi}$.

The navigation filter also includes descriptions of the dominant inertial instrument errors, i.e., gyro drift and accelerometer bias. The filter attempts to estimate these states inferentially through GPS/INS residual measurement of position and velocity. Gyro drift and accelerometer bias errors are modeled as first-order Markov processes, as shown in Table 4.

In the loosely coupled GPS/INS architecture, the receiver provides estimates of vehicle position and velocity derived from its internal Kalman filter. These are then differenced with INS estimates, in ECEF coordinates, and transformed to the navigation frame using the corrected C_e^n to obtain the inputs $\underline{z}^n$ sent to the navigation filter. The position and velocity components of $\underline{z}^n$ are given by

$$\underline{z}_x^e = \underline{x}_{INS}^e - \underline{x}_{GPS}^e \qquad \underline{z}_v^e = \underline{v}_{INS}^e - \underline{v}_{GPS}^e \quad (4)$$

$$\underline{z}_x^n = C_e^n \underline{z}_x^e \quad \underline{z}_v^n = C_e^n \underline{z}_v^e \quad (5)$$

These measurements may now be related directly to filter states $\underline{\theta}$ and $\delta\underline{v}$ through the measurement equation

$$\underline{z} = \begin{pmatrix} \underline{z}_x^n \\ \underline{z}_v^n \end{pmatrix} = H\underline{x} \quad (6)$$

where the 16-element navigation filter state vector is defined as

$$\underline{x} \equiv (\underline{\theta}, \delta\underline{v}, \underline{\phi}, \delta h, \underline{\varepsilon}, \underline{\nabla})^T \quad (7)$$

and the measurement matrix H is taken as

$$H = \begin{bmatrix} H_x & 0_{3\times3} & 0_{3\times3} & \underline{u} & 0_{6\times6} \\ 0_{3\times3} & I_{3\times3} & 0_{3\times3} & 0_{3\times1} & 0_{6\times6} \end{bmatrix} \quad (8)$$

Table 4. Kalman filter error equations

$$\delta\underline{\dot{v}}^{\,n} = C_b^n \underline{\nabla}^b + \underline{a}^{\,n} \times \underline{\phi} - (2\underline{\Omega}^{\,n} + \underline{\rho}^{\,n}) \times \delta\underline{v}^{\,n} - (2\delta\Omega^{\,n} + \delta\underline{\rho}^{\,n}) \times \underline{v}^{\,n} + \delta\underline{g}^{\,n} + \underline{w}_v(t)$$

$$\dot{\underline{\theta}} = \underline{\theta} \times \underline{\rho}^{\,n} + \delta\underline{\rho}^{\,n} + \underline{w}_\theta(t)$$

$$\dot{\underline{\phi}} = -C_b^n \underline{\varepsilon} - (\underline{\Omega}^{\,n} + \underline{\rho}^{\,n}) \times \underline{\phi} + \delta\underline{\Omega}^{\,n} + \delta\underline{\rho}^{\,n} + \underline{w}_\phi(t)$$

$$\delta\dot{h} = -\delta v_z + w_z(t) \qquad \dot{\underline{\nabla}} = -\beta_\nabla \underline{\nabla} + \underline{w}_\nabla(t)$$

$$\dot{\underline{\varepsilon}} = -\beta_\varepsilon \underline{\varepsilon} + \underline{w}_\varepsilon(t) \qquad \delta\underline{\Omega}^{\,n} = -\underline{\theta} \times \underline{\Omega}^{\,n}$$

$$\delta\underline{\rho}^{\,n} = \frac{1}{R_0}(\hat{\underline{u}} \times \delta\underline{v}^{\,n}) \qquad \delta\underline{g}^{\,n} = \left[\, 0 \quad 0 \quad \frac{-2g_0}{R_0}\delta h \,\right]^T$$

with

$$H_x = \begin{bmatrix} 0 & -R_0 & 0 \\ R_0 & 0 & 0 \\ 0 & 0 & 0 \end{bmatrix} \quad \underline{u} = (0\ ,\ 0\ -\ 1\ )^T \quad (9)$$

and R_0 is equatorial earth radius.

The previous linear dynamic system equations and measurement equations form the basis for the Kalman filter, which estimates the navigation system errors. The standard equations of the Kalman filter may be found in References 13 and 14.

Filter estimates of gyro drift and accelerometer bias errors are continually fed back to the navigator in order to compensate the instruments at the instrument sample rate of 500 Hz. The compensated IMU measurements are computed from

$$\underline{a}(t) = \underline{a}_{IMU}\,(t) - \underline{\nabla}_k\,(+) \quad (10)$$

$$\underline{\omega}(t) = \underline{\omega}_{IMU}\,(t) - \underline{\varepsilon}_k\,(+) \quad (11)$$

where $\underline{\nabla}(+)$ and $\underline{\varepsilon}(+)$ represent the updated filter values, which are exponentially decayed between updates consistent with the Markov model. The gyro drift and accelerometer bias estimates are accumulated over the entire duration of filter operation.

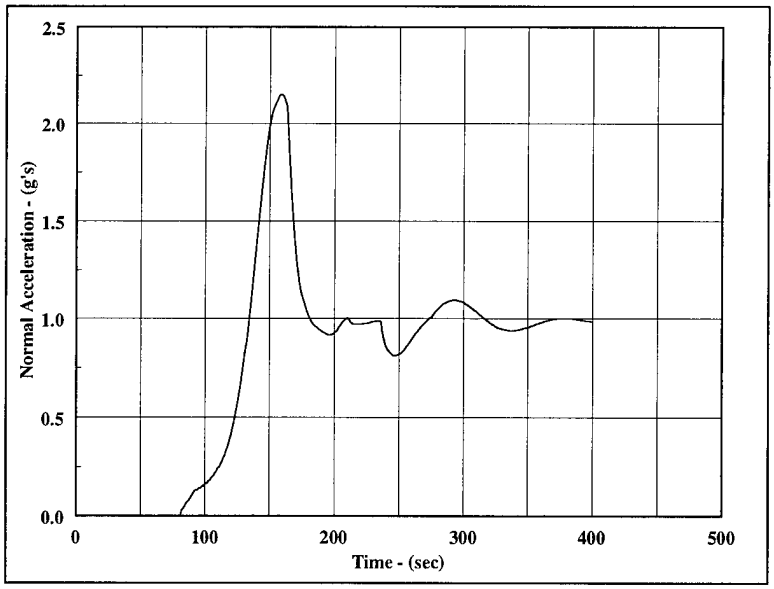

Figure 7. EX-171 normal acceleration history - maximum range trajectory

A similar process is used to update navigation state variables after each GPS measurement at a nominal 1-Hz rate. Missile position estimates are used to correct C_n^e:

$$C_n^e(+) = C_n^e(-) - C_n^e(-)\Theta(+) \quad (12)$$

Missile attitude corrections are made directly to C_b^n:

$$C_b^n(+) = C_b^n(-) + \Phi(+)C_b^n(-) \quad (13)$$

Velocity and altitude corrections are implemented as

$$\underline{v}(+) = \underline{v}(-) - \delta\underline{v}(+) \quad (14)$$

$$h(+) = h(-) - \delta h(+) \quad (15)$$

After each measurement update, corrections to the IMU and INS are performed, and the filter state variables are reset to zero.

Preliminary Analysis of ERGM System Performance

Nominal Navigation System Performance

The performance of the GPS-aided navigation system was evaluated during support of the NSFS EX-171 ERGM Program. Using the 6-DOF simulation developed for this effort, trajectory and IMU data were generated along the EX-171's maximum range trajectory shown in Figure 3. The data reflect a gun launch at White Sands Missile Range with a muzzle velocity of 2908 ft/sec, time of flight of 400 sec, and maximum range of 146 km.

Figure 7 shows the normal acceleration along the ERGM's maximum range trajectory. Of particular note is the normal acceleration behavior in response to the optimal lift/drag glide algorithm, which is activated after apogee at t = 83.7 sec. This steady

1-g specific force greatly enhances the observability of the navigation errors and the performance of the navigation Kalman filter, particularly in estimating inertial instrument errors used for IMU compensation.

Uncorrupted accelerometer and rate gyro data were recorded along the maximum range trajectory (at a frequency of 500 Hz), in addition to the vehicle's true position, velocity, and attitude. These data were then processed by the GCAM model and used for filter tuning and navigation system performance studies. The perfect IMU measurements were corrupted with IMU and navigation system errors, which are representative of flight hardware being fabricated for early demonstration flights; these errors do not represent the higher quality IMUs that may be available later in the EX-171 development program.

The navigation filter was tuned by adjusting process noise spectral densities to achieve acceptable filter performance. The values used are not necessarily optimal, but were selected on a trial and error basis until the filter error covariance behavior became consistent with the true error behavior. During these initial studies, GPS measurements were approximated by true position and velocity data corrupted by Gaussian white noise, with position and velocity root-mean-square (rms) values of 10 m and 1 m/sec, respectively.

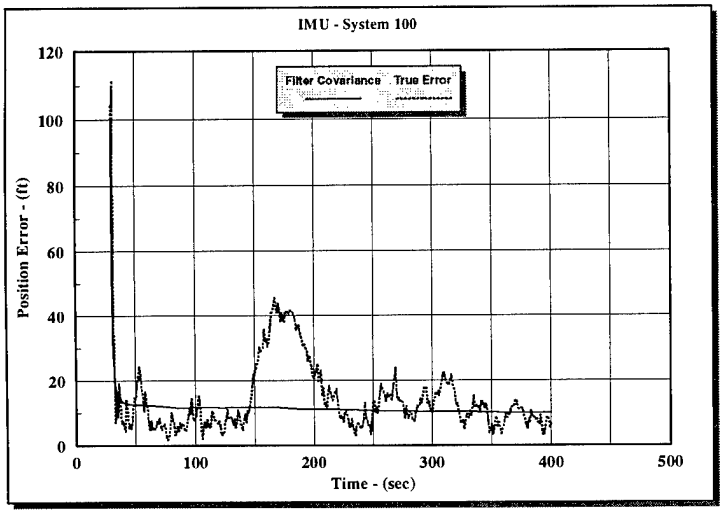

Figure 8. EX-171 navigation position error

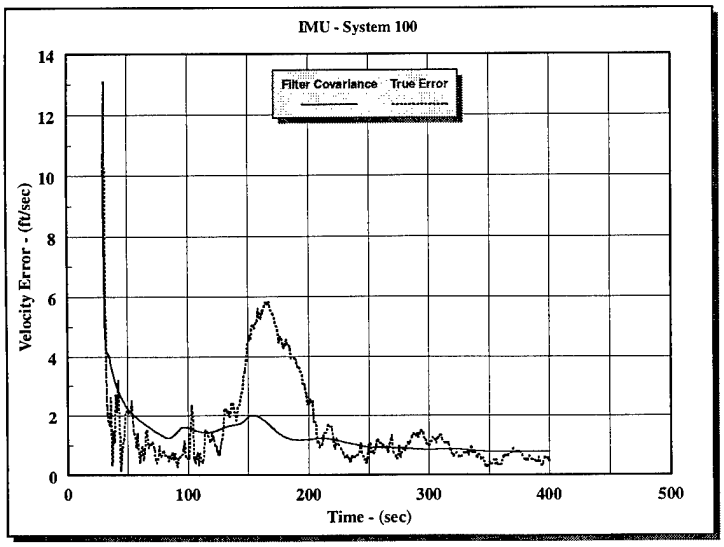

Figure 9. EX-171 navigation velocity error

Figures 8 through 11 show typical behavior of the GPS-aided navigation system over the EX-171's maximum range trajectory. In this simulation, processing of GPS measurements is delayed for approximately 30 sec after muzzle exit. This delay simulates navigation system initialization, rocket motor burn, and GPS satellite acquisition. Position and velocity errors decay rapidly from fairly large initial values because of the GPS aiding. However, missile attitude and IMU inferential states are much more difficult to estimate until the glide algorithm is activated shortly after apogee. At this point, missile attitude and IMU errors become more observable under the influence of normal acceleration, as shown in Figures 10 and 11. A reasonable period of time is required to compensate IMU errors to acceptable levels. Over shorter range flights, this may imply that attitude and IMU errors will not be fully removed before impact.

The results of Figures 8 through 11 show good nominal performance, with position and velocity errors

driven down to about 10 ft and 1 ft/sec 1-σ after about 200 sec of flight. The vehicle's attitude errors are reduced to the level of about 3 mrad 1-σ over the same period. The filter correctly identifies the gyro drift and accelerometer bias and corrects the IMU with small residual errors on the order of 2 deg/hr and 3 mg, by the end of the flight.

The exact requirements for uncompensated IMU and INS errors have yet to be determined for the EX-171 development program. These requirements are driven by cost and performance tradeoffs between inertial instrument precision, quality of GPS estimates, and the potential vulnerability of the tactical system to countermeasures. The GCAM model was developed precisely for this purpose and will be used to conduct system-level studies addressing system requirements and tactical employment issues.

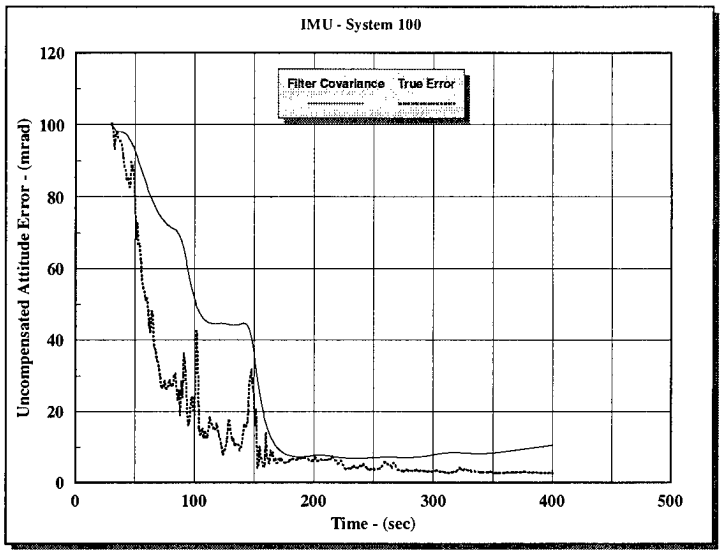

Figure 10. EX-171 navigation attitude error

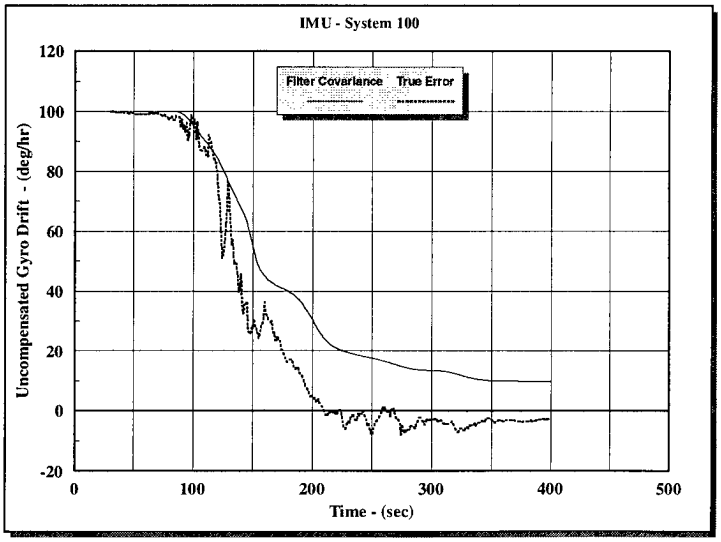

Figure 11. EX-171 navigation gyro drift

Effect of Jamming on Navigation Accuracy

Employment strategies for GPS-aided weapons systems must address the potential vulnerability of the navigation system to various forms of jamming. Preliminary studies have been conducted to evaluate navigational accuracy in the event that GPS measurements are lost during flight as a result of countermeasures. The initial studies were performed in a parametric fashion with respect to GPS "break-lock" range, without attempting to associate these ranges with a specific J/S ratio, jammer power, or geometry. Later studies calculated the break-lock ranges resulting from particular jamming scenarios and power levels. These assumed several candidate GPS antenna patterns and were evaluated for specific ERGM trajectories. Several navigation systems of varying degrees of precision were analyzed, representing possible instrument accuracies that ranged from present day demonstration system hardware to very precise inertial instruments that might be available in the future.

Jamming sensitivity studies were conducted by first generating vehicle truth data using a 6-DOF trajectory simulation. These data were then processed by the GCAM model, which contains the INS and the GPS/INS navigation filter. The navigation filter uses GPS measurements to estimate and

Table 5. Initial INS errors

Navigation System Error	IMU System					
	100	70	50	20	10	1
Position Error (ft)	100	100	100	100	100	100
Velocity Error (ft/ sec)	10	10	10	10	10	10
Attitude Error (mrad)	100	70	50	20	10	1
Gyro Drift (deg/ hr)	100	70	50	20	10	1
Gyro Scale Factor (ppm)	1000	700	500	200	100	10
Accelerometer Bias (mg)	100	70	50	20	10	1
Accelerometer Scale Factor(ppm)	1000	700	500	200	100	10
GPS Position Error (m)	10	10	10	10	10	10
GPS Velocity Error (m/ sec)	1	1	1	1	1	1

Table 6. Navigation system position errors at impact

Inertial Measurement Unit Precision	Position Error at Impact (ft)					
Range-to-go at Break-Lock (km)	0	3	6	9	12	15
IMU System 100	4.2	8.6	14.4	37.0	76.8	150.5
IMU System 70	4.2	8.1	12.9	36.0	61.5	123.6
IMU System 50	4.2	7.8	12.1	33.7	55.8	111.9
IMU System 20	3.8	6.8	10.5	26.4	47.3	76.8
IMU System 10	3.7	6.2	9.9	25.8	39.9	68.7
IMU System 1	3.2	4.5	7.0	19.4	34.5	48.6

remove INS errors, and for in-flight calibration of the inertial instruments. The study assumed a number of INS systems of varying quality, which are shown in Table 5. The nomenclature "SYSTEM X" is used, where "X" denotes the level of instrument accuracy as well as the size of initialization errors. For example, "SYSTEM 100" denotes an IMU having off-the-shelf errors of 100 mg for accelerometer bias and 100 deg/hr for gyro drift, initialized with 100 mrad of attitude error. Navigator initial position and velocity errors were chosen for convenience in displaying results. Nominal errors at impact are shown in Table 6 and assume uninterrupted GPS measurements at 1-sec intervals throughout the flight.

The accuracy of each notional IMU system was evaluated under the assumption that GPS measurements were lost at break-lock ranges between 0 and 15 km from the nominal impact point. These correspond to times-to-go between 0 and 84 sec, respectively, along the ERGM's maximum range trajectory. At the break-lock range, GPS measurements ceased, and the INS and navigation filter were no longer updated. Residual navigation and inertial instrument errors existing at this point were propagated for the remainder of the trajectory. A tabulation of navigation system performance for each break-lock range and IMU system is shown in Table 6.

Figure 12 shows the navigation system position error at impact as a function of break-lock range for the various IMU systems investigated. These results are very encouraging in that they show the potential for reasonable navigation system accuracy when GPS information is denied for a significant portion of the trajectory. The results also indicate that the relationship between IMU precision and navigation accuracy under these conditions is not linear.

To assess the effects of jammer geometry and power levels on the ranges at which break-lock occurs, additional studies were performed in which the receiver processed data along the ERGM's maximum range trajectory. The J/S ratio was computed along the trajectory, and threshold levels were assigned to determine when loss-of-track or

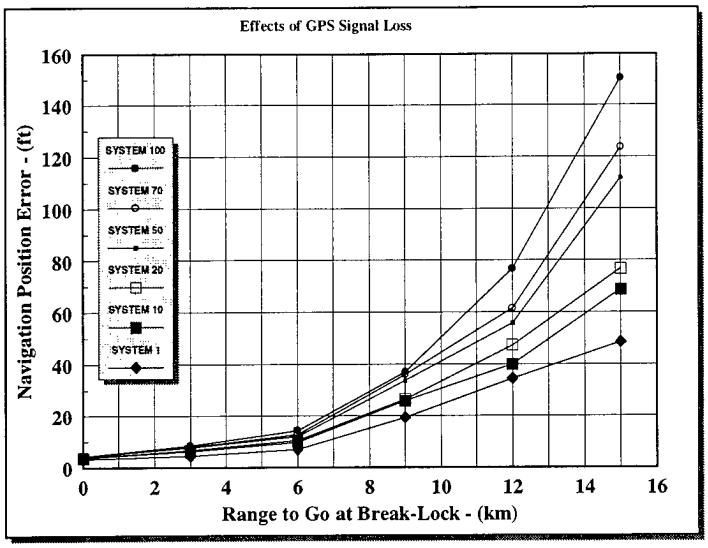

Figure 12. Effect of GPS signal loss on navigation accuracy at impact

denial-of-acquisition occurred. For this study, 45 dB was taken as the threshold for GPS acquisition, and 65 dB as the threshold for firm track.

The assumed receiver antenna patterns were found to have a strong effect on the results. Two types of antenna patterns were considered. The first was a spherical, isotropic pattern having a gain of one in all directions. The second pattern assumed that either through vehicle roll control or dynamic antenna gain control, the resulting pattern can be tailored to provide coverage mainly in the upper hemisphere. To accommodate variations in the trajectory, a small 8-deg cutout zone on the upper side of the vehicle was also enforced. The resulting pattern appears as a cone of 82 deg half-angle about the body vertical axis, as shown in Figure 13. This antenna has a gain of one within the upper cone-shaped pattern for good satellite reception, with a −30 dB gain outside the cone to reject jamming signals.

The J/S ratios were computed for the spherical antenna as a function of range-to-go to the target. For this initial study, the total radiated jammer power was placed at the target or vehicle aim point. Jammer power levels between 1 W and 50 kW were considered. The results indicated that the all-directional antenna offered minimal jamming resistance.

For a jammer power of 100 W or more, the receiver would not be able to acquire at any time, using the 45 dB threshold. If the GPS signal was being tracked when a 100-W jammer turned on, loss-of-lock would occur at about 15 km from the target, with the 65 dB threshold. Based on these results, it is obvious that an all-directional antenna is inappropriate in scenarios where jamming is present.

When the modified antenna pattern is used, the results change dramatically. Figure 14 shows the J/S ratios vs. range-to-go for this case. For a jammer power of 1000 W, acquisition is possible to within 15 km of the target, and the GPS signal can be tracked up until 1.4 km from the target. For a very large 10-kW jammer, acquisition

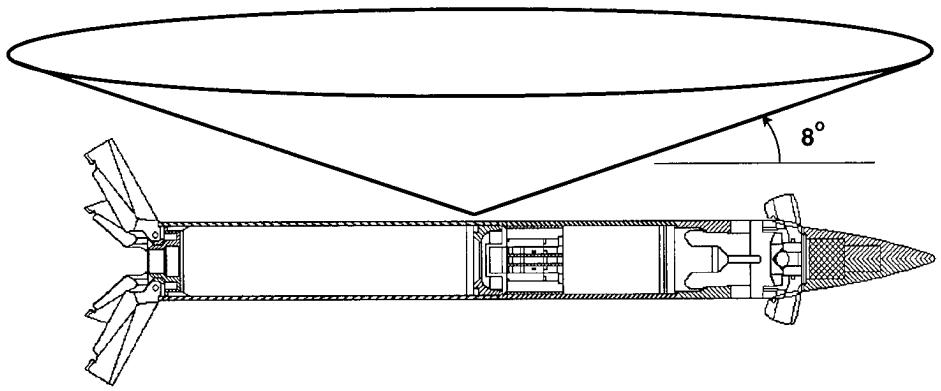

Figure 13. Hemispherical antenna gain pattern with 8-deg cutout

can be accomplished prior to approximately 50 km range-to-go, and break-lock will occur at a range-to-go of 4.7 km—a substantial capability in the presence of a very severe jamming environment.

The break-lock ranges for the two antenna types are plotted in Figure 15. From these results, it is clear that selective tailoring of the antenna design can result in greatly improved performance in a jamming scenario. Based on one feasible antenna pattern modification, the fairly small break-lock ranges that were achieved, even at large jammer power levels, is highly encouraging.

These results are preliminary in nature and will no doubt be refined as the EX-171 system becomes better defined. However, they do indicate the potential accuracies achievable under the modest assumptions of this study. It is quite possible that the performance observed may be further improved through the use of additional trajectory shaping, tailoring of the antenna pattern, improvements in receiver signal processing, and improvements in navigation filter design, even when additional system error sources are considered.

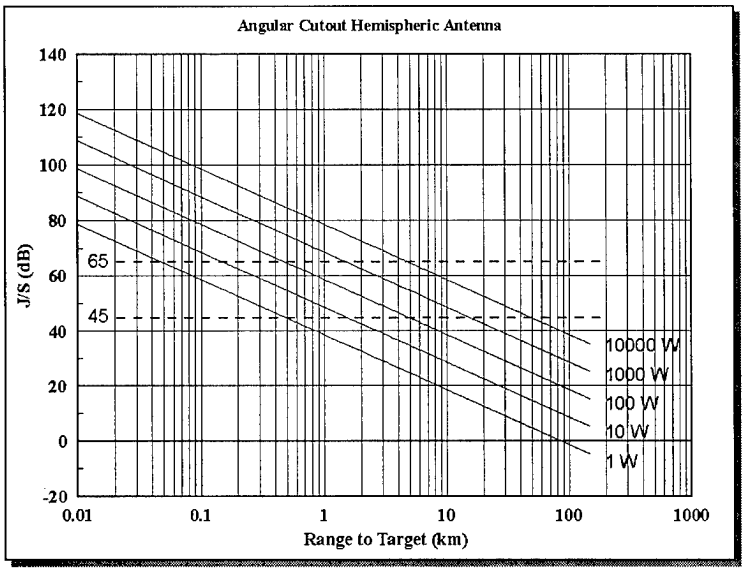

Figure 14. J/S ratio vs. range-to-go

Summary and Future Directions

The combined use of GPS and inertial navigation is an emerging trend that will continue to be incorporated into a variety of new system applications. This stems from simultaneous advances in both the GPS and INS arenas. The high accuracy and easy availability of GPS, combined with new, high-performance receiver technology, makes it an attractive option for the updating of navigation systems. In the area of inertial navigation technology, a revolution is occurring that will result in miniaturized, micro-machined instruments[23-25] that are extremely small, reasonably accurate, and very inexpensive. The synergism between GPS and INS is creating a new technology, out of which will emerge many new system applications of GPS-aided inertial navigation and guidance—making very high terminal accuracies possible.

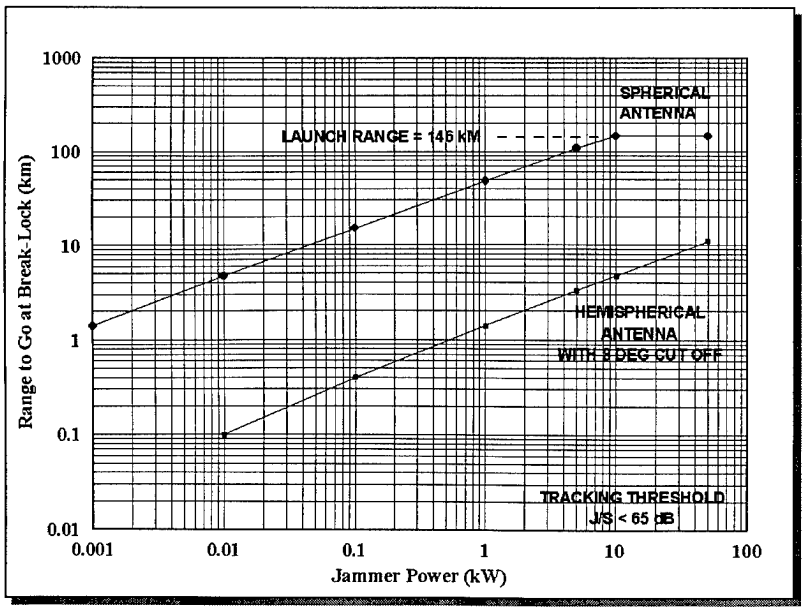

Figure 15. GPS break-lock range vs. jammer power

New military applications continue to be developed. GPS-guided bombs led to extended-range guided projectile and rocket applications. Applications of GPS to the Navy Land Attack STANDARD Missile (LASM) and the Army Tactical Missile System (TACMS) will produce surface-to-surface weapons with greatly improved accuracy. GPS-aided weapons that can maintain bounded levels of delivery errors as the range increases open the door to the development of more energetic propulsion systems that further extend operational range. These long-range, GPS-guided weapons create a need for more precise target location. This, in turn, has led to GPS/INS developments for unmanned air vehicles (UAV) for reconnaissance and precision targeting, and the growing use of relative or differential GPS positioning techniques[26] for accurately directing weapons to designated impact points.

The emergence of KW technology, combined with development of advanced versions of the Navy STANDARD Missile, has produced TBMD interceptor systems such as SM-X, which utilizes GPS and ship-based radar to aid navigation and guidance. Effective use of weapons with narrow sensor acquisition windows necessitates that attitude errors be kept to a minimum. New uses for GPS allow a direct determination of vehicle attitude by processing data from a dual antenna GPS receiver, together with an INS, using a Kalman filter for data fusion.[27] Many other examples exist that address mission requirements from a system perspective involving the appropriate blending of GPS/INS technology and operational strategies.

GPS can also be a very effective resource in support of test and evaluation. When used on interceptor and target vehicles, it can provide a highly accurate means of measuring body-to-body miss distance during flight tests. Precise kinematic on-the-fly GPS relative positioning has demonstrated subdecimeter accuracy for baselines of up to 30 km.[28] This relative positioning capability, combined with INS attitude information, can accurately reproduce the impact point along an extended body and the attitude geometry associated with the collision (or near miss) of two vehicles. This also allows a precise visual depiction, or animation, of a test vehicle's flight motion history. This capability has important ramifications for test and evaluation of hit-to-kill systems that utilize aim point selection to optimize lethality. GPS appears to offer a revolutionary new approach to the analysis and reduction of dynamic flight test data that is less expensive and more accurate than competing methods.

The spread of military applications for GPS/INS technology has led to concerns regarding potential vulnerability of GPS, especially to jamming. Well-designed GPS/INS systems can mitigate the effects of jamming using a variety of possible techniques. Some of these include:

- Directional and steered antennas
- Direct acquisition of the Y-code
- Tightly coupled aiding from the INS
- Improved GPS receivers that
  - employ large numbers of correlators
  - contain signal processing enhancements
  - implement electronic countermeasures

System-level simulations of the type described in this paper can play an important role in evaluating GPS jamming susceptibility. The effects of satellite selection, antenna gain patterns, and vehicle attitude dynamics on J/S ratios, receiver acquisition, and tracking capabilities can be assessed with GPS/INS simulations of this type. In addition, new or proposed countermeasures such as receivers with improved antijam margin and Y-code acquisition as a function of vehicle dynamics, clock accuracy, and jamming environment can be evaluated.

Many of the military GPS/INS applications to date have utilized receivers that internally process raw GPS measurements and produce position and velocity. When these are combined with an INS and a Kalman filter to derive navigation solution updating, the implementation is termed a

loosely coupled system. This has been a popular system configuration because many existing receivers and navigation systems are difficult to integrate with raw GPS pseudo-range and phase measurements. An additional problem is that the raw GPS measurements are treated as classified after they have been corrected for selective availability.

However, the predominant trend for future systems is clearly moving in the direction of tight coupling for the GPS/INS. There are significant advantages to having a tightly coupled integration in which raw GPS measurements are directly used to update the Kalman filter. Some of the benefits are:

- More direct exploitation of fundamental measurement data
- More direct aiding of the receiver tracking process by the filter and INS
- Higher likelihood of maintaining firm satellite tracks
- Better resiliency to poor satellite geometry, high vehicle dynamics, data dropouts, IMU errors, and jamming

A system-level simulation can be a valuable tool for assessing alternative system architectures for a tightly coupled GPS/INS and for quantifying the performance benefits obtained.

In addition to the military market, commercial maritime and aviation industries have benefited from GPS/INS technology. This technology is being utilized to an increasing extent in future ship, aircraft, and landing systems. Emergency and transport vehicles are beginning to rely more heavily on GPS, and it appears that GPS will become more routinely available in future automobile and "intelligent" highway transportation systems. Because of the heavy commercial and civilian utilization of GPS, and demands for better positioning accuracy from users all over the world, the U.S. government has decided to phase out the DoD-controlled selective availability over a 10-year period. Elimination of selective availability will force the DoD to develop and implement new technologies for achieving high GPS positioning accuracies (for U.S. military applications during times of conflict), while denying potential adversaries that capability.

References

1. Hurn, J., "GPS, A Guide to the Next Utility," Trimble Navigation, Sunnyvale, CA, 1989.
2. Wells, D., *Guide to GPS Positioning*, Canadian GPS Associates, Fredericton, New Brunswick, Canada, 1987
3. Hoffman-Wellenhof, B.; Lichtenegger, H.; and Collins, J., *GPS Theory and Practice*, Third Revised Edition, Springer-Verlag, New York, NY, 1994.
4. Parkinson, B.W.; Spilker, J.J.; Axelrad, P.; and Enge, P., *Global Positioning System: Theory and Applications*, Vols. I and II, American Institute of Aeronautics and Astronautics, Washington, DC, 1995.
5. Naval Surface Warfare Center, *Proceedings of the GPS "True Facts" Symposium*, Dahlgren, VA, Aug 1995.
6. GPS Joint Program Office, *NAVSTAR GPS User Equipment-Introduction*, USAF Space Systems Division, Los Angeles AFB, CA, 1991.
7. Bibel, J.E., *A Brief Overview of the Integration of GPS and INS for Guided Missile Navigation*, Naval Surface Warfare Center White Paper, Dahlgren, VA, Apr 1994.
8. Savage, P.G., "Strapdown Inertial Navigation Lecture Notes," by Strapdown Associates, Inc., Plymouth, MN, Sep 1991.
9. Britting, K.R., *Inertial Navigation System Analysis*, Wiley-Interscience, New York, NY, 1971.
10. Sutherland, Jr., A.A., and Gelb, A., *Application of the Kalman Filter to Aided Inertial Systems*, NWC TP 4652 by The Analytic Sciences Corporation for Naval Weapons Center, China Lake, CA, Aug 1968.
11. Bose, S.C., "Radar Updated Strapdown Inertial Midcourse Guidance Performance Analysis for Missiles," *Proceedings of AIAA Guidance and Control Conference*, Boulder, CO, Aug 1979, pp. 218-229.
12. Ohlmeyer, E.J. and Packard, M.E., *Error Modeling of the Tomahawk Ground-Launched Cruise Missile (GLCM) Inertial Navigation System*, Naval Surface Weapons Center TR 84-301, Dahlgren, VA, Jun 1985.
13. Brown, R.G. and Hwang, P.Y.C., *Introduction to Random Signals and Applied Kalman Filtering*, 2nd Ed., John Wiley, New York, NY, 1992.
14. Gelb, A., Ed., *Applied Optimal Estimation*, M.I.T. Press, Cambridge, MA, 1974.

15. Evans, A.G. and Hermann, B.R., "Feasibility of Using a GPS Receiver to Navigate a Naval Gun-Launched Projectile to a Target," *Proceedings of ION National Technical Meeting*, San Diego, CA, Jan 1992.
16. Hagan, J.D., "Future Gun Weapon System Technology," *Technical Digest*, Dahlgren Division, Naval Surface Warfare Center, Dahlgren, VA, 1996.
17. Ohlmeyer, E.J.; Pepitone, T.R.; Miller, B.L.; Malyevac, D.S.; Bibel, J.E.; and Evans, A.G., *System Modeling and Analysis of GPS/INS for Extended Range Guided Munitions*, TR-96/159, Dahlgren Division, Naval Surface Warfare Center, Dahlgren, VA, Aug 1996.
18. Griffiths, J., *Radio Wave Propagation and Antennas: An Introduction*, Chapter 1, Prentice-Hall, Englewood Cliffs, NJ, 1987.
19. Regan, F.J., *Strapdown Systems, Part II, Algorithms*, Naval Surface Weapons Center TN 81-409, Silver Spring, MD, Nov 1981.
20. Defense Mapping Agency, *Department of Defense World Geodetic System 1984*, DMA TR 8350.2, Washington, DC, Sep 1987.
21. Ohlmeyer, E.J., *INS Covariance Model With Gyro Drift Rate Compensation*, Naval Surface Warfare Center White Paper, Dahlgren, VA, Sep 1993.
22. Moore, T.; Rudolph, K.; Ziolkowski, F; and Luckau, A., "Use of the GPS Aided Inertial Navigation System in the Navy Standard Missile for the BMDO/Navy LEAP Technology Demonstration Program," *Proceedings of ION GPS-95*, Palm Springs, CA, Sep 1995.
23. Gustafson, D.; Hopkins, R.; Barbour, N.; and Dowdle, J., "A Micromechanical INS/GPS System for Guided Projectiles," CSDL-P-3444, *Proceedings of the ION 51st Annual Meeting*, Colorado Springs, CO, Jun 1995.
24. Bryzek, J.; Petersen, K.; and McCulley, W., "Micromachines on the March," *IEEE Spectrum*, May 1994, pp. 20-31.
25. Barbour, N.; Connelly, J.; Gilmore, J.; Geiff, P.; Kourepenis, A.; and Weinberg, M., "Micromechanical Silicon Instruments and Systems Development at Draper Laboratory," AIAA Guidance, Navigation, and Control Conference, San Diego, CA, Jul 1996.
26. Schmidt, G. and Setterlund, R., *Precision Strike Concepts Exploiting Relative GPS Techniques*, Charles Stark Draper Laboratory, Cambridge, MA, 1995.
27. Miller, B.L.; Phillips, C.A.; Evans, A.G.; and Bibel, J.E., "A Kalman Filter Implementation for a Dual-Antenna GPS Receiver and an Inertial Navigation System," *Proceedings of ION GPS-93*, Sep 1993.
28. Hermann, B.R.; Evans, A.G.; Law, C.S.; and Remondi, B.W., "Kinematic On-the-Fly GPS Positioning Relative to a Moving Reference," *Proceedings of ION GPS-94*, Sep 1994.

The Authors

Ernest J. Ohlmeyer

ERNEST J. OHLMEYER joined the Division in 1968 after receiving a B.S. degree in physics from Loyola University. His early career focused on the free-flight dynamics of projectiles and design and development of the Navy 5-inch and 8-inch Guided Projectiles. In 1982, he obtained an M.S. degree in engineering from the Naval Postgraduate School as part of the Full-Time Advanced Study Program. His subsequent activities have emphasized analysis and performance evaluation of tactical missile systems including Tomahawk, Wide Area Defense missile, Standard Missile, Surface Launched Weapon Technology, Advanced Self Defense Missile, and Tactical Ballistic Missile Defense programs. Mr. Ohlmeyer has twice been a Principal Investigator in the NSWCDD Independent Research Program. Since 1985, he has been Group Leader for flight dynamics, guidance, and control in the Aeromechanics Branch. His current interests include: robust and nonlinear control, system design optimization, guidance algorithms for missiles, and applications of GPS/INS. Mr. Ohlmeyer is a member of AIAA, IEEE, and Sigma Xi.

THOMAS R. PEPITONE received the B.S. degree in aerospace engineering from the Georgia Institute of Technology in 1965 and the M.S. and Ph.D. degrees in aerospace engineering from the University of Virginia in 1968 and 1977, respectively. From 1968 through 1986, he was employed by the Naval Surface Warfare Center and participated in several research and development programs ranging from guided munitions to strategic missile systems. After working in private industry for several years, in 1990 he founded Aerospace Technology, Inc., an engineering consulting firm that specializes in the areas of missile dynamics, guidance, navigation, and control. Dr. Pepitone is a member of the IEEE and a senior member of the AIAA.

Thomas R. Pepitone

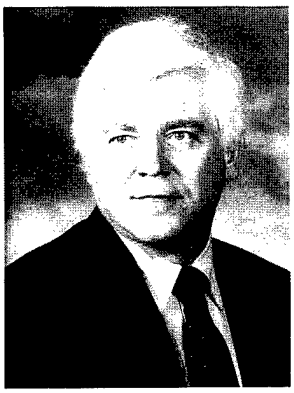

B. LARRY MILLER received a B.A. degree from Western Kentucky University in 1967 and an M.A. degree in mathematics from the University of Louisville in 1971. He was a staff meteorologist at Vandenberg AFB until 1972, and has since been employed at NSWCDD in the Space Sciences Branch. Since 1974, he has worked on numerous aspects of the GPS, including satellite constellation design, concept evaluation of ground and space applications, and development of the first spaceborne GPS navigational unit.

B. Larry Miller

D. STEPHEN MALYEVAC received a B.S. and M.S. degrees in mechanical engineering from Virginia Polytechnic Institute and State University in July 1986 and May 1988, respectively. He joined the Division in 1988 and works in the Aeromechanics Branch in the areas of guidance, control, simulation, and performance analysis for tactical missiles. He is a member of the American Institute of Aeronautics and Astronautics.

D. Stephen Malyevac

JOHN E. BIBEL received a B.S. degree in aerospace engineering from the Pennsylvania State University in May 1984. Since then, he has been employed at NSWCDD, where he has been involved with simulation; performance analysis; and guidance, navigation, control and estimation technologies for tactical missile systems. Mr. Bibel is currently completing requirements toward an M.S. degree in aerospace engineering from Virginia Polytechnic Institute and State University and is a member of the American Institute of Aeronautics and Astronautics. Over the past couple of years, Mr. Bibel was the lead aeromechanics engineer for the NATACMS demonstration, was co-chair of the marinized-ERINT missile concept definition team for the Navy TBMD COEA, and has supported the AEGIS, ESSM, and SLWT programs.

John E. Bibel

ALAN G. EVANS has been working in Global Positioning System (GPS) applications at NSWCDD since 1981. He received a B.S.E.E. degree from Widener University in 1964 and M.S. and Ph.D. degrees in electrical engineering from Drexel University in 1967 and 1972, respectively. In the area of GPS, Dr. Evans has contributed to static and dynamic relative positioning and orientation, signal multipath analysis, the determination of geodetic quantities, and receiver development.

Alan G. Evans

The Automation of Finding the Intersection, Union, or Set Difference of Two Planar Polygons

Armido R. DiDonato

EW
EXPEDITIONARY
WARFARE

This article describes the general features of an algorithm for automating, by computer, the determination of the intersection, union, or set difference of two polygons in a plane. The algorithm, with the details given for the intersection case, has many applications in computer graphics: finding locations of defended areas, establishing launch zones for strikes against multiple targets, designing computer-aided design/computer-aided modeling (CAD/CAM) systems, and analyzing geographical data. Few algorithms have been published; their implementation into code is lacking or unavailable. The present algorithm allows simple polygons, extensions to those which have polygonal holes, coincident vertices, and overlapping edges. Self-intersecting polygons are not admissible. Some examples are given. The program is robust, efficient, and available in 32-bit DOS-EXTENDED executable code.

Introduction

Given two polygons A and B in the xy–plane, and specifying a point by (x, y), the intersection, union, and set difference of A and B follow the definitions of set theory,[1] namely

$$A \cap B = \{(x,y) : (x,y) \in A \text{ and } (x,y) \in B\}$$
$$A \cup B = \{(x,y) : (x,y) \in A \text{ or } (x,y) \in B\}$$
$$A - B = \text{closure}\,\{(x,y) : (x,y) \in A \text{ and } (x,y) \notin B\}$$

This article describes a solution to these computational geometry problems by an algorithm that is implemented into a Fortran 77 computer program. Details are given for $A \cap B$.

Determination of the intersection, union, and set difference of A and B has important computer graphic applications: Two of considerable importance to the Navy are establishing the locations of defended areas and determining the launch zones against multiple targets. Other applications include the design of CAD/CAM systems and the analysis of geographical data. References 2 and 3 contain applications dealing with defended areas and launch zones. References 4 through 7 are basic papers. Reference 6 provides some of the definitions we use, as well as additional references.

A closed polygon P in the xy–plane is specified by its vertices; i.e., $N + 1$ points: $\mathbf{p}_1, \mathbf{p}_2, \ldots \mathbf{p}_{N+1}$, with $\mathbf{p}_i \neq \mathbf{p}_{i+1}$, $1 \leq i \leq N$, $N \geq 2$, and $\mathbf{p}_1 = \mathbf{p}_{N+1}$. The notation $\mathbf{p}_i$ is used to denote the point with coordinates (x_i, y_i), and it is also

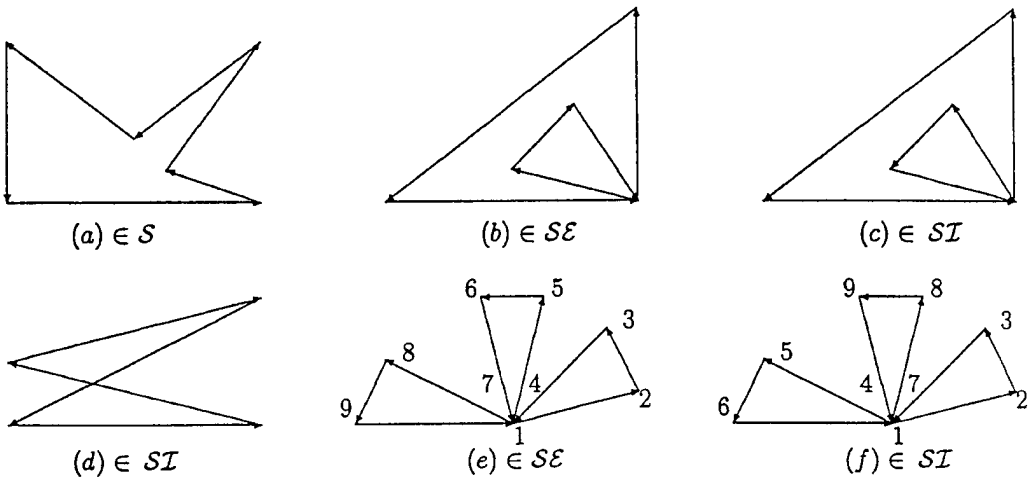

Figure 1. Examples of polygons in $\mathcal{S}$, $\mathcal{SE}$, and $\mathcal{SI}$

used as a vector emanating from the origin with its endpoint at (x_i, y_i). The closed boundary of P, ∂P, is composed of a sequence of N ordered, directed straight line segments called *edges*. Letting $\overline{\mathbf{p}}_i$ denote the i^{th} edge, it is easy to show for any point $\mathbf{q}$ on $\overline{\mathbf{p}}_i$ that

$$\mathbf{q} = (1 - t)\,\mathbf{p}_i + t\,\mathbf{p}_{i+1}, \quad 0 \le t \le 1 \qquad (1)$$

Our algorithm will apply to the class $\mathcal{S}$ of positively-oriented simple polygons and to an extension of this class called $\mathcal{SE}$. A *simple* polygon P has at least three distinct vertices, and a nonzero area, and no pair of edges share a point unless they are consecutive, in which case they have exactly one point in common where the end of one edge joins the beginning of the other. We say P is *positively-oriented* (PO) [*negatively-oriented* (NO)], if its interior is on the left [right] as ∂P is traversed in the direction of increasing order of the vertex indices (Figure 1(a)). One can determine the orientation of P by its *signed-area*, AR(P), which is positive if P is PO and negative if P is NO; where, with $\mathbf{p}_i = (x_i, y_i)$,

$$AR(P) = \frac{1}{2}\sum_{i=1}^{N} x_i(y_{i+1} - y_{i-1}), \quad y_o \equiv y_N \qquad (2)$$

A *self-intersecting* polygon is said to be in the class $\mathcal{SI}$. Such polygons are not admissible for our algorithm. They have the property that either two or more nonconsecutive edges cross (Figure 1(d)); and/or they have the more subtle property that three or more edges meet at a point c such that crossings occur when some of these edges are slightly offset from c in a sufficiently small neighborhood of c, N(c). In the first case, two edges, $\overline{\mathbf{p}}_i$ and $\overline{\mathbf{p}}_j$, are said to *cross* if there exist t and s in (0, 1) such that

$$(1 - t)\,\mathbf{p}_i + t\,\mathbf{p}_{i+1} = (1 - s)\,\mathbf{p}_j + s\,\mathbf{p}_{j+1} \qquad (3)$$

In the latter case, $P \in \mathcal{SI}$ if there exists a vertex c such that ∂P cannot be traversed without some path in and out of c crossing ∂P (Figures 1(c) and 1(f)).

To illustrate the self-intersecting property for Figure 1(f), consider Figure 2, which shows N(c) with c located at the point where vertices 1, 4, and 7 meet. The endpoint of $\overline{\mathbf{p}}_6$ cannot join $\mathbf{p}_7$ without crossing the connected

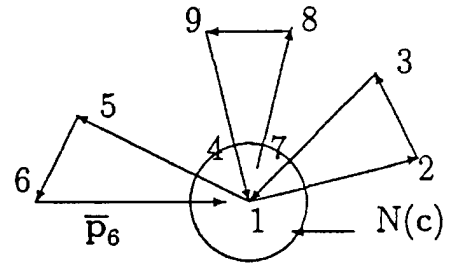

Figure 2. Shows the self-intersecting property for Figure 1(f)

line made up of $\bar{p}_3$ and $\bar{p}_4$. Thus, the polygon of Figure 1(f) is in $\mathcal{SI}$. Sometimes renumbering the vertices without changing the geometrical properties of P takes P from $\mathcal{SI}$ to $\mathcal{SE}$. Compare Figure 1(e) with 1(f).

A polygon P is said to be in $\mathcal{SE}$ if it is not *self-intersecting*. Polygons in $\mathcal{SE}$ may have *polygonal holes*, vertices meeting at a point with *degree* > 1, and overlapping edges. A *polygonal hole* is made up of a subset of consecutive vertices of P that form a closed NO polygon. The *degree* of a point **p**, at which coincident vertices meet, is an integer that equals the number of vertices meeting at **p** (Figures 1(b) and 1(e)). We also classify such P as PO with the understanding that the interior of P, when well-defined, is on the left as ∂P is traversed in the direction of increasing vertex indices. The finite area of P is given by Equation (2) and is nonnegative. The restriction to PO polygons can be made without loss of generality since an NO polygon $\bar{B}$, associated with a set operation, can be replaced by a PO polygon B with the same vertex points but with a different set operation. For example, $A - B$ = *closure* $(A \cap \bar{B})$. This relationship is important in its own right, since it shows that the set difference $A - B$ can be obtained by simply listing the vertices of B in reverse order and using the intersection algorithm with some minor changes.

Algorithm (Preliminaries)

Let A and B be in $\mathcal{SE}$ with NX and NU vertices, respectively. This section contains additional definitions, preliminary remarks and procedures, and rules that govern the algorithm for finding $A \cap B$. Analogous statements can be made for $A \cup B$, but with a few exceptions, our remarks will refer to the determination of $A \cap B$.

Let the vertices and edges of A be denoted by $\mathbf{a}_i$, $\bar{\mathbf{a}}_i$, and those of B by $\mathbf{b}_j$, $\bar{\mathbf{b}}_j$. With $\mathbf{a}_i = (x_i, y_i)$ and $\mathbf{b}_j = (u_j, v_j)$, the coordinates x_i, y_i, and u_j, v_j are stored in the input arrays X, Y, and U, V, respectively.

Initially, all meetings of $\bar{\mathbf{a}}_i$ with $\bar{\mathbf{b}}_j$ are found by solving Equation (4) for t and s, where

$$(1-t)\,\mathbf{a}_i + t\,\mathbf{a}_{i+1} = (1-s)\,\mathbf{b}_j + s\mathbf{b}_{j+1},$$

$$t, s \in (0, 1],\ 1 \le i \le NX1,\ 1 \le j \le NU1, \qquad (4)$$

with NX1 = NX − 1 and NU1 = NU − 1.

A meeting point of A, B (*MP*) is classified as one of the following: (*c*), (*w*), (*ve*), (*ev*), (*oa*), (*ob*), (*oab*). Examples of *MPs* are shown in Figure 3. A (*c*) *MP* occurs as a *crossing* between an edge of A and an edge of B such that $t \in (0, 1)$, $s \in (0, 1)$. A (*w*) *MP* specifies a *meeting* of a vertex of A and a vertex of B such that $t = 1$, $s = 1$. A (*ve*) *MP* is a *meeting* of a terminal endpoint of an edge of A and an interior point of an edge of B so that $t = 1$, $s \in (0, 1)$; or if the roles of A and B are reversed, then $t \in (0, 1)$, $s = 1$, and the meeting is an (*ev*) *MP*. Note that neither $t = 0$ nor $s = 0$ is used in identifying *MPs* since such points would have been previously detected and accounted for. An (*oa*), (*ob*), or (*oab*) meeting occurs when $\bar{\mathbf{a}}_i$ and $\bar{\mathbf{b}}_j$ are parallel and have more than one point in common. The edges are said to *overlap*. If the terminal endpoint of $\bar{\mathbf{a}}_i$ and an interior point of $\bar{\mathbf{b}}_j$ are the same, this point is taken as an *MP*; if the terminal endpoint of $\bar{\mathbf{b}}_j$ and an interior point of $\bar{\mathbf{a}}_i$ are the same, this point is also taken as an *MP*; the configuration is classified (*oab*). See (*oab*) of Figure 3. If only the first condition is satisfied, the *MP* type is

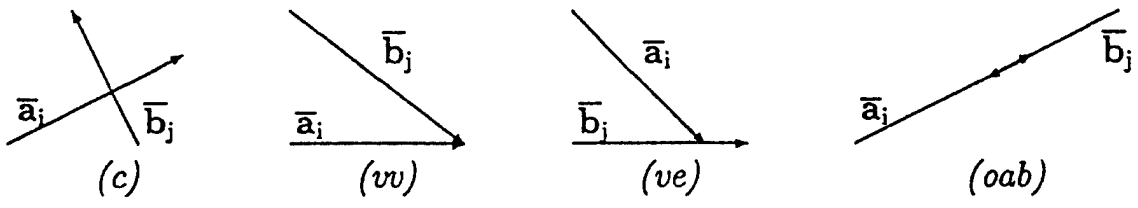

Figure 3. Various types of meetings of two edges

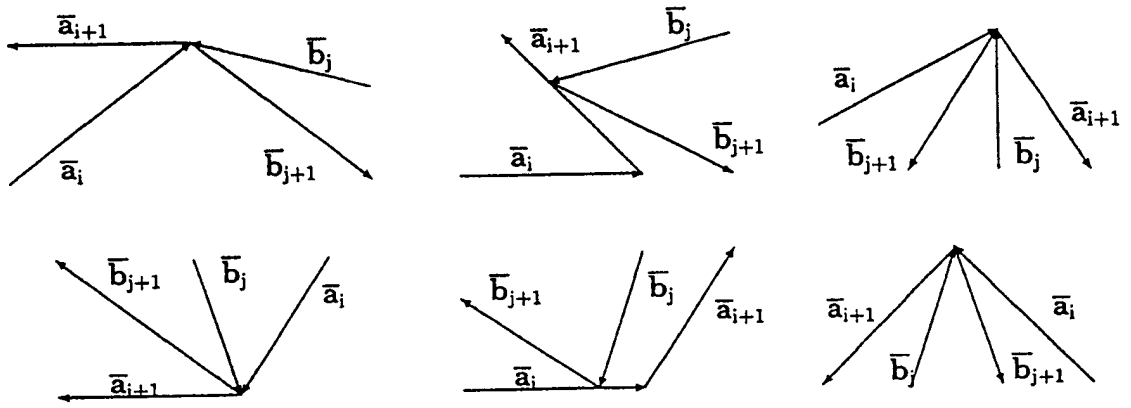

Figure 4. Examples of isolated *MP*s (top row) and removable *MP*s (bottom row)

denoted by (*oa*); if only the second holds, by (*ob*).

Once an *MP*, denoted by **d**, is found, it is examined for certain geometrical properties. First, if neither of the meeting segments, $\bar{a}_i$ and $\bar{b}_j$, points into the interior of the other polygon, then **d** is called an *isolated MP*. It is immediately stored as part of the output—an isolated intersection region made up of one point—and it is dropped from further consideration. Such points can occur only for (*iv*), (*ie*), and (*ev*) type meetings. See the top row of Figure 4 for examples. Of the remaining *MPs*, the ones to be *retained* are called *RMPs*. Let $[\bar{p}_j, \bar{p}_{j+1}]$ denote the connected line of two consecutive edges of a polygon. The *RMP* class is made up of the following :

(α) Types(*c*), (*oa*), (*ob*), and (*oab*).

(β) Type (*iv*). Provided the connected lines made up of $[\bar{a}_i, \bar{a}_{i+1}]$ and $\hat{b} = [\bar{b}_j, \bar{b}_{j+1}]$ cross at **d** such that $\bar{a}_i$ without **d** lies on one side of $\hat{b}$, and $\bar{a}_{i+1}$ without **d** lies on the other; or else more than one point of $\bar{a}_{i+1}$ lies along $\bar{b}_{j+1}$. See (a) and (b) of Figure 6 for examples.

(γ) Type (*ie*). Provided the connected line $[\bar{a}_i, \bar{a}_{i+1}]$ *crosses* $\bar{b}_j$ at **d**. *Crosses* here means that all the points of $\bar{a}_i$ except **d** are on one side of $\bar{b}_j$, and all the points of $\bar{a}_{i+1}$ except **d** lie on the other; or else more than one point of $\bar{a}_{i+1}$ lies along $\bar{b}_j$. See Figure 7 for examples.

(δ) Type (*ev*). Provided an obvious similar set of conditions as given in (γ) are met.

MPs that are not in *RMP* (and not isolated) are called *removable*. These points always occur at the vertex of at least one of the polygons. They will be taken into account later. See the bottom row of Figure 4 for examples.

Assume now that all *MPs* to be treated are in *RMP*. Continuing, for a given $\bar{a}_i$, each $\bar{b}_j$ is found that meets the i^{th} edge of A. If there are m such $\bar{b}_j$, $m \geq 1$, their indices are ordered according to the increasing square of the distance of the *MPs* from a_i along $\bar{a}_i$. The index of $\bar{a}_i$ is stored in m consecutive elements of array IA, and the m indices of the $\bar{b}_j$ are stored in corresponding elements of array IB in the order stated above. If an *MP* occurs at the endpoint of $\bar{b}_j$ for a given j, and that vertex coincides with other edges of B (Figure 1(b),(e)), then distances along $\bar{a}_i$ for these edges will be the same. A set of *MPs* with equal distances for a given i is called an EQDA set. For such sets, a separate strategy is necessary to order the indices of those intersecting $\bar{b}_j$'s. The ordering procedure our algorithm uses in these cases will be described later.

A parameter MO is assigned an integer to identify the *MP* type. Thus,

$$\begin{aligned} &MO = 2 \Rightarrow (c), MO = 3 \Rightarrow (iv), MO = 4 \Rightarrow (ie) \\ &MO = 5 \Rightarrow (ev), MO = 6 \Rightarrow (oa), \\ &MO = 7 \Rightarrow (ob) \end{aligned} \qquad (5)$$

The MO values are stored in the array IAO. The integer values stored in IA and IB for a given *MP* are unique as a pair, except when (*oab*) occurs. In this case, the same pair of indices may appear more than once in IA and IB, with IAO containing MO = 6 or 7. Note, however, that their *MPs* will not be the same and, consequently, the algorithm will have no difficulty here. Two arrays, WA and ZA, contain the values of the coordinates (w_k, z_k) of the *RMPs*.

After the *RMPs* have been obtained and each characterized by a value of MO, the decisions remain of how to process these data to obtain the desired result, $A \cap B$. The basic decision the algorithm must make is to determine whether to move from the *RMP* at $\bar{a}_i$ and $\bar{b}_j$ along $\bar{a}_i$ ($\bar{a}_{i+1}$ if MO = 3,4,7) or $\bar{b}_j$ ($\bar{b}_{j+1}$, if MO = 3,5,6). Of course this depends on whether $A \cap B$ or $A \cup B$ is wanted. In the first case, one should always choose the segment that captures some of $A \cap B$; and in the latter case, choose the segment that captures some of $A \cup B$. For example, let $\bar{a}_i$ and $\bar{b}_j$ meet at **d** with MO = 2. Let $\bar{c}_{ij} = \bar{a}_i \times \bar{b}_j$ denote the vector cross product of $\bar{a}_i$ and $\bar{b}_j$ so that $\bar{c}_{ij} = c_{ij}\,\mathbf{k}$, where $c_{ij} = (x_{i+1} - x_i)(v_{j+1} - v_j) - (y_{i+1} - y_i)(u_{j+1} - u_j)$, and **k** is the unit vector normal to the xy–plane consistent with a right-handed coordinate system. If $c_{ij} > (<)0$, then $\bar{b}_j(\bar{a}_i)$ passes into the interior of A(B) from **d**, and the next point to process would be the next listed *RMP* from **d** along B(A). If $A \cup B$ is wanted and if $c_{ij} > (<)0$, then $\bar{a}_i(\bar{b}_j)$ passes into the exterior of B(A) at **d**, and the next point to process would be the next listed *RMP* from **d** along A(B).

The processing for MO = 2 as described is straightforward. If MO = 3, a vertex of A meets a vertex of B; there are 48 different geometrical configurations possible. Of these, 24 are removable and 8 are isolated *MPs*. Our Fortran function MO3 is used to determine whether the *MP* is isolated or removable or, if not, whether to proceed along $\bar{a}_{i+1}$ or $\bar{b}_{j+1}$. If MO = 4(5), the endpoint $\mathbf{a}_{i+1}$ ($\mathbf{b}_{j+1}$) meets the edge $\bar{b}_j$ ($\bar{a}_i$); there are 12 different configurations, of which one is an isolated *MP*, and five are removable *MPs*. A Fortran function MO4 (MO5) is called to determine whether the *MP* is isolated or removable, or whether to proceed along $\bar{b}_j$ ($\bar{a}_i$) or along $\bar{a}_{i+1}$($\bar{b}_{j+1}$). If MO = 7(6), the edges overlap; there are four different configurations. In this case, MO7 (MO6) is used to determine whether to move along $\bar{a}_i$($\bar{b}_j$) or along $\bar{b}_{j+1}$ ($\bar{a}_{i+1}$). Some of the analysis used in MO3 and MO4 will be given in a later section.

Now let K denote the total number of *RMPs*. If K = 0, the routine LOCPT1, from the Naval Surface Warfare Center, Dahlgren Division (NSWCDD) Math Library,[8] is called. It determines if a point is inside, on, or outside a given polygon. If the midpoint on $\bar{a}_1$ is contained in the interior of B, then $A \cap B$ = A; if not, LOCPT1 is asked if the midpoint of $\bar{b}_1$ is in the interior of A. If yes, then $A \cap B$ = B; if not, $A \cap B$ = 0. Note that K cannot equal one, because the only possible *MP* would either be isolated or removable and, consequently, would not belong to the *RMPs*. Therefore, it will be assumed hereafter that $K \geq 2$.

For a more detailed discussion, Example 1 is presented and shown graphically in Figure 5(a). The edges of B are in bold. The example displays some of the difficulties the algorithm must treat. Note that the polygons A and B are in $\mathcal{SE}$. Tables 1 and 2 help to clarify the discussion. They will be followed, in the next section, by Tables 3 through 6, which contain the data actually generated by the algorithm.

The second and third columns of Table 1 represent arrays X and Y that contain the coordinates (x_i, y_i) of the ordered vertices of A. The fourth and fifth columns carry the coordinates (u_j, v_j) of the ordered vertices of B in arrays U and V. The sixth and seventh columns hold the indices of the edges or segments of A and B, respectively, which generate the *RMPs* with coordinates (w_k, z_k). These coordinates, shown in the ninth and tenth columns, are stored in arrays WA and ZA, as mentioned above. The type of intersection or meeting is described by the value of MO, which is stored in the array IAO as listed in the eighth column. Thus, the

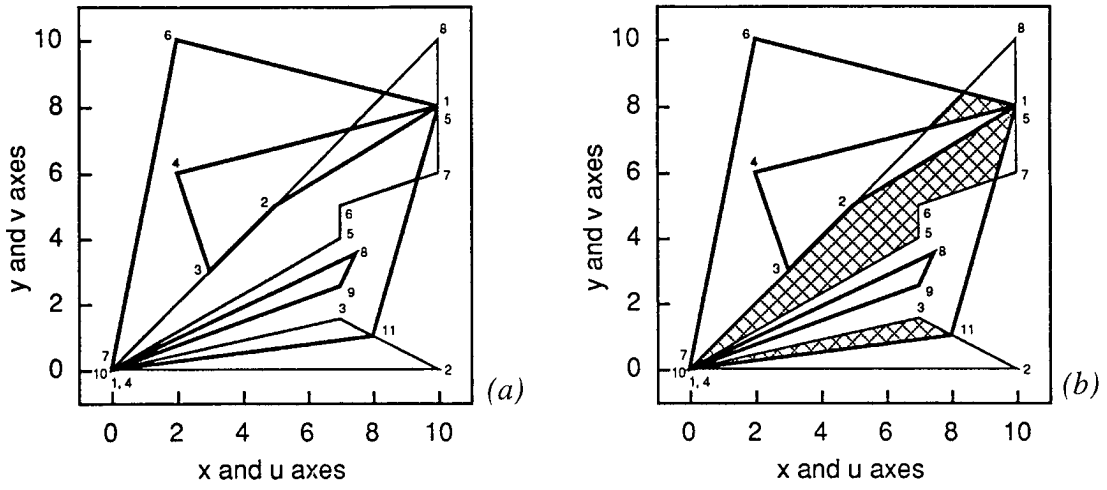

Figure 5. Input polygons A and B and $A \cap B$, respectively

first line in the tabulated data of Table 1, k = 1, starting with column six, states that the endpoint of edge $\overline{b}_{10}$ meets (since MO = 5) segment $\overline{a}_2$ at $w_1 = 8.0$ and $z_1 = 1.0$.

Note that three removable *MPs* that occur at the intersections of $(\overline{a}_7, \overline{b}_4)$, $(\overline{a}_7, \overline{b}_{11})$, and $(\overline{a}_8, \overline{b}_9)$ are not listed. The first two of these points at (10.0, 8.0) will make up part of the final output. It will be shown later how they are recognized and properly inserted into the output.

The next interim set of the arrays for Example 1 is given by Table 2. Columns 2 through 7 of Table 2 are based on *RMPs* found by fixing i and finding all $\overline{b}_j$ that meet $\overline{a}_i$, with these points ordered in increasing distance from a_i along $\overline{a}_i$. This is done for all i, as was explained earlier. These data will be called List-A. The remaining six columns, called List-B, refer to polygon B and are obtained by sorting the *RMPs* such that for a given j, all the $\overline{a}_i$ that meet or intersect $\overline{b}_j$ are

Table 1. Interim arrays(1) of Example 1 (Figure 5(a))

			NX = 9	NU = 12		K = 9			
k	**X**	**Y**	**U**	**V**	**IA**	**IB**	**IAO**	**WA**	**ZA**
1	0.0	0.0	10.0	8.0	2	10	5	8.0000	1.0000
2	10.0	0.0	5.0	5.0	3	6	3	0.0000	0.0000
3	7.0	1.5	3.0	3.0	3	9	3	0.0000	0.0000
4	0.0	0.0	2.0	6.0	6	11	2	9.3684	5.7895
5	7.0	4.0	10.0	8.0	8	5	2	8.4000	8.4000
6	7.0	5.0	2.0	10.0	8	4	2	7.3333	7.3333
7	10.0	6.0	0.0	0.0	8	1	5	5.0000	5.0000
8	10.0	10.0	7.5	3.5	8	2	6	3.0000	3.0000
9	0.0	0.0	7.0	2.5	8	6	3	0.0000	0.0000
10	x.x	x.x	0.0	0.0	2	10	5	8.0000	1.0000
11	x.x	x.x	8.0	1.0	x	x	x	x.xxxx	x.xxxx
12	x.x	x.x	10.0	8.0	x	x	x	x.xxxx	x.xxxx

ordered according to their increasing distance from $\mathbf{b}_j$ along $\bar{\mathbf{b}}_j$. This is done for each j. For example, with k = 1 there is a meeting of $\bar{\mathbf{b}}_1$ with $\bar{\mathbf{a}}_8$; the indices are stored as IBT(1) = 1, IAT(1) = 8. Note that IA(7) = 8 and IB(7) = 1. The IAB and IBA arrays are defined such that an element of IAB contains the value of k at which the same *MP* is located in List-B, and IBA contains the value of k at which the same *MP* of List-B appears in List-A. Thus IAB(7) = 1 "points" to the first *MP* given in List-B and IBA(1) = 7 "points" to the seventh and same *MP* in List-A. If some of the distances are equal for a given j, that set of *RMPs* is called an EQDB set. The *RMPs* at *k* = 5, 6 of List-B constitute such a set.

The information contained in each element of IAO(IBO) is now expanded by packing, with its MO value, additional data that specify whether to proceed from **d** along the A polygon or along the B polygon. Interpreting the elements of IAO(IBO) in terms of 32-bit words, with the bits numbered from right to left, the zeroth, first and second bits make up the value of MO for **d**. If also the 29th and 30th bits are set, then the algorithm moves to the next item in List-A(B), which means one moves from **d** along the edges of A(B) until the next *RMP* is encountered. If only the 29th bit is set, the algorithm moves to the next item in List-B(A); hence one moves from **d** along the B(A) polygon to the next *RMP*. Thus, for k = 7 of Table 2, IA(7) = 8, IB(7) = 1 and

$$\text{IAO}(7) = 0110\ 0000\ 0000\ 0000\ 0000\ 0000\ 0000\ 0101 = (60000005)_H \rightarrow 6\square 5$$

The elements of IAO and IBO are given in the concise MN-notation, M□N, which represents the bit pattern in hexadecimal notation M000000N, where M takes the value 2 or 6, and N may have values 2 through 7. Thus, IAO(7) states that the seventh *RMP* is of type (*ev*) with MO = 5, and that the next *RMP* to process, since M = 6, is in List-A at k = 8. If, for example, the algorithm were located at k = 8 of List-B, IBO(8) states that the eighth *MP* in List-B is of type (*ve*) with MO = 4 and, since M = 2, the algorithm moves to List-A at k = IBA(8) = 10.

The reader may have noticed at this point that a more sophisticated computer program could have reduced the 12 arrays of Table 2 to 8 or fewer. We refrained from this in order to achieve a minimum computing time to reach the end result. In this spirit, we point out a

Table 2. Interim arrays(2) of Example 1 (Figure 5)

NX = 9 NU = 12 K = 9												
	LIST-A						LIST-B					
k	**IA**	**IB**	**IAO**	**IAB**	**WA**	**ZA**	**IBT**	**IAT**	**IBO**	**IBA**	**WB**	**ZB**
1	2	10	6□5	8	8.0000	1.0000	1	8	2□4	7	5.0000	5.0000
2	3	6	6□3	5	0.0000	0.0000	2	8	2□7	8	3.0000	3.0000
3	3	9	2□3	7	0.0000	0.0000	4	8	6□2	6	7.3333	7.3333
4	6	11	2□2	9	9.3684	5.7895	5	8	2□2	5	8.4000	8.4000
5	8	5	6□2	4	8.4000	8.4000	6	3	2□3	2	0.0000	0.0000
6	8	4	2□2	3	7.3333	7.3333	6	8	6□3	9	0.0000	0.0000
7	8	1	6□5	1	5.0000	5.0000	9	3	6□3	3	0.0000	0.0000
8	8	2	6□6	2	3.0000	3.0000	10	2	2□4	10	8.0000	1.0000
9	8	6	2□3	6	0.0000	0.0000	11	6	6□2	4	9.3684	5.7895
10	2	10	6□5	8	8.0000	1.0000	1	8	2□4	7	5.0000	5.0000

very significant saving in computing time that can be realized with this algorithm. Vertex points that belong to A and/or B and also $A \cap B$, which are not treated as *RMPs*, are called *interior points (INTPs)*. Although there can be up to (NX) (NU) *RMPs*, in many (NX1) (NU1) applications there are relatively few compared to the number of *INTPs*. However, to find *INTPs* using a routine like LOCPT1 to determine if a point is inside a polygon is computationally expensive. Our algorithm, on the other hand, does not find these points by such means. Instead, as the *RMPs* are processed, the *INTPs* are found directly, in their proper order, by a simple analysis of the IA and/or the IBT array elements. Examples of such points are $\mathbf{a}_5$ and $\mathbf{a}_6$ of Figure 5(a). The rule for obtaining a sequence of *INTPs* of A(B), if they exist, is called *Rule A(B)*.

Rule A: The 29th and 30th bits of IAO(k) must have the value 1 so that the next element to process will be in List-A. There are two cases to consider, depending on the value of k:

(a) If the value of k satisfies $1 \le k \le K-1$, then let

$$IA(k) = I, \quad IA(k+1) = J, \quad LL \equiv J - I > 0,$$

and

$$mm \equiv \begin{cases} 1 & \text{for} \quad MO = 2,5,6 \\ 2 & \text{for} \quad MO = 3,4,7 \end{cases} \tag{6}$$

Let $\{X\}$ denote a sequence of points of an ordered subset of the vertices of A, i.e.,

$$\{X\} = \{(x_{iL}, y_{iL})\}, \quad iL = I + m, \quad m = mm, mm+1, \ldots, LL$$

(b) If k = K, then since IA(K + 1) = IA(1), by referring to the notation in (a) above, LL< 0. In this case,

$$LL = J - I + NX1, \tag{7}$$

$$iL = \begin{cases} I + m & \text{for } I + m \le NX1 \\ (I+m) \bmod (NX1) & \text{for } I + m > NX1 \end{cases}$$

The sequence $\{X\}$ makes up a set of *INTPs*. The x-coordinate and y-coordinate of each is stored sequentially in the output arrays W and Z following the storage of the *RMP* at WA(k), ZA(k).

Rule B: Rule A with the following changes:

IBT → IA, IBO → IAO, u → x, v → y,
NU1 → NX1, WB → WA, ZB → ZA

It will be shown in the next section that for $\mathbf{a}_5$, $\mathbf{a}_6$, Rule A can be applied, at k = 3 of Table 3, with mm = 2, I = 3, J = 6, LL = 3, iL = 5, 6.

Before obtaining and processing the final tables below, we return to two items to be discussed. Namely EQDA, EQDB sets, and removable points. Let an EQDA set consist of a total of n *RMPs* ($2 \le n \le K - k + 2$), which begin at the k^{th} row of List-A; then the following conditions must be satisfied:

$$\begin{aligned} IA(k) &= IA(k+1) = \cdots = IA(k+n-1) \\ WA(k) &= WA(k+1) = \cdots = WA(k+n-1) \\ ZA(k) &= ZA(k+1) = \cdots = ZA(k+n-1) \end{aligned} \tag{8}$$

The EQDB points are recognized in List-B by similar requirements, where IA in Equation (8) is replaced by IBT and WA, ZA by WB, ZB. Thus, an EQDA (EQDB) set would be characterized geometrically as an edge of A(B) being met n times at the same point by edges of B(A). Of course, there can be many such sets that the algorithm must handle, but this discussion will be limited to one in each list. In Table 2, there is an EQDA set of two points at k = 2,3, and there is also an EQDB set of two points at k = 5,6. Note that they are ordered in increasing values of the IB elements and the IAT elements, respectively; i.e., IB(2) < IB(3), and IAT(5) < IAT(6). Initially, EQDA (EQDB) sets are always ordered in this way. The reordering of these sets, when necessary, will be based on an overall ordering of the entire IAO(IBO) array. It is understood that any reordering of some of the elements of IAO or IBO implies reordering all the arrays of List-A and List-B in the same manner.

A very simple rule, *Rule C*, dictates the overall ordering that is required. It states that

the M values of M□N must alternate row by row in each list, with one exception as stated below. The ordering, as given by Rule C, is necessary to insure that no *INTPs* are passed over and also that no erroneous ones are introduced into the output. There are two ways to satisfy this rule, in case it does not hold initially. First, if there exist EQDA (EQDB) sets, then cyclic permutations, within each set, can be carried out towards satisfying the rule. If there remain groups of elements of IAO(IBO) for which Rule C is still not satisfied, then in each of these groups, all the elements are removed except one. The one kept, whenever possible, has an N value in M□N of two. If there is no such element, then the first element of the group is retained and the others are discarded. The one exception to Rule C occurs if all the M values throughout List-A are the same, and likewise for List-B. In this case, the algorithm processes the lists directly.

Algorithm (Main)

Three final sets of arrays, Tables 3 through 5, one for each intersection region of Figure 5(b), are generated by applying the algorithm to the example of Figure 5(a). The tables contain sufficient information to obtain $A \cap B$. Removable points that are needed to generate $A \cap B$ are picked up in their proper order as *INTPs*. This will be shown in the example. Table 3 differs from Table 2 because of Rule C. In List-A of Table 3 at k = 2, 3 (an EQDA set), the rows are interchanged from those of Table 2. An EQDB set exists at k = 4, 5 of Table 3, where an interchange has occurred from the corresponding rows at k = 5, 6 of Table 2. The k values in List-B of Table 3 are off by one in this interchange, because in Table 3, Rule C required the deletion of the second row of List-B and the corresponding row at k = 8 in List-A of Table 2.

At this point, the algorithm is in a position to process Table 3. Two new arrays, W and Z, as shown in Table 6, will contain the coordinates (w_L, z_L) of each point of $A \cap B$ in their proper order for each intersection region. These regions will be in $\mathcal{SE}$. Each element of array IC will contain the number of points in one such region, and a parameter IAN will contain the number of elements of IC; i.e., the number of regions in the output. The first and last points for any

Table 3. Final intersection data(1) of Example 1 (Figure 5)

NX = 9 NU = 12 K = 8												
	LIST-A						LIST-B					
k	IA	IB	IAO	IAB	WA	ZA	IBT	IAT	IBO	IBA	WB	ZB
1	2	10	6□5	7	8.0000	1.0000	1	8	2□4	7	5.0000	5.0000
2	3	9	2□3	6	0.0000	0.0000	4	8	6□2	6	7.3333	7.3333
3	3	6	6□3	5	0.0000	0.0000	5	8	2□2	5	8.4000	8.4000
4	6	11	2□2	8	9.3684	5.7895	6	8	6□3	8	0.0000	0.0000
5	8	5	6□2	3	8.4000	8.4000	6	3	2□3	3	0.0000	0.0000
6	8	4	2□2	2	7.3333	7.3333	9	3	6□3	2	0.0000	0.0000
7	8	1	6□5	1	5.0000	5.0000	10	2	2□4	9	8.0000	1.0000
8	8	6	2□3	4	0.0000	0.0000	11	6	6□2	4	9.3684	5.7895
9	2	10	6□5	7	8.0000	1.0000	1	8	2□4	7	5.0000	5.0000

Table 4. Final intersection data(2) of Example 1 (Figure 5)

NX = 9 NU = 12 K = 6												
	LIST-A						LIST-B					
k	IA	IB	IAO	IAB	WA	ZA	IBT	IAT	IBO	IBA	WB	ZB
1	3	6	6□3	5	0.0000	0.0000	1	8	2□4	5	5.0000	5.0000
2	6	11	2□2	6	9.3684	5.7895	4	8	6□2	4	7.3333	7.3333
3	8	5	6□2	3	8.4000	8.4000	5	8	2□2	3	8.4000	8.4000
4	8	4	2□2	2	7.3333	7.3333	6	8	6□3	6	0.0000	0.0000
5	8	1	6□5	1	5.0000	5.0000	6	3	2□3	7	0.0000	0.0000
6	8	6	2□3	4	0.0000	0.0000	11	6	6□2	2	9.3684	5.7895
7	3	6	6□3	5	0.0000	0.0000	1	8	2□4	5	5.0000	5.0000

particular region will always be the same, unless it has only one isolated point, so that these regions are always closed.

When a row of List-A(B) is processed, the 31st bit of that row element in IAO(IBO) is set. After a closed region of the output has been found, then all such rows in List-A(B) and their corresponding rows in List-B(A) are deleted. The remaining rows are renumbered sequentially, with the first row of the new lists repeated as the last row. Thus, a new table is generated and used to obtain the next region of the output. In stepping through the table, note the way the removable points are recovered, as well as the way the *INTPs* are obtained, all in their proper order. It will be helpful in following the discussion to use Table 6 as well as Figure 5.

Starting with IA(1) and IB(1), then W(1) = WA(1), Z(1) = ZA(1). Now IAO(1) is unraveled. It carries the information that MO = 5, an (ev) *RMP*, and that one must proceed to the next *RMP* in List-A, which is IA(2) = 3, IB(2) = 9. Before storing WA(2) and ZA(2), Rule A is used to get the *INTP*, $\mathbf{a}_3$ = (7.0,1.5) (see Table 1 for the coordinates of $\mathbf{a}_3$), which is stored in W(2), Z(2), then W(3) = WA(2), Z(3) = ZA(2). From IAO(2) with IAB (2) = 6, the algorithm points to List-B at k = 6, 7. Here, W(4) = WB(7), and Z(4) = ZB(7). From IBO(7) and IBA = 9, proceed to k = 9 of List-A. Since the starting point and the present point at k = 9 are the same, a closed output polygon specified by four points (IC(1) = 4), has now been obtained. At this stage, all the rows that have been used are deleted, and the remaining rows renumbered to obtain Table 4.

An analysis of Table 4 at k = 1,2 of List-A yields *INTPs* $\mathbf{a}_5$ and $\mathbf{a}_6$. As the table is processed, another *INTP* is found from List-B at k = 6, 7 using Rule B. It is the removable point from the meeting of $(\bar{\mathbf{a}}_7, \bar{\mathbf{b}}_{11})$ at $\mathbf{b}_1$ = (10, 8). Thus, we see that a removable point is recovered, if required, as an *INTP*.

The region found from Table 4 is defined by seven points (IC(2) = 7) that are listed in the W, Z arrays in elements 5 through 11. By deleting the used rows of Table 4, Table 5 is obtained.

From Table 5, an *INTP* is found in List-B at k = 1, which is the removable point resulting from the meeting of $\bar{\mathbf{a}}_7$ and $\bar{\mathbf{b}}_4$ at $\mathbf{b}_5$ = (10, 8). Carrying out the steps indicated in the table yields the third intersection region made up of four points (IC(3) = 4), which are stored in the elements 12 through 15 of W and Z.

The total algorithmic process is summarized in four major steps:

1. The input polygons A and B are in $\mathcal{SE}$ and are defined by NX, NU vertices with their coordinates stored in arrays X,Y and U,V, respectively. Polygons in $\mathcal{SI}$ are not admissible.

Table 5. Final intersection data(3) of Example 1 (Figure 5)

NX = 9 NU = 12 K = 2												
	LIST-A						LIST-B					
k	IA	IB	IAO	IAB	WA	ZA	IBT	IAT	IBO	IBA	WB	ZB
1	8	5	6□2	2	8.4000	8.4000	4	8	6□2	2	7.3333	7.3333
2	8	4	2□2	1	7.3333	7.3333	5	8	2□2	3	8.4000	8.4000
3	8	5	6□2	2	8.4000	8.4000	4	8	6□2	2	7.3333	7.3333

2. All *MPs* are found and classified. Isolated points, stored separately, and removable points are not included as *RMPs*. The *RMPs* are characterized, and their processing order is specified by the contents of IAO and IBO.
3. The *RMP* points make up List-A and List-B. It may be necessary to reorder or remove rows from these lists, according to Rule C, if some of the *RMPs* are of degree > 1. *INTPs* are found directly when the lists are processed by Rules A and B.
4. The output consists of IAN and arrays IC, W, and Z. The number of intersection regions is given in IAN. IC contains in its i^{th} element the number of vertices that make up the i^{th} intersection region. The coordinates of the vertex points of $A \cap B$ are stored, in proper order, in consecutive elements of the W and Z arrays.

Table 6. The output intersection data of Example 1 (Figure 5)

IAN =3 IC(1) = 4 IC(2) = 7 IC(3) = 4			
W(l) = 8.00000	Z(l) = 1.00000	W(9) = 10.0000	Z(9) = 8.00000
W(2) = 7.00000	Z(2) = 1.50000	W(10) = 5.00000	Z(10) = 5.00000
W(3) = 0.00000	Z(3) = 0.00000	W(11) = 0.00000	Z(11) = 0.00000
W(4) = 8.00000	Z(4) = 1.00000	W(12) = 8.40000	Z(12) = 8.40000
W(5) = 0.00000	Z(5) = 0.00000	W(13) = 7.33333	Z(13) = 7.33333
W(6) = 7.00000	Z(6) = 4.00000	W(14) = 10.0000	Z(14) = 8.00000
W(7) = 7.00000	Z(7) = 5.00000	W(15) = 8.40000	Z(15) = 8.40000
W(8) = 9.36842	Z(8) = 5.78947		

Intersection Analysis of (vv) and (ve)

In this section, we expand the discussion of two types of *MPs*. In the case of a *(vv) MP*, a vertex of A meets a vertex of B. As mentioned earlier, there are 48 possible configurations with 16 in *RMP*. Examples of two are shown in Figures 6(a) and 6(b). In analyzing these figures, one should keep in mind that A and B are PO, and the desired result is $A \cap B$. Hence, in Figure 6(a) one would process the next *RMP* in List-A, since $\bar{\mathbf{a}}_{i+1}$ points to the interior of B. Five cross products, with a proper sign for each of their magnitudes, are used to establish the last statement. Given the coordinates of $\mathbf{a}_i$, $\mathbf{a}_{i+1}$, $\mathbf{a}_{i+2}$ and $\mathbf{b}_j$, $\mathbf{b}_{j+1}$, $\mathbf{b}_{j+2}$, the MO3 Fortran function picks from six possible cross products the five given in Equation (9). If the signs of their magnitudes are as shown, then MO3 recognizes the geometry of Figure 6(a) and outputs M□3 with M having the value that requires processing the next point in List-A.

$$\begin{cases} \bar{\mathbf{a}}_i \times \bar{\mathbf{a}}_{i+1} = c\mathbf{k}, & c<0 \\ \bar{\mathbf{b}}_j \times \bar{\mathbf{b}}_{j+1} = d\mathbf{k}, & d>0 \\ \bar{\mathbf{a}}_i \times \bar{\mathbf{b}}_{j+1} = e\mathbf{k}, & e<0 \\ \bar{\mathbf{a}}_{i+1} \times \bar{\mathbf{b}}_j = f\mathbf{k}, & f<0 \\ \bar{\mathbf{a}}_{i+1} \times \bar{\mathbf{b}}_{j+1} = g\mathbf{k}, & g<0 \end{cases} \qquad (9)$$

In Table 3 at k = 2 of List-A, a *(vv) RMP* is indicated. The geometry of that *MP* is shown in Figure 6(b). Hence, referring to the

figure, one would move from A to B to process the next *RMP* since $\bar{b}_{j+1}$ points to the interior of A. This follows from the signs of the magnitudes of the five cross products given below in Equation (10) as determined by MO3 and is indicated in Table 3 by the value stored in IAO(2).

$$\begin{cases} \bar{a}_i \times \bar{a}_{i+1} = C\mathbf{k}, & C<0 \\ \bar{b}_j \times \bar{b}_{j+1} = D\mathbf{k}, & D>0 \\ \bar{a}_i \times \bar{b}_j = E\mathbf{k}, & E>0 \\ \bar{a}_i \times \bar{b}_{j+1} = F\mathbf{k}, & F>0 \\ \bar{a}_{i+1} \times \bar{b}_j = G\mathbf{k}, & G>0 \end{cases} \quad (10)$$

Figure 6(c) shows an example of a removable (*w*) *MP*.

For the case of a (*w*) *MP*, a vertex of A meets an interior point of an edge of B. There are 12 possible configurations, but only 6 are in the *RMP* class. Four have crossings between $\bar{b}_j$ and the line made up of $\bar{a}_i$, $\bar{a}_{i+1}$. The other two require that $\bar{a}_{i+1}$ overlaps $\bar{b}_j$. These situations are identified by the Fortran function MO4 using a pair of vector cross products and a dot product given below. The geometries are shown in Figures 7(a), (b), (c), (d). For Figure 7(a) (7(b)), G and H are negative (positive) in Equation (11), and MO4 finds that one must process the next *RMP* in List-B(A), where

$$\begin{cases} \bar{b}_j \times \bar{a}_i = G\mathbf{k} \\ \bar{b}_j \times \bar{a}_{i+1} = H\mathbf{k} \end{cases} \quad (11)$$

One may note that the *RMP* shown in Figure 7(a) also appears in Figure 5(a), with the roles of A and B interchanged (see Table 3 at k = 7 of List-B).

For Figure 7(c), G is positive, H = 0, and the vector dot product $(\bar{b}_j \cdot \bar{a}_{i+1}) < 0$, and MO4 requires processing the next *RMP* in List-A. For Figure 7(d), H = 0 and $(\bar{b}_j \cdot \bar{a}_{i+1}) > 0$, and MO4 processes the next *RMP* in List-B.

Subprograms

The following subprograms, coded in Fortran 77, are used to obtain $A \cap B$.

1. XINT—The master routine. It calls SOLVA to find and characterize each *MP*. It uses (QSORTI, QSORTR, IORDER, RORDER, LOCPT1)[8] to order the *RMPs* along each edge or segment. It decides from IAO and IBO whether the next *RMP* is processed from List-A or List-B. It uses IAB (IBA) to point from List-A(B) to the corresponding elements in List-B(A). It calls routines 3 through 7 below. It identifies *INTPs*. It decides when an intersection region has been found. It identifies the output elements and stores them in the W and Z arrays, and assigns appropriate values to IAN and the elements of IC.

2. SOLVA—Linear equation solver. This routine solves Equation (4) for s and t, and also sets the value of MO, which identifies the type of intersection found.

3. MON—Sets the value of M (2 or 6) in M□N of arrays IAO and IBO, where N takes the values 2 through 7.

4. PSORT6—Recognizes EQDA and EQDB sets and carries out their initial

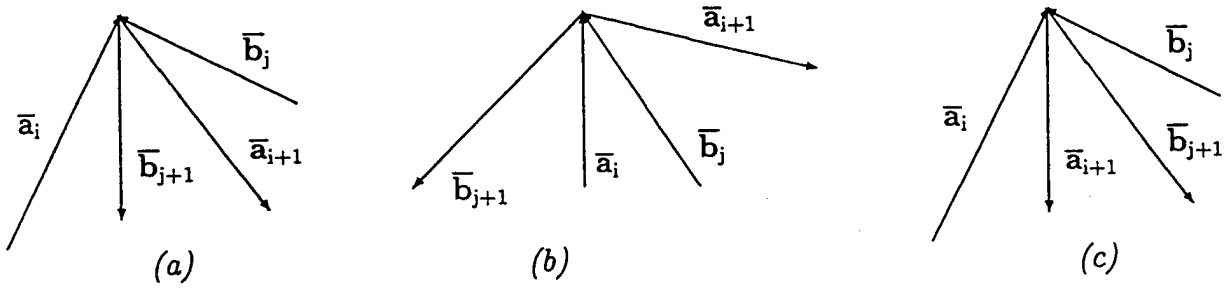

Figure 6. Several configurations of (*vv*) intersections

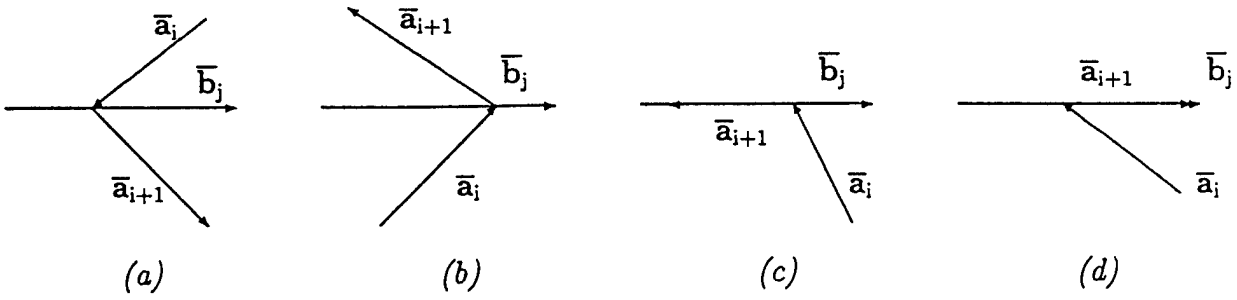

Figure 7. Several configurations of (*ve*) intersections (RMPs)

ordering using QSORTI, IORDER, then calls EX if the sets require further reordering according to Rule C.

5. REORD2—Identifies the rows of List-A and List-B to be deleted according to Rule C, after EQDA and EQDB sets have been ordered.

6. DEL—After an intersection region is found, this routine deletes the rows of List-A and List-B where the 31st bit is set in the elements of IAO and/or IBO.

7. LOCPT1—Given a polygon P in E^2, the xy–plane, LOCPT1 determines if a given point in E^2 is inside, on, or outside ∂P.

8. CYPERl—This routine is called by EX to cyclically permute, according to Rule C, the rows of List-A and List-B that contain EQDA and/or EQDB sets.

9. EX—This routine determines whether CYPER1 should be called. It is called by PSORT6.

Inherent Difficulties

An inherent difficulty of our algorithm, as with any such algorithm, arises from the use of floating point arithmetic. The well-known problems of whether or not two lines actually meet, or if a point is or is not in a polygon are examples of where problems can arise. Although floating point operations are kept to a minimum by working mainly with integer arrays, they nevertheless are unavoidable and are needed in subroutines 1 through 4 and 7 of the previous section. In general, the code should be run in double precision. This will reduce floating point problems, but not eliminate them entirely.

In order to make maximum use of the computer's word length, the algorithm uses a small positive machine-dependent parameter $\in$. This is accomplished by basing tolerances used by the floating point subroutines on $\in$. It is chosen as the smallest positive number such that $1 + \in > 1$. For IBM PCs, we have

$$\in = \begin{cases} 1.1920929\left(10^{-7}\right) & \text{(single precision)} \\ 2.2204605\left(10^{-16}\right) & \text{(double precision)} \end{cases} \quad (12)$$

Two Additional Examples

Examples 2 and 3 are presented to display the robustness of the algorithm. In Example 2, Figure 8, polygon A is made up of two disjoint polygons connected by lines, and B is composed of three such polygons. The connecting lines, or edges, are chosen so that A and B are in $\mathcal{SE}$. We see in this example that the intersection of more than a pair of polygons can often be found with only one application of the algorithm. Example 3, Figure 9, is interesting because all the *MPs* are at the same point in the plane.

Table 7 contains the input data required to specify A and B for both examples. The discussion of both examples is brief, but follows essentially the same order as was given in Example 1 with Tables 3 through 6. In both figures the edges in bold belong to B. Figure 9 does not show the indices at the center point (5,5) for lack of space; however, the reader should have no difficulty supplying them. Note that A has five coincident vertices, and B has four at that point. Tables 8 through 11 contain the algorithm-generated

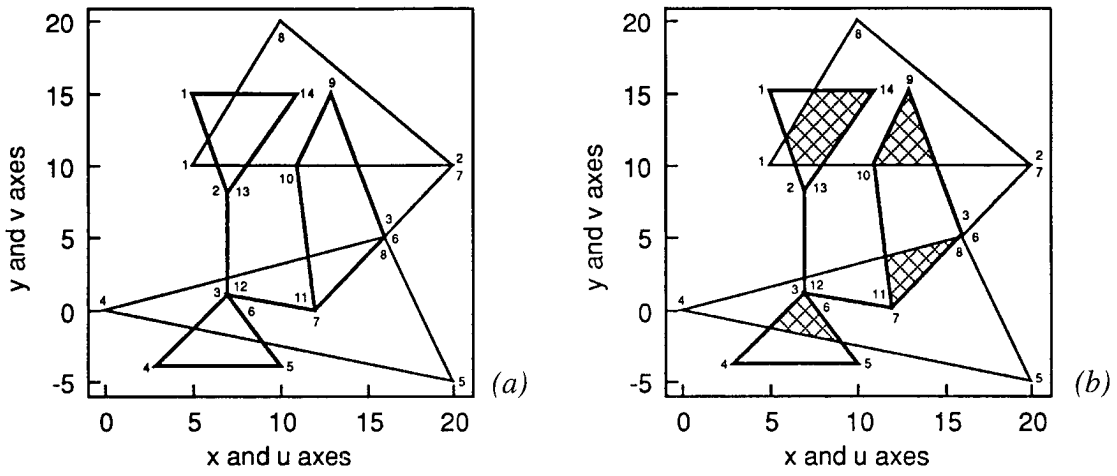

Figure 8. Input polygons A and B and $A \cap B$, respectively

arrays for Example 2, and Tables 12 and 13 contain the arrays for Example 3.

In Example 2, a removable *MP* occurs at $(\bar{a}_5, \bar{b}_7)$, which has coordinates (16.0, 5.0). This *MP* was not needed in the final output, hence it was not picked up as an *INTP*.

In Example 3, there are 16 removable *MPs* that are not listed in view of space considerations. One of these, at $(\bar{a}_{10}, \bar{b}_{10})$, appears in the final output.

Acknowledgments

The author thanks Sibille Tallant for bringing the problem and some of the references to his attention. The author would like to recognize Greg Tallant for his assistance on this article. Several errors were found in an original version of the code by Russ Gnoffo during a translation from Fortran to C++. The graphics in the paper were generated by Dottie Burgess. The presentation was markedly improved by comments and suggestions of Jean DiDonato and William Ormsby. The author was supported in this work by William Ormsby and James Sloop.

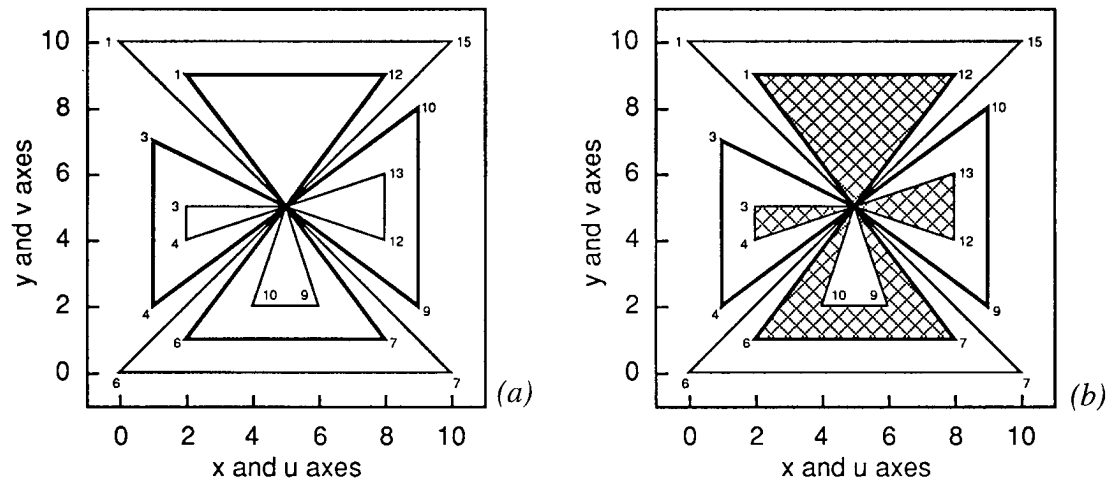

Figure 9. Input polygons A and B and $A \cap B$, respectively

Table 7. Input data for Examples 2 and 3 (Figures 8 and 9)

Example 2					Example 3				
NX = 9 NU = 15					NX = 16 NU = 13				
k	X	Y	U	V	k	X	Y	U	V
1	5.0	10.0	5.0	15.0	1	0.0	10.0	2.0	9.0
2	20.0	10.0	7.0	8.0	2	5.0	5.0	5.0	5.0
3	16.0	5.0	7.0	1.0	3	2.0	5.0	1.0	7.0
4	0.0	0.0	3.0	-4.0	4	2.0	4.0	1.0	2.0
5	20.0	-5.0	10.0	-4.0	5	5.0	5.0	5.0	5.0
6	16.0	5.0	7.0	1.0	6	0.0	0.0	2.0	1.0
7	20.0	10.0	12.0	0.0	7	10.0	0.0	8.0	1.0
8	10.0	20.0	16.0	5.0	8	5.0	5.0	5.0	5.0
9	5.0	10.0	13.0	15.0	9	6.0	2.0	9.0	2.0
10	x.x	x.x	11.0	10.0	10	4.0	2.0	9.0	8.0
11	x.x	x.x	12.0	0.0	11	5.0	5.0	5.0	5.0
12	x.x	x.x	7.0	1.0	12	8.0	4.0	8.0	9.0
13	x.x	x.x	7.0	8.0	13	8.0	6.0	2.0	9.0
14	x.x	x.x	11.0	15.0	14	5.0	5.0	x.x	x.x
15	x.x	x.x	5.0	15.0	15	10.0	10.0	x.x	x.x
16	x.x	x.x	x.x	x.x	16	0.0	10.0	x.x	x.x

Table 8. Final intersection data (1) of Example 2 (Figure 8)

NX = 9 NU = 15 K =12												
	LIST-A						LIST-B					
k	IA	IB	IAO	IAB	WA	ZA	IBT	IAT	IBO	IBA	WB	ZB
1	1	1	6□2	2	6.4286	10.0000	1	8	6□2	12	5.9091	11.8182
2	1	13	2□2	11	8.1429	10.0000	1	1	2□2	13	6.4286	10.0000
3	1	9	6□5	8	11.0000	10.0000	2	3	6□2	8	7.0000	2.1875
4	1	8	2□2	7	14.5000	10.0000	3	4	2□2	9	5.1667	-1.2917
5	2	7	6□3	6	16.0000	5.0000	5	4	6□2	10	8.9412	-2.2353
6	3	10	2□2	9	11.6364	3.6364	7	2	2□3	5	16.0000	5.0000
7	3	12	6□2	10	7.0000	2.1875	8	1	6□2	4	14.5000	10.0000
8	3	2	2□2	3	7.0000	2.1875	9	1	2□4	3	11.0000	10.0000
9	4	3	6□2	4	5.1667	-1.2917	10	3	6□2	6	11.6364	3.6364
10	4	5	2□2	5	8.9412	-2.2353	12	3	2□2	7	7.0000	2.1875
11	8	14	6□2	12	7.5000	15.0000	13	1	6□2	2	8.1429	10.0000
12	8	1	2□2	1	5.9091	11.8182	14	8	2□2	11	7.5000	15.0000
13	1	1	6□2	2	6.4286	10.0000	1	8	6□2	12	5.9091	11.8182

Table 9. Final intersection data(2) of Example 2 (Figure 8)

NX = 9 NU = 15 K = 8												
	LIST-A						LIST-B					
k	IA	IB	IAO	IAB	WA	ZA	IBT	IAT	IBO	IBA	WB	ZB
1	1	9	6□5	6	11.0000	10.0000	2	3	6□2	6	7.0000	2.1875
2	1	8	2□2	5	14.5000	10.0000	3	4	2□2	7	5.1667	-1.2917
3	2	7	6□3	4	16.0000	5.0000	5	4	6□2	8	8.9412	-2.2353
4	3	10	2□2	7	11.6364	3.6364	7	2	2□3	3	16.0000	5.0000
5	3	12	6□2	8	7.0000	2.1875	8	1	6□2	2	14.5000	10.0000
6	3	2	2□2	1	7.0000	2.1875	9	1	2□4	9	11.0000	10.0000
7	4	3	6□2	2	5.1667	-1.2917	10	3	6□2	4	11.6364	3.6364
8	4	5	2□2	3	8.9412	-2.2353	12	3	2□2	5	7.0000	2.1875
9	1	9	6□5	6	11.0000	10.0000	2	3	6□2	6	7.0000	2.1875

Table 10. Final intersection data (3) of Example 2 (Figure 8)

NX = 9 NU = 15 K = 6												
	LIST-A						LIST-B					
k	IA	IB	IAO	IAB	WA	ZA	IBT	IAT	IBO	IBA	WB	ZB
1	2	7	6□3	4	16.0000	5.0000	2	3	6□2	4	7.0000	2.1875
2	3	10	2□2	5	11.6364	3.6364	3	4	2□2	5	5.1667	-1.2917
3	3	12	6□2	6	7.0000	2.1875	5	4	6□2	6	8.9412	-2.2353
4	3	2	2□2	1	7.0000	2.1875	7	2	2□3	7	16.0000	5.0000
5	4	3	6□2	2	5.1667	-1.2917	10	3	6□2	2	11.6364	3.6364
6	4	5	2□2	3	8.9412	-2.2353	12	3	2□2	3	7.0000	2.1875
7	2	7	6□3	4	16.0000	5.0000	2	3	6□2	4	7.0000	2.1875

Table 11. The output intersection data of Example 2 (Figure 8)

IAN = 3 IC(1) = 6 IC(2) = 4 IC(3) = 11			
W(1) = 6.42857	Z(1) = 10.0000	W(11) = 16.0000	Z(11) = 5.00000
W(2) = 8.14286	Z(2) = 10.0000	W(12) = 11.6364	Z(12) = 3.63636
W(3) = 11.0000	Z(3) = 15.0000	W(13) = 12.0000	Z(13) = 0.00000
W(4) = 7.50000	Z(4) = 15.0000	W(14) = 7.00000	Z(14) = 1.00000
W(5) = 5.90909	Z(5) = 11.8182	W(15) = 7.00000	Z(15) = 2.18750
W(6) = 6.42857	Z(6) = 10.0000	W(16) = 7.00000	Z(16) = 1.00000
W(7) = 11.0000	Z(7) = 10.0000	W(17) = 5.16667	Z(17) = -1.29167
W(8) = 14.5000	Z(8) = 10.0000	W(18) = 8.94118	Z(18) = -2.23529
W(9) = 13.0000	Z(9) = 15.0000	W(19) = 7.00000	Z(19) = 1.00000
W(10) = 11.0000	Z(10) = 10.0000	W(20) = 12.0000	Z(20) = 0.00000
		W(21) = 16.0000	Z(21) = 5.00000

Table 12. Final intersection data (1) of Example 3 (Figure 9)

NX = 16 NU = 13 K = 4												
	LIST-A						LIST-B					
k	IA	IB	IAO	IAB	WA	ZA	IBT	IAT	IBO	IBA	WB	ZB
1	1	1	6□3	1	5.0000	5.0000	1	1	2□3	5	5.0000	5.0000
2	4	4	2□3	2	5.0000	5.0000	4	4	6□3	2	5.0000	5.0000
3	7	7	6□3	3	5.0000	5.0000	7	7	2□3	3	5.0000	5.0000
4	13	10	2□3	4	5.0000	5.0000	10	13	6□3	4	5.0000	5.0000
5	1	1	6□3	1	5.0000	5.0000	1	1	2□3	5	5.0000	5.0000

Table 13. The output intersection data of Example 3 (Figure 9)

IAN = 1 IC(1) = 16			
W(1) = 5.00000	Z(1) = 5.00000	W(9) = 4.00000	Z(9) = 2.00000
W(2) = 2.00000	Z(2) = 5.00000	W(10) = 5.00000	Z(10) = 5.00000
W(3) = 2.00000	Z(3) = 4.00000	W(11) = 8.00000	Z(11) = 4.00000
W(4) = 5.00000	Z(4) = 5.00000	W(12) = 8.00000	Z(12) = 6.00000
W(5) = 2.00000	Z(5) = 1.00000	W(13) = 5.00000	Z(13) = 5.00000
W(6) = 8.00000	Z(6) = 1.00000	W(14) = 8.00000	Z(14) = 9.00000
W(7) = 5.00000	Z(7) = 5.00000	W(15) = 2.00000	Z(15) = 9.00000
W(8) = 6.00000	Z(8) = 2.00000	W(16) = 5.00000	Z(16) = 5.00000

References

1. Apostol, T.M., *Mathematical Analysis*, Addison-Wesley Co., Reading, MA, 1974, pp. 41-42.
2. Tallant, S.U., *A Comparison of Great Circles, Rhumblines, and Chords for Representing Weapon Range-Circles on a Spherical Earth*, Naval Surface Warfare Center, Dahlgren, VA, NSWCDD/TR-95/105, Jul 1995.
3. Tallant, S.U. and Harter, T.L., *On the Use of Planar Union and Intersection Algorithms for Polygons on a Spherical Earth*, Naval Surface Warfare Center, Dahlgren, VA, NSWCDD/TR-96/29, (to be published) Jun 1996.
4. Barton, E.E. and Buchanan, I., "The Polygon Package," *Computer aided Design*, Vol. 12, No. 1, 1980, pp. 3-11.
5. Krishnan, D. and Patnaik, L.M., "Systolic Architecture for Boolean Operations on Polygons and Polyhedra," *Computer Graphics Forum*, Vol. 6, No. 3, 1987, pp. 203-210.
6. Margolit, A. and Knott, G.D., "An Algorithm for Computing the Union, Intersection or Difference of Two Polygons," *Computers & Graphics*, Vol. 13, No. 2, 1989, pp. 167-183.
7. Shijie, C. and Fuyan, Z., "A Fast Algorithm for Polygon Operations," *Journal of Computer Science and Technology (English Language Edition)*, Vol. 6, No. 1, 1991, pp. 91-96.
8. Morris, A., *NSWC Library of Mathematics Subroutines*, Naval Surface Warfare Center, Dahlgren, VA, NSWCDD/TR-92/425, Jan 1993.

The Author

ARMIDO R. DIDONATO received a B.S. in mathematics from Duquesne University, 1950; an S.M. in mathematics from the Massachusetts Institute of Technology, 1951; and a Ph.D. in mathematics from Carnegie-Mellon University, 1972. From 1951 to 1953, he was a mathematician at duPont deNemours. Then from 1953 to 1954, Dr. DiDonato was a mathematical physicist at Melpar, Inc. Then in March of 1954, the author came to NSWCDD, where he headed Applied Mathematics of the Science and Mathematics Research Group from 1957 through 1967. The author has written publications in fluid dynamics, dynamic elasticity theory, viscoelasticity, ship waves, maximum likelihood analysis, computation of special functions and mathematical probability functions, trajectory analysis, and computational geometry. He is also a recipient of the Navy Meritorious Civilian Service Award.

Armido R. DiDonato

Advanced Processors—From Concept to Demonstration

O. Thomas Holland, Robert L. Stiegler, Wendy L. Poston, and Charles W. Steadman

The Advanced Processors (AP) section, in Naval Surface Warfare Center, Dahlgren Division's (NSWCDD's) Munitions Branch, is very active in developing and applying new technologies fundamental to the Navy's thrust in expeditionary warfare. Several of this section's amphibious-warfare and naval-surface, fire-support tasks involve algorithms and hardware for automatic target recognition, sensor data processing, modeling and simulation, and data visualization. Among these tasks are Advanced Processors for Weapons Sensor Fusion (APWSF), Advanced Systems for Air Defense (ASAD), and the Technology Evaluation Assessment Modeling and Simulation (TEAMS) facility. This article describes the contributions made by the AP section to these efforts, especially as they apply to expeditionary warfare, and presents a summary of technical results that are finding application to various Navy and Marine Corps interests.

EW
EXPEDITIONARY
WARFARE

"To maintain near perfect real-time knowledge of the enemy and communicate that to all forces in near real time."
Dr. Anita Jones, DDR&E, 3/24/94

"Improved situational awareness: precision location of own-force and enemy assets and state of readiness and accurate, timely IFF."
RADM W. P. Houley, U. S. Navy

Introduction

To prepare the battle space and successfully accomplish their missions, Naval Expeditionary Forces (NEFs) rely on an integrated, yet disparate, collection of sensors deployed by various means throughout the amphibious operating area. However, through the Science and Technology (S&T) Round Tables for Expeditionary Warfare and Littoral Warfare, the Belisarious Series of Workshops and Wargames, and the Littoral Operations 2020 Game Series, wide-ranging deficiencies have been identified in current sensor capability.

Innovative technologies for weapon and targeting sensors, particularly the integrating software and processing, are essential. Future weapons will have significantly greater ranges and lethality. Target acquisition must extend beyond the ranges of those weapons. And in a significantly more dynamic and fluid battlefield, greater situational awareness and positive target identification are imperative. Innovative algorithms and advanced processors for specific targeting and weapon system sensors are fundamental to the success of NEF in the future battle space.

The concept for future NEF operations is presented in FMFRP 14-21, *Operational Maneuver From the Sea*,[1] (OMFTS). This concept was reiterated at

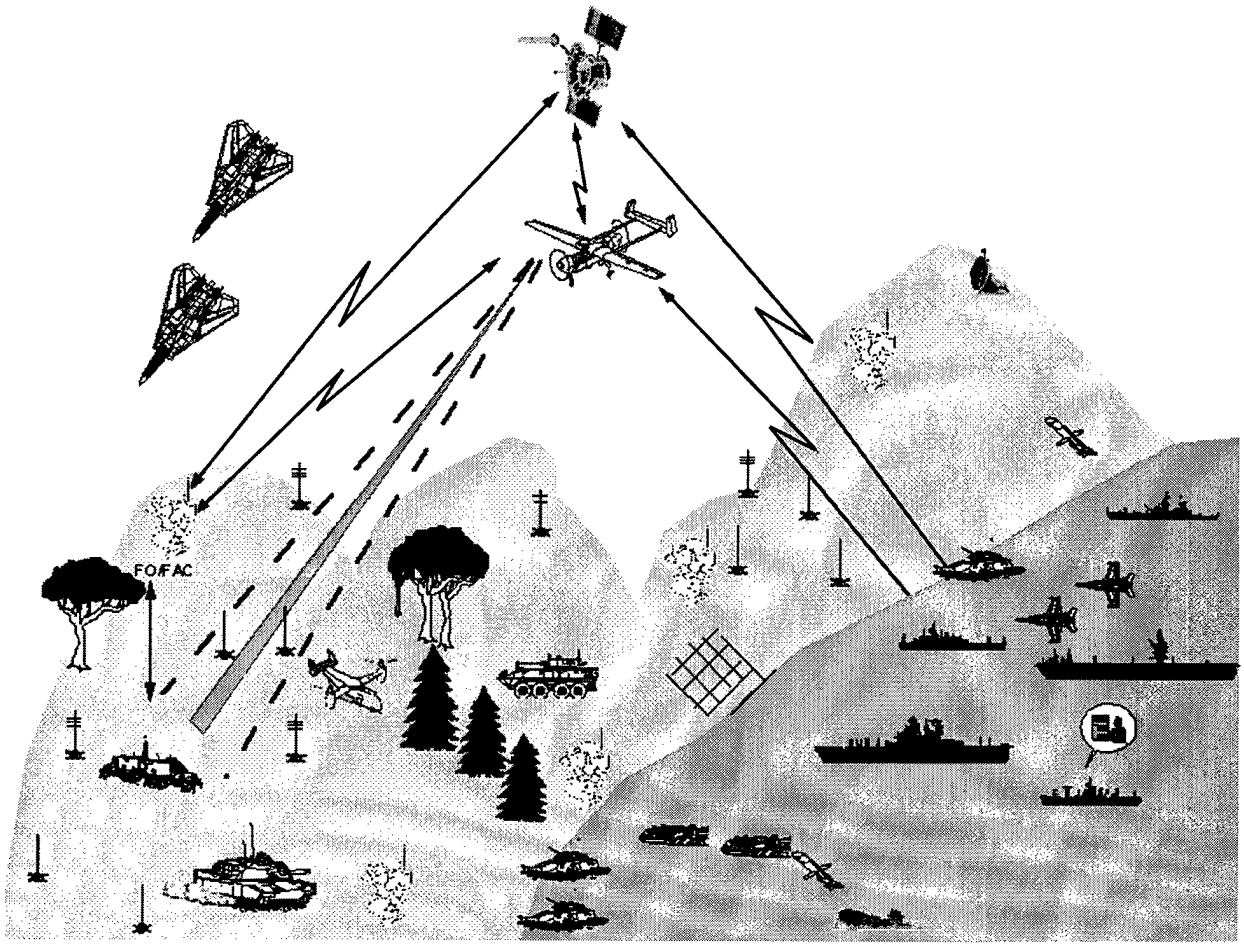

Figure 1. "Sensor-to-shooter" engagement environment of naval expeditionary forces

the Commandant's Warfighting Laboratory, *Sea Dragon* Brief to Industry, 19 December 1995. Figure 1 depicts the complex NEF "sensor-to-shooter" engagement environment with forces deployed ashore.

The AP section at NSWCDD has contributed an evolving expertise to numerous Navy and U.S. Marine Corps (USMC) tasks involving innovative technologies for weapon and targeting sensors: digital signal processing, embedded processors, application-specific processors, and algorithms for automatic target recognition and digital signal processing. In this article, we highlight some of the expeditionary warfare, in particular USMC, supportive tasks in which the AP section has been and continues to be involved.

Advanced Processors for Weapons Sensor Fusion

The USMC's APWSF project grew out of an Independent Exploratory and Development (IED) program at NSWCDD. Initiated in October 1988, the program concluded in 1990 with a demonstration of a system that could identify any one of five land-based military platforms from their infrared video imagery.[2] The significance of this effort was twofold: it demonstrated (1) that a system could be implemented with the capability of identifying targets with greater than 83 percent accuracy (from any viewing profile and with degraded data), and (2) that an artificial neural system (ANS) could be implemented with conventional hardware

techniques and integrated into a usable target identification system.

Recognizing the potential applications of the technology demonstrated in the IED program, the USMC tasked NSWCDD in 1991 to investigate the application of advanced technologies such as ANS to future USMC weapons. This initial effort identified extensive application of ANS and other neoteric sensor processing technologies to USMC systems under development. Realizing that advanced sensor processing technology would be at the heart of future weapon systems, the USMC created the 6.2 exploratory development task APWSF[3] in FY92 to pursue the development of advanced sensor processing, multiple and disparate sensor fusion, and target detection and recognition.

The APWSF 6.2 exploratory development project developed algorithms and system architectures for target classification and identification that have been incorporated in several man-portable or remotely delivered sensor system prototypes. One of these techniques, which has been demonstrated in the USMC's Expendable Acoustic Remote Sensor (EARS), has the ability to:

1. Determine statistically that possible target acoustic signals are present
2. Extract fundamental acoustic frequencies and their associated harmonics
3. Separate (sift) signals related to one target from others in a target-rich acoustic sample

Figure 2. EARS sensor

This third technique, called Enhanced Harmogram Analysis (EHA),[4,5] is determined from the Fourier transform and an estimate of background noise of a sample signal. Originally developed to detect helicopters and provide a feature set for classification, EHA was used in EARS to detect and provide a feature set for ground-based vehicles. Figure 2 shows the EARS sensor: a gun-launchable, acoustic target detection and classification sensor. Figure 3 shows the spectogram of an M60 tank at one kilometer, and Figure 4 shows the harmogram spectra related to the engine of the M60.

Another contribution of APWSF to acoustic sensor advancement is in the use of wavelet transformations for helicopter identification.[6] Detecting the presence of a helicopter is achievable with EHA methods; however, helicopters of the same type tend to be deployed in a group, which cannot be separated with this algorithm. Their signals are further complicated by the spurious and transient signals of field artillery and other weapons. Such additive and nonperiodic

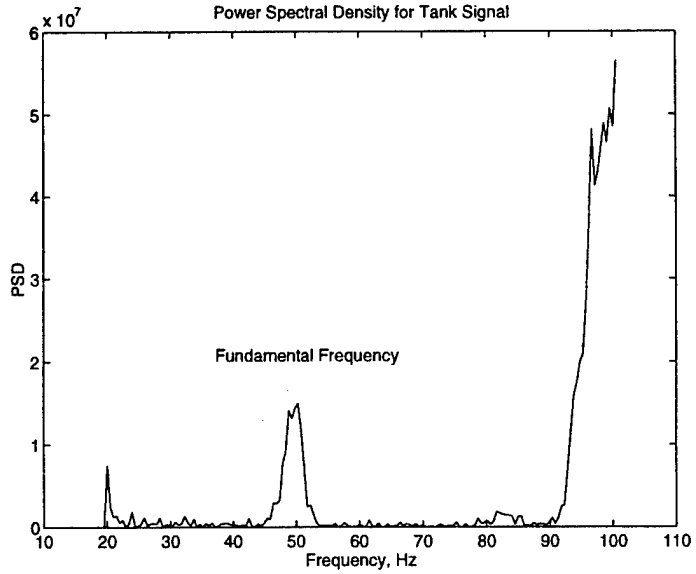

Figure 3. Power spectral density for M60

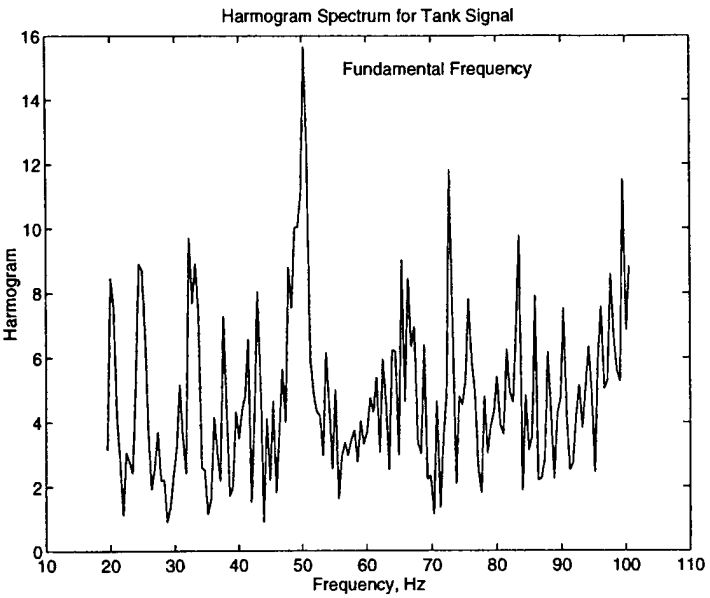

Figure 4. Harmogram spectra for M60

signals tend to decrease the effectiveness of spectral analysis techniques, such as EHA. This presents the challenging problem of distinguishing individual helicopters operating at the same blade rotation rates, etc., from within a group. One of the results of the investigation into wavelet transforms indicated the possibility of using wavelet transforms of a sample signal to locate short-term transients associated with unique characteristics of individual helicopters. Other results demonstrated the ability to use a wavelet transform to remove (i.e., filter) artillery blast from the signal of interest; these results showed that a wavelet could provide a very good feature set for target classification.

Advanced Sensor for Air Defense

Marine Air-Ground Task Forces can deploy anywhere in the world and must maintain freedom of maneuver to position themselves to defeat and/or control the threat. Ground-based air defense (AD) fire units equipped with passive sensors can effectively detect, identify, and engage low- to medium-altitude air threats (at night and during adverse weather) while reducing the probability of detection by enemy forces.

The Avenger and the Man-Portable Air Defense System (MANPADS) fire units currently rely on external radar cueing and visual air search, both of which have deficiencies, for target acquisition. Passive sensor technology being explored includes electronic support measures (ESM) and acoustic systems. ESM sensors exploit the radio frequency (RF) emissions of aircraft avionics equipment, while acoustic sensors exploit the aircraft's acoustic signature. Both sensors have the ability to provide weapons system cueing as well as noncooperative target recognition (NCTR). The multisensor integration of these two technologies is being pursued for Avenger and MANPADS applications. Sensors will be mounted on (i.e., organic to) the fire units to provide a stand-alone target acquisition capability. The ability to sense while on-the-move is also being addressed for Avenger.

The principle objective of the ASAD program is to demonstrate technologies to provide a passive target acquisition capability for Avenger (pedestal-mounted STINGER) and MANPADS (shoulder-launched STINGER) fire units. ASAD has demonstrated the ability to passively detect, acquire, and classify fixed-wing, rotary-wing, and unmanned aerial vehicle (UAV) targets in an operational environment within the engagement envelope of shore-based AD (SHORAD) weapons systems. ASAD has reduced technology risks and provided technology alternatives for the demonstration and evaluation phase of the acquisition cycle.

ASAD has achieved its objectives by developing:

1. A vehicle-mounted ESM and acoustic-sensor capability that is fully integrated with Avenger and that has demonstrated the ability to detect, classify, identify, and track targets in a realistic battlefield environment
2. A man-portable ESM and acoustic-sensor capability to support target alert and cueing, with emphasis on trade-offs for maximizing performance while minimizing size, weight, power, and cost

3. Modeling and simulation tools for atmospheric acoustics that will help facilitate the design and deployment of acoustic sensor technology on the Marine Corps battlefield

ESM and acoustic passive sensors have been developed and demonstrated for both the Avenger and MANPADS fire units. Priorities are for Avenger first, followed by MANPADS. Maximum commonality between vehicle- and man-portable applications have been pursued. The Avenger's passive sensors will also have application to light armored vehicle (LAV)-AD fire units. The sensors will be integrated with the fire units and linked to the USMC Expeditionary Air Defense System (EADS) via the single channel ground-to-air radio system (SINCGARS) remote terminal unit, which will be used as the passive sensor display and fusion device. Data fusion (active and passive target tracks) has been demonstrated, where practical, within the scope of the effort. Sensor performance against fixed-wing, rotary-wing, and UAV targets will be measured, and the benefits gained over the unaided gunner (e.g., detection range, reaction time) will be evaluated.

Army Forward Area AD (FAAD) NCTR sensor technology will also be evaluated and modified, if necessary, to meet notional requirements for Avenger, where applicable. ESM and acoustic sensor prototypes developed at NSWCDD, along with industry support, have been used to demonstrate the desired capability for the MANPADS. In addition, algorithms from the underwater sonar community have been adapted for air acoustic solutions, wherever appropriate.

The Avenger project will demonstrate a vehicle-mounted ESM and acoustic dual-NCTR sensor capability that is fully integrated with the fire unit and the EADS. Performance will be evaluated in the presence of vehicle and generator-interference noise sources and typical RF environments.

The prime candidate for the ESM sensor of the Avenger system is the USMC's enhanced AN/VSX-2, which transitioned from the Amphibious Warfare Technology Directorate to the Program Manager-AD in fourth quarter 1994. The enhanced AN/VSX-2 was fabricated by Magnavox in FY95. Changes to the baseline AN/VSX-2 include a coarse direction-finding capability (rear 270 degrees), the ability to operate on-the-move, an improved processor, and other refinements to increase performance and reliability. Technical demonstration occurred during first quarter 1996. Test results, along with affordability issues, were used to support a decision in second quarter 1996 for a low-rate initial production. ESM sensors developed for the MANPADS can complement the AN/VSX-2 or serve as backups for the Avenger system.

For the STINGER MANPADS, this project has demonstrated two independent, man-portable, ESM and acoustic sensors that can provide the STINGER gunner a target-alert and cueing capability. Algorithms that can classify and identify targets have been and continue to be evaluated.

A user/developer consortium will be assembled to begin development of an authoritative, atmospheric acoustic modeling and simulation capability. Efforts will concentrate on:

- Evaluation of the existing modeling and simulation capability
- Identification of viable options to provide a near-term capability to support ASAD efforts
- Long-range planning to support the USMC's unique requirements
- A distributed interactive simulation (DIS) implementation for atmospheric acoustics

This program transitioned technology from an Applied Research (6.2) effort that demonstrated the potential of onboard NCTR and alert and cueing sensors for Avenger, LAV-AD, and MANPADS fire units. Work on the vehicle-based sensor was in cooperation with the Army. The MANPADS work was conducted in-house at NSWCDD with industry support. The ASAD program was a new start in FY93 and is managed by NSWCDD. Figures 5 through 8 show the ESM sensors (Avenger and MANPADS) developed at NSWCDD under ASAD.

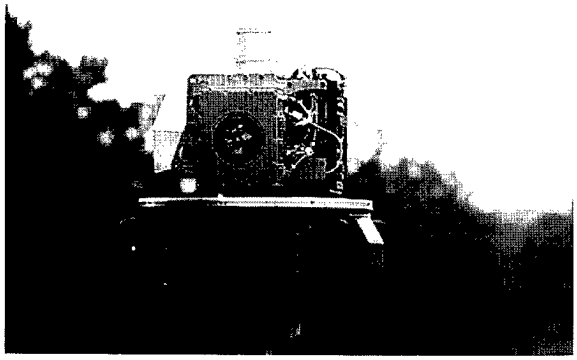

Figure 5. ASAD sensor close up

Figure 6. ASAD in test

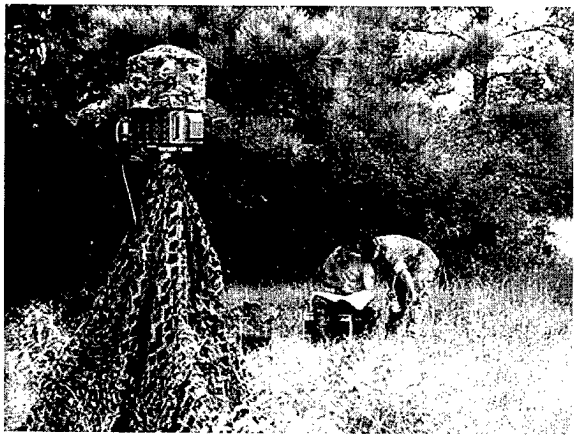

Figure 7. ASAD under USMC evaluation

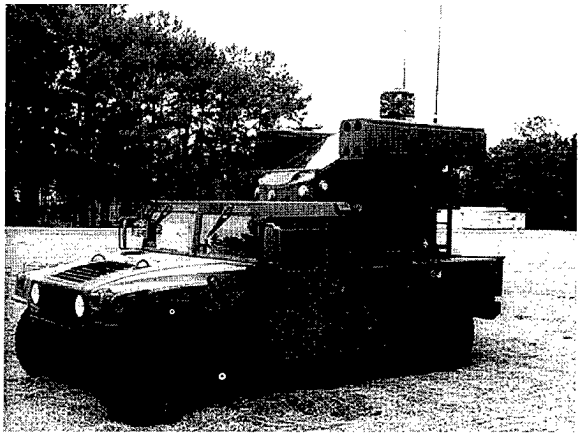

Figure 8. ASAD mounted on Avenger

Technology Evaluation Assessment Modeling and Simulation Facility

Beginning in FY97, USMC proof-of-concept demonstrations will be conducted within the physical context of an evolving TEAMS facility. Integration will be achieved with emergent NEF modeling and simulation capabilities. Operationally, Marine Light Regiment and Naval Strike Force assets and capabilities will be supported in the conduct of USMC operations. Measures of effectiveness will be determined at the engagement level.

Tactical and phenomenological realism will enable detailed system performance and military impact assessments to be performed. Material and combat developers who are charged with developing, procuring, and deploying effective sensor-to-shooter systems will have a much needed facility. Expeditionary warfare and USMC concept developers will be able to use the facility to support and execute Advanced Warfighting Experiments to assess OMFTS concepts, doctrines, and technology developments. Developers will have a facility that supports combat development, acquisition, and engineering processes. Test and evaluation specialists can also use the tool to plan, assess, and augment their processes as well. Engineers, analysts, and other technology developers are expected to be the principal users of the TEAMS facility.

Operationally, the primary benefit of the TEAMS facility will be the capability to enhance operational effectiveness by ensuring that the correct sensor is in the right place at the right time, and that the best shooter is provided

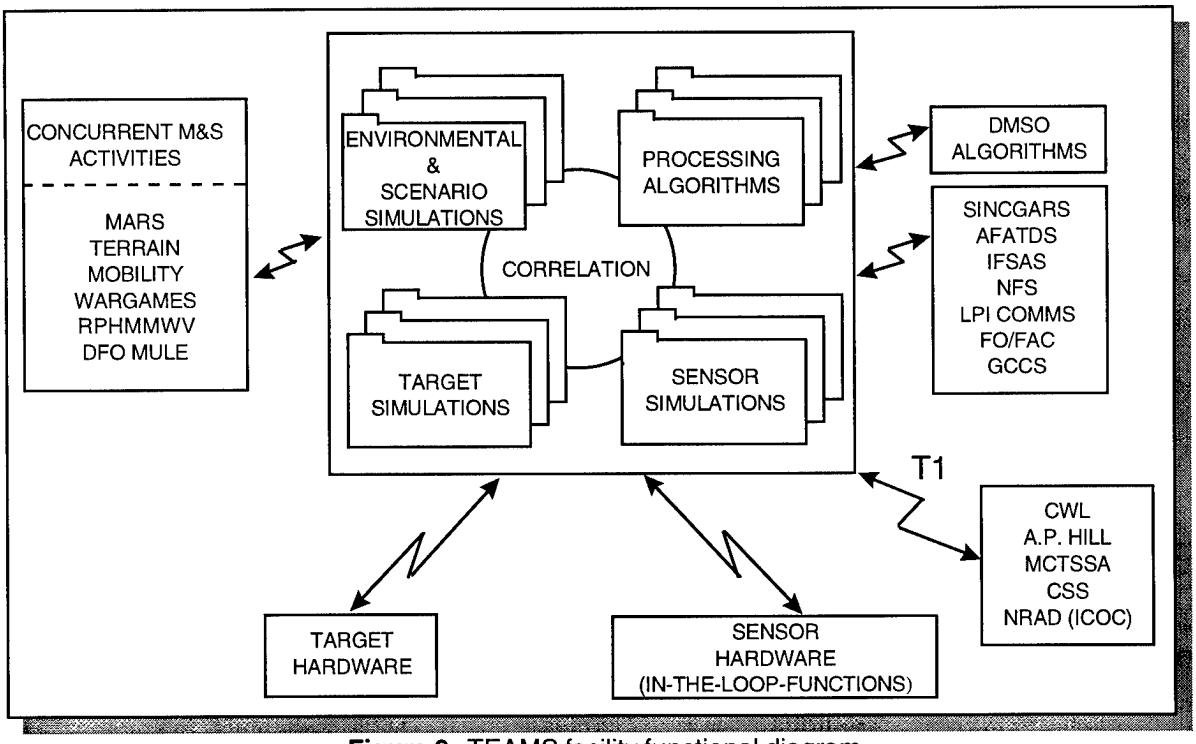

Figure 9. TEAMS facility functional diagram

the necessary information for successful engagement. This will, in turn, enable the NEF to successfully accomplish its mission in a timely fashion with significantly fewer resources and lower costs. Based on technology developed and assessed at the TEAMS facility, combat leader and battle staff training in the employment of sensor arrays can be similarly enhanced by providing a more realistic simulated environment.

The TEAMS facility will provide a high fidelity, synthetic, sensor-to-shooter engagement environment for detailed analysis and evaluation. Emphasis is placed on the tactical level, with aggregation to desired operational levels possible. Tactically relevant, high-resolution phenomenology of algorithms, sensors, targets, atmospherics, and obscurants can be evaluated, assessed, developed, and simulated with the technical focus on the sensor-to-shooter interaction. Lethality effects can be emulated for engagement fidelity with emphasis on the littoral domain.

Figure 9 depicts the functional and process design of the TEAMS facility. The facility possesses a core functionality that effectively integrates and correlates a very high fidelity environment, tactical force representation, and network management. The design allows for ease of entry to existing and emergent sensor simulators and models.

Representations of exploratory system concepts can be efficiently integrated for performance and military-worth assessments. The force manager can host MODSAF and Multiwarfare Analysis and Research Simulation (MARS) representations in standard and conceptual configurations.

Internal and external networking employs both DIS and MARS protocols and supports object-oriented data structures providing maximum reuse and flexibility without duplication. Emergent high-resolution Terrain is employed as a setting for the detailed phenomenology of the sensor-to-shooter interaction.

Leading edge technologies for simulating dynamic sensor-to-shooter interactions and phenomenology are applied. The environmental dynamics, tactical situation, sensor performance features, sensor array deployment, and target characteristics can be

variable, providing a thorough understanding of a sensor's technical and tactical performance.

Simulations can host a comprehensive aerial and ground-based tactical sensor array of remotely deployed and platform-based sensors. Aerial sensors can be simulated on platforms with a variety of flight profiles. Ground sensors can be mobile or stationary. Existing and emergent electro-optic, laser, magnetic, radar, and acoustic sensors can be hosted.

The capability to accept or emulate intelligence data from higher levels and joint-source sensors can be explored. Sensor fusion simulation technology can be explored and developed, and communication functions can be effectively emulated. Direct and indirect fire can be simulated with probabilistic battle-damage assessment provided as a result of the sensor-to-shooter interaction. Methods of engagement will be developed and integrated into the exploratory system during development.

The facility will be fully integrated into the NEF modeling and simulation system. The appropriate applications are being utilized to enable aggregated linkage through the desired battle staff hierarchy. Detailed interfaces are being developed that enable single and multiple tactical commander/leader real-time interface. Connectivity to selected Advanced Distributed Simulation Sites will be attained via designated MARS and DIS nodes. Command and coordination interface can be made with the designated simulation or communication system. Supporting scenarios and engagement vignettes can also be developed in coordination with the USMC to ensure operational relevance. The scenarios and vignettes support concepts of OMFTS, light regiment employment, and various NEF engagement options.

Additionally, combat and material developers need a robust, high fidelity facility to support concept evaluation and performance assessment in tactically and environmentally realistic simulation environments. TEAMS will allow user-friendly man-in-the-loop and system-in-the-loop operations. Developers will be able to evaluate the algorithms, sensors, and targeting systems in a nearby real (e.g., Fort A.P. Hill) or simulated battle space environment starting in the preparation phase and continuing through successful mission completion. The battle space environment covers the depth and breadth of the 2020 amphibious operating area and possesses the ability to focus on a system-level microcosm. Such ability will greatly enhance the effectiveness and quality of the engineering effort and support the decisions of acquisition and proponent managers from concept exploration through system fielding.

Currently under construction at NSWCDD, the TEAMS facility is staffed by personnel from NSWCDD's Systems Research and Technology, Ship Defense Systems, and Weapons Systems departments.

The Future

The goal of the AP section is to investigate and develop sensor and information processing capabilities that can be applied to new systems requiring the ability to detect and recognize targets in a *real-time* battlefield environment. The technology that has developed within the AP section has broad application to surveillance, scouting, targeting, fire control, information processing, and battlefield management in a variety of military systems. We can expect to continue to see advances across the spectrum of science. Already, new technologies have produced modern weapons systems with advanced features such as:

- Terrain mapping radar
- Fire-and-forget operation
- Laser-guided operation

The exponential growth of technology is transforming the modern battlefield into a high-tech conundrum where the weapons of war perform their missions at speeds beyond the human ability to assimilate information. Compounding the challenge, these capabilities are proliferating as technically advanced

nations, driven by increasingly competitive world economics, make even more advanced technologies not only available for any to purchase, but affordable as well. It can be argued that threat capabilities are available to the independent terrorist that were once available only to world superpowers.

Countering such numerous and diverse threats will require weapon and tactical intelligence systems of the future to deal with large amounts of loosely correlated data and to react accurately to rapidly changing information and conditions. Data from multiple, disparate sensors will have to be quickly and concurrently integrated into an accurate representation of the threat environment. The success of future weapons systems hinges on their ability to automatically detect and recognize targets of interest in a chaotic battlefield environment.

Through continued innovations, the AP section will continue to investigate and develop advanced sensor data-processing technologies, to provide future expeditionary-warfare weapons systems with the capabilities of automatic target detection, accurate target classification and, where appropriate, autonomous operation.

References

1. Marine Corps Combat Development Command, FMFRP 14-21, *Operational Maneuver from the Sea* (coordinating draft), 31 Mar 1995.
2. Holland, T.; Tarr, T.; and Farsaie, A., *An Artificial Neural System for Target Identification Using IR Imagery Data,* Independent Research and Independent Exploratory Development, pp. 5-30 through 5-33, Naval Surface Warfare Center, 1990.
3. Marine Corps Research, Development and Acquisition Command, Marine Corps Exploratory Development Program FY 1991 Block Plan, Marine Corps Air-Ground Technology CC1A PE 62131M, 30 Aug 1990.
4. Holland, O.T.; Poston, W.L.; and Nichols, K.R., "Enhanced Harmogram Analysis Techniques for Extraction of Principal Frequency Components," proceedings of The International Conference on Signal Processing Applications and Technology, Volume 2, pages 906 - 914, Nov 1992.
5. Poston, W.L., Holland, O.T.; and Nichols, K.R., *Enhanced Harmogram Analysis Techniques for Extraction of Principal Frequency Components,* 1993 NSWCDD Technical Report NSWCDD/TR-92/313, 1992.
6. Solka, J.L.; Priebe, C.E.; Hayes, H.I.; and Rogers, G.W., *Wavelet Transformations for Helicopter Identification Via Acoustic Signatures,* 1994 NSWCDD Technical Report NSWCDD/TR-93/169, 1993.

The Authors

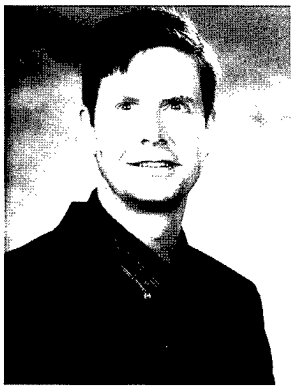

O. Thomas Holland

O.THOMAS HOLLAND received a B.S. degree in electrical engineering from Tennessee Technological University and an M.S. degree in electrical engineering from Virginia Polytechnic Institute and State University. Mr. Holland has published numerous technical reports and papers on signal processing, processing architectures, automatic target recognition, and nondestructive inspection. His work in the application of artificial neural systems to target identification from infrared imagery was selected for ONT accomplishments report and was a runner-up for the 1990 Independent Exploratory Development Award. Mr. Holland holds three patents for electronic devices and has a patent pending on a system for determining the roughness of manufactured surfaces. He presently directs the AP group in NSWCDD's Munitions Branch, holds a position on the Independent Research Information Sciences Panel, and serves as technical advisor to USMC research and development efforts.

ROBERT L. STIEGLER, Program Manager for Maneuver Warfare Technology in Dahlgren Division's Weapon Systems Department, received a B.S. degree in electrical engineering from the University of Wisconsin; an M.B.A. from Roosevelt University - Chicago; and is currently working on a Ph.D. in public administration at Virginia Tech. After serving six and a half years in the U.S. Air Force, he began his civilian career as a radar technician on EC-121 Airborne Early Warning Aircraft. After two years as a quality assurance specialist on the MK-48 Torpedo Program, he joined the Naval Training Systems Center (NTSC) where, over a 15-year period, he established two training system support activities in support of shipboard, antisubmarine warfare (ASW), Aviation, and Marine Corps Training Devices. He was Head of NTSC's Aviation and Marine Corps Engineering Division from 1986 to1988, after which he served over two years as Science Advisor to the CG, FMFLANT, for which he received the Navy Superior Civilian Service Award. He joined NSWCDD in 1990 as Assistant Director of the Naval Science Assistance Program, subsequently as a branch head in the Strike Systems Department. Currently, Mr. Stiegler is the Program Manager for Maneuver Warfare Technology supporting U.S. Marine Corps (USMC) Science and Technology and Deputy of the NSWC Center of Excellence for Expeditionary Warfare Technology. Mr. Stiegler received the Technology to Sea Award in 1995 and was awarded the Navy Meritorious Civilian Service Award by the USMC in 1996.

Robert L. Stiegler

WENDY L. POSTON received her bachelor's degree with high honors from Cameron University in 1989, with majors in physics and mathematics. She received a master's degree in aerospace engineering in 1991 from George Washington University and a doctorate in computational statistics from George Mason University in 1995. Dr. Poston has been employed at NSWCDD since 1991. Her research interests are in the development of real-time automatic target recognition systems, nondestructive testing, and signal processing. She conducts basic research in support of NSWCDD's Independent Research program and the USMC, in statistics and signal processing. She won the Independent Research Excellence Award in 1995 for her work in probability density estimation. Dr. Poston has written over 35 papers, has been granted three patents in artificial intelligence, and has a patent pending on a system for determining the roughness of manufactured surfaces.

Wendy L. Poston

CHARLES W. STEADMAN, JR. received a B.S. degree in electrical engineering from West Virginia Institute of Technology in May 1985. Since then he has been employed at NSWCDD, where he is primarily a hardware design engineer with experience in designing microprocessor and DSP systems, high-clock-rate digital and ECL circuits, high-speed communication, and full-motion video. He has worked on two NSWCDD Independent Exploratory Development programs, one of which was the IED project of the year in 1990. His work in the Munitions Branch has been in missile simulation, guidance, and control; most recently, he works as principal design engineer on the Marine Corps' ASAD project.

Charles W. Steadman

FO/FAC Brings A Digital Link to the Forward Fire Support Teams

Craig T. Melton

To shatter the enemy's cohesion and limit their capability to resist, Marine Air-Ground Task Forces (MAGTFs) rely heavily upon the synergism between two force elements: the mobility of their ground combat units and the fire power of supporting arms. The supporting arms employed may be organic mortar and artillery units from ground combat elements, aircraft from the MAGTF air combat element or, in a joint environment, assets from Navy, Army, Air Force, or allied forces. Key to the success of supporting arms is the transmission of accurate and timely target coordinates from the forward fire-support team to the correct coordinating agency for action. Reducing the time line from "sensor" to "shooter" increases both the effectiveness of supporting arms and the survivability of the observer. The Naval Surface Warfare Center, Dahlgren Division (NSWCDD), acting as the technical direction agency for the Marine Corps Systems Command (MARCORSYSCOM) Forward Observer/ Forward Air-Controller (FO/FAC) program, has developed a system to quickly and accurately calculate target coordinates and transmit them to the correct fire-support coordinating agency for action. The system uses an eye-safe laser rangefinder, a magnetic compass and tilt angle sensor, a Global Positioning System (GPS) precise-code (P-code) receiver, and a digital modem.

EW
EXPEDITIONARY
WARFARE

Introduction

Expeditionary forces are those which are able to function where no supporting infrastructure exists. The U.S. Marine Corps (USMC) has traditionally been the expeditionary force relied upon to rapidly deploy in possibly austere environments in support of National Command Authority tasking. To be effective in such an environment, the USMC must be light and mobile, yet not sacrifice the firepower necessary to succeed in their mission. This firepower is generated through combined arms, where infantry, armor, artillery, tactical aviation, and naval gunfire capabilities are integrated into an overwhelming force.

For combat missions, USMC units are commonly organized in MAGTFs. Each MAGTF has one or more ground combat elements, each of which may include artillery and armor units, and an air combat element combining fixed- and/or rotary-wing aircraft. These elements must be capable of drawing upon their own and other elements' supporting arms to achieve combined arms. Various fire-support agencies are developed throughout the MAGTF hierarchy, through which fire-support requests are received and evaluated against the commander's intent. The goal for these fire-support agencies is to approve requests for fire in less time than it takes the tasked supporting-arms unit to be ready to fire—a typical goal being 60 sec for artillery, naval gunfire, or mortar requests. However, before requests for supporting arms are received by the fire support agencies, targets must be located and identified by some source. The most important source of targeting information is the foot-mobile soldier.

Fire support teams are defined as forward observers (FOs) for artillery and mortars, forward air-controllers (FACs) for close air support (CAS), and Air Naval Gunfire Liaison Company (ANGLICO) teams for naval gunnery and aviation. Each team has the basic requirement of locating and classifying targets and transmitting this information back to their respective fire-support controlling agency. Up to a few years ago, these teams relied heavily upon maps, a compass, and a lot of experience to do their job. A good fire-support team could call in fire to within approximately 200 m of a target on the first shot and adjust to within 50 m (typically considered the required accuracy) with two more shots. All position calculations and adjustments were done by hand and rules of thumb, and relayed to the fire-support agency by voice over a radio, typically a very slow process. During the time the observers are calculating this information, voicing it over the radio, and adjusting fire, they could be detected by the enemy, who would make themselves less vulnerable and take action against the observers. Recent deployment of GPS receivers and the AN/GVS-5 laser rangefinder have helped reduce the mission time line by allowing observers to quickly orient themselves to the map and determine an accurate range to a target. However, errors in estimating azimuth angle still introduced large first-shot miss distances, and voicing data over the radio led to target data lateness and error.

NSWCDD, acting as the technical direction agency for MARCORSYSCOM's FO/FAC program, has developed a system that utilizes an eye-safe laser rangefinder, magnetic compass, tilt angle sensor, GPS P-code receiver, and digital modem to quickly and accurately calculate target coordinates and transmit them to the correct fire-support coordinating agency for action. The field user simply acquires the target with the laser rangefinder, fires, and the target's location is calculated utilizing information from sensors in the laser-rangefinder unit and GPS receiver. The observer then needs only to push a button to send the data digitally across the radio net to the correct fire-support agency.

System Hardware

The FO/FAC Advanced Technology Demonstration system consists of three primary subsystems: the mission module, the control display unit (CDU), and the targeting subsystem (see Figure 1). This modular approach allows each subsystem to be modified with minimum impact on other subsystems. Total system weight is under 18 lb, making FO/FAC man-portable. In addition to the three primary subsystems, a mission planning station (MPS) was developed to facilitate rapid preplanning of tactical scenarios.

The mission module is the centerpiece of the FO/FAC program (see Figure 2). It contains a miniaturized, precision lightweight GPS receiver; an Automatic Target Handoff System II (ATHS-II) digital modem; a commercially available control processing unit; and a power management board. The GPS receiver

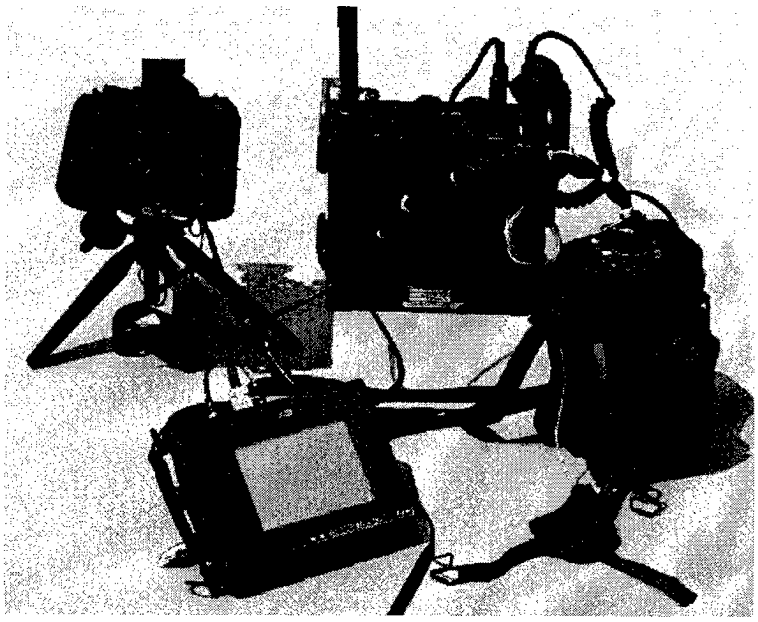

Figure 1. *The FO/FAC system*

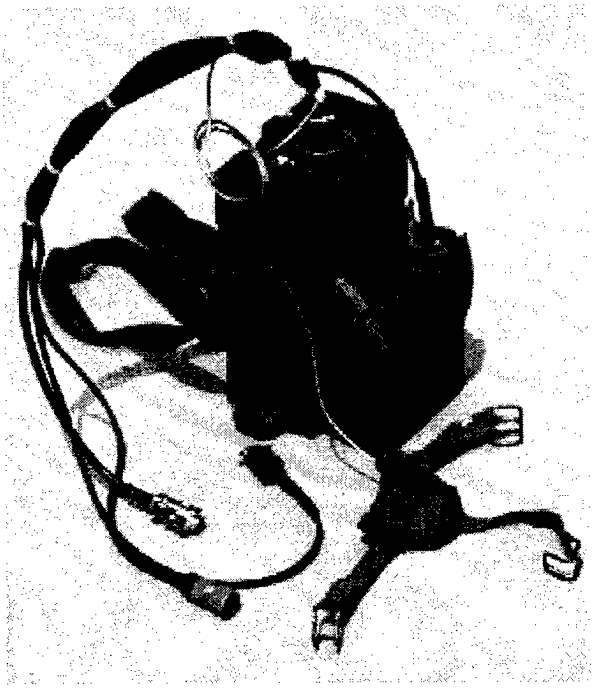

Figure 2. FO/FAC mission module

utilizes P-code and determines the position of the system to within 16-m spherical error probable (SEP) using a helmet-mounted GPS receiver.

The ATHS-II modem is a tactical data modem manufactured by Rockwell International, Collins Avionics and Communications Division. The modem supports a variety of data-link, digital-message-device, and transmission formats, including USMC Marine Tactical System (MTS), U.S. Army Tactical Fire Direction System (TACFIRE), and U.S. Air Force Applications Program Development (AFAPD) protocols. The ATHS-II modem is currently being integrated into the USMC AV-8B *Harrier* aircraft and is a tentative upgrade to the F-18/D *Hornet*.

The CDU is the man-machine interface to the FO/FAC Advanced Technology Demonstration system (see Figure 3). The current CDU is a commercially available Hardbody PC, magnetic pen-based computer. This computer utilizes a menu-driven, touch-sensitive display to enact system commands. The CDU has the capability to read a floppy disk, which can be preprogrammed with relevant fire mission data from the MPS to lessen the observer's workload. Custom software was developed so that observers entered mission information in a sequence derived from the way current fire-support teams run their missions. Combined with the touch-sensitive, menu-driven display, observers were consistently able to operate the FO/FAC system within minutes of picking it up.

The primary targeting system for FO/FAC is the AN/PVS-6 Miniature Eye-Safe Laser Infrared Observation Set with Compass Vertical Angle Measurement module (MELIOS C/VAM) (see Figure 4). This rangefinder is a

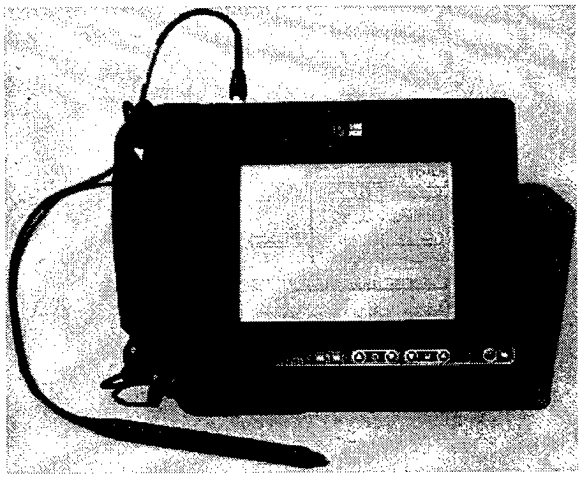

Figure 3. FO/FAC control display unit

Figure 4. MELIOS C/VAM

class IIIa, erbium glass laser operating at 1.54 μm, making it eye-safe. Weighing 4.5 lb, the MELIOS C/VAM can be handheld or mounted on a tripod. While this system gives accurate target location coordinates, it has no laser designation capability. A second targeting system for FO/FAC is the AN/PAQ-3 Modular Universal Laser Equipment (MULE). This currently fielded system provides laser designation capability, but at a significant penalty: it operates at a wavelength of 1.06 mm (not eye-safe). In addition, the MULE weighs close to 40 lb.

System Accuracy

One of the key requirements of the FO/FAC system is the calculation of an accurate target coordinate. The GPS receiver utilizes P-code to determine user location to within 16 m SEP. The targeting subsystem then determines the range, azimuth, and elevation angles to the target. This information is combined to calculate a 10-digit Military Grid Reference System coordinate based upon the World Geodetic System 1984 (WGS-84) datum.

Given the demonstrated accuracy of P-code GPS, the key to computing an accurate target coordinate was the performance of the MELIOS C/VAM. Errors in computed range, azimuth, and elevation angles to the target translate into inaccurate target grids. In order to characterize the performance of the system, a test was conducted on NSWCDD's main range. For this test, a number of visible targets were surveyed, and their coordinates were translated into WGS-84 10-digit grids. The FO/FAC system was operated from a known point and used to calculate the grids to these targets on several different test days. The targets were located over an entire 360-deg azimuth sweep, and successive targets were lased after moving through significant azimuth deltas.

The MELIOS C/VAM system was calculated to have 1-σ accuracy of 15 mil in azimuth, 5 mil in elevation, and 3 m in range. Combining these with GPS errors results in the error distribution shown in Figure 5. For ordnance with steep approach angles, the altitude error becomes less important and, typically, a circular error probable (CEP) is calculated. The CEP is simply the radius of a circle within which 50 percent of the rounds will fall. The CEP for the system was calculated utilizing an algorithm that incorporates uncorrelated elliptical Gaussian distributions.[1] The CEP for the FO/FAC system is plotted in Figure 6.

From Figure 5, it is clear that the major source of error is the azimuth measurement. The C/VAM unit determines azimuth by sensing the local magnetic field and correcting for any magnetic anomalies determined in the

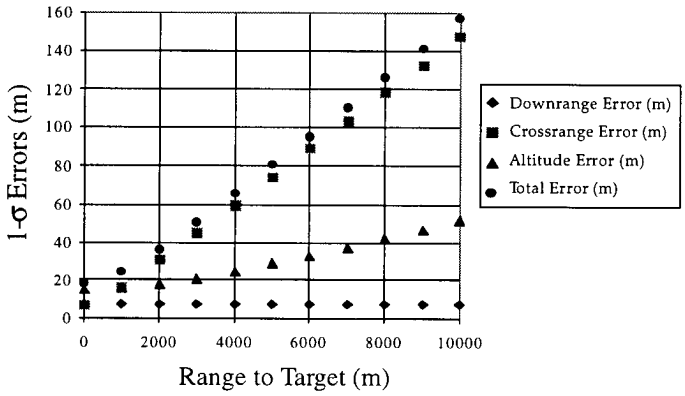

Figure 5. FO/FAC 1-σ errors for target at same altitude as observers

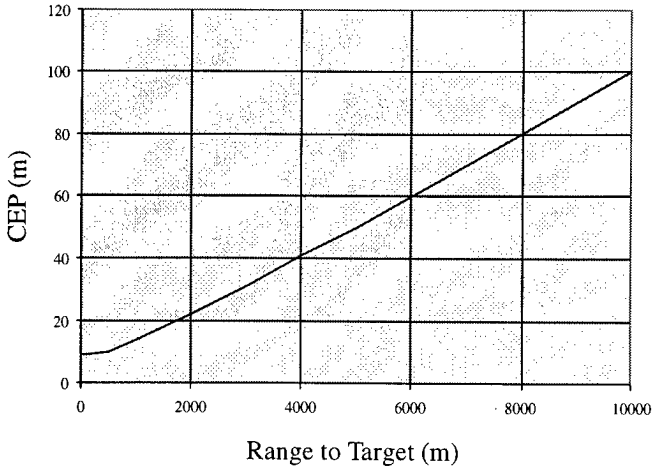

Figure 6. FO/FAC CEP vs. range

C/VAM calibration. The calibration procedure begins with taking azimuth measurements in a predetermined pattern, from which a set of corrective constants are determined. The error in this correction plus the measurement error of the device yields the total measurement error. In addition, these corrective constants are accurate only for the magnetic field at the time of calibration, and any local magnetic changes will introduce additional error.

Test Scenarios

To test the viability of the FO/FAC concept, the system underwent extensive testing in simulated operational environments. Basic scenarios were developed for CAS, field artillery, and naval gunfire missions (see Figure 7). Relevant digital messages were developed in the appropriate protocols for the given scenarios to check mission flow and ease of operator use.

The CAS missions were run with an ATHS-II equipped AV-8B *Harrier* at China Lake, 29 Palms, and Chocolate Mountain Gunnery Range in California. Mission flow included:

- The aircraft sending the FAC an on-station report (OSR) message
- The FAC sending the pilot a nine-line brief
- The pilot modifying the nine-line brief as appropriate and sending it back to the FAC for mission confirmation
- The pilot sending the FAC a departing initial point (IP) message
- The FAC sending a "cleared-hot" or "abort" message as appropriate

All messages were sent in the MTS format over an AN/PRC-113 radio. The OSR message is sent from the aircraft once it reaches the control point designated for the sortie. This message lets the FAC know that the plane is available for a mission. The FAC then creates a nine-line brief which contains all relevant mission information, such as the target coordinate, IP from which the plane is to approach, egress point from which the plane will leave, target type, suggested ordnance, etc. The pilot then changes any parameters that cannot be met and sends these back to the FAC in the

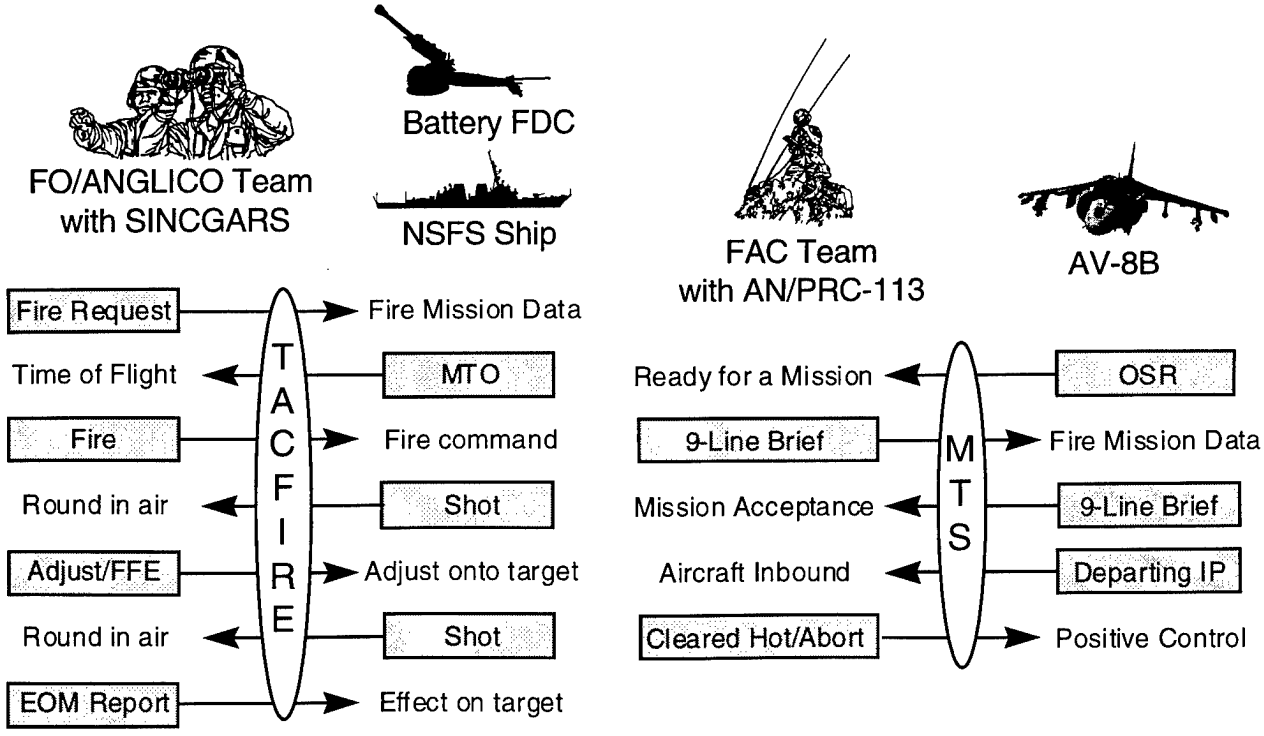

Figure 7. FO/FAC operational scenarios

"negotiation" phase. Once the pilot is satisfied with the mission, it is accepted by the *Harrier's* mission computer with the press of a button. The FAC-computed target coordinate is then displayed on the *Harrier's* head-up display. The pilot sends a departing IP message to the FAC advising that the plane is inbound on an attack profile. The FAC then attempts to visually acquire the aircraft approaching from the IP and clears it "hot" if it is approaching from the right direction and nothing significant has changed in the target area, or aborts the mission if the tactical situation has changed. This is referred to as positive control of the aircraft—the aircraft cannot drop ordnance unless the FAC can see it, and both the FAC and the pilot can see the target. This technique is applied to avoid casualties from friendly fire.

The FO/FAC system achieved great operational success with the AV-8B in these tests. Over 20 Mk 76 practice bombs were dropped at 29 Palms on a variety of targets at ranges up to 7 km from the FAC. All bombs were dropped on uncorrected FAC-generated coordinates, and all had effect on the target.

Field artillery missions were run with the 10th Marines at Fort Bragg, North Carolina. The missions run included fire-for-effect (FFE) and adjust-fire missions, utilizing "when ready" and "at my command" as control techniques. Basic mission flow included:

- Sending the battery Fire Direction Center (FDC) a call for fire
- Receiving a message-to-observer (MTO) from the battery
- Sending a fire command to the battery
- Receiving a shot command from the battery
- Sending adjust-fire missions to the battery
- Sending end-of-mission (EOM) messages to the FDC

Messages were sent in the TACFIRE protocol over a single-channel, ground-to-air radio system (SINCGARS) radio. The call-for-fire message is similar to the CAS 9-line brief in that it contains target coordinates, target type, suggested ordnance, etc. Once the call for fire is accepted, an MTO is sent relaying, among other things, the predicted time of flight of the projectile. When the battery sends the shot command to the FO, a countdown clock appears; when the count reaches zero, the round should impact. Any necessary adjustments are made by the FO's lasing where the round impacted; the relevant corrections are automatically computed and sent back to the battery with the touch of the CDU pen. The EOM message relays the effect achieved on the target back to the FDC.

Evolutionary or Revolutionary?

The current FO/FAC system was developed with commercial off-the-shelf equipment to demonstrate an improved capability to the Marine Corps. As such, it was designed to operate under current supporting arms doctrine. However, exploration of new possibilities for the system is just beginning. The digitization of the battlefield holds much promise in making smaller forces more effective by enhancing battlefield awareness and unit capabilities across the entire spectrum of conflict. The current evolutionary FO/FAC system may demonstrate revolutionary capabilities on the battlefield.

Nonvisual Close Air Support

The FO/FAC system may be the first step toward safe and effective nonvisual CAS. Nonvisual CAS occurs when the FAC cannot see the aircraft, and the aircraft cannot see the target. Performing nonvisual CAS, sometimes referred to as "bombing on coordinates," allows release of weapons from higher altitudes, thereby reducing aircraft losses to surface threats. In addition, CAS could be performed in inclement weather and at night. According to the Center for Naval Analysis, the five steps required for nonvisual CAS include:

1. Acquire a target and establish that it is legitimate (i.e., that it belongs to the enemy).
2. Determine the three-dimensional coordinates of the target with respect to a common geodetic datum or frame of reference (e.g., WGS 84).

3. Pass those three-dimensional coordinates to the CAS aircraft over a quick, secure, and reliable link.
4. Maneuver the aircraft to enable the weapon to reach the target.
5. Obtain prescribed weapon function to achieve kill criterion on the target, but avoid incapacitation of friendly troops in the area.

The current FO/FAC system performs the first three of these requirements during daylight operations, using the observer's visual inspection of the target to classify it as an enemy. The addition of night-vision optics or a forward-looking infrared device would expand options to night and conditions of degraded visibility, and an identification, friend or foe (IFF) capability would allow nonvisual CAS even on a cluttered battlefield.

Combat Identification

Combat identification, or IFF capability, has become an increasingly important consideration for the dynamic battlefield of the future. The FO/FAC system, coupled with an advanced Command, Control, Communications, and Intelligence (C^3I) network, shows great promise in relaying IFF data back to the command element to improve situational awareness. The army recently purchased several FO/FAC systems for integration into their experimental Battlefield Combat Identification System hardware. This vehicle-mounted system will not only lase the target to get its coordinates, but also interrogate the target to determine if it is friend or foe. This information is relayed back to the command element for overall situational awareness, or to the incoming CAS aircraft to indicate which forces are friendly, and which are not, in a cluttered battlefield.

Rapid Force Projection Initiative (RFPI)

The RFPI program is an army-sponsored program that employs observers at echelons lower than the battalion. The RFPI concept was initiated as a result of the slow buildup of heavy forces in the Gulf War. It was recognized that rapidly deployed, light forces were initially vulnerable because of lack of firepower. The RFPI model involves groups of highly mobile "hunters" infiltrating an area and engaging targets with heavy fire-support elements, or "killers." These hunter teams, backed by killer assets, give light forces the punch they need to survive until heavy friendly forces arrive. The RFPI program has purchased five FO/FAC systems for evaluation as possible hunter systems.

Unmanned Aerial Vehicle (UAV) Integration

The integration of a FO/FAC-type system in a UAV will allow remote sensing of targets, further reducing the time an observer is exposed to the enemy. The airborne system will lase on a target signature provided by a sensor, and calculate the grid point of that target. The data will then be relayed to the observer or to the coordinating agency for action. This capability can be used to greatly enhance situational awareness and improve the assessment of effects achieved on targets due to indirect fires. A new program designated Automatic Target Acquisition FO/FAC has recently been initiated at Dahlgren. This program integrates the FO/FAC system with a UH-1N helicopter, which simulates a UAV.

Conclusions

The FO/FAC program has successfully demonstrated that a foot-mobile, supporting arms observer can quickly determine an accurate target coordinate and digitally hand off this coordinate to a fire-support element in a useful format. This capability significantly enhances survivability of the observer and effectiveness of fire support. In addition, the availability of a reliable digital link in forward positions has spawned interest in a number of areas relevant to the expeditionary nature of battle in the 21st century.

Acknowledgments

The author would like to acknowledge Joe Sholander for contributions to this article and

for leading the FO/FAC program from its inception.

Reference

1. DiDonato, A.R. and Jarnigan, M.P., *A Method for Computing the Generalized Circular Error Function and the Circular Coverage Function*, NWL Report No. 1768, U.S. Naval Weapons Laboratory, Dahlgren, VA, Jan 1962.

The Author

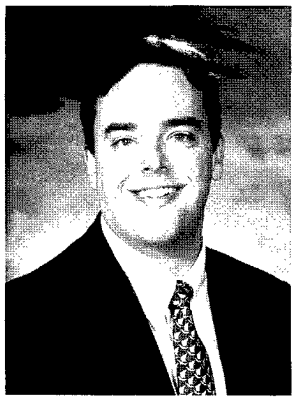

Craig T. Melton

CRAIG T. MELTON received his B.S. degree in aerospace engineering from the University of Maryland in May 1990. He joined the NSWCDD Munitions Branch in December of that year and began working in the area of aeroballistic modeling and simulation for a variety of projectiles. His most recent work has focused on Marine Corps tactical sensors. He recently received an Award of Merit for Group Achievement, for work on the Electrothermal Chemical Gun team, and a Technology to Sea Excellence Award and Marine Corps Achievement Award for his work on the FO/FAC program. Mr. Melton graduated from the Naval War College in May 1996 and is currently working toward an M.S. in aerospace engineering from the Virginia Polytechnic Institute and State University.

Horizon Infrared Surveillance Sensor: Applied Research for Infrared Search and Track Systems

Robert Headley, Ken Hepfer, Patrick Dezeeuw, Bill Trahan, and Angela Plante

EW
EXPEDITIONARY
WARFARE

The Horizon Infrared Surveillance Sensor (HISS) project is a multiyear effort to investigate Infrared Search and Track (IRST) technologies for surface navy applications. Areas investigated include single-scan target detection, single infrared-(IR-)band target detection, and IRST operation within a multisensor integration (MSI) context. Each phase of the HISS project investigates particular characteristics of IRST operation and provides a system with specific capabilities to support scheduled MSI experiments and test events. This article discusses IRST systems and the construction of HISS systems. In addition, the article presents data collected during the most recent series of land-based tests.

Introduction

The U.S. Navy and other navies of the world have been experimenting with IRST systems for more than 20 years. These systems work passively to detect inbound missiles based on the thermal contrast between the missile and its background. Since faster missiles tend to have more thermal signature, the IRST can provide target detection against those missiles that are most stressing to current combat systems. Because of the frequencies at which they operate, IRST systems are immune to radio frequency (RF) multipath effects that influence the performance of current radar systems. With the resolution of IRST systems, these sensors can provide extremely accurate target positional information.

Early IRST system designs were at times hampered by limitations in technology areas, such as detector manufacture, computing power and speed, and stabilization capabilities. Through the years, IR technologies have progressed to the point where it is now possible to procure commercially available components and, with only slight modification, integrate those components as an IRST system. These systems can be operated in a military environment, they can be used to confirm existing theory, and they can be used to investigate IR phenomenology.

In 1992, the Naval Surface Warfare Center, Dahlgren Division (NSWCDD), established a program of applied IRST research in support of ongoing efforts in the area of MSI. The program that was established

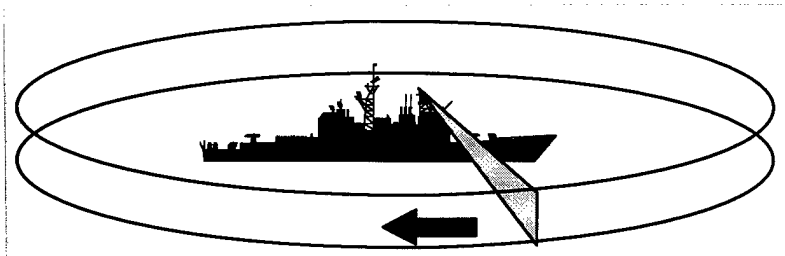

Figure 1. Scan pattern for an IRST

investigates particular areas of IRST design while providing equipment to support MSI testing and demonstration.[1]

This article discusses IRST systems, the structure of the HISS project, the construction of HISS systems, and the measured performance of HISS systems during field tests. In addition, the article provides some examples of observed IR phenomenology. The range performance data presented were collected during an MSI test event that was held at the Naval Surface Warfare Center, Wallops Island Detachment, from November 1993 through April 1994.[2] System accuracy data were collected during an MSI test event that was held at the Search and Track Sensor Test Site at NSWCDD from June through September 1995.

Infrared Search and Track Systems

A shipboard IRST system scans a sector or swath in space in order to passively detect antiship cruise missiles (ASCMs), as shown in Figure 1. IRST systems work in the midwave infrared (MWIR) (3 to 5 μm) or longwave infrared (LWIR) (8 to 12 μm) bands of the electromagnetic spectrum. IRST systems have been used in ground-based and airborne applications to detect targets. For these systems, the expected targets, the environment, and the battle space are different than in the shipboard application. The differences will influence design choices for scan rate, field of regard, IR spectral band, and type of signal processing, among others.

IRST systems have also been developed for surface navy applications. The French Navy currently has two *Veille Air Mer Panoramique Infrarouge* (*VAMPIR*) IRST systems in operation, as shown in Figure 2. The Royal Dutch Navy has extensively tested their IRSCAN system, which is used in conjunction with their GOALKEEPER self-defense system. The Israeli Navy has tested a unit that they call SPIRTAS, but that unit was not fielded on an operational ship. The U.S. Navy, in cooperation with the Canadian Department of National Defence, developed a shipboard IRST system known as the AN/SAR-8, shown in Figure 3. That unit was tested at a land-based test site and on a test ship, encountering some 600 target sorties during the test program.[3] A programmatic decision was made not to procure more than the two engineering development models produced under the AN/SAR-8 program.

IRST systems work by sensing the thermal contrast between a target and its background. They scan a region of space, most commonly 360 deg in azimuth with a narrower elevation angle. Scan rates commonly used are on the order of 30 to 60 rpm,

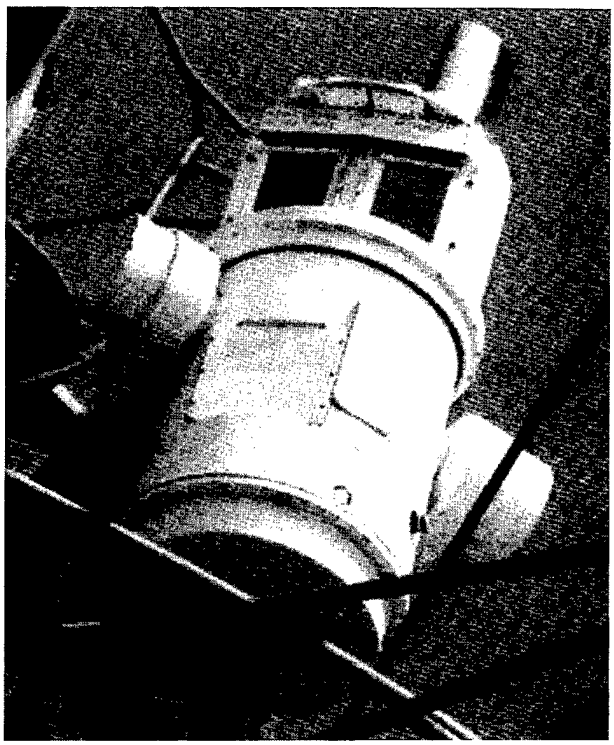

Figure 2. French Navy VAMPIR IRST system

although scan rates outside of these bounds have been tested. IRST systems generally develop target detection reports and, usually, target tracks that are reported to an external engagement system.

In operation, the atmosphere between the target and the IRST sensor attenuates the received signal. Atmospheric transmission is dependent on the weather, on the area of operation (i.e., maritime, ground, air), on the specific IR band of operation, and on the altitude of the sensor. For a sensor operating in the maritime environment, at sea level, the target signal is greatly reduced after being transmitted through the atmosphere. Therefore, transmission, or—more generally—the weather, greatly affects the performance of IRST systems. Models used to predict the performance of IRST systems sometimes employ large weather databases and develop a statistical prediction of the performance of these systems in "worldwide" environments.[4] A plot of the transmissions derived from just such a weather database is provided in Figure 4.

Figure 4 shows transmission data calculated from the "Random 384" worldwide weather database, also referred to as the "R384." The R384 is a database of weather observations collected in four locations: 96 observations to represent the Baltic Sea, 96 observations to represent the Yellow Sea, 96 observations to represent the Persian Gulf, and 96 observations to represent the Caribbean Sea. These 384 observations, representing a "statistically significant" sample, are useful in predicting the performance of IRST systems because they provide a large mix of weather profiles and, therefore, actual transmissions that can be expected in the worldwide environment.

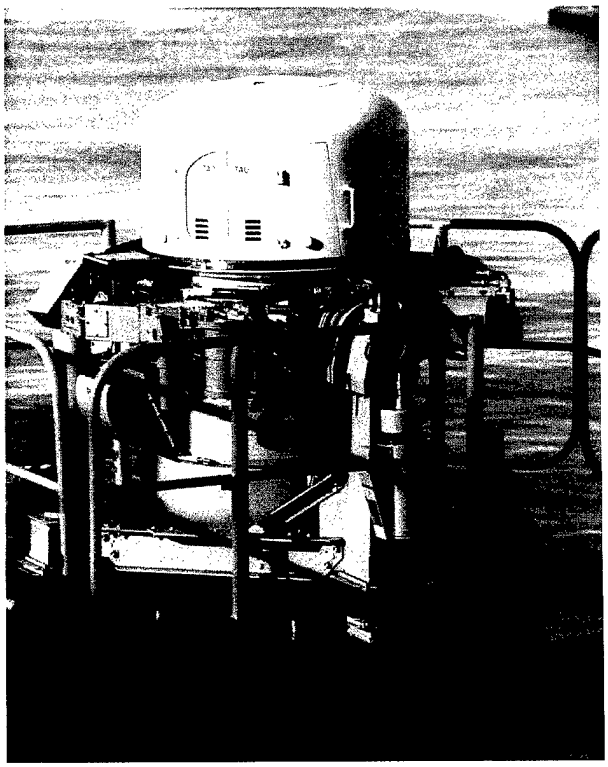

Figure 3. U.S. Navy AN/SAR-8, IRST designation system

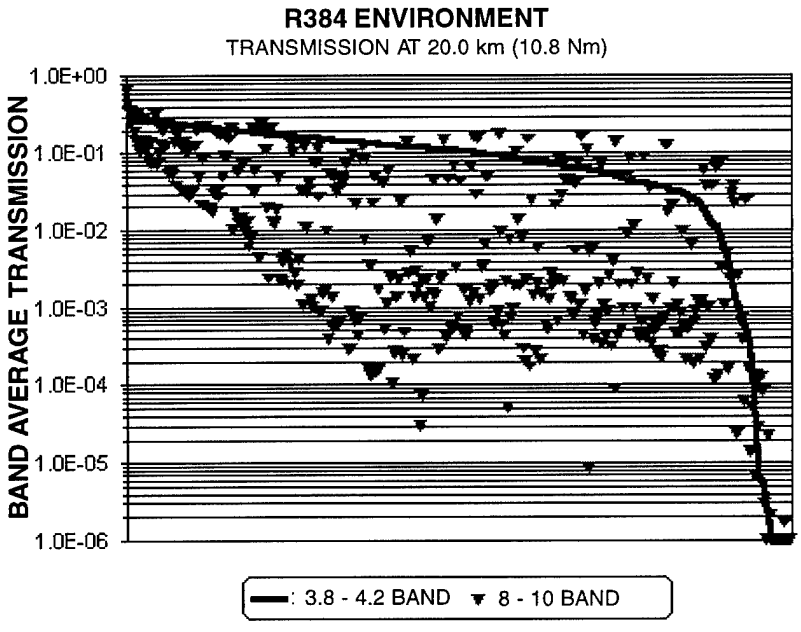

Figure 4. A comparison of the transmission, over a 20-km path in MWIR and LWIR bands for the R384 Worldwide Weather File

The MWIR transmission data in Figure 4 have been sorted from best transmission to worst transmission (left to right) before being plotted. For each observation in the R384 sample, the LWIR transmission data in Figure 4 are plotted at the same abscissa as the

corresponding MWIR transmission point. The figure shows that transmission in the MWIR band is generally more consistent over all of the weather environments. In 15.36 percent of the cases in the R384, transmission in the LWIR is slightly better. In the remainder of cases, the MWIR offers better transmission, and quite often, *much* better transmission.

Another aspect to be considered is the signature of the target. Figure 5 shows target signature caused by aerodynamic heating alone. These notional signatures do not include any contribution from hot engine parts or from exhaust plumes. These are calculated signatures based solely on speed, size, and emissivity of the airframe. Three curves are provided, for Mach 1, Mach 2, and Mach 3 targets. The signatures have a peak, which moves towards the lower wavelengths as target speed increases. For very fast targets, the MWIR band becomes the band of most utility. It has the most target signature and the best transmission. For slower targets, the selection of band is not as obvious. There may be enough of a target signature benefit in the LWIR, for slow targets, to outweigh the lack of transmission in that band.

The Horizon Infrared Surveillance Sensor Project

The HISS project is a multiyear effort to investigate IRST technologies, specifically in the areas of single-scan target detection, single IR-band target detection, and IRST operation within an MSI context.[5,6] The project is executed in multiple phases in order to investigate particular characteristics of IRST operation and provide systems with specific capabilities to support scheduled MSI experiments and tests.

The objectives of the HISS project are to:

- Verify the contribution of IRST in highly interactive MSI experiments
- Validate single-scan target detection for supersonic targets
- Determine the merits of IR dual sub-band target/clutter discrimination
- Act as a surrogate during tests and demonstrations that require the presence of an IRST system

The project is performed in three phases that explore and provide prototype equipment for different aspects of the IRST target detection problem. The Photonic Systems Branch at NSWCDD is the project's program management office and the integrator of the

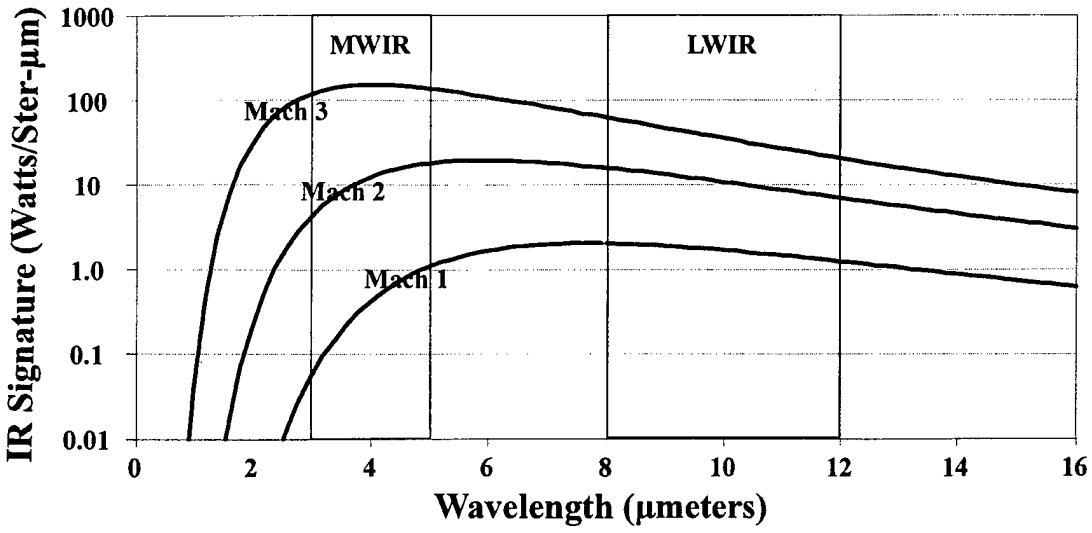

Figure 5. Target signature caused by aerodynamic heating for three target speeds

system components. Major system components are obtained by contracting for specific equipments. The goals of each phase are as follows:

Phase 1

- Develop a prototype sensor of requisite sensitivity and resolution for "horizon limited" detection of supersonic targets
- Participate in joint IR/RF data collection exercises
- Collect and record seaside IR data with the prototype sensor
- Develop single-scan target detection algorithms that operate on the recorded data

Phase 2

- Develop a prototype real-time signal processor that implements the algorithms developed under phase 1
- Develop a prototype sensor and stable platform to scan a limited sector with the required sensitivity, resolution, and positional accuracy
- Develop a real-time interface to an MSI processor
- Participate in MSI field experiments

Phase 3

- Develop prototype IR scanner and detective assemblies to provide full 360-deg coverage
- Upgrade the signal processor capability to include multiscan detection and track initiation
- Participate in MSI field experiments
- Evaluate dual sub-band target/clutter discrimination using recorded data

Field Test Experience With HISS Systems

Data were collected using the HISS phase 1 sensor in March and April 1992.[7] The phase 1 system was composed of an MWIR focal plane array (FPA) imaging sensor, a positioning mount to point the sensor, and a data collection, digitization, and recording station. The digital sensor video was used in the development of non-real-time target detection algorithms after the data collection event.

The HISS phase 2 system was used as a data collection and real-time target detection device during testing from November 1993 to April 1994 and again from June through September 1995. Operated at waterside, land-based test facilities, the system provided target detections in real time to an external MSI processor. The system components included an electromagnetic interference-(EMI-)tight equipment van, an MWIR FPA sensor, a scanning pedestal system, a real-time signal processor, a system control center, a real-time external interface, and assorted instrumentation. The HISS phase 2 equipment is shown in Figures 6 and 7.

The data collected were also used in studies of IR propagation. There is an ongoing project at NSWCDD that is examining the degree of correlation, either positive or negative, between RF and IR propagation conditions.[8,9]

The HISS phase 2 system was composed of available components obtained under

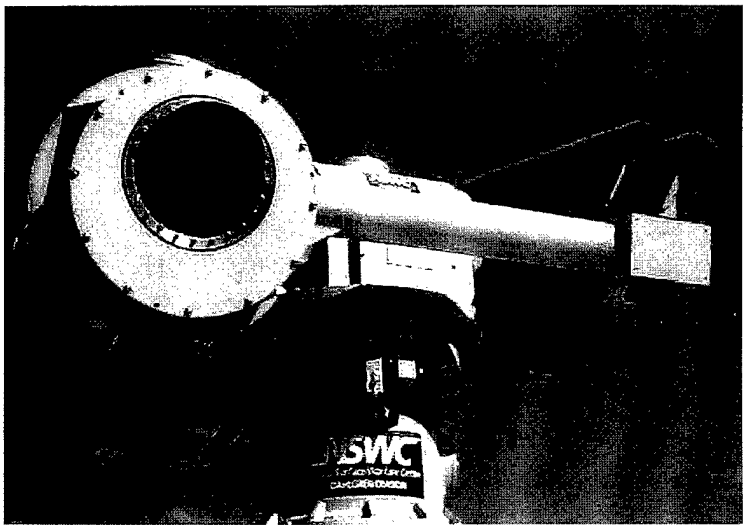

Figure 6. HISS phase 2 sensor and scanning pedestal system

Figure 7. HISS phase 2 control and processing electronics

separate contracts[10,11,12] and integrated by NSWCDD. Where possible, nondevelopmental items or commercial equipment was selected. In many of the components, slight adjustments were made either to component interfaces or to performance in selected areas to achieve required overall system performance. Top-level system performance parameters are summarized in Table 1. The single-scan target detection algorithms were developed by NSWCDD during the analysis of HISS phase 1 data. The algorithms were integrated into the signal processing hardware through a series of contractor/government working groups.[13] The phase 2 system does not have a track initialization function; that will be added in the next phase. A block diagram of the system is provided in Figure 8.

Measured Performance of the HISS Phase 2 System

During testing, actual ASCMs are generally not available to use as test targets. Therefore, this section will discuss the performance of the HISS phase 2 system against simulated ASCM targets. Data will be provided on quantification of system detection range, system reporting latency, and system accuracy. Two specific test targets have been used to measure these properties.

One of the test targets was a TLX height-keeping, towed target with IR augmentation. The target was towed behind a Learjet on 6000 ft of cable. IR augmentation is required because the target is being dragged through the air at subsonic speeds (~240 kn) and has no inherent sources of signature. IR augmentation was provided by an APC-6 plume generator fitted with a hot metal emitter (HME). With the addition of the HME, hot gasses from the generated plume heat a rear-mounted plate, which provides broadband emissions that can be observed from the forward aspect. The source radiant intensity of the TLX target was approximately 10 W/sr in the band of the HISS phase 2 sensor.

Table 1. HISS phase 2 system parameters

System Parameter	System Performance
Sensor Type	staring FPA imaging sensor
Number of Detectors	256 x 256 array
Sensor Spectral Band	3.8 to 4.2 μm
System Sensitivity (while scanning)	approximately 2 x 10-14 W/ cm2
Instantaneous Field of View	80 μrad x 80 μrad
Search Sector	15° azimuth sector with 1.17° of elevation
Revisit rate (at the center of scan)	approximately once per second
Processing - real-time data rate	4 million, 12-bit samples per second
Processing - operations	approximately 200 operations per data sample

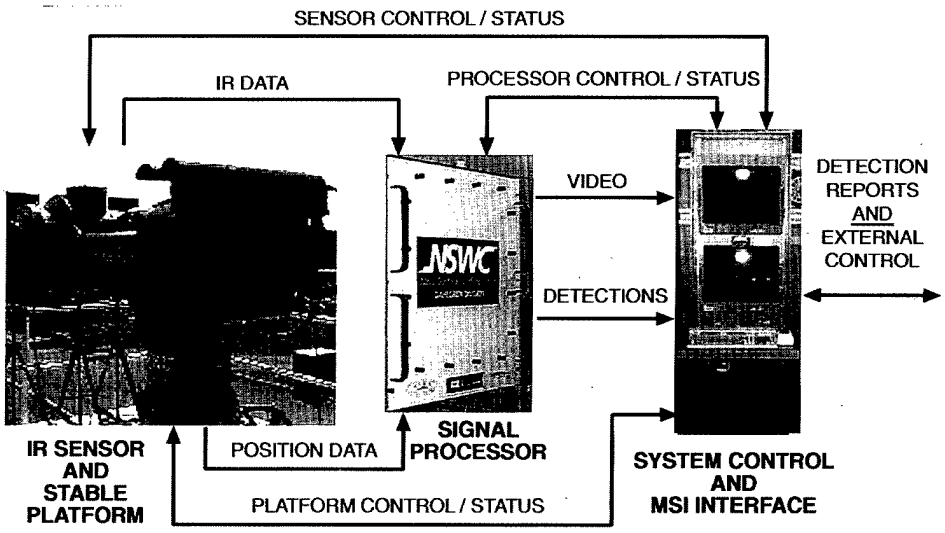

Figure 8. HISS phase 2 system block diagram

The second test target is a 60-ft, ocean-going, "sport fisherman" boat. This boat is an NSWCDD target asset known as SEA LION. Strip heaters were mounted at the bow and stern at approximately 12 ft above water level. The strip heaters provided a target signature of approximately 20 W/sr in the full MWIR band, and something less than that in the HISS spectral band. The strip heaters are approximately 2-in. high by 14-in. wide, and temperatures measured during testing ranged from 700° to 900°F.

Detection Range

The HISS system is used in conjunction with other sensors coupled by an MSI processor. The HISS system can operate with a low false-alarm rate, in a "stand-alone" fashion, but this particular system was designed with an adjustable reporting threshold to be operated in conjunction with other sensors. With the application of this reporting threshold, the reported detections can be limited to those having the most "target-like" characteristics, and the number of reported detections can be controlled. The observable benefit from using multiple sensors for target detection is increased initial detection range for the MSI system against a variety of targets in a variety of weather conditions. For reporting HISS detections, threshold false-alarm rates of 10 per second, 1 per second, 1 per 10 seconds, and 1 per 100 seconds were investigated in real time and post-test.[2,14] This adjustment in reporting threshold was used to study the ability of the MSI system and external sensors to respond to "cues" from the HISS system, and to study the effects of various false-alarm rates on overall system performance.

Figure 9 shows an example of the targets reported by the HISS system to the MSI processor over a period of 150 sec. Detections are reported if they exceed a threshold based on a ranking of how "target-like" the detectors appear. The ranking function is referred to as the comprehensive target metric (CTM). CTM is calculated for every HISS system detection in a single scan. In this example, CTM is the vertical axis, and azimuth and elevation are the other two axes. Three targets are shown in the figure. From left to right, they are (1) a Learjet at approximately 40 NM; (2) the test target mounted on SEA LION, near the horizon; and (3) a helicopter at approximately 7 NM, flying a vertical sawtooth pattern from 15 to 1500 ft.

Figure 10 provides a histogram of the measured probability of first detection against the TLX towed target for 25 successful target presentations. The bin sizes on the histogram are + 0.5 NM. The detection ranges shown

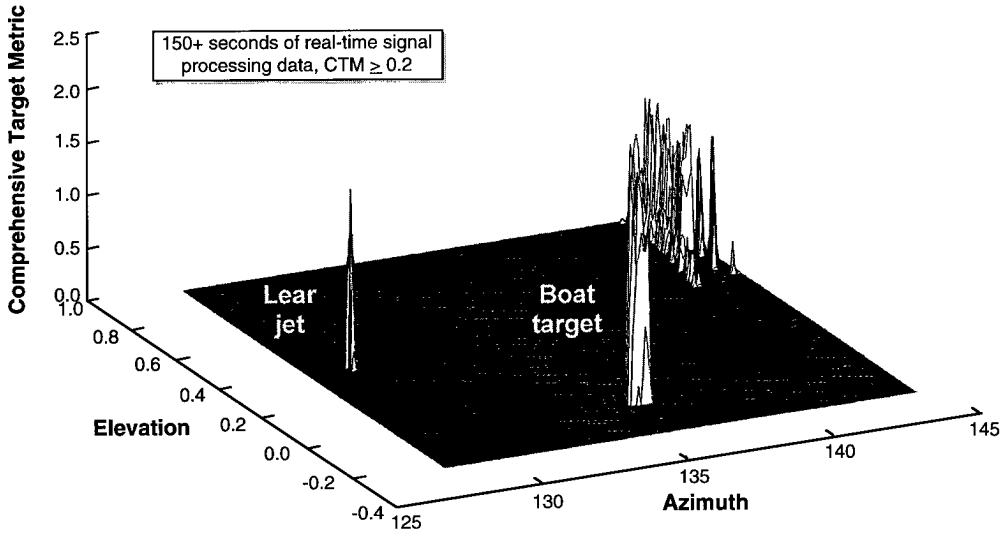

Figure 9. Elevation versus azimuth versus CTM of three targets, CTM reporting threshold = 0.2

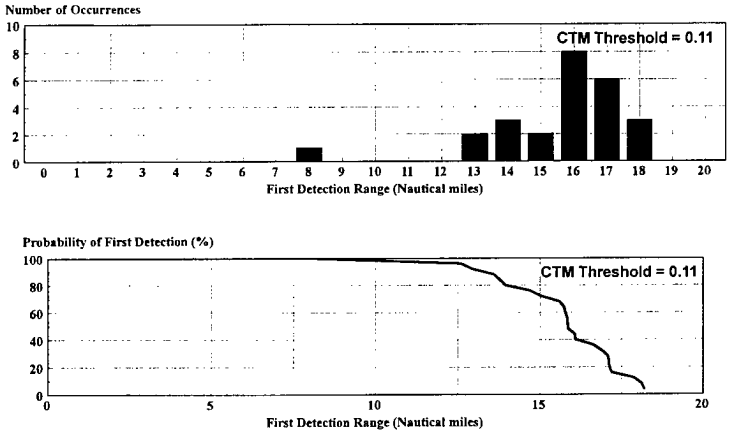

Figure 10. Probability of detection: TLX towed target, 25 presentations

here are for a constant CTM reporting threshold of 0.11. This value was chosen for the analysis because it provides a false-alarm rate of approximately one per second, and selecting one reporting threshold facilitates performance comparisons. Other texts provide data at alternate reporting thresholds.[14,15]

From the figure, one can see that maximum first detection range is approximately 18 NM, and minimum is approximately 8 NM, with a median of 16 NM. In the 25 presentations that constitute this graph, the TLX is flying between 30 and 240 ft in altitude. Approximately half of these target runs are at an altitude of less than 50 ft.

The performance of the system can be predicted for other operating areas through the use of statistical weather databases.[4] Figure 11 shows the HISS phase 2 system performance that can be expected against four notional targets whose signatures are 2.5, 5, 10, and 20 W/sr in R384 weather environments. These targets are all assumed to be flying at an altitude of 15 m, and the CTM reporting threshold is fixed at 0.11.

Reporting Latency

Another important system value is the latency with which target data are reported. Because IR sensor data are time-tagged as they are received at the signal processor, and the detection report message is time-tagged as it leaves the system, latency can be determined directly from recorded system data. Figure 12 shows the reporting latency under several different signal processing loads. Latency, as shown here, is the time at which the detection message is sent across the external interface minus the time at which the signal processor receives data on the first pixel from the sensor. All 65,536 pixels are read out every 60th of a second. Therefore,

the figure should show the latency involved in performing signal processing, arranging and formatting the data for external reporting and internal system transmission delays.

Four latency values are shown for each load. They are the latency for the first and last detections in each of the two frames being processed. The signal processor operates on two frames of sensor video at a time, for purposes of efficiency in using the available array memory. The first frame of a pair that is received will incur a delay, while the second frame is being read into the signal processor. Therefore, the latency on the first frame of the pair will always be approximately 16 ms longer than the second frame. The figure shows that the reporting latency will vary depending on where in the scene the detection occurs. Maximum latency for all load conditions is 85.445 ms. Minimum latency for all load conditions is 46.728 ms. There is a very slight trend for reporting latency to increase as the detection load increases. The maximum load of 34 detections per message represents a signal processing load of approximately 1000 detections per second.

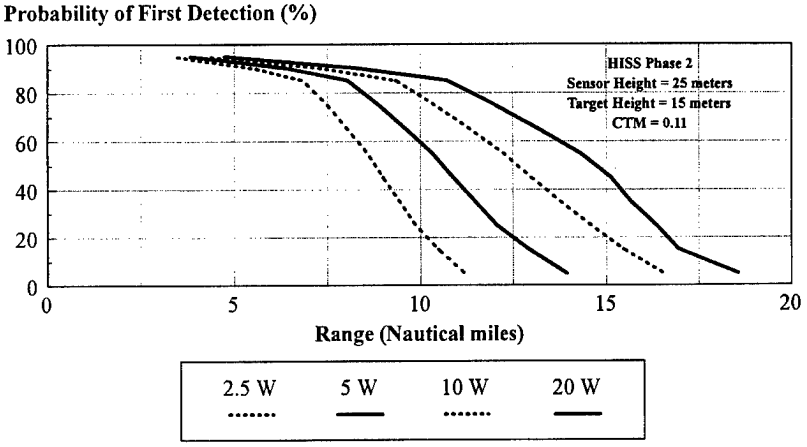

Figure 11. Predicted performance of the HISS phase 2 system against four notional targets in the R384 weather environments

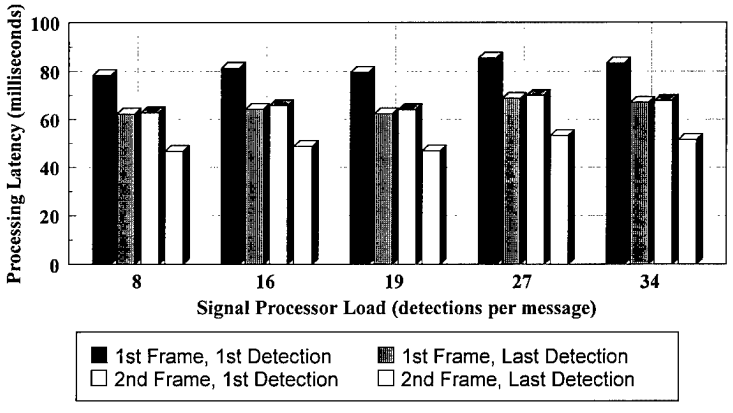

Figure 12. Observed reporting latency for various signal processor loadings

System Accuracy

The system components of the HISS phase 2 were procured independently and integrated at NSWCDD. The resolution of the IR sensor and the pointing accuracy of the stable platform are primary contributors to the accuracy of the system. Other components of the system, and the asynchronous manner in which system data are combined, lead to a larger inaccuracy than can be derived from the accuracies of the sensor and the platform. One of the best ways to measure the overall reporting accuracy of a system is to analyze the reported position of a stationary target, or in the case of this analysis, a *nearly* stationary target. A SEA LION run was selected at random for analysis.

The reported data are shown in Figure 13. This figure shows 3 min of data collected during a SEA LION run. The scale of the azimuth data, at 15 deg, is representative of the azimuth zone scanned during operation. The elevation scale was selected to reduce clutter on the graph, but is only slightly larger than the elevation field-of-view of the system. So, conceivably, this graph may be thought of as the motion that a system operator would perceive, in azimuth and elevation, as the target was being reported and displayed. The target is at

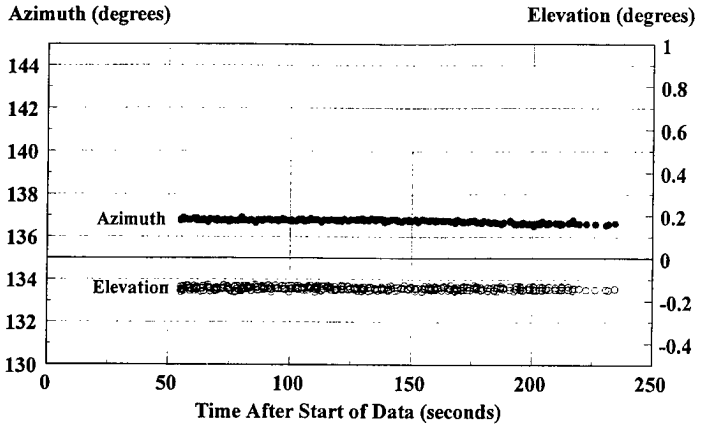

Figure 13. Reported azimuth and elevation of the SEA LION boat target

approximately 137 deg in azimuth and −0.15 deg in elevation.

Because the target is not stationary, but will change position over this 3-min period, the data in this figure include the motion of the target. A direct calculation of the reported position and the variation of that position from these data would therefore include the system's reporting inaccuracy and the motion of the target. To remove the target motion from the analysis, these data were divided into 30-sec increments. The arithmetical means of these 30-sec increments were determined and subtracted from the data—effectively removing most of the long-term target motion, because SEA LION is a relatively slow-moving target.

Figure 14 provides graphs of the variation of the reported azimuth and elevation about the calculated means for the 30-sec intervals. As you can see in the left-most graph (azimuth), there is still some residual left-to-right target motion in the data. This motion is indicated by the downward slope of the data and will result in a slightly larger error value for azimuth than if this residual motion had been removed. The elevation data appear to be evenly distributed around the mean.

The standard deviation for the reported azimuth is 0.042 deg, which is equivalent to 0.727 mrad. The standard deviation for the reported elevation is 0.007 deg, which is equivalent to 0.126 mrad. The peak-to-peak variation in azimuth and elevation,

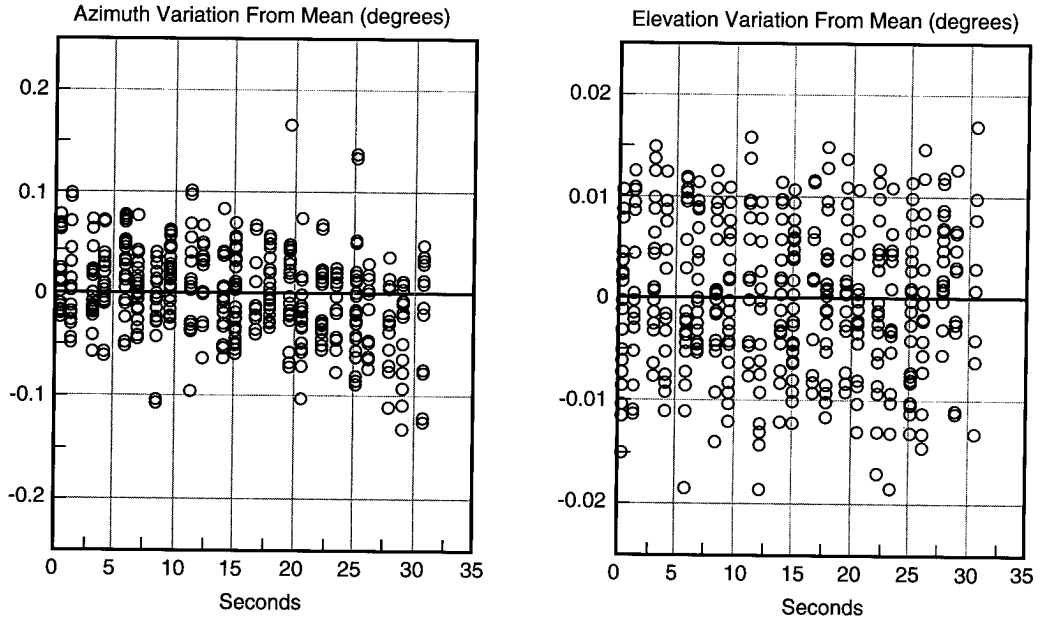

Figure 14. Variation in reported azimuth and elevation about the mean taken over 30-sec increments

Table 2. Summary of reporting accuracy analysis

	Azimuth	Elevation
Standard Deviation from Mean (°)	0.04	0.01
Standard Deviation from Mean (mrad)	0.73	0.13
Peak-to-peak Variation (°)	0.30	0.04
Peak-to-peak Variation (mrad)	5.18	0.62

respectively, is 0.297 deg and 0.035 deg. These data are summarized in Table 2.

Areas of Continuing Study

The data collected and analyzed during these field tests have allowed the quantification of the performance of an IRST system designed for shipboard use. The system has provided target detections in real time to an MSI processor for quantification of the benefits that can be derived from an IRST system. As with any body of research, there are some areas that will be pursued in the future. This section will discuss some of these continuing areas of study.

HISS Phase 3

The HISS phase 2 system was last used at NSWCDD in support of the multisensor detection (MSD) project at the end of FY95. This system was disassembled. Some of the components—namely, the scanning pedestal system, the sensor, the equipment van, and assorted instrumentation—will be used in conjunction with an Office of Naval Research project.[16] The remainder of the system components will be used in the HISS phase 3 system.

The block diagram for HISS phase 3 is shown in Figure 15. All of the major components of the phase 3 system are under contract and should be delivered in 1995. All that remains before realization of a complete phase 3 system is the development of software and integration of components. The primary differences in the construction of the HISS phase 3 are in the IR scanner and the sensor, and in the functionality of the signal processor.

A mirror-stabilized IR scanner has been procured[17] that will provide a continuous 360-deg horizon scan at 60 rpm. Two MWIR-detective assemblies have been integrated into the scanner.[18] Energy is split between the two bands by a dichroic beam splitter within the scanner. In operation, one MWIR band will be processed in real time for target detection. Data will be recorded in the

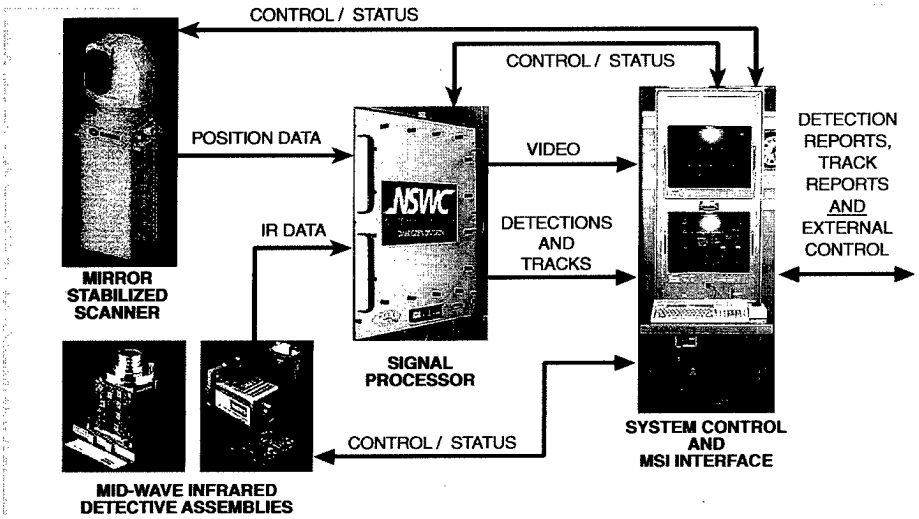

Figure 15. HISS phase 3 system block diagram

second MWIR band for post-test analysis. This analysis will comprise definition of dual-band clutter rejection techniques.

The signal processing hardware used in the HISS phase 2 system will be used in the new system. Because of the new sensor and scanner, the physical interfaces will be modified. The new input devices also increase the required capacity of the signal processor from 4 million samples per second to approximately 35 million 12-bit samples per second. A track initiation and maintenance function and a multiscan target discrimination function will be defined for the new system.

Development of the System Control Center and the internal and external interfacing software—essentially a new design—will begin next fiscal year. New interfaces will be developed for single point-of-control for the scanner and detective assemblies. The existing interfaces to the signal processor will be modified to accommodate new functionality. The external interface will also be modified to allow intrusive modification of system setup.

Refraction Effects

Refraction, the bending of light rays as they pass obliquely through a propagation medium, is caused by changes in the index of refraction of that propagation medium. In the atmosphere, the index of refraction at visible and IR wavelengths varies with its density. Temperature, humidity, and pressure are the primary factors determining the density of the air. Although the variations are small, the long path lengths make the effect measurable. Data collected with the HISS phase 1 sensor at Wallops Island in 1992 indicated that refraction is a major factor in the detection of IR targets at the horizon. Since that time, an effort has begun at NSWCDD to study the effects of IR refraction as part of an overall study of RF and IR propagation.

A useful gauge of the change in the refractive index of the atmosphere for a marine environment is the air-sea temperature difference (ASTD). ASTD is used because the air temperature profile is difficult to measure directly. Air temperature, in this metric, is measured at a given height, and sea temperature is measured with a sensor in contact with the water at or near the surface. Since the atmosphere is in thermal contact with the sea's surface, water temperature is assumed to equal the temperature of the air just above the water. For a neutral atmosphere, the air temperature and sea temperature are equal, and the ASTD is therefore zero. For a negative ASTD, the position of the horizon limit is predictable, based on a measurement of the ASTD with some degree of accuracy using available models. Refraction models may perform poorly under positive ASTD conditions.

Figure 16 shows the maximum detection ranges that were measured with the HISS phase 1 system during a series of field tests. The target is a boat-target, like SEA LION, with an IR target mounted at an altitude of

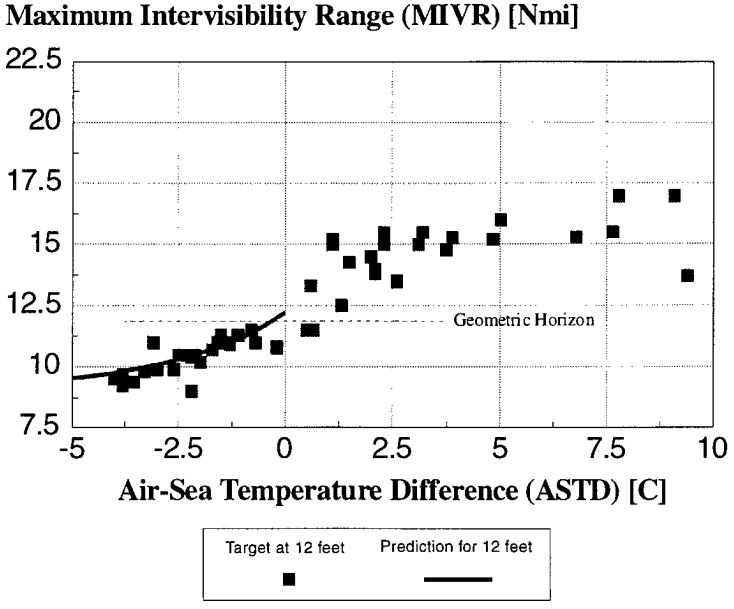

Figure 16. HISS phase 1 measurements of maximum intervisibility range, 17 March through 16 April 1992

12 ft. Figure 16 provides measurements of the maximum detection range against that target for a number of test days over a period of one month. This target is horizon-limited, and the maximum detection range represents the point at which the boat-target has gone over the horizon. Therefore, what is shown is a direct measure of the position, and change in position, of the horizon-limited range, or maximum intervisibility range (MIVR).

In Figure 16, the MIVR varies from approximately 8 NM to approximately 17 NM. The detection range is plotted against ASTD, and there is an apparent correlation, particularly with negative ASTD. A prediction of the MIVR is provided with the data. The "geometric horizon" on the graph indicates the maximum detection range to the target if the effects of refraction were neglected. For shipboard IRST systems detecting ASCM targets at the horizon, refraction effects will continue to be an important area of study.

Infrared Mirages

Another aspect of IR refraction in the atmosphere is the occurrence of IR mirages, or multiple images of the target. This phenomenon, illustrated in Figure 17, continues to be studied.[19,20] Mirages are transitory phenomena that occur at particular geometries of observer position and target position. During the tests at Wallops Island in 1994, mirages were observed on a number of test days.

It can be briefly summarized that there are three basic atmospheric conditions: unstable, neutral, and stable, which are generally associated with (respectively) negative ASTD, zero ASTD, and positive ASTD. In unstable atmospheric conditions, "inferior mirages" will generally occur. An inferior mirage can be described as a second image of the target that appears below the original image. In stable atmospheric conditions, a "superior mirage" may occur in the presence of an atmospheric inversion layer above the height of the observer. A superior mirage can produce one or more images of the target that appear above the original image. Figure 18 provides a breakdown of the observed mirage effects for a 29-day test period.

Figure 19 provides a dramatic example of the effects of a superior mirage. The figure includes (a) detections by the HISS system against an outbound Learjet and (b) image slices that show the formation of multiple images of the target by a superior mirage. The gap in detections between 100 and 125 sec (approximately 12 to 13.5 NM) is apparently caused by a region where no energy was received from the target. However, for the gap in detections that occurs after 160 sec

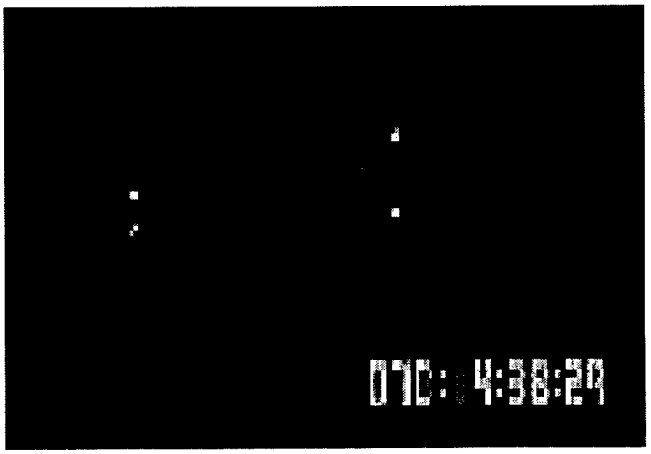

Figure 17. Mirages observed during testing

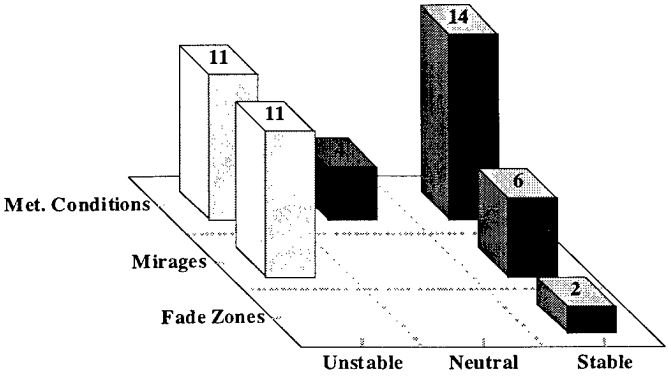

Figure 18. Breakdown of meteorological conditions

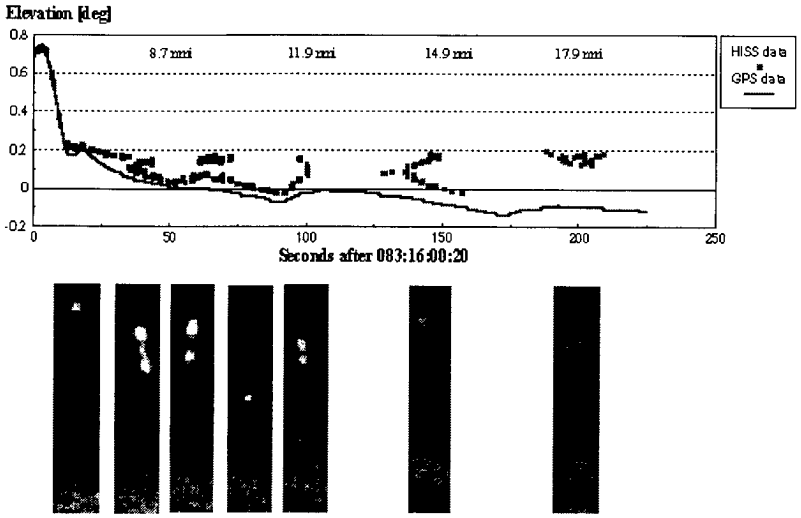

Figure 19. HISS detections against superior mirage of outbound Learjet and accompanying image slices

(approximately 16 NM), the lowest image of the target remains visible in the imagery data. The target, at this point, does not have enough signal strength to exceed the HISS detection threshold. The target is detected again at approximately 17.5 NM and finally disappears from the target detection record and from the imagery data.

The effects of refraction need to be considered when working with IR devices in a maritime environment. One of those effects is the occurrence of inferior or superior mirages. This is clearly an important area of study and will grow in importance as we increase the availability of IR devices on U.S. Navy ships and begin to use these devices in an integrated combat system.

Summary

This article provides an introduction to the HISS project. The general characteristics and composition of the systems used in each phase of the project have been addressed. In addition, data collected during phase 1 and phase 2 field testing have been presented. Certain measured performance areas in the phase 2 system have been presented. The next phase of the project was introduced, and the plans for construction of that system were addressed. Additionally, continuing work in the areas of IR refraction and mirages was presented.

References

1. Presentation entitled "Surface Navy IRST Program," 27 Aug 1992, by J.P. Shipp, Dr. K.C. Hepfer, and R.M. Headley, Jr.
2. Wiss, V. and Stapleton, R., *Multi-sensor Integration Data Reduction and Analysis Report for the Wallops Island Multi-sensor Integration Experiment*, NSWCDD/TR-94/89, Jan 1995.
3. Yee, D., "AN/SAR-8 Developmental Testing (DT IIA and DT IIB) Test Report," NSWSES letter, Jul 1991.
4. Austin, D. et al., *Use of the NSWCDD Weather Databases for Prediction of Atmospheric Transmission in Common Thermal Imaging Sensor Bands*, NSWCDD/TR-94/89, Jan 1995.
5. Martin, J. and Stapleton, R., *An Evaluation of Infrared Sensor Data to Support Radar Cueing*, NSWCDD/TR-95/34, Dec 1994.
6. Horman, S. et al., "Interactive Integration of Passive Infrared and Radar Horizon Surveillance Sensors to Extend Acquisition and Firm Track Ranges," presented at the 19th Annual Tri-Service Radar Symposium.
7. Hepfer, K. et al., unpublished paper entitled "Horizon Infrared Surveillance Sensor (HISS), Phase I - Field Test Results," Feb 1993.

8. Stapleton, J. et al., *Correlation of Microwave and Mid-wave Infrared Low Elevation Propagation Data*, NSWCDD/TR-95/60, in preparation.
9. Queen, J. et al., *Wideband Low Elevation Microwave Propagation Measurements*, NSWCDD/TR-95/18, in preparation.
10. Contract N60921-93-C-A308 between NSWCDD and Loral Defense Systems - Akron: for a "Signal Processor for the Horizon Infrared Surveillance Sensor System," Oct 1992.
11. Contract N60921-93-C-A313 between NSWCDD and Rockwell International Corporation: for a "Mid-wave Infrared Focal Plane Array Sensor System," Nov 1992.
12. Contract N60921-93-C-A315 between NSWCDD and Andrew Kintec, Inc.: for a "Scanning Optical Pedestal System," Dec 1992.
13. Loral Defense Systems - Akron document entitled "Software Requirements Specification for the Horizon Infrared Surveillance Sensor Signal Processor," Apr 1993.
14. Hepfer, K., *False Alarm Analysis, Horizon Infrared Surveillance Sensor; Analysis of Test Data Collected at NSWCDD, Wallop's Island Detachment, January - April 1994*, NSWCDD/MP-94/271, Dec 1994.
15. Dezeeuw, P., *Detection Range Performance, Horizon Infrared Surveillance Sensor; Analysis of Test Data Collected at NSWCDD's Wallops Island Detachment, March - April 1994*, NSWCDD/MP-94/363, Dec 1994.
16. Horman, S. et al., "Uniformity Compensation for High Quantum Efficiency Focal Plane Arrays," presented at the 1995 meeting of the IRIS Specialty Group on Passive Sensors, Mar 1995.
17. Contract N00014-93-C-0033 between the Office of Naval Research and Societe d'Applications Generales d'Electricitie et de Mecanique (SAGEM): for an "Infrared Sensor System," Dec 1992.
18. Contract N00014-93-C-0186 between the Office of Naval Research and Hughes Aircraft Company: for "MWIR FPA/Electronics Equipment," Jul 1993.
19. Rivera, H. and Trahan, J., NSWCDD report entitled "Infrared Propagation Experiment At Wallops Island; Test Setup and Data Description," Nov 1994.
20. Trahan, J., *Infrared Refraction and Mirages, Wallops Island, Feb - Apr, '94*, NSWCDD/TR-94/365, Dec 1994.

The Authors

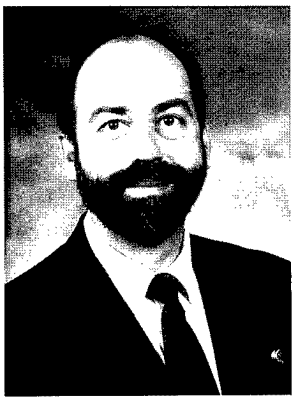

Robert Headley

ROBERT HEADLEY is the program manager for the HISS project at NSWCDD. He has worked at NSWCDD for 22 years and is currently group leader for IRST systems in the Photonic Systems Branch. Mr. Headley was previously program manager, system engineer, and prime mission equipment engineer for the Technical Direction Agent on the U.S. Navy's AN/SAR-8 IRSTD program. Prior to that, he was a design engineer and field test engineer for the Laser Fire Director project at NSWCDD and has spent many years as a designer of test equipment and test instrumentation. Mr. Headley has accepted invitations to speak at the National IRIS and IRCM IRIS, and he is author of a number of papers and technical reports.

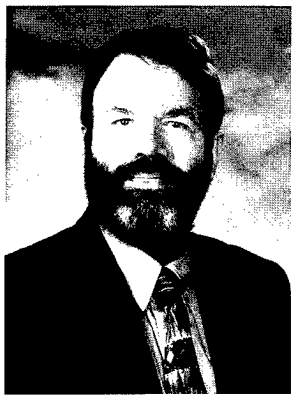

KEN HEPFER has 25 years of experience in surface navy electro-optics. He received a B.S. in physics from Florida State University in 1964, an M.S. in physics from Carnegie Institute of Technology in 1966, and a Ph.D. in physics from Carnegie-Mellon University in 1970. Since joining NSWCDD in 1970, Dr. Hepfer has developed performance analysis methodologies and has done performance and system design analyses that have provided direction for all major developments in electro-optical fire control and surveillance systems of the Surface Navy. He is currently the Chief Scientist/Systems Analyst of the Photonic Systems Branch at NSWCDD and provides requirements and system performance analysis support to a number of programs.

Ken Hepfer

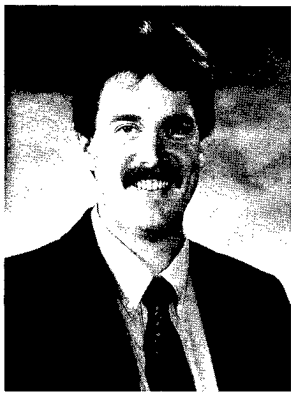

PATRICK DEZEEUW began working in the Photonic Systems Branch at NSWCDD in 1979 as a participant in the Cooperative Education Program. Mr. Dezeeuw graduated with a B.S. in physics from Mary Washington College in 1986. Since graduation, he has specialized in the area of collection and analysis of radiometric imagery. Mr. Dezeeuw was the test site engineer for NSWCDD's Search and Track Sensor Test Site from 1988 through 1992 and has considerable experience in field testing of research and development systems. He is currently the systems engineer on the HISS project.

Patrick Dezeeuw

ANGELA PLANTE received a B.S. in electrical engineering from Virginia Polytechnic Institute in 1992, and an M.S. in electrical engineering from Virginia Polytechnic Institute in 1994. Ms. Plante's masters thesis was on "Photoinduced Fresnel Reflectors in Optical Fibers," and her field of study was in the area of fiber-optic sensors. Ms. Plante has been working with the HISS project as a test engineer and is responsible for the analysis of HISS detection data in the areas of refraction and system accuracy.

Angela Plante

Shipboard Chemical Warfare Agent Detection

Daniel C. Driscoll and Diane H. LaMoy

EW
EXPEDITIONARY
WARFARE

The Navy faces a growing threat from the use of chemical and biological warfare agents. In response to this threat, the Naval Surface Warfare Center, Dahlgren Division (NSWCDD), has been developing a variety of specialized sensing technologies for fleet use. This article will focus on sensors for the detection of chemical warfare agents. Two specialized technologies will also be described:

- *The application of charge coupled device (CCD) imaging spectroscopy to the detection of chemical warfare agents in liquid droplet form*
- *The detection of chemical warfare agent vapors by ion mobility spectroscopy (IMS) for point detection and compartment monitoring*

The engineering of systems of this type presents a unique challenge. Sensitive analytical instruments must be put in a sufficiently rugged package to survive and be reliable in a very harsh environment. By utilizing mature technologies and including survivability and logistical requirements in design decisions from the start, such systems are being successfully developed and deployed to the fleet.

Introduction

As many as 25 countries are developing, or are suspected of developing, chemical weapons. Ten nations have biological weapons programs and another ten are suspected to have such programs. By the year 2000, these numbers are projected to increase. These weapons can be delivered by surface-to-surface missiles, aircraft bombs and rockets, spray, or other, more unconventional means.

The U.S. Navy's experience in Operation Desert Storm highlighted the increased risk that naval forces have of encountering chemical and biological agent contamination. Department of Defense (DoD) defense guidance[1-3] policy and OPNAVINST S3400.10E require that deployable U.S. Navy surface ships and high-threat overseas shore installations be provided with chemical, biological and radiological (CBR) defense capabilities. CBR defenses must include a multilayered chemical detection suite consisting of:

- Intelligence
- Standoff detection capabilities that will enable:
  - ship avoidance maneuvers
  - activation of shore-based CBR defense systems
- Onboard detection and monitoring of exterior areas and interior compartments.

Defensive systems for the detection of chemical agents are currently in development at NSWCDD. These systems include a standoff capability for chemical warfare agent vapors—the Chemical Agent Remote Detection

System (CARDS); a point sensor for chemical warfare agent vapors—the Improved Point Detection System (IPDS); a detector for chemical warfare agent aerosols (droplets)—the Shipboard Automatic Liquid Agent Detector (SALAD); and a man-portable version of the IPDS—the Shipboard Chemical Agent Monitor Portable (SCAMP), being developed for compartment monitoring and survey.

An extensive biological-agent detection effort is also ongoing at NSWCDD. The Interim Biological Agent Detection System (IBADS) has been developed and is being installed on selected Navy ships and shore installations. A follow-on Biological Point Detection System (BPDS) is the goal of a joint services development effort.[4]

In this article we shall focus on the sensors for detection and warning of chemical warfare agents. The IPDS, which has recently completed operational evaluation (OPEVAL),[5-7] has been approved for introduction in the fleet. SALAD is about to begin OPEVAL. CARDS and SCAMP are still in development. These systems, when completed, will form an integrated suite of chemical warfare agent detectors to meet the needs of the fleet.

Current Capabilities

As stated above, doctrine requires that U.S. Navy ships be provided with a multilayered suite of chemical-warfare-agent detection capabilities. At present, these requirements are at least partially fulfilled by:

- The AN/KAS-1 and AN/KAS-1A
- The Chemical Agent Point Detection System (CAPDS)
- The M256 chemical detection kit

Standoff chemical detection (of nerve agents) is provided by the AN/KAS-1 and AN/KAS-1A. This device is a forward-looking infrared (FLIR) viewer fitted with optical filters that are manually put in place by the operator to discriminate an agent cloud from background. It is also fitted with a video monitor so that what the operator sees can also be seen by personnel in the combat information center (CIC).

Fixed-point chemical vapor detection is provided by the CAPDS. This system consists of two through-bulkhead units (TBUs) to sample external air, and two detector units, which analyze the air sample and communicate with alarm display units located in damage control central (DCC) and on the bridge. Each detector unit has a single baffle-type ion mobility cell that detects nerve agent vapor only.

Compartment monitoring and survey is currently performed using the M256 chemical detection kit. This kit includes M8/M9 paper, to check surfaces for liquid contamination, and a color-change card based on reagents that must be mixed by the operator. Response time of the reagent-based detection ticket is 10 to 15 minutes. The response time of the M8/M9 paper is on the order of several minutes depending on how much agent is present.

Systems in Development

The systems currently in development will enhance fleet capabilities in each of the areas of chemical detection mentioned above: CARDS in standoff detection, IPDS and SCAMP for vapor detection, and SALAD for detection of liquid agents.

SALAD

SALAD is based on a different technology than are IPDS and SCAMP, and indeed any other chemical-agent detector in development by any of the services. Rather than detecting vapor, SALAD detects the presence of liquid agent droplets on an exposed roll of chemically sensitive paper (M8/M9). The paper will turn specific colors when exposed to chemical warfare agents; an optical scanner system then detects the color changes and produces an alarm, thus automating one of the simplest but most specific detection technologies (M8 paper).

The M8 detector paper used for SALAD is impregnated with three chemical dyes that react immediately and specifically to liquid

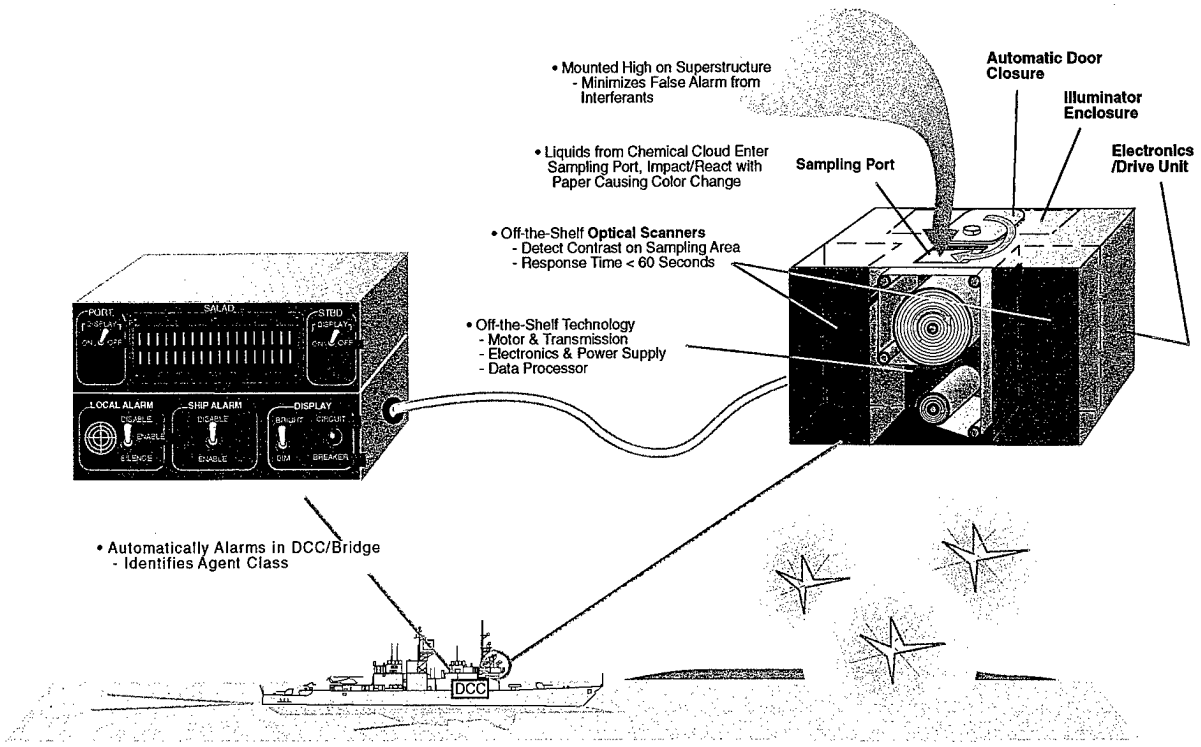

Figure 1. Standard shipboard installation of the Shipboard Automatic Liquid Agent Detector (SALAD)

nerve and blister chemical warfare agents. On the M8 paper, GD (Soman) droplets produce a bright yellow stain, HD (Blister) droplets produce a red stain, and VX (nerve agent) droplets dissolve the blue and yellow dyes to create a dark green stain.

Figure 1 shows a schematic of a standard shipboard installation of SALAD. The SALAD system consists of a single detector unit (mounted topside) connected to remote control/display units (collocated with the control display units of the IPDS (DCC and bridge)). The image scanning system that provides the automated reading of the M8 paper is an electronic CCD. The detector unit has two such scanning devices with illumination sources that scan a roll of M8 paper that is moving through the field of view of each scanner. One scanner performs a prescan function to examine the paper for any defects or previously stained areas. The automatic paper feeder then moves the paper into the field of view of the second scanner. The data from each scanner are digitized and read simultaneously by an embedded, high-speed, digital signal processor. The detection algorithm resident in the embedded microprocessor analyzes the data from the two CCD images in real time and compares the spectral signatures to a library of (previously recorded) agent and interferant signatures. This approach ensures a high probability that agents will be detected and an alarm sounded, while nonagents will have a low probability of causing a false alarm.

The SALAD unit has physical dimensions (in inches) of 24 (d), 18 (w), and 12 (h). It weighs approximately 50 lb and runs on 110-Vac/15-amp power.

IPDS

The IPDS is a (fixed) point detector for nerve and blister (mustard) chemical warfare agent vapors. It is designed to be a replacement for the CAPDS and to fulfill the role of point sensor for monitoring air on the exterior of the ship.[8,9]

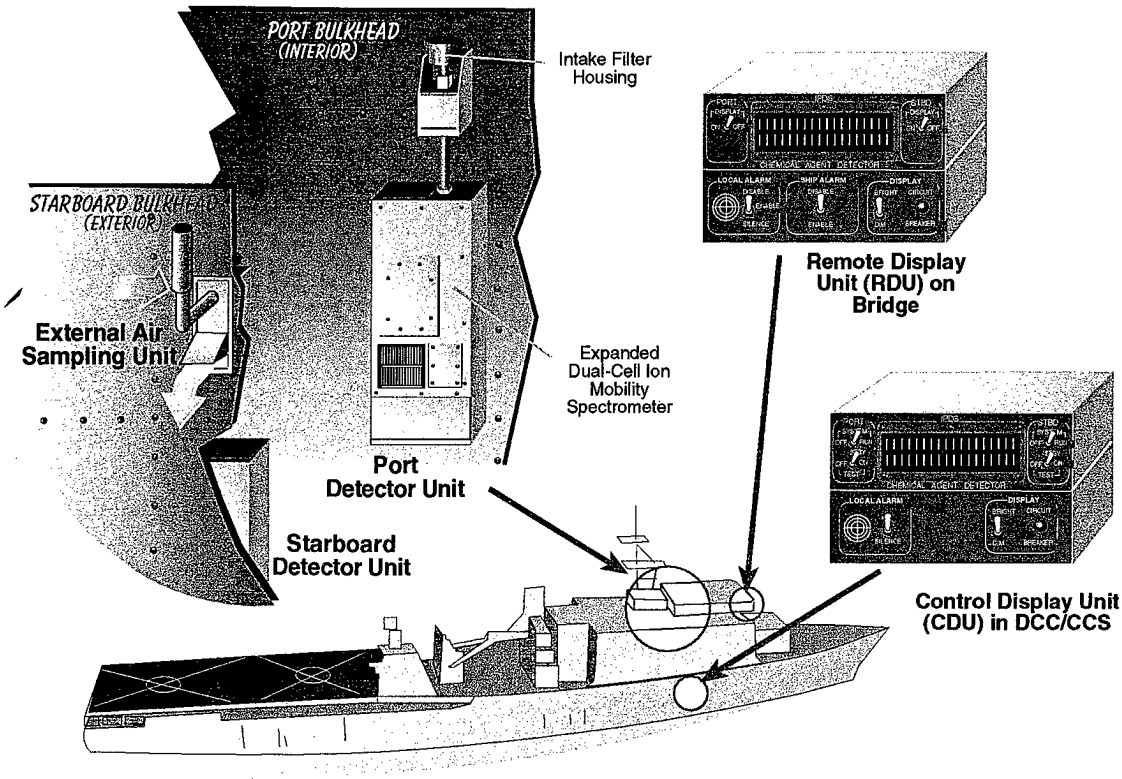

Figure 2. Standard shipboard installation of the Improved Point Detection System (IPDS)

Figure 2 is a schematic of a standard shipboard installation of IPDS. Two external air sampling units (EASUs), mounted on the port and starboard sides of the ship, take in large samples of external air. A small sample flow is skimmed off and goes to the detector unit mounted near each EASU on the interior of the ship. After sampling by the detector unit, the sample flow is exhausted through the EASU back to the exterior of the ship.

The IPDS makes use of IMS to generate, separate, and detect cluster ions, formed by chemical warfare agent molecules, and reagent or "reactant" (ion) clusters produced in the ionization region of the IMS cell. A small radiation source (Am^{241} 100 μCi) ionizes residual H_2 (from water), and polar species, such as acetone, will then cluster around an H^+ ion. Ion molecule reactions between these cluster ions and any (neutral) molecule having a higher proton affinity than acetone result in (agent) molecules replacing one, two, or three acetones on the cluster to form monomer, dimer, or trimer peaks whose relative intensities depend upon the concentration of the agent present. A similar process operates in the negative ion mode where electronegative species (such as mustard gas) compete for space in negative ion clusters formed around OH^- ions resulting from ionization of residual water vapor. Because nerve agents react to form positive ions, while blister agents (mustard and lewisite) react to form negative ions, two IMS cells are present in the IPDS detector unit to allow simultaneous detection of nerve and blister chemical warfare agents.

The IPDS detector unit consists of:

- Positive and negative IMS cells in a heated enclosure
- An acetone source for the positive cell
- Pumps

- A filter/sieve pack
- Signal processing electronics inside a radio frequency interference/ electromagnetic interference (RFI/EFI) shielded enclosure

The IPDS system consists of two such detector units, two EASUs to draw in outside air and transfer it to the detectors, and two remote control and display boxes to control the system and provide status information and alarms to the user. (Remote control and display units are mounted in the DCC (control) and on the bridge (remote display).)

Each detector unit continuously draws air samples into a manifold and through membrane holder assemblies, and then exhausts it (back through a transfer line to the exhaust of the EASU). A portion of the sample passes through silicone membranes into each IMS cell. Ion clusters are generated by the ion-molecule reactions described previously. The clusters are then injected into the drift region of the IMS cell by pulsing the gate electrode (normally closed) that normally repels ions from the drift region. The pulse lowers the potential at this gate sufficiently to allow ions into the drift region. In the drift region, ions of different size separate by their mobility in the uniform electric field of that region. The time of arrival of the ions and their respective signal strengths are measured and compared to data in a library of materials' signatures in the central processing unit (CPU). The presence of interferants is ignored, and agent and simulant data are displayed. If agents are detected, an alarm signal is produced.

The detector unit has physical dimensions (in inches) of 9.5 (d), 11 (w), and 24 (h). It weighs approximately 100 lb, and requires 110-Vac/15-amp power.

SCAMP

SCAMP is based on the same technology as the IPDS. The IMS cells at the heart of the SCAMP detector are nearly identical to those found in the IPDS detector unit. The design/development effort in the SCAMP program has focused on taking the proven IPDS design concept and, through reductions in size, weight, and power consumption, turning it into a man-portable package.[10] While reducing the weight from roughly 100 lb to less than 25 lb, the essential functional characteristics of the detector unit must be retained. For example, in order to maintain the same sensitivity, the IMS cells must be operated at an elevated temperature, which requires placing them in some kind of heated enclosure. The flow characteristics of the pneumatic system cannot be changed drastically since any changes in flow affect the IMS signatures. The acetone dopant must still be provided to the positive cell (only), and the recirculating (closed) airflow loop passing through the cells must pass through a desiccant cartridge (scrubber) in order to keep the relative humidity low and remove any organics (sample) from the air stream after analysis.

The signal processing performed by the SCAMP detector unit is identical to that performed by the IPDS detector. There is no remote display/alarm to communicate with, so the communications tasks to be performed by the electronics are simplified. However, the CPU must still monitor the operational status of the detector (flows, temperature, and operating mode) and run the detection algorithm—that is, analyze the IMS signatures from each cell and determine if agent (or simulant) is present.

As currently envisaged, the goal is for SCAMP to occupy the same volume as the XM-22 Automatic Chemical Agent Alarm (ACADA), a portable detector under development by the Army. While there are a number of differences in the philosophies behind these two systems, both in design and doctrine of use, the two seem to be approximately the right size package for portable detectors. Figure 3 is a preliminary design of the SCAMP fit to the ACADA envelope.

The SCAMP unit has physical dimensions (in inches) of 6.5 (d), 6 (w), and 10 (h). It weighs approximately 25 lb and runs on either 110-Vac or 24-Vdc batteries.

A number of areas have been identified where the size of components in the

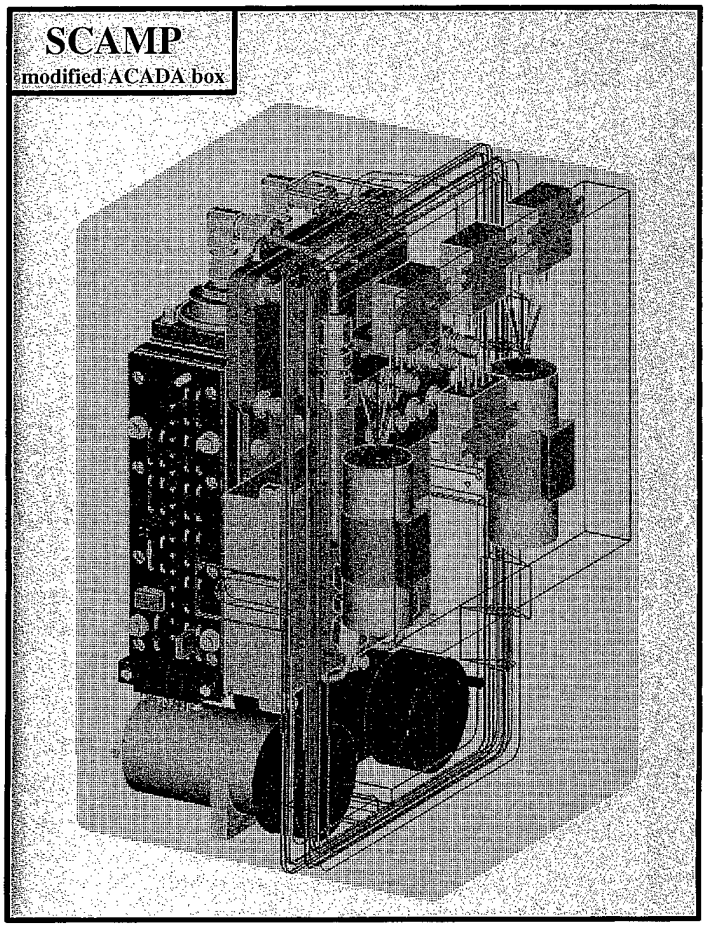

Figure 3. Preliminary design drawing of the Shipboard Chemical Agent Monitor Portable (SCAMP) fit to the envelope of the XM-22 ACADA

pneumatic system can be reduced. Since the pneumatic system in IPDS is almost entirely made of stainless steel, any reduction in component size translates into substantial savings in weight. Three components in particular for which savings in size/weight have been identified are the desiccant cartridge, the acetone source, and the interface between the IMS cells and the semi-permeable membrane.

Theories Of Operation

IMS

Both IPDS and SCAMP use IMS drift tubes as the central sensing element of the detector. In an IMS drift tube, ion clusters are created in the ionization region and then admitted to the drift region by a voltage pulse applied to the gate electrodes ("gate pulse"). Different ionic species are then separated by their mobilities in the uniform electric field of the drift region. For an ion in the drift region, mobility is defined in Equation (1) by the relation:

$$V_d = K * E \qquad (1)$$

where V_d is the magnitude of the drift velocity, E is the electric field strength, and K is the mobility.

When defined by Equation (1), the mobility seems simple enough. However, in terms of fundamental quantities such as ion charge, mass, temperature, and pressure (of the "bath" gas), K is not a simple function. In practice, limiting cases must be considered and some simplifying assumptions applied in order to calculate K. In the weak field limit, for an ion of charge e, at a (fixed) temperature T, K is related to the diffusion coefficient D as in Equation (2):

$$K = (eD/k_BT) \qquad (2)$$

where k_B is Boltzman's constant. K and D are unique for a given fixed temperature combination of ion and neutral gas. The weak field limit is defined as the electric field strength being such that ions do not acquire velocities well above their thermal velocities; or, in other words, only a few collisions are normally needed for the ion to reach thermal equilibrium with the neutral molecules. The weak field limit is the condition normally found in IMS cells.

Much of the fundamental physics and chemistry of ions moving through a neutral gas can be learned from measurement of mobility. A basic expression of the mobility for an ion of mass m and charge e, moving through a bath of neutral molecules of mass

M and number density N, is given by Equation (3):[11,12]

$$K = (3e/16N)(2\pi/\mu k_B T_{eff})^{1/2} \times [(1+\alpha)/(\omega_D T_{eff})] \quad (3)$$

where $\mu = mM/(M+m)$ is the reduced mass of the ion-neutral collision pair, T_{eff} is the effective temperature of the ions, ω_D is the collision cross section, and α is a correction factor (generally less than 0.02 for $m > M$). The collision cross section, ω_D, depends on the model chosen for the ion-neutral interaction potential, and much work has been done in analytical applications of IMS measuring the mobility experimentally to evaluate the validity of different models of the ion-neutral potential.

In the application of IMS to detection of chemical warfare agent vapors, what is, in effect, a measurement of the mobility is used to identify the chemical species present in the air being sampled. The raw data produced are in the form of an ion chromatogram—that is, ion current as a function of time measured from the gate pulse admitting the ion clusters into the drift region of the IMS cell. Since the electric field strength and the length of the drift region (and hence V_d) are known quantities, from Equation (1) one can see that each peak in the chromatogram (IMS signature) corresponds to a unique value of the mobility. The ion drift times (mobilities) compared to signatures taken from known samples stored in a library in the detection algorithm are the data used to make an identification of the chemical warfare agents.

CCD Video/SALAD

SALAD images the stains produced on M8 paper by collecting spectral image data from the illumination intensity received by the CCD sensors. The CCD comprises systematically arranged metal oxide semiconductor (MOS) capacitors. The MOS capacitors are divided into two sections: the photo sensor, which converts incident light into charges (and accumulates charge), and the charge transfer section, which transfers those charges (generating the raw signal). The sensor gate pulse determines the timing at which the charges transfer from the MOS capacitors to the vertical registers of the scanner. When the photo sensor is emptied of charge, it begins again accumulating charge from the effect of incident light. Because of this, the output of the CCD is proportional to the product of incident light intensity and accumulation time.

After an incident chemical agent (or simulant) falls on the exposed paper detection medium, the detector unit scans the paper by scrolling it through the field of view of the CCD devices as described previously. The output of the illumination source is filtered through a color wheel that resolves the visible (460 nm to 700 nm) white light into 12 spectral bands at 20-nm intervals. The CCD charges induced by each of the 12 spectral bands are collected, digitized, and compared to a library of spectral data for each known agent (or simulant). Upon detection of agent or simulant, an alarm signal is sent to the remote control/display units.

Control of the camera, illuminator, and paper scrolling mechanism is done through a commercial off-the-shelf (COTS) input/output (I/O) with customized drive circuitry. A COTS frame grabber converts the image data to a digital signal, and a COTS processor board processes the image data for spectral content. Two factors driving the choice of processing technology to use are the sampling rate of the "real world" analog signal and the amount of signal processing required to produce the desired output or decision.

The sampling rate must be greater than the Nyquist rate. The Nyquist rate is defined as two times the bandwidth of the signal. Bandwidths for many standard signals are well-known, such as for voice or video. Unknown bandwidths can be determined using a spectrum analyzer or by performing a Fourier transform on a time-domain signal.

The faster data is digitized, the more rapidly that data needs to be stored, either temporarily in a buffer or more permanently to random access memory (RAM) or disk.

Temporary data storage time depends primarily on the speed of the processor. Many processors clock in 100 MHz or more. If data is transferred every clock cycle on a 32-bit wide bus, then four 8-bit wide bytes of data can be moved every 10^{-8} second or 4 MB in 1 second into the buffer, assuming the buffer has 4-MB capacity.

Permanent data storage is usually more limited by backplane speed than processor speed. The backplane contains the data highway that connects the components located on different printed circuit boards. This data highway is called a bus. Some common bus architectures are the standard 16-bit Industry Standard Architecture (ISA) and 32-bit Enhanced Industry Standard Architecture (EISA) buses that are used in the desktop computer. Throughput on these buses is about 8 MHz.

The new standard Peripheral Component Interconnect (PCI) bus, which is an upgrade for the desktop computer, is 32-bits wide and has a current 32-MHz throughput, although the specification for PCI allows for clock speeds up to 66 MHz. This is the fastest bus on the market, and many vendors are now offering COTS analog-to-digital conversion boards for audio and video as well as for more generic applications.

The Versa Module Eurocard (VME) bus has a 16-MHz system clock and is 32 bits wide. VME is available in a ruggedized version but tends to be a larger overall system because of its board size.

The Standard (STD) bus and STD 32 have 8-MHz throughput, but the overall system, including card cage and power supply, is relatively compact.

The second consideration in the choice of technology is the algorithm or data processing requirement, including I/O, such as serial data or motor control. The microprocessor is the engine to do these tasks. The time needed to run a particular algorithm depends on processor speed as well as instruction cycle time. Processors vary not only in how fast they run (25 MHz, 33 MHz, 66 MHz), but also in how many cycles it takes to do a particular task. If greater processing speed is required, a second processor board is sometimes added, or a processor is specially designed for the task at hand. For example, the TMSC320CX is a popular processor designed specifically for digital signal processing.

The SALAD design relies heavily on COTS components: the result is a system that will cost less and ultimately reach the fleet in a more timely manner.

Future Improvements/Capabilities

Standoff chemical detection will be addressed by CARDS. CARDS is intended to be an automated detector that will be sensitive to both nerve and blister chemical warfare agents. Some technical parameters of this system are still being determined; a passive infrared sensing (or imaging) detector is planned as the heart of the system. If it is practical to include imaging in this system, the system will be open to multiple uses (surface surveillance, mines, swimmers, and others).

Fixed-point chemical vapor detection will be addressed by IPDS. As mentioned above, IPDS has passed Milestone III, and delivery of the first production units is anticipated for FY97. IPDS was designed to be a direct replacement for CAPDS, and the first ships equipped with IPDS will be those with existing CAPDS installations. As IPDS replaces CAPDS, it will add the capability of detecting blister as well as nerve agents with improved sensitivity (0.1 mg/m^3 for G-series nerve agents with IPDS as opposed to 0.3 mg/m^3 for CAPDS) and a reduced false alarm rate.

Fixed-point liquid agent detection will be addressed by SALAD. This type of detection will constitute a new capability, as there is currently no system on U.S. Navy ships to perform this task.

Compartment monitoring and survey will be addressed by SCAMP. As opposed to the M256 kit, SCAMP will provide a much more timely (under 1 minute) and sensitive

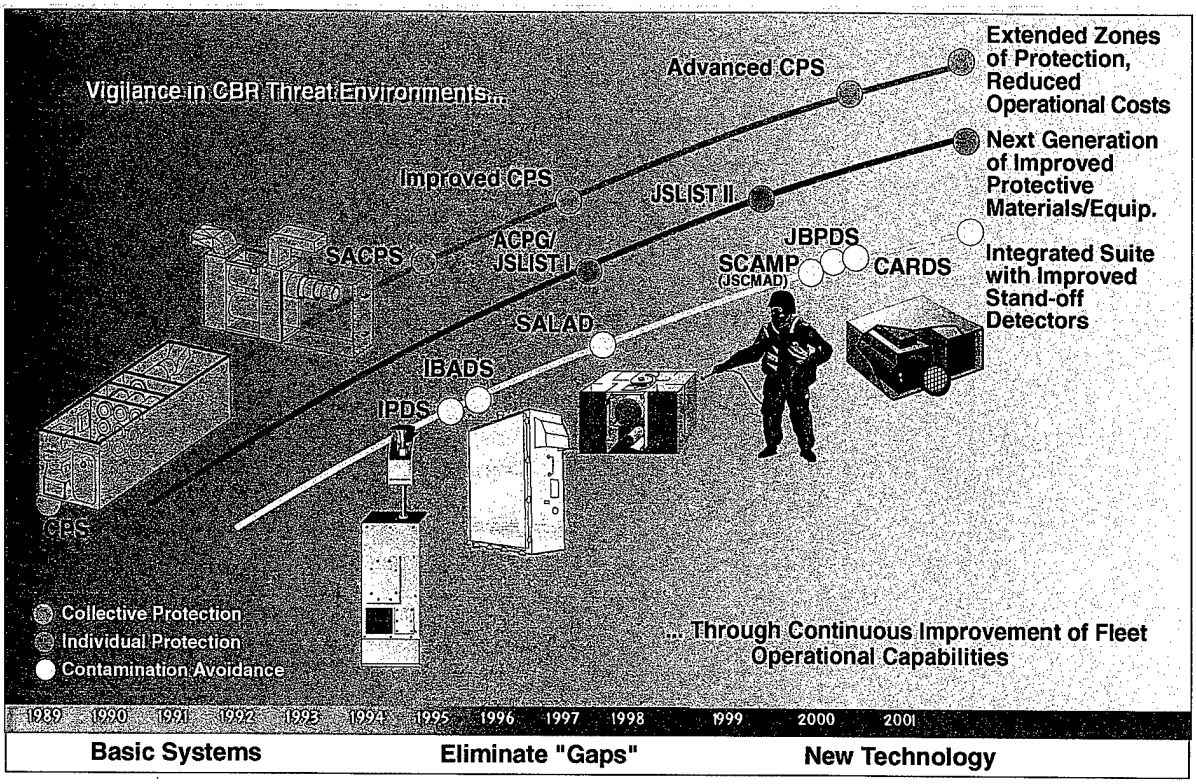

Figure 4. Development schedule through the year 2001 for the major Navy protection and detection programs

(0.1 mg/m^3 for nerve, 10 mg/m^3 for blister) analysis of the air inside enclosed spaces in the ship. If fitted with a heater attachment, it will also provide a rapid reading of surface contamination.

Conclusion

Figure 4 shows the projected time line for development of CBR protection and detection systems through 2001. The detection of chemical and biological warfare agents (in a maritime environment) presents unique challenges, both to the basic technology employed and from the standpoint of systems engineering. Instruments that were previously found only in the laboratory (or in the case of biological agents, where no single instrument existed to do the job) must be ruggedized to stand up to a very harsh environment while maintaining a high level of sensitivity and accuracy. Starting with mature technologies, making use where practical of COTS technology, and making testing an integral part of the development process, detection systems that are highly reliable, sensitive, and accurate are being successfully developed and fielded.

References

1. *Surface Ship Survivability*, Chief of Naval Operations (N86D), NWP 62-1 Rev D, Jan 1993.
2. *Naval Ships Technical Manual*, Chapter 470, "Shipboard BW/CW Defense and Countermeasures," S9086-QH-STM-000/CH-470, 1 Sep 1991.
3. *Chemical Biological, and Radiological Defense for Surface Ships*, Chief of Naval Operations (N11), NTP X-00-8201B, 7 Aug 1992.
4. Byrne, J.A., *Evaluation of the Interim Biological Agent Detection System (IBADS) From September 1993 to April 1994*, NSWCDD/TR-95/147, Dahlgren, VA, Jun 1995.

5. Pompeii, M.A.; Fitzgerald, Jr., R.A.; Johnson, G.P.; Driscoll, D.C.; and Machlinski, K.J., *Developmental Testing (DT-IIB) of the Improved (Chemical Agent) Point Detection System (IPDS),* NSWCDD/TR-95/118, Dahlgren, VA, Jul 1995.
6. Fitzgerald, Jr., R., *Test Report for Improved (Chemical Agent) Point Detection System Advanced Development Model 1,* Naval Surface Warfare Center, Dahlgren, VA, NSWCDD Letter Report to NAVSEA 05R14, 23 Aug 1991.
7. Fitzgerald, Jr., T.; Driscoll, D.; and Johnson, G., *Developmental Testing, Phase IIA (Shipboard) of the Improved (Chemical Agent) Point Detection System Engineering Development Model 1,* NSWCDD/TR-93/217, Dahlgren, VA 24 Mar 1993.
8. *Technical Manual for Improved (Chemical Agent) Point Detection System (IPDS), Description, Operation, and Maintenance,* S9437-A8-MMM-010 (Draft), 7 Apr 1994.
9. *Training Module, Improved Point Detector System (IPDS)* (Draft), Chief of Naval Technical Training (N11), NTPX-00-8201B, 7 Aug 1992.
10. Byrne, J.A., *Shipboard Chemical Agent Monitor Portable (SCAMP) Design Analysis,* NSWCDD/TR-93/121, Dahlgren, VA, Mar 1995.
11. Eiceman, G. and Karpas, Z., *Ion Mobility Spectrometry,* CRC Press, Ann Arbor, 1994.
12. Mason, E.A. and McDaniel, E.W., *Transport Properties of Ions in Gases,* John Wiley & Sons, New York, 1987.

The Author

Daniel C. Driscoll

DANIEL C. DRISCOLL graduated from Syracuse University in 1979 with a B.S. in physics. After graduate studies at Northeastern University and three years working in industry in the area of thin film deposition and characterization, he resumed graduate studies at Syracuse, receiving an M.S. in physics in 1986 and a Ph.D. in chemical physics in 1987. He was an Office of Naval Technology (ONT) postdoctoral fellow at the Naval Research Laboratory for three years, during which time he worked in the areas of plasma and combustion chemistry. He joined NSWCDD in 1991 and works in the Systems Research and Technology department; his main area of effort has been the development of sensors for chemical warfare agents. He was involved in the development and testing of IPDS. He is currently the technical point-of-contact for the Navy in the Lightweight Standoff Chemical Agent Detector (LSCAD) program, a joint program to develop, test, and field a passive infrared remote detector for chemical warfare agents. If successful, this program will provide a standoff chemical agent detection capability to surface combatants and overseas port facilities.

Using Fractal Features to Perform Automated Detection of Mines in Cluttered Sonar Images

Susan M. Tuovila and Susan R. Nelson

EW
EXPEDITIONARY
WARFARE

Recent changes in global political and military climates have resulted in a restructuring of the Navy's priorities, in particular, a shift in emphasis from open ocean warfare to coastal operations. Mine countermeasures (MCM) operations, including reconnaissance, mine hunting, and mine clearance, are a crucial part of maintaining coastal security and protecting naval assets. To support these missions, there has been a drive to produce more effective tools for the detection, classification, and identification of mines. The automated target recognition problem is twofold: the classification of minelike targets, and the rejection of false targets. An automated algorithm has been developed to perform both target classification and clutter rejection in side-scan sonar images. This fractal-based analysis (FBA) algorithm produced a minelike target classification rate similar to human operators; a low false target rate was also achieved through the successful identification and rejection of image clutter.

Background

Because of recent changes in global military conditions, there has been a shift in emphasis in naval readiness from open ocean warfare to coastal warfare. Preparing for conflicts in the shallow-water coastal regions of the world necessitates the development of strategies for covert coastal surveillance and location of ordnance in shallow coastal waters. The recent conflict in the Persian Gulf underlined the importance of MCM effectiveness to protect Navy assets and allow for zone clearance in preparation for amphibious assault missions.[1] In addition to new mission needs, the continuing drive to achieve higher area coverage rates during MCM operations and the expanding use of remotely operated vehicles have promoted a growing need for computer-automated detection of sea mines, especially in the noisy shallow-water domain. Because the shallow domain contains high levels of both physical bottom clutter and reverberation (image clutter), the identification of clutter is a necessary part of the automated target recognition process. Although the classification of minelike targets is obviously important, the principal problem in MCM operations is the elimination of false targets.[2]

Introduction

The classification algorithm developed at the Naval Surface Warfare Center, Dahlgren Division (NSWCDD), Coastal Systems Station (CSS) is an

FBA algorithm[3,4] that uses fractal characteristics to differentiate between minelike targets, image background, and image clutter in side-scan sonar images. The image clutter may represent physical bottom clutter or may be other types of image clutter, such as reverberation, high gain, and noise components, created by sonar data collection and processing procedures. Many naturally occurring phenomena, including topological features and noise signals, have been successfully modeled using fractals.[5] Manmade structures, which typically consist of Euclidean shapes, do not have fractal characteristics and can, therefore, be distinguished from natural structures. This methodology shows promise for successfully differentiating minelike targets from the sea bottom and noise in sonar images.

A fractal set, process, or surface is one in which the effective, or fractal, dimension is greater than the topological dimension and is not constrained to be an integer. As well as being characterized by real-valued fractal dimensions, fractal surfaces also possess the qualities of irregularity and self-similarity. Irregularity means that the surface cannot be defined by smooth boundaries, and so the area of the surface cannot be exactly measured or calculated. Self-similarity means that, over some range of measurement scales, each scaled piece of the surface displays the same form as the whole surface; that is, the appearance and statistical properties of the surface do not appreciably change. One often-cited, naturally occurring example is the jagged coastline, any magnified segment of which is similar to another segment on another scale. The measured length of a segment of an irregular coastline is dependent on the resolution of the measuring instrument. It should be noted here that any naturally occurring phenomenon is not exactly fractal, but can be expected to contain both random and nonfractal components. However, it may be properly analyzed by its fractal properties if, over some appropriate range of measurement scales, the requirement of statistical self-similarity is fulfilled.

Measurement of Fractal Dimension

There have been a variety of methods devised to calculate fractal dimension. Most involve the measurement of the slope of some empirically derived function that describes jaggedness (in one-dimensional cases), texture (in two-dimensional cases), or "bumpiness" (in higher dimension cases). For the two-dimensional case of sonar images considered here, larger slopes infer greater variation in acoustic pixel intensity that would result in an increase in the calculated fractal dimension value for an image area. Many methods of determining fractal dimension are not well suited for use on sonar images, which have many gray-level values (in our case, 256) and few structures easily definable as sharp edges. The method used for this study was the 3-D method.[6] This method is based on the proposition that an image's intensity variations are a good reflection of the roughness of the imaged surface and that, if the surface has fractal characteristics, then so will the image. To calculate fractal dimension, an image area was covered with rectangular boxes, and the pixel intensity for the image area was then analyzed box by box.

A two-dimensional image actually has two calculable fractal dimensions, one for each of its two topological dimensions. These two fractal dimensions correspond to the average variation in texture, or pixel intensity, in the x and y directions. Also, one average fractal dimension for the whole image region may be calculated. Each fractal dimension over a given image area should have a value between 2 and 3 for a two-dimensional image. Although an actual portion of sea bottom has a third topological dimension, measuring the height of structures above the bottom, a side-scan sonar image maps the bottom with a two-dimensional acoustical "snapshot." This snapshot reduces geographical information, as well as target echoes and sonar-related acoustical phenomena, such as speckle and reverberation, into a single pixel intensity for each bottom portion.

The fractal dimension represents how pixel-intensity statistics within an image area change with changing image resolutions, that is, the

degree of self-similarity over different measurement scales. The statement of self-similarity is

$$E\left(|\Delta I_{\Delta x}|\right) \; \|\Delta x\|^{-H} = E\left(|\Delta I_{\Delta x=1}|\right), \quad (1)$$

where $E(|\Delta I_{\Delta x}|)$ is the expected value of the change in intensity over Δx pixels, and $\|\Delta x\|$ is the norm of the n-dimensional vector Δx. If statistical self-similarity exists, then there is a real value of H for any given image region. Analysis of background areas in our side-scan sonar images indicates that self-similarity does exist over a range of measurement scales. Equation (1) may also be used to determine the value of H. Solving for H yields

$$H = \frac{\log\left(E\left(|\Delta I_{\Delta x}|\right)\right) - \log\left(E\left(|\Delta I_{\Delta x=1}|\right)\right)}{\log\left(\|\Delta x\|\right)} \quad (2)$$

H may be thought of as a persistence factor, with larger values of H corresponding to smoother surfaces. The fractal dimension, D_f, is

$$D_f = (D_t + 1) - H = 3 - H \quad (3)$$

where D_t is the topologic l di. ension of an image. Equation (3) is b: sed on the definition of fractional Browni in n tion. A fractional Brownian pro_ess, $I(x)$, is one in which, for all x and Δx,

$$\Pr\left\{\frac{I(x+\Delta x) - I(x)}{\|\Delta x\|^{H}} < y\right\} = F(y) \quad (4)$$

where $F(y)$ is a cumulative distribution of a random variable y, and $0<H<1$. The increments of I are said to be statistically self-similar with parameter H; that is,

$$I(x) - I(x_0) \text{ and } \frac{I(rx) - I(x_0)}{r^{H}} \quad (5)$$

have the same statistical characteristics.

In practice, the size of the image area used to calculate fractal dimension will have an effect on the resulting dimensional value. With small areas, the small number of points on which to perform the regression will allow noise components, such as image speckle and quantization noise, to have a significant effect on the calculated slope. Using larger areas will reduce the noise effect but will also introduce smoothing of roughness characteristics within the area.

Application to Sonar Images

A side-scan sonar is an active sonar that projects a beam, or beams, perpendicular to the direction of motion of the sensor platform. Each sonar transmission, or "ping," ensonifies a bottom segment that is narrow in the along-track (ping) direction and wide in the range dimension. An image of the sea bottom is formed as the sonar platform moves forward. The resulting image is composed of gray-scale pixels; the area of sea bottom represented by each pixel depends on sonar design parameters and sampling rates. Pixel resolutions in the range and ping dimensions need not be the same. An example of a side-scan sonar image is shown in Figure 1. As sonar images go, this is a very "clean" image; that is, it is relatively free from system noise, gain saturation, bottom clutter, motion distortions, and acoustic anomalies. Also, it is a good image for study because it

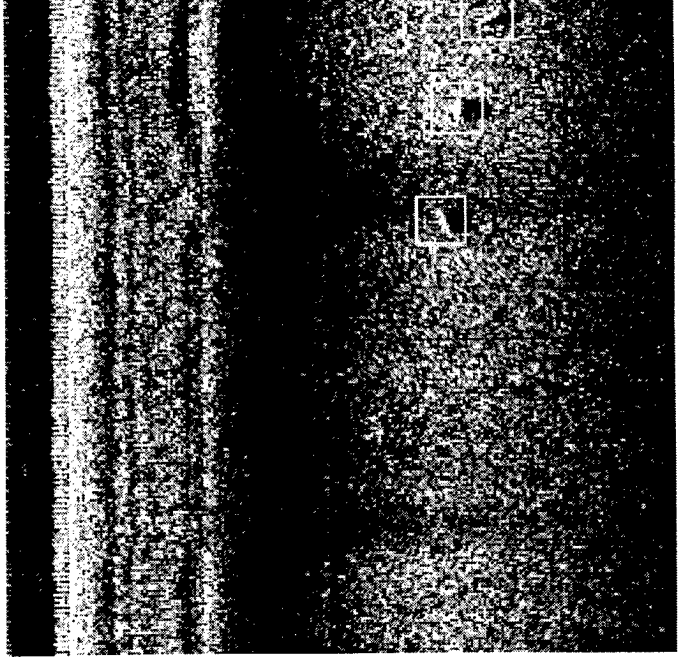

Figure 1. Side-scan sonar image

has three well-defined targets that display both strong highlights and good shadows. This image was taken using a side-scan sonar with a variable aperture that produced constant resolution in the range dimension. Each element has two vertical segments. The top segment has a wide beam to cover the near-range area. The bottom segment has a narrow beam; when sufficient time has elapsed for this beam to reach the sea bottom, this segment is activated to ensonify farther ranges, and the wider segment is turned off. Each sonar image contains 512 range samples, 420 pings, and 256 gray levels.

Although a side-scan sonar images a sea bottom that may be fractal in nature, the image itself will always contain nonfractal features that stem from recording and displaying processes. The image in Figure 1 displays qualities typical of side-scan sonar images. The path of the sonar platform runs vertically up the left side of the image. Scanning the image from left to right (near range to far range), a series of vertical bands can be seen. The first dark band is the sonar return from the water volume. This is followed by a bright band that represents the first bottom return. The bright and dark bands following this are caused by ripples in the vertical beam pattern of the wide beam segment. Notice that these bands are not straight lines from the bottom to the top of the image, but have areas of curvature. The curves indicate motion deviations from a straight-line path of the sonar platform. The motion deviations are very small in this image. The dark area following these narrow bands shows signal attenuation with range for the wide-beam segment. The narrow segment is activated at about one-third of maximum range, and its signal attenuates to low levels at maximum range. This is a beamformed image to which both time-varying gain (range direction) and automated gain control (ping direction) signals have been added. The targets lie in an area of relatively high gain.

Figure 2 shows the same sonar image as shown in Figure 1 after it has been background-normalized. The goal of background normalization is to remove artifacts—such as

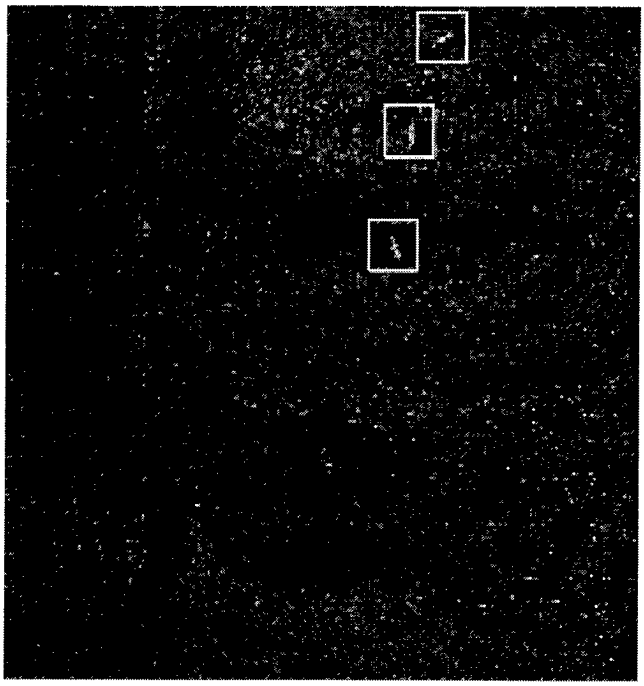

Figure 2. Background-normalized image

signal attenuation with range, effects of gain functions, and transient events—while retaining target highlights and shadows. Before a series of images can be productively analyzed by automated computer algorithms, it is necessary to imbue the images with a consistent background-intensity distribution against which targets can be compared. The normalization algorithm applied here is part of the Iterative Statistics Algorithm (ISA) developed at NSWCDD CSS. It uses running arithmetic means in both the range and along-track dimensions to produce a background- normalized image; it was developed with the purpose of reducing background variation without significantly degrading small targets.

Three features of these images are of particular interest and relevance as to their effect on the fractal nature of the sonar image.

First, because images were produced using a narrowband sonar, there is a high level of random speckle in the image that represents areas of constructive and destructive interference of the sonar returns. This speckle acts as a random noise signal that overlays the fractal characteristics of the physical sea bottom, and it has the effect of increasing fractal dimension values.

Second, a quantization noise signal is produced during the analog-to-digital conversion process when an analog voltage is converted to a digital (integer) pixel intensity. This signal is not of significant magnitude in the images shown because 256 gray levels were sufficient to cover the dynamic range of the sonar signals.

Third, the background-normalization procedure can be expected to have a significant effect on the fractal qualities of an image. Because normalization imposes regularity of background intensity on an image, it is by definition not a fractal process.

Three important points should be made about the analysis of images using fractal features.

First, because the fractal dimension relationship shown in Equation (3) is based on a Brownian signal, when attempting to compare two image areas using fractal features, the calculated features indicate not only the difference in texture between the two areas, but also how much the underlying spectral structure of each area differs from Brownian, or $1/f^2$, noise.

The second important point to remember when applying fractal methods to actual images is that sonar and other types of

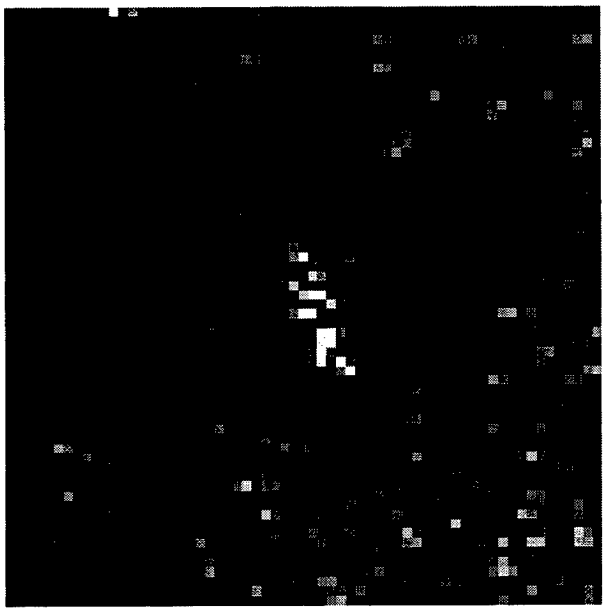

Figure 3. Imaged minelike target (Zoom = 8)

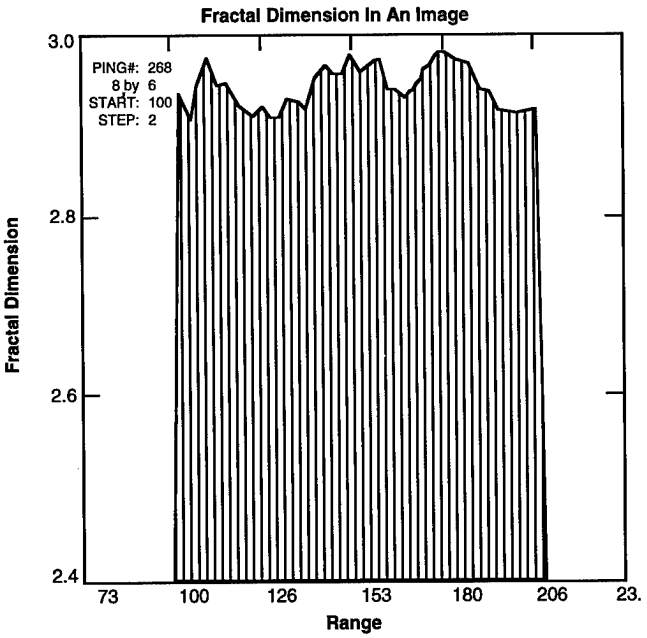

Figure 4. Fractal dimension across a background area

images contain speckle, nonlinear gain adjustments, and other imaging effects resulting from the type of sensors and displays used to form the images. The statistical structure of these "noise" components will have a direct, and sometimes significant, effect on the calculated fractal features. Moreover, different fractal methods will be affected differently, depending on the underlying assumptions made by each method.

Finally, the fractal dimension value for each image area will depend on the extent to which that area has fractal characteristics.

Figure 3 shows a magnified image that contains the bottom-most target from Figure 2. Low pixel values in the target highlight and high values in the shadow indicate the level of speckle contamination. Some of the pixels in this background are of sufficiently high intensity to be classified as target highlight pixels. This figure demonstrates the difficulty of developing detection/classification features, from any target classification model, that will differentiate target highlights, target shadows, and nontarget areas. Figure 4 shows the variation in fractal dimension across a horizontal slice through an area of background. In this and the next figure, the x-axis is a neighborhood of range cells from the sonar image and the y-axis is fractal dimension.

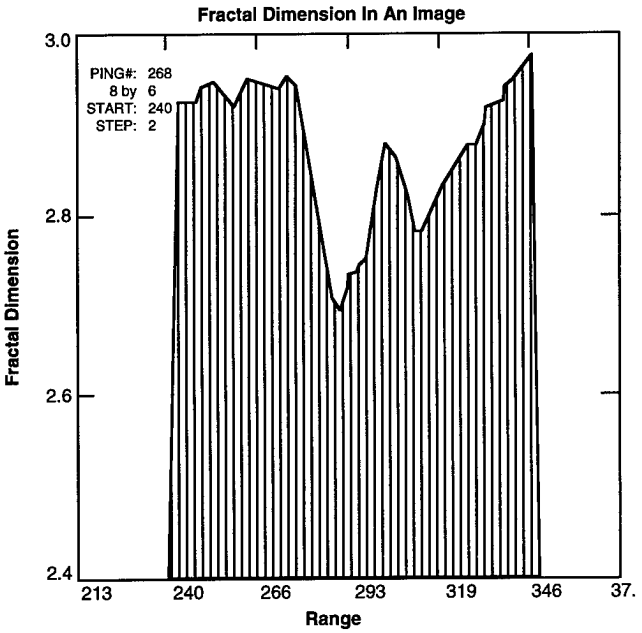

Figure 5. Fractal dimension across a strong target

Figure 5 shows the variation in fractal dimension across a horizontal slice of image containing the bottom-most target in Figure 2. The two dips in Figure 5 represent the acoustic highlight followed by the target shadow.

Automated Target Detection Methodology

Sonar images contain a number of characteristics, derived from sonar-design attributes, image-display practices, and acoustic transmission effects, that complicate the process of automated target recognition.

First, the probability of successful target recognition is limited by the number of image pixels that constitute a target highlight. Because sea mines are relatively small objects, the entire target highlight may comprise only one to three dozen pixels, far fewer than available in typical radar and electro-optic images. The small number of pixels on target also limits the amount and types of processing that can be performed on an image, because any smoothing or averaging process will partially smooth out the target as well.

Second, because side-scan sonars typically have narrowband projectors and receivers, there is a high level of random speckle in the resulting images. This random speckle has the effect of obscuring targets by lowering the signal-to-noise ratio of target highlights and shadows.

Third, side-scan sonars tend to have narrow beam apertures to achieve adequate resolution. This narrow beam produces good forward reflection off angled targets, so at some target angles, not much signal energy gets reflected back to the sonar receiver. This produces an imaged target (a) defined mostly by its acoustic shadow and (b) possessing only a small or weak highlight. It is very difficult to achieve automated detection of target shadows because the shadow is embedded in the background, and both shadow and background are contaminated by speckle. Shadow-to-background pixel intensity ratios are typically much smaller than highlight-to-background ratios.

A set of fractal features was derived to characterize areas within an image by converting a side-scan sonar image to a corresponding fractal dimension image, then performing a series of windowing, filtering, and thresholding operations. Figures 6 and 7 show the resulting fractal dimension images for two different box sizes. Using a small box retains much of the speckle that contaminated the original image, but also retains the targets. Using a bigger box reduces the level of both the speckle and the targets. Both of these box dimensions, as well as the magnitude of their difference, are useful features. If the two box sizes yield much the

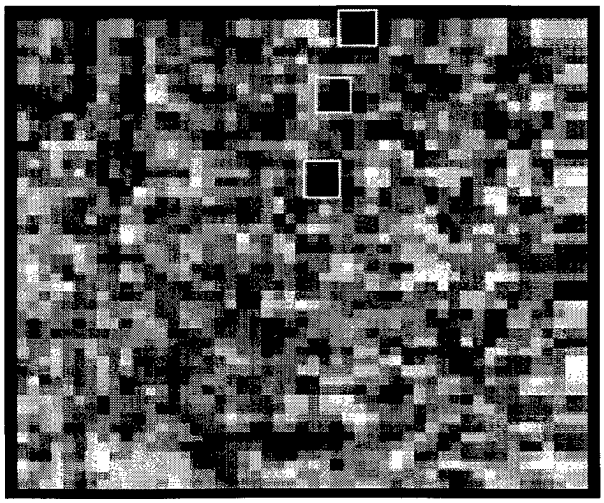

Figure 6. Small box fractal dimension

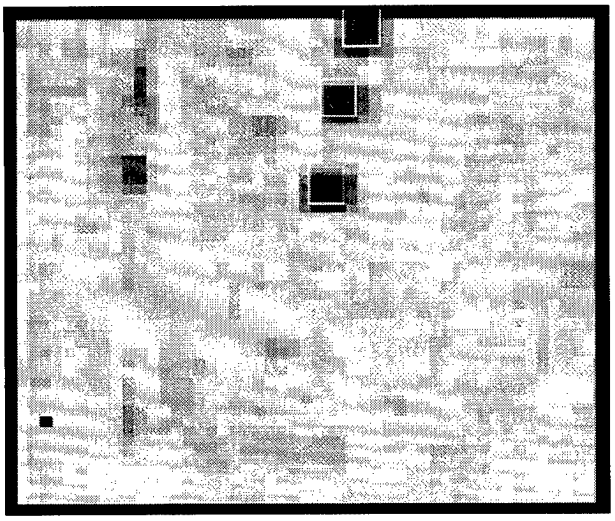

Figure 7. Big box fractal dimension

same value of dimension, that is an indication that the sonar image in that area is fairly uniform and, so, is probably a background or other nontarget area because the small box dimensions were set at sizes sufficient to include targets of interest.

Once an image area has been identified as an area of interest by a detector, that area is characterized by the calculation of higher-order fractal features. For illustrative purposes, an area of background is analyzed in Figure 8. In this figure, the center point in range is identified with a black circle. A window is formed around this point, and the fractal features within this window are compared to those in adjacent image windows. The fractal dimension is calculated about those points denoted by the four empty circles. For the three windows in a background area, the small-box fractal dimension has virtually the same value (about 2.95) at all four points of measurement. This large value represents the high level of speckle produced in images taken with this sonar. The difference, *FDIF*, between the big-box and small-box fractal dimensions is near zero. The average slope is also small, as positive and negative fluctuations in background intensity and speckle are about equal in magnitude. Other fractal features calculated for these windows also have either identical or very similar values.

Figure 9 shows an analysis of the image area around the same strong target previously

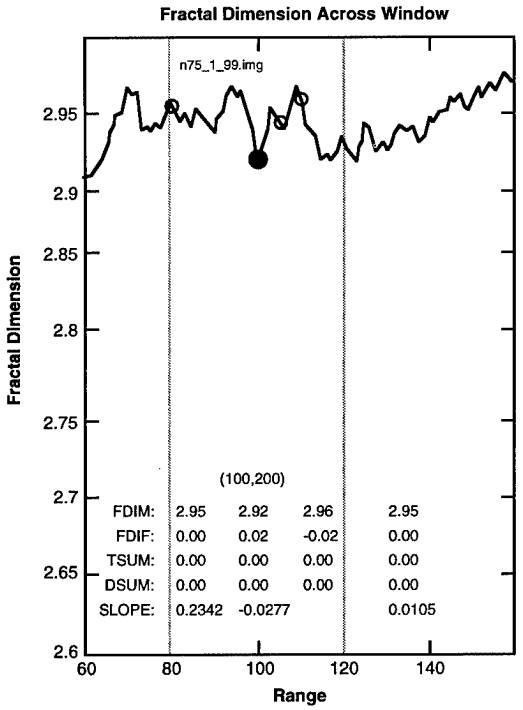

Figure 8. Fractal features across a background area

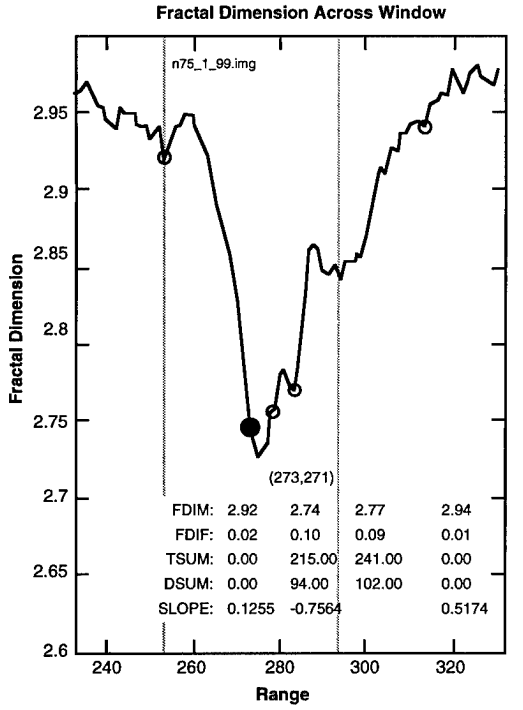

Figure 9. Fractal features across a strong target

discussed. The large dip in the center window represents the target highlight, and the smaller dip just beyond it is the target shadow. This figure immediately makes apparent the difficulty of detecting even a strong shadow because of its small size. The strong, stable highlight, however, stands out clearly. The center window has a small-box fractal dimension about 0.18 smaller than the adjacent windows. Also, the difference between the big and small box dimensions is about six times higher for the center window than in the adjacent windows. The average slope and other calculated fractal features are also significantly different.

All the analysis in the previous sections has been performed on the image in our data set with the least noise and motion, the strongest targets, and no bottom clutter. Images that have less desirable characteristics make the job of target detection and classification much harder. The presence of image clutter is particularly troublesome because the clutter typically produces a high false target rate (FTR). Figure 10 shows an image with heavy clutter that represents physical debris. In general, the more complex and problematic the image, the more high-order fractal features are required to successfully identify both targets and clutter.

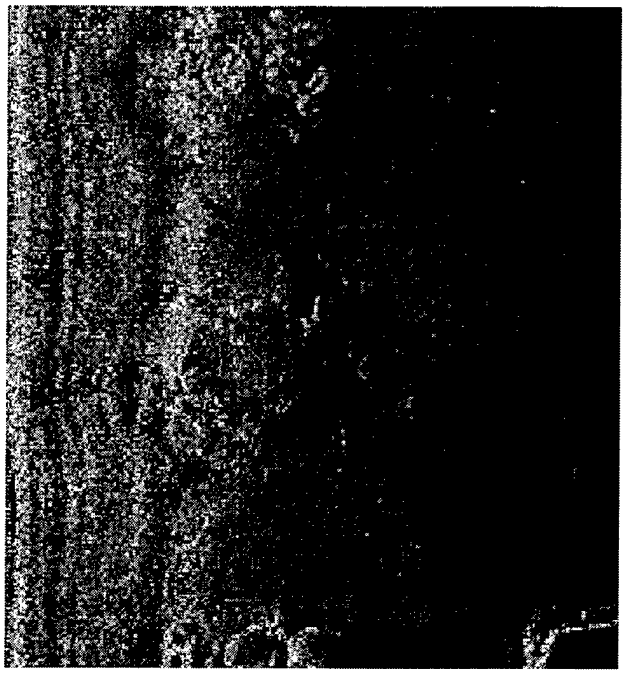

Figure 10. Highly cluttered image

Results

Sixty images were analyzed using an FBA target classifier. Target detection was performed using the ISA, which identified image areas of possible interest and passed the center coordinates (x_c, y_c) of each detection square to the FBA classifier. The 60 sonar images were assigned to two groups: a 30-image training set and a 30-image testing set. The training set was used to develop successful image analysis techniques and to set target classification thresholds. This training set was analyzed multiple times until optimum results were obtained. The resulting classification scheme was then applied to the testing set. FBA-classified targets were then compared to a list of sanctioned targets whose locations were known from groundtruth taken during the sonar test. A very conservative approach was taken to calculating probability of detection/classification (PDPC) scores. An imaged object was considered a minelike target if it was on the list of sanctioned targets, regardless of the size or strength of its acoustic signature within the image. Likewise, an imaged object was considered a false target regardless of its imaged appearance if it was located in an area for which there was no available groundtruth.

Classification thresholding for detected objects was done in three stages: (1) minimum thresholding for object acceptance, (2) thresholding for minelike target classification, and (3) identification of clutter. Values of the calculated fractal features were highly consistent with the visual appearance of the imaged object. Strongly minelike targets had feature values well different from the threshold values, whereas weak or small targets had values close to the thresholds. Known targets (from the groundtruth target list) that were not classified as minelike were weak targets. This analysis was also successful in discriminating against clutter. Most of the false targets classified in images containing target

fields were actually field markers, such as buoys and icosahedrons. False targets classified in cluttered images were typically isolated bright highlights that were separated from an extended highlight structure.

The resulting training set PDPC was 0.78, and the FTR was an average of 1.7 false targets per image. The testing set results were a PDPC of 0.72 with an FTR of 1.6 per image. The training set of images was shown to four human operators, who were assigned PDPC and FTR scores by comparing their list of targets to the sanctioned target list. The operator who achieved the best PDPC score on the training set was also shown the testing set. A comparison of performance scores for tested operators and the fractal-based analysis procedure are presented in Table 1.

Conclusions

The fractal features of a side-scan sonar image can be used to distinguish minelike targets from nontarget areas. For the image set studied, FBA achieved PDPC scores comparable to the average human operator. FTRs were higher than for human operators. The higher FTR appears to be mostly due to the classification of false targets that lie isolated from, but are part of a larger area of bottom clutter or reverberation. These types of false targets are easier for human operators to reject because the targets can be visually examined in the larger context of the whole image. Also, the human operators learned not to accept field markers as minelike targets.

The automated target recognition task is more difficult for images that contain motion distortions, heavy clutter, gain saturation, or other noise problems. Its success also depends on the achievable resolution of the sonar, how many pixels comprise a minelike target, and the number of gray levels allowable in the image. The use of FBA of sonar images is likely to be most successful at target classification, with the minimum achievable FTR, when used in conjunction with other signal and image processing modules, such as neural networks, which can mimic the human process of acquiring experience.

Increasingly sophisticated image processing techniques, such as FBA, and the increasing speed of hardware processors, give promise of advancing the state of the art in automated target recognition. In practice, these techniques will always be limited by the quality of the image, which is, in turn, limited by the resolution and stability of the sonar. Also, sonar signal processing techniques used during data collection are now geared toward producing an image scaled for human display. This practice usually results in images that have been scaled and clipped to produce very bright target highlights and correspondingly brighter shadow areas. Storage of signal data before it has been rescaled for human display would provide a more suitable image with greater dynamic range for computer analysis.

Table 1. Performance Scores for FBA Classifier

	COMBINED SETS		TRAINING SET	TESTING SET
	OPERATOR AVERAGE[1]	BEST OPERATOR[2]	FBA[3]	FBA[3]
PDPC	.71	.85	.78	.72
FTR (per image)	.75	.72	1.7	1.6

[1] Four operators were used for the training set, one for the testing set.
[2] The best operator from the training set was used for the testing set.
[3] Fractal-Based Analysis. (see 1&2)

Also, the ability to successfully process sonar images for target detection is greatly enhanced by proper site groundtruth; that is, by recording environmental, target, operational, and other supplementary data at the same time as sonar data are collected.[7]

Acknowledgments

This work was funded by the Office of Naval Research (Dr. Wally Ching, ONR 321) under the Sensor Signal/Image Processing Project (RN15C83A) within the Mine Reconn/ Hunter Program.

References

1. Walsh, E.J., "Navy Adopts New Doctrine, New Technologies to Address Changing Mine Countermeasures," *Defense Electronics*, Jul 1992, pp. 40-46.
2. Skinner, D.P., "Mine Countermeasures (MCM) Sensor Technology Drivers," Keynote Address, *Proceedings of the SPIE Conference on Detection Technologies for Mines and Minelike Targets*, 17-21 Apr 1995, Orlando, Florida, vol. 2496, pp. 608-613.
3. Nelson, S.R. and Tuovila, S.M., "Fractal-Based Image Processing for Mine Detection," *Proceedings of the SPIE Conference on Detection Technologies for Mines and Minelike Targets*, 17-21 Apr 1995, Orlando, Florida, vol. 2496, pp. 454-465.
4. Nelson, S.R. and Tuovila, S.M., "Automated Recognition of Acoustic Image Clutter," *Proceedings of the SPIE Conference on Detection Technologies for Mines and Minelike Targets*, 8-12 Apr 1996, Orlando, Florida.
5. Mandelbrot, B.B., *The Fractal Geometry of Nature*, W.H. Freeman and Company, 1983.
6. Pentland, A.P., "Fractal-Based Description of Natural Scenes," *IEEE Transactions on Pattern Analysis and Machine Intelligence*, Vol. PAMI-6, No. 6, Nov 1984, pp. 661-674.
7. Tuovila, S.M., *Supplementary Data Collection to Enhance Sonar Testing*, CSS TN 1108-92, Coastal Systems Station, Dahlgren Division, Naval Surface Warfare Center, Oct 1992.

The Authors

Susan M. Tuovila

SUSAN M. TUOVILA is a senior mathematician at NSWCDD CSS in Panama City, Florida. She has worked in the areas of environmental science, sonar simulation and data analysis, sonar image processing, and automated target recognition.

Susan R. Nelson

SUSAN R. NELSON is a senior mathematician at NSWCDD CSS in Panama City, Florida. She has extensive experience in signal and image processing, computer modeling, and software design. In recent years, she has been involved in the development of automated target recognition algorithms for the detection and classification of sea mines.

High Resolution Array Processing for the High Area Rate Reconnaissance Side-Look Sonar

Jo Ellen Wilbur, Christopher A. Sermarini, R. Lee Thompson, and James F. Bryan

EW
EXPEDITIONARY
WARFARE

The High Area Rate Reconnaissance (HARR) side-look sonar (SLS) contains a periodically spaced, real receive array designed for detection and classification of bottom and close-tethered mines. The work reported here is taken from an examination of the utility of high resolution array processing (HRAP) and noise reduction techniques as related to the HARR SLS. Issues specific to the SLS and its operational requirements greatly impact the applicability of different HRAP methods to the SLS. The HARR SLS is an imaging sonar whose primary noise contribution is bottom backscatter. It is an oversampled, filled array that operates in the near-field Fresnel zone of the array. Very high resolution, model-based or autoregressive (AR) array processing techniques have limited use in the HARR SLS. The overlapped-subarray correlogram (OSC) and the minimum variance distortionless response (MVDR) processors each have advantages; however, their correlation matrices must be defined to maximally decorrelate noise while simultaneously maintaining range and cross-range resolution. The work presented here concentrates on a relative comparison in resolution and noise reduction between Fast Fourier Transform (FFT) beamforming and the OSC, MVDR, and AR processors.

Introduction

Much research has been done in the area of array processing; however, most of the work has focused on arrays that satisfy conditions that typically are not satisfied by mine-hunting sonar. Since mine-hunting sonars are active, noise can consist of bottom reflections, surface reflections, and volume reverberation, each correlated to the transmit signal, as well as thermal noise that is not correlated. Many of the usual assumptions fundamental to sophisticated array processing algorithms (for example $\lambda/2$ element spacing, constant angle resolution, uncorrelated Gaussian noise, and far-field operation) do not apply to the SLS. Relative performance of array processing algorithms frequently focuses on bearing resolution between targets at a fixed range. The SLS is an imaging sonar in which range resolution is also a factor. Issues specific to mine-hunting sonar greatly impact the type of array processing that has potential for the SLS. The SLS is designed for bottom and close-tethered mine detection and classification; because the dominant source of noise is bottom reflections, the noise is correlated to the transmit signal. Consequently, the gain in resolution obtained from array

processing methods applied to SLS stave data can be shown to vary with bottom type. In fact, without proper modification, some high resolution array processors could actually yield a lower resolution than conventional beamforming in, for example, the case of a gravel bottom. These same processors would produce extremely high resolution when operating over a mud or silt bottom.

Designed for operation in the near field, the SLS is a variable-length aperture, line array of contiguous filled elements, with spacing between element centers on the order of 27λ. It is an imaging sonar designed for detection and classification of bottom and close-tethered mines. This makes model-based high resolution array processing methods limiting for the SLS. Furthermore, in the array processor, the correlation matrix must be modified to achieve an improvement in cross-range resolution without imposing any degradation in range resolution.

The periodic real array was chosen as a basis for the SLS design because of its versatility and relative tolerance to platform motion. That is, roll, pitch, and yaw will affect all the array elements uniformly. The array is 3.8 m comprising 38 contiguous 10-cm elements. The projector pattern in the horizontal plane is formed by a four-element, bizonally shaded, 14.24-cm long, half-cylinder array. The bizonal shading yields maximum side lobes of -18 dB in the horizontal plane. The projector array pattern is a unique arrangement designed to minimize the deleterious effects of surface reverberation in shallow water. Acoustic energy is prevented from reaching the surface by the mechanical arrangement comprising a 5-cm diameter, half-cylinder array placed directly beneath a large acoustic mirror countersunk into the bottom of the tow vehicle. This results in a "brick wall," 180-deg, verticle plane pattern.[1]

Array Processing of the HARR SLS

The SLS forms a spatial isomorphism to zoom or band-select spectral estimators[2] where the decimation factor for the SLS is 53. The array elements are not omnidirectional, and the SLS configuration maintains a 27λ spacing between elements, which is significantly undersampled relative to the Nyquist criterion of λ/2 intrinsic to most high resolution array processing algorithms. As stated, the array comprises 38 contiguous elements with center spacings 10 cm apart. For a continuous wave (CW) transmission frequency of 400 kHz, the Nyquist rate is 1.875 mm. A 53-fold decimation to the 10-cm spacing results in aliasing of the 53 spatial bands. In the spatial folding process, this yields aliased main lobes at spacings of 2.15 deg. Unless the beam is steered more than 1 deg, signal bandwidth-related aliasing in the spatial sampling process is nominal. The aperture fill acts as the spatial bandpass filter in the zoom process with nulls at 2.15 deg. (See addendum, page 13, for details.)

Figure 1 gives the sound pressure levels for a single element, given that the HARR SLS is operating 40 m above a sandy bottom in 200 m of water and given a sea state of 3. From Figure 1, the dominant source of noise in the SLS is seen to be bottom backscatter. Although the ensonified area in the beamwidth of each element increases with range, the backscattering coefficient decreases as the grazing angle becomes smaller with range. Therefore, the effective strength of the bottom backscatter at the output of each array element is relatively constant over range. Because attenuation losses for the target and backscatter are the same, the relative difference in sound pressure levels for the target and bottom backscatter are constant over range. More specifically, the signal-to-noise ratio (SNR) at the stave output is constant over range. Recall that the SLS is a side-scan designed for constant range cell resolution, which means the output SNR will increase with range in the beamforming process. For example, the relative increase in SNR from the output of a conventional time-delay or phase-shift beamformer increases as a function of the number of elements used to

form the beam, coupled with the relative coherency of both target and noise between each element. At 205 m, all 38 elements are used in beamforming to produce a cross-range cell resolution of 20 cm. To effect the same resolution at 45 m, nine elements are used for beamforming. Given a sandy bottom, the SNR input to the beamformer, or the output for each filled element, is seen in Figure 1 to be on the order of 4 dB. The corresponding output SNR from the beamformer is a function of the relative coherency between elements for the target return versus the coherency between elements for the noise. For the ideal case of complete coherency across all elements for the target return and incoherency for the noise over all elements, an FFT or phase-shift beamformer yields a maximum SNR potential of 13.5 dB at minimum range, increasing to 19.8 dB at maximum range. As the ratio of target coherency to noise coherency across the array decreases, the output SNR from the beamformer is degraded. Effective signal designs can be employed to maximize this ratio.

To test different array processors, SLS stave data for the HARR were simulated using a ray tracing model in which the ocean bottom was simulated as a collection of random scatterers, uniformly distributed on the plane of the seafloor and Gaussian in scattering amplitude. Point source targets or rectangular targets could then be placed at

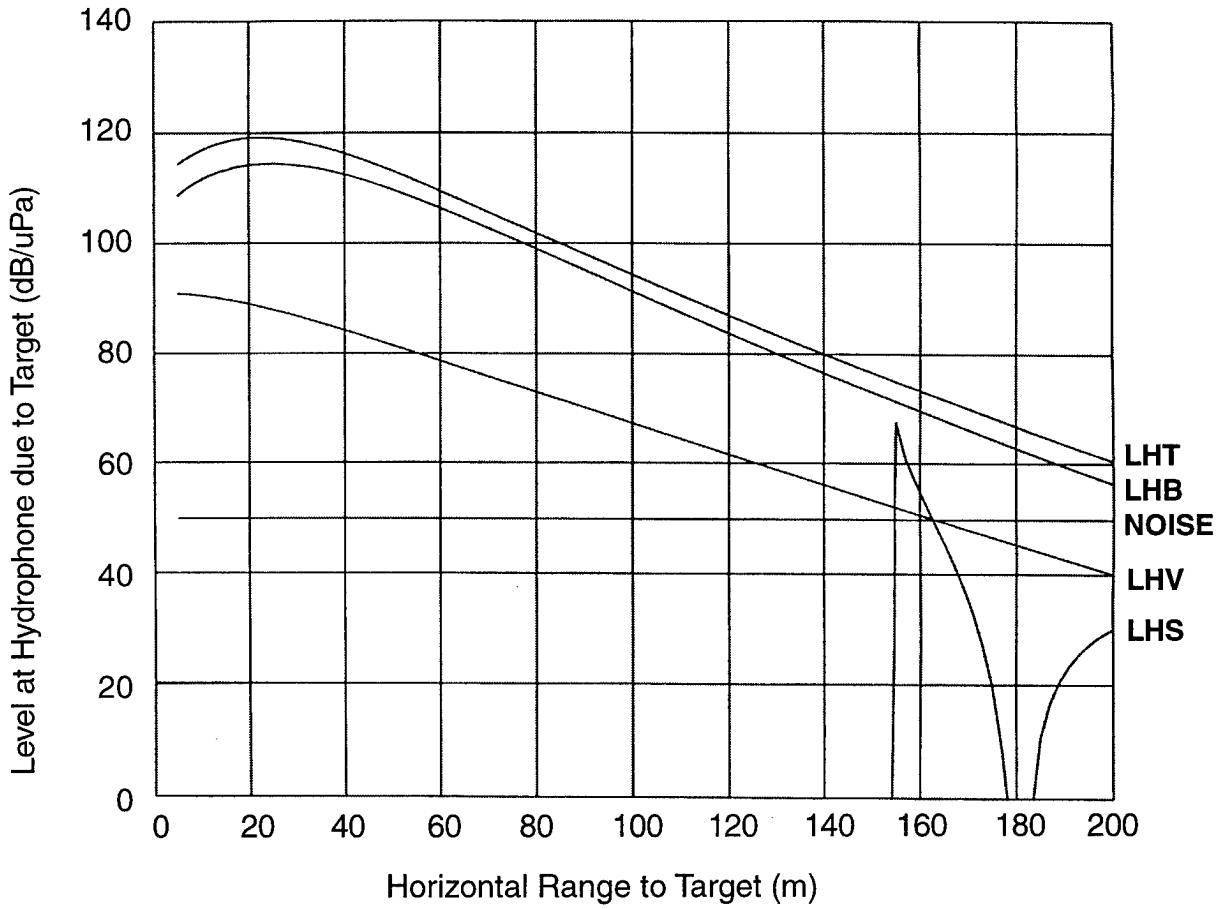

Figure 1. Sound pressure levels for a single element given 266 μs CW pulse, a water depth of 200 m, soundhead height above the bottom of 40 m and tilt angle of -30 deg, a target strength of -20 dB, a sea state of 3, and a sandy bottom. LHT denotes the level at the hydrophone due to the target as a function of range, LBT corresponds to bottom return, LHV to volume reverberation, and NOISE to ambient noise

various azimuth and range separations in this simulated environment. A software simulation of the data acquisition system for the SLS was incorporated into the simulator.

FFT Beamforming

Stave data are down-converted in frequency, separated into in-phase and quadrature-phase components, then digitized. The beamforming is done in software in which the time samples are termed "snapshots." Given θ, the direction of propagation of the incoming wave, the beamformer output at each snapshot, t_n, can be expressed in matrix form as

$$\begin{aligned} y(t_n, \theta) &= \mathbf{a}^H \mathbf{x} \\ \mathbf{x} &= (x_0\ x_1\ \cdots\ x_{M-1})^T \\ \mathbf{a} &= (a_0\ a_1\ \cdots\ a_{M-1})^T \end{aligned} \quad (1)$$

for **a**, the beamformer filter coefficients, where T = *transpose* and $x_m = s_m^a(t_n, \theta)$ is the heterodyned, filtered, analytic, sampled output of the mth stave.

The energy in each beam is defined by the spatial variance or spread of the beamformer[3]

$$\|y\|^2 = \mathbf{a}^H \mathbf{R}_{xx} \mathbf{a} \quad (2)$$

where $\mathbf{R}_{xx} = \mathbf{x}\mathbf{x}^H$ is the spatial correlation matrix. For a given target, the minimum mean-square error solution as a function of θ to Equation (1) yields the case for which

$$\mathbf{a} = \left(1 \quad e^{-j\frac{2\pi}{\lambda} d\sin\theta} \quad \cdots \quad e^{-j\frac{2\pi}{\lambda}(M-1)d\sin\theta} \right)^T \quad (3)$$

such that the beam points in the direction of the incoming wave. For $\mathbf{R}_{xx} = \mathbf{x}\mathbf{x}^H$, Equation (1) defines an FFT or phase-shift beamformer where, even in the absence of noise, maximum resolution is limited by the aperture length, $L = md$, with m being the number of elements used to form the beam.

Figure 2 gives the image and array pattern from the FFT beamformer for the return from a point source at maximum range, where the SNR of the stave data is 4 dB and is dominated by bottom reflections. The transmit signal was a 266-µs CW pulse corresponding to 20-cm resolution in the range direction. The results are identical to that of a phase shift beamformer.

Overlapped-Subarray Correlogram Processor

When the elements of the correlation matrix $\mathbf{R}_{xx}$ are estimated over an ensemble of snapshots such that **x** becomes an $N \times M$ matrix of N-dimensional vectors of the form

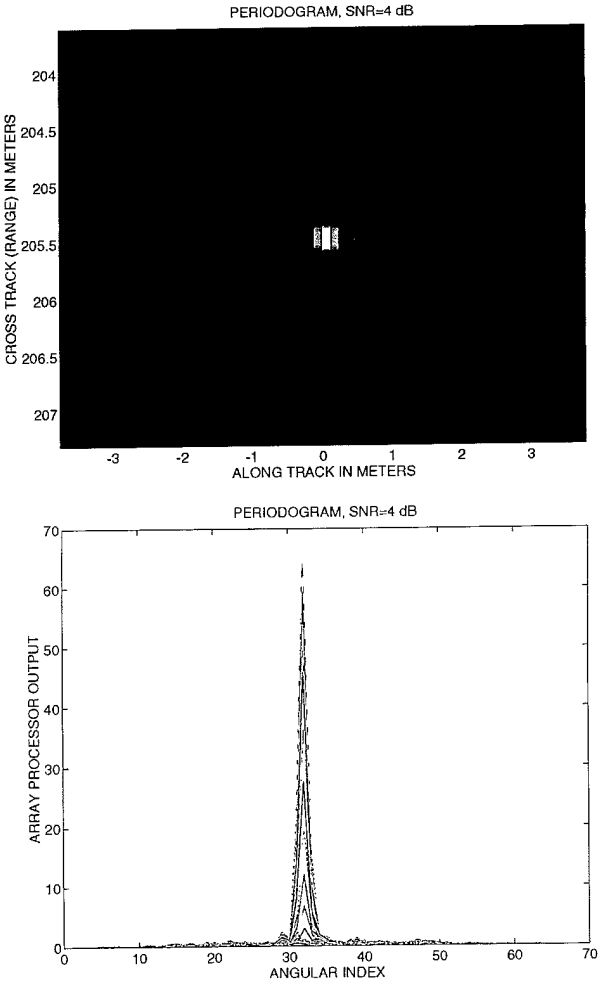

Figure 2. Image and array pattern of the FFT beamformer for the return from a point source at 205.5 m, given a 266 µs CW transmission and 4 dB SNR

$$\mathbf{x} = (\mathbf{x}_0, \mathbf{x}_1, \ldots \mathbf{x}_{M-1})^T, \quad (4)$$

the beam energy pattern in Equation (1) is defined by the spatial equivalent to the Blackman-Tukey correlogram spectral estimator.[3,4] The collection of snapshots defines the ensemble of waveforms where ensemble averaging is used to raise the SNR. This form of array processor is termed the correlogram and applies when the element spacing is on the order of $\lambda/2$ or when beamforming is used for bearing estimation.

The SLS is an imaging sonar that transmits a 266-μs CW pulse. Therefore, ensemble averaging is limited to less than 20 cm. This means averaging out noise contributions is limited to less than 10 cm in the range direction. However, across array elements, where the element samples are separated by more than 25λ, the noise per sample is significantly less correlated. Therefore, for the SLS to yield maximum SNR, while at the same time preserving both range and cross-range resolution, the correlation matrix elements are calculated by forming subarrays and averaging across array elements, instead of ensemble averaging.

The OSC is calculated by replacing the matrix elements in Equation (2) with:

$$r_{xx}(i,j) = \frac{1}{M-|i-j|} \sum_{m=0}^{M-|i-j|-1} x^*_{m+i-j} x_m \quad (5)$$

where $r_{xx}(i,j)$ is the i-j lag autocorrelation estimate for the ith row, jth column matrix element in $\mathbf{R}_{xx}$.

Equation (5) gives the unbiased autocorrelation estimate. The resultant beamwidth is related to the total array length used in the OSC and is directly related to the beamwidth of the spatial transform of the effective window defined by the array length and element shading. That is, for an unshaded array, the effective window is a rectangle of length $L = md$, and the corresponding transform is the digital sampling function, or Dirichlet kernel,

$$D(\lambda,\theta) = \frac{\sin\left(\frac{\pi md}{\lambda}\sin\theta\right)}{\sin\left(\frac{\pi d}{\lambda}\sin\theta\right)} \quad (6)$$

where m is the number of elements used in the beamformer at a given range. The angular distance between 3 dB points in the unbiased OSC is $D(\lambda, \theta_{3_{dB}}) = \frac{1}{2}D(\lambda, 0)$, which at maximum range, or 205 m, yields $\theta_{3dB} = 0.058$ deg corresponding to a cross-range resolution of $\Delta r = 20.24$ *cm*.

Figure 3 gives the image and array pattern from the OSC processor for the return from a point source at maximum range, given 4 dB SNR. The correlation matrix elements were estimated by averaging over two-thirds the length of the aperture at each range. Averaging across the array has effectively raised the SNR over that of the conventional FFT beamformer. Although averaging the correlation matrix increases the SNR and the beamwidth appears narrower, resolution, when defined as the ability to spatially resolve two point sources, is still limited by the aperture length, L.

Notice that Equation (1) yields negative side lobes. An alternative correlogram processor uses the biased autocorrelation estimate

$$r^b_{xx}(i,j) = \left(1 - \frac{|i-j|}{M}\right) r_{xx}(i,j) \quad (7)$$

for $r_{xx}(i,j)$ defined in Equation (5). The correlogram estimator defined by Equation (7) yields a beam pattern corresponding to the transform of the triangular function, or $\frac{1}{2}D^2(\lambda, \theta/2)$.

High Resolution Model-Based Processing

Model-based array processors[3] are high resolution processors; however, their application to the SLS is limited. Figure 4 gives the

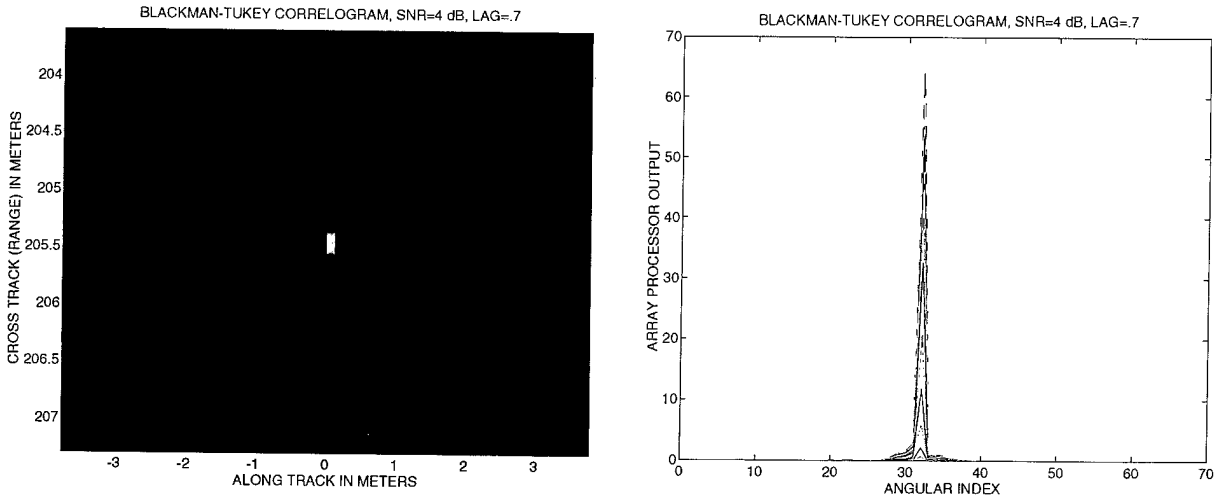

Figure 3. Image and array pattern of the OSC array processor for the return from a point source at 205.5 m, given a 266 μs CW transmission and 4 dB SNR

image and array pattern from an AR array processor for the return from a point source at maximum range, given 4 dB SNR. The model order was defined to equal two-thirds the number of array elements used at each range, and subarrays were used to form the covariance matrix. Because the model order was large relative to the number of elements used to form the beam, the modified covariance method was used to prevent spurious peaks attributed to line splitting, which can occur in the Burg algorithm.[3]

At maximum range, the AR processor can be seen from Figure 4 to produce a very high resolution, high SNR image. However, as the number of stave elements is reduced, the performance of the SLS is considerably degraded. Still, the SLS is likely to reserve high resolution processing for the outer half of the sonar operating range. First, the limiting resolution is defined by the resolution that can be achieved at maximum range where all elements are used in the beamforming, whereas doubling the resolution over the first half-range can be achieved by doubling the number of elements used to form the beam. Further, the number of degrees of freedom is related directly to the number of elements used in the beamformer, allowing for more flexibility in the array

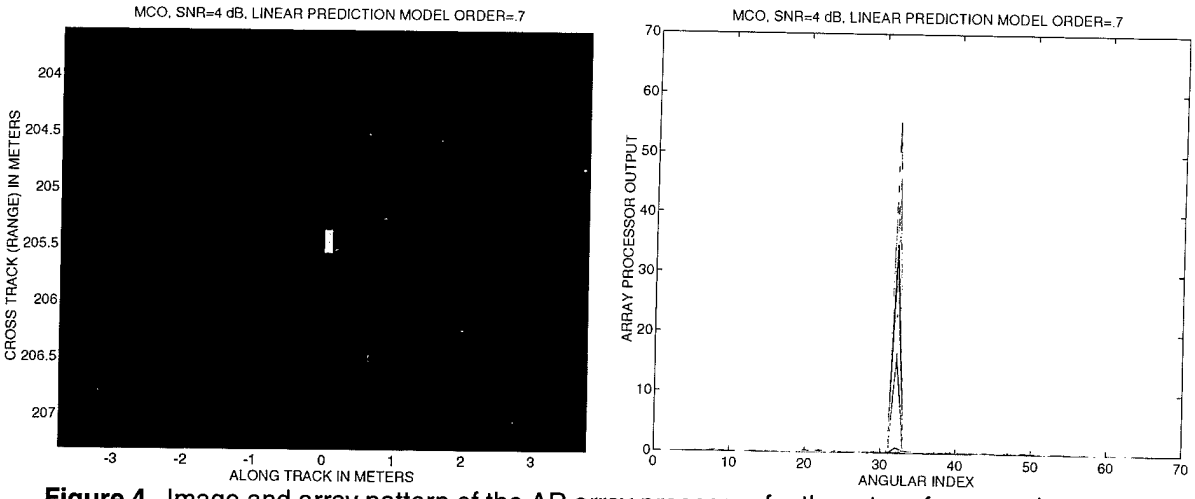

Figure 4. Image and array pattern of the AR array processor for the return from a point source at 205.5 m, given a 266 μs CW transmission and 4 dB SNR

processing algorithm over the second half of the sonar operating range. However, keeping a constant cross-range resolution over range can be problematic, especially since resolution is a function of SNR. Further, the AR processor maintains a nonlinear relationship to power, making conversion from processor output into sonar image difficult, especially since the SLS is a bottom search sonar where noise is dominated by scattered reflections off the bottom and correlated to the transmit signal.

Minimum Variance Distortionless Response

An alternative HRAP method for which the output peaks are linearly related to the power in the beam is the linearly constrained MVDR estimator. Although the improvement in resolution is not as great as for model-based array processing, the linearly constrained MVDR does not produce spurious peaks, and, by definition, the output maintains a linear relation to power.

The MVDR is designed to minimize Equation (1) subject to the constraint that the signal vector passes undistorted.[5,6] That is, for N sources, design the filter such that Equation (1) is minimized subject to the constraint

$$\mathbf{a}_{MVDR}^{H}\mathbf{c} = 1 \tag{8}$$

where

$$\mathbf{c} = \begin{pmatrix} 1 & e^{-j\frac{2\pi}{\lambda}d\sin\theta} & \cdots & e^{-j\frac{2\pi}{\lambda}(M-1)d\sin\theta} \end{pmatrix}$$

in the direction of propagation of the incoming wave, and 1 denotes a unity vector of dimension L. The signal vector $\mathbf{x}$ is an $L \times M$ matrix of L-dimensional vectors

$$\mathbf{x} = (\mathbf{x}_0\ \mathbf{x}_1\ \cdots\ (\mathbf{x}_{M-1})^{T} \tag{9}$$

where

$$\mathbf{x}_i = (x_0\ x_1\ \cdots\ x_{L-1})$$

for L, the number of spatial lags. As with the OSC, estimation of the correlation matrix elements for the SLS is calculated by averaging across the array instead of over snapshots. The MVDR filter becomes

$$\mathbf{a}_{MVDR} = \frac{\mathbf{R}_{xx}^{-1}\mathbf{c}}{\mathbf{c}^{H}\mathbf{R}_{xx}^{-1}\mathbf{c}} \tag{10}$$

which yields the following expression for the output beam energy:

$$\|y\|^2 = \frac{1}{\mathbf{c}^{H}\mathbf{R}_{xx}^{-1}\mathbf{c}} \tag{11}$$

Figure 5 gives the image and array pattern for the MVDR array processor for the return

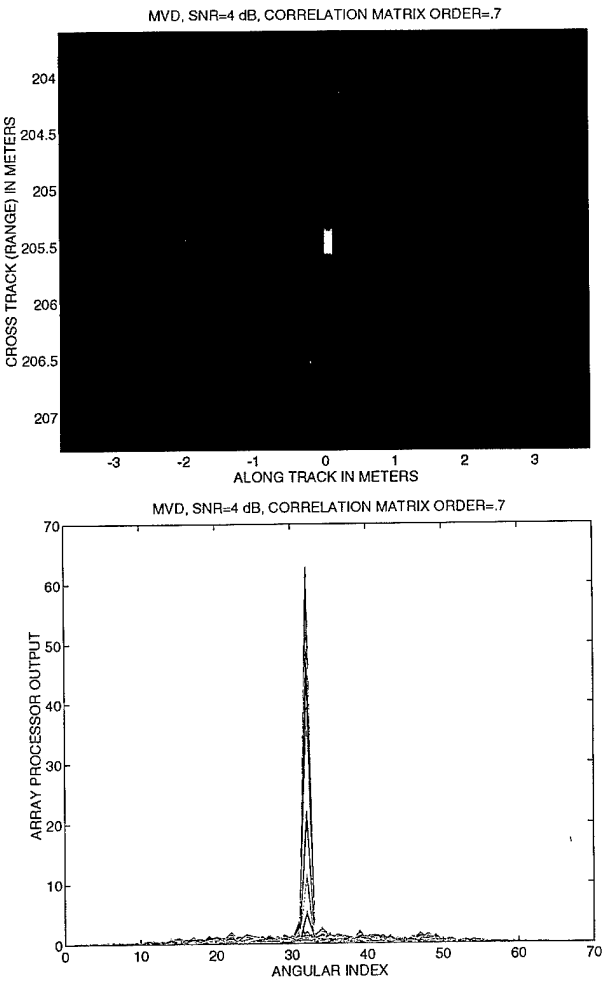

Figure 5. Image and array pattern of the MVDR array processor for the return from a point source at 205.5 m, given a 266 μs CW transmission and 4 dB SNR

from a point source at maximum range and 4dB SNR. The MVDR yields higher resolution, whereas the OSC produced a higher SNR. The relative beam resolution for the MVDR is, by definition, dependent upon SNR. The higher the SNR, the greater the gain in resolution achieved over conventional beamforming. Figures 6 and 7 give the respective output from the FFT beamformer and the MVDR for a point source at maximum range in 0-dB SNR.

Subspace processing can be used to increase the SNR in the MVDR. The effectiveness of subspace processing, when applied to the MVDR, is sensitive to the number of singular values retained.

Concluding Remarks

This article examined the application of array processing and associated high resolution array processing to the HARR SLS. The SLS is an imaging sonar designed for detection and classification of bottom and close-tethered mines. The correlogram is a classical processor in that the trade-off between side lobe leakage and resolution is limited by the length of the array. However,

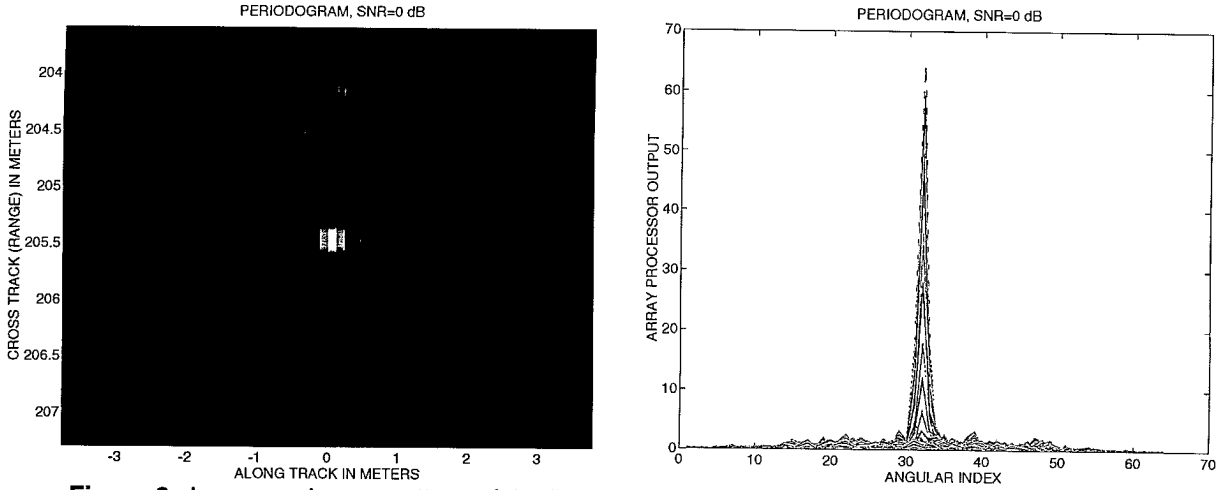

Figure 6. Image and array pattern of the FFT beamformer for the return from a point source at 205.5 m, given a 266 μs CW transmission and 0 dB SNR

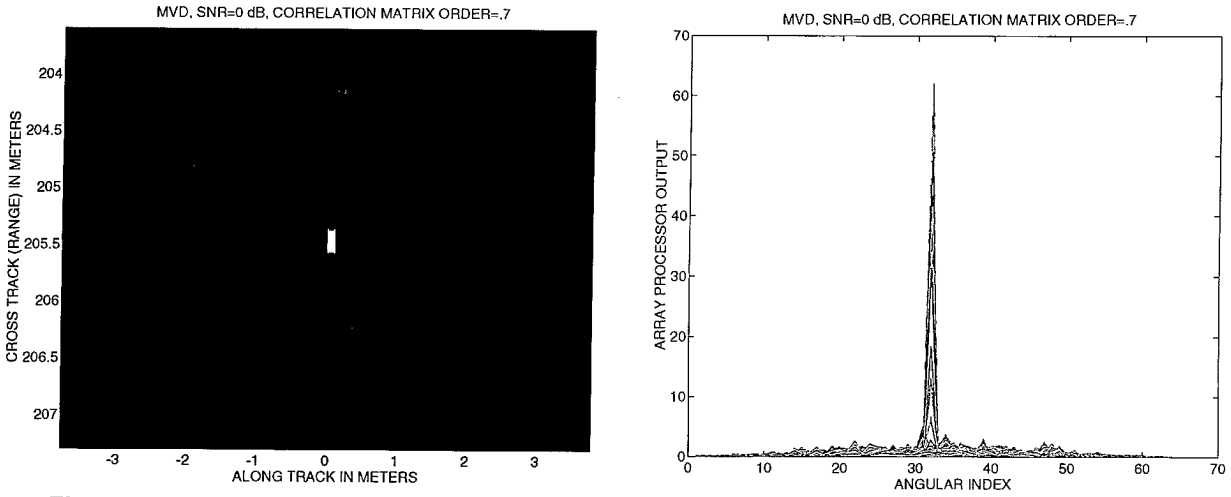

Figure 7. Image and array pattern of the MVDR array processor for the return from a point source at 205.5 m, given a 266 μs CW transmission and 0 dB SNR

when the correlation matrix is properly defined, the OSC processor yields relatively high SNR over conventional FFT beamforming. Also, resolution is tied to bottom type, as is the case with HRAP processors. For the SLS, ensemble averaging in the estimation of the correlation matrix should be replaced by element subarrays to yield a high SNR. Although parametric model-based array processing, in principle, maintains high resolution, the nonlinearity associated with these processors, coupled with the sensitivity to model order, makes them somewhat unstable for the HARR SLS.

The resolution for the MVDR processor is not as high as theoretically possible with parametric models; however, the MVDR yields a higher resolution than classical array processors without the problems associated with the nonlinearity of other high resolution processors. The performance of the MVDR is, by definition, dependent upon input noise. Resolution is greatest for a high SNR and when the dominant source of noise is uncorrelated to the signal. For typical operation of the HARR SLS, as given in Figure 1, noise is primarily due to bottom backscatter and on the order of 4 dB. Here, the MVDR yields higher resolution (however, no improvement) in SNR over the beamformer.

Resolution is a function of bottom type in the MVDR and AR processors. The cases cited above were for a sandy bottom. A mud or silt bottom will yield greater resolution in the MVDR. A gravel bottom will result in less resolution than with the sandy bottom. When the correlation matrix is estimated by averaging across the array, the MVDR still maintains an appreciable performance advantage over standard FFT beamforming, even in low SNR.

Addendum

To see the relation between the SLS and the band-select process, let the input to the mth array element be denoted $u(t,\theta)$, where θ defines the angle of the direction of propagation referenced from the axis perpendicular to the line array. The output of the mth element of length d then expresses as

$$s_m(t,\theta) = \int_{-d/2}^{d/2} u\left(t + dt_x(\theta)\right) dx \qquad (1)$$

where dx denotes the incremental distance along the array axis, and $dt_x(\theta)$ denotes the incremental time delay of the propagating wave across the element aperture. Equation *(1)* can be converted to a time convolution or filtering operation for the line array. The incremental time delay across the array is

$$dt_x(\theta) \equiv \frac{dx \sin\theta}{c} \qquad (2)$$

which gives an expression for the incremental distance of

$$dx = \frac{c}{\sin\theta} dt_x(\theta) \qquad (3)$$

Application of Equation *(3)* into Equation *(1)* yields the following expression for the output of the mth array element:

$$s_m(t,\theta) = \frac{c}{\sin\theta} \int_{-T(\theta)/2}^{T(\theta)/2} u\left(t + dt_x(\theta)\right) dt_x(\theta) \qquad (4)$$

for $T(\theta) = d \sin\theta / c$, which equates to a convolution in time of the form

$$s_m(t,\theta) = \frac{c}{\sin\theta}\left(u(t) *_t rect\left(\frac{t}{T(\theta)}\right)\right) \qquad (5)$$

where

$$rect\left(\frac{t}{T(\theta)}\right) \equiv \left\{ \begin{array}{l} 1, |t| \le T(\theta)/2 \\ 0, |t| > T(\theta)/2 \end{array} \right\} \qquad (6)$$

Equation *(6)* has several important implications. The aperture fill acts as a spatial filter, which becomes apparent in the expression for the beamformer response function. The convolution relation also imposes a restriction on the allowable bandwidth of the transmit relative to steering angle. This becomes

particularly important if steering is used to incorporate motion compensation into the beamforming algorithm.

Equation *(6)* effectively serves as the spatial filter in the folding process. The corresponding beam pattern is the spatial transform of Equation *(6)* as given below:

$$R(\lambda,\theta) = S_a\left(\frac{\pi d}{\lambda}\sin\theta\right) \qquad (7)$$

where $S_a(x) \equiv \sin x / x$ is the sampling function. Cascaded with the proper decimation, the beam pattern is aliased into spatial subbands, which allows for the narrower beam, without aliasing, from the undersampled array.

The SLS transmits a narrowband signal with carrier frequency $f_c = 400\ kHz$, which corresponds to a Nyquist sampling rate for the array of

$$d_s = \frac{c}{2f_c} = 1.875mm \qquad (8)$$

and a decimation factor of

$$P = \frac{L}{d_s}\Big/ N_e \qquad (9)$$

The array length is 3.8 m comprising 38 contiguous elements with 10-cm spacing between element centers which, from Equation *(9)*, yields $P \cong 53$. For the sound speed in water, $c = 1500\ m/s$, the $\lambda_c = 0.375\ cm$ which, applied to Equation *(7)*, yields spatial nulls in the element pattern at 2.15 deg.

Acknowledgments

This work was supported by the Office of Naval Research.

References

1. Zehner, B., "SLS Hydrophone Arrays," Technical Specification, NCSC SPEC N1230-92-001, Mar 1994.
2. Otnes, R.K. and Enochson, L., *Digital Time Series Analysis*, John Wiley & Sons, Inc., NY, 1972.
3. Johnson, D.H., "The Application Spectral Estimation to Bearing Estimation Problems," *Proceedings of the IEEE*, 70(9), 1982.
4. Van Veen, B.D. and Buckley, K.M., "Beamforming: A Versatile Approach to Spatial Filtering," *IEEE ASSP Magazine*, Apr 1980.
5. Owsley, N.L., "Sonar Array Processing," Ch. 3, *Array Signal Processing*, ed. S. Haykin, Prentice Hall, Inc., NJ, 1985.
6. Vaidyanathan, C. and Buckley, K.M., "Performance Analysis of the MVDR Spatial Spectrum Estimator," *IEEE Trans. Signal Processing*, 43(6), 1995.

The Authors

JO ELLEN WILBUR received a B.S. in electrical engineering from Virginia Polytechnic Institute (1982) and M.E. (1984) and Ph.D. (1987) degrees in electrical engineering from the University of Florida, with her specialty in the areas of Communication Theory and Digital Signal Processing. She was an assistant professor in the Department of Electrical and Computer Engineering at Clemson University from 1987 to 1989. Since 1989, she has been employed with the Acoustic, Sonar, and Signal Processing Division at the Coastal Sytems Station, in Panama City, Florida. From 1992 to 1995 she served as an Elected Member of the IEEE Signal Processing Technical Committee on Statistical Signal and Array Processing (IEEE SSAP). She is currently serving an additional term as a nonvoting member and home-page reprints editor for the IEEE SSAP (1995-1998). She was a member of the IEEE Executive Committee, Piedmont Section (1987-1989). In 1991 she received an ONR Certificate of Commendation as coauthor of the best CSS FY91 independent research paper: "Nonlinear Analysis of Cyclically Correlated Spectral Spreading in Modulated Signals," *Journal of the Acoustical Society of America*, 1992.

Jo Ellen Wilbur

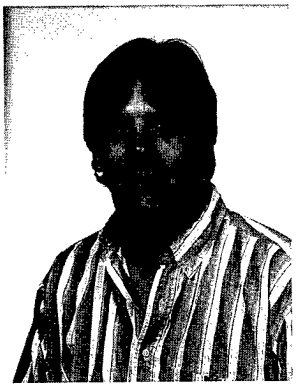

CHRISTOPHER A. SERMARINI received B.S. and M.S. degrees in electrical engineering from Florida State University, Tallahassee, FL, in 1987 and 1991, respectively. He is currently seeking a Ph.D from the Uiversity of Southern California, Los Angeles. He has worked on underwater communications and sonar applications of digital signal processing for the Naval Coastal Systems Station in Panama City, FL, since 1988.

Christopher A. Sermarini

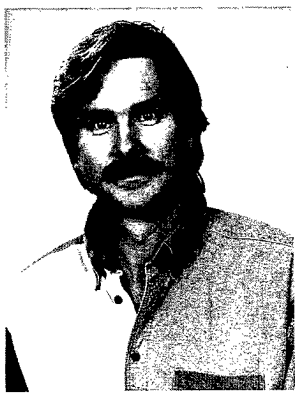

R. LEE THOMPSON received a B.S. degree with honors in ocean engineering from Florida Atlantic University in 1989, and an M.S. degree in electrical engineering from the University of Texas at Austin in 1995. He has been employed by Coastal Systems Station since 1990. He has contributed to the development of several unmanned underwater vehicle systems through his work on vehicle sensor fusion, high resolution sonar signal processing, and sonar simulation. His primary focus has been in the areas of sonar signal classification techniques, stave level sonar simulations, and broadband array processing. He is a member of Tau Beta Pi, the IEEE Oceanic Engineering Society, and the IEEE Signal Processing Society.

R. Lee Thompson

JAMES F. BRYAN received a B.S. degree in electrical engineering in 1985 and an M.S. degree in electrical engineering in 1986, both from the Georgia Institute of Technology. He has been employed at the Coastal Systems Station since 1986. He developed the data display for the Sonar Adaptive Countermeasure program. He is currently developing the conventional beamformer for a side-look sonar for the High Area Rate Reconnaissance project. He is a member of the IEEE Signal Processing Society.

James F. Bryan

Systematic Mine Countermeasures: A Structured Approach In Support Of Expeditionary Warfare

Donald W. Shepherd

EW
EXPEDITIONARY
WARFARE

This article presents a systematic structure that clearly delineates the functional relationships of mine countermeasures (MCM) in an expeditionary warfare context. MCM is a complex warfare area that will play an increasingly important role in naval operations as the Navy continues to implement the new forward-deployment strategy. In the past, MCM was regarded primarily as operations undertaken by specialized naval components independent of main battle-force components. In the future, implementation of naval strategy will require that main battle-force components possess organic capabilities to deal with the threat of mines. This shift in view requires a structured approach to MCM in support of expeditionary warfare.

This article focuses on articulating an overall structure composed of three basic components: (1) a theater-level vision of MCM, (2) an associated concept of operations for implementing that vision, and (3) a top-level functional architecture illustrating the allocation of MCM systems across associated functions. This overall framework can be regarded as the point of departure toward a true systems engineering approach to MCM.

Introduction

With the end of the Cold War, the armed forces of the United States began the process of redefining roles and missions. The new role for the Navy was first articulated in the policy paper . . . *From the Sea* and further amplified in the subsequent issue, *Forward . . . From the Sea.* The new concept articulated in these papers is that of a forward-deployed Navy. Emphasis is placed upon the notion of the Navy as an integral warfighting partner with the other services in the arena of joint littoral warfare. Accomplishment of its missions within this warfighting context requires that the Navy have a strong expeditionary warfare capability. By its very nature, expeditionary warfare connotes bringing forces to bear in areas distant from the shores of the United States for the purposes of achieving national policy.

Implementation of this overall warfare strategy hinges upon the Navy's ability to effectively control the total battle space, or theater, associated with warfare in the littoral environment. This need leads naturally to the concept of theater warfare, with Navy Expeditionary Forces as the foundation enabling U.S.

forces to effectively shape the battle space, attain battle-space dominance, project power from the sea, and sustain operations ashore.

In this forward-presence, theater-level, expeditionary warfare-focused arena, the Navy will be forced to increasingly deal with the threat of enemy sea and land mines. The sea mine has evolved from simple, moored devices—which must be physically contacted by the target vessel—to complex, sophisticated weapons that exploit acoustic, magnetic, and other signature characteristics to determine the presence of the target and detonate when the target comes within lethal range of the mine's warhead. Effective, technically advanced mines are readily available at modest prices on the world arms market. A general purpose, moored contact mine can be expected to range in cost from $1,000 to $6,000. Simple influence mines can be purchased for as little as $10,000. A multiple-influence mine, utilizing modern, signal-processing technology, can be purchased for considerably less than $100,000. Furthermore, the ability of an adversary to employ mines effectively depends neither on a strong industrial base, nor on an indigenous technical development and production capability. To third-world, littoral nations, sea mines have become the weapon of choice to oppose any assault from the sea.

At the same time, the U.S. Navy's ability to deal with the sea mine as a threat has not kept pace with other warfare areas. During the last 40 years, more U.S. ships have fallen victim to sea mines than to all other antiship weapons combined (see Figure 1). In 1988, USS *Samuel B. Roberts* was put out of action for 18 months at a total repair cost of $41 million when it struck a moored contact mine in the southern Persian Gulf. In Desert Storm, a bottom influence mine inflicted $18 million in damages to USS *Princeton*, and a conventional moored mine inflicted $3.5 million in damage to USS *Tripoli*.

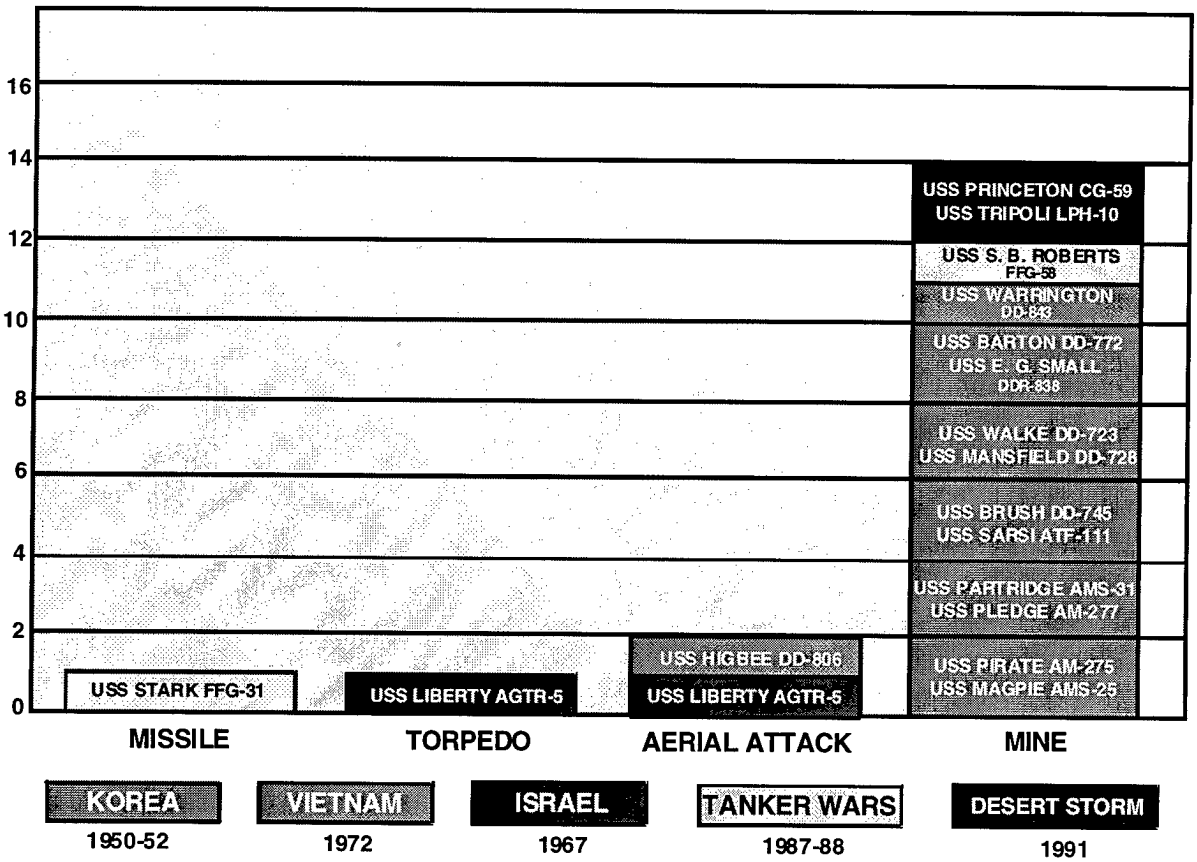

Figure 1. U.S. ship casualties during the last 40 years

During this same 40-year period, the Navy's approach to countering the mine threat focused on having available what eventually became a nominal MCM force that could be dedicated to the problem as necessary. Although the threat showed a steady growth in terms of complexity, sophistication, number of mines, and technical capability, the amount of effort, in terms of fiscal resources and platform force levels, committed to the MCM problem by the U.S. Navy failed even to come close to keeping pace.

This situation is the result of many factors. One of the principal contributing factors has been a lack of understanding of the mine warfare problem, particularly the MCM aspects of the problem that are the focus of this article. The complexity of MCM operations is little understood and appreciated outside that small Navy community that has focused on the operational and technical aspects of the problem.

This article provides a systematic and structured exposition on the essential elements of MCM. To present a coherent and consistent discussion, this article has three primary objectives:

- First, to provide an explanation of the essential features of MCM for the non-MCM community, both within the Navy and in the public and private sectors
- Second, to describe the overall operational concept that permits the integration of MCM into the war-fighting structure of the Navy
- Third, to articulate a unifying structure—an architecture—that clearly illustrates the functional relationships of the components of the MCM system. This architecture has proven to be extremely useful in understanding the functional relationships of MCM systems.

Scope of the MCM Problem

An appreciation of the broad scope of the MCM problem is essential to an understanding of the diverse factors that combine to define the operating environment within which MCM operations must be conducted. An understanding of this operating environment and primary influencing factors are likewise a fundamental precept of the top-level MCM architecture. The overall MCM problem can be articulated in terms of *drivers* and *boundary conditions*. The drivers are those major factors that establish the fundamental ground rules of the envisioned MCM operation. The drivers combine in various ways to set the boundary conditions upon the contemplated operations. The general relationship between the drivers and the boundary conditions is illustrated in Figure 2.

Drivers

Mobilization State. The mobilization state is determined by national priorities and the warning time associated with the impending military operation. The mobilization state influences the timeline associated with deployment of dedicated MCM forces to the geographic location at which they are required. Of course, the possibility always exists that dedicated MCM forces will already be deployed in the potential area of conflict.

Geographic Location. The geographic location of the impending military action has a profound influence on potential MCM operations since the location essentially determines the physical parameters of the operating environment. MCM is particularly sensitive to the effects of the environment since the majority of operations are conducted in water depths of less than 600 feet. The particular environmental characteristics that affect MCM operations are water depth, bottom type, bottom gradients, magnetic and acoustic propagation characteristics of the operating area, and sea state. These factors are all clearly beyond the control or influence of U.S. forces.

MCM Mission. The major MCM mission of U.S. forces will henceforth be to support the forward-deployed concept. The most dominating need, from an MCM perspective, is an ability to support the power projection portion of the Navy's forward-presence role. Broadly translated, there is a pressing need for organic MCM

capabilities that will support naval task groups during the transit phase of maritime operations. There is a need as well for a break-in/break-out capability at forward ports. The need to support amphibious operations will remain critical. In a benign environment—such as after cessation of hostilities—there will be a continuing need to accomplish administrative MCM operations.

Therefore, naval forces must be capable of performing five distinct MCM missions in support of the forward- deployed, joint littoral warfare concept of Navy operations. The major MCM missions that are to be accomplished by U.S. forces can be categorized as:

- Port break-in/out
- Transit support
- Amphibious assault support
- Fleet operating area support
- Administrative operations after cessation of hostilities

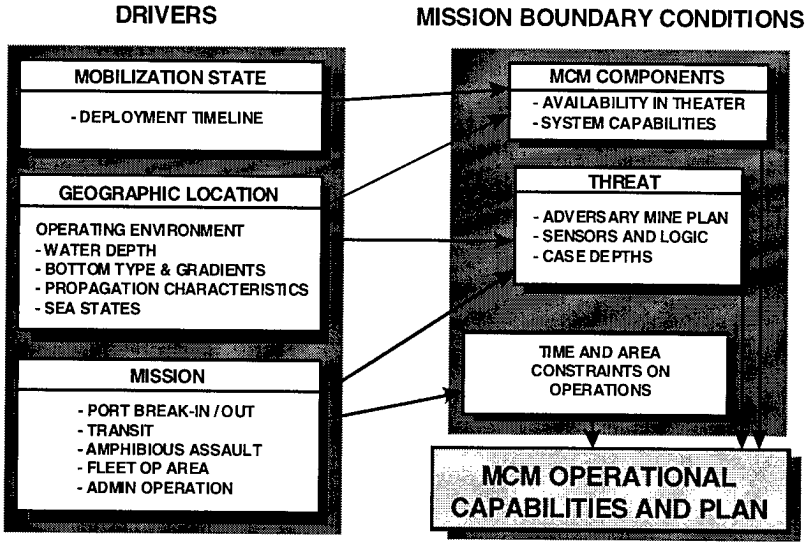

Figure 2. Scope of the MCM problem

A brief description of each of these missions is provided in Figure 3.

Although these five typical missions are not doctrinally recognized by the Navy, they are useful in understanding the overall context within which MCM operations can be expected to occur.

Boundary Conditions

MCM Components. This boundary condition is an expression not only of the quantity of MCM components available in

Port Break-In/Out — Operations undertaken at forward ports to ensure that enemy mines do not impede access to the port by U.S. and Allied forces.

Transit Support — The use of naval assets, usually organic to individual ships or the battle force, to ensure that NEF, ARG, and CVBG components are not delayed or damaged by mines during movements from open ocean areas, through straits and choke points, and into their assigned littoral operating areas.

Amphibious Operating Area (AOA) Support — The full spectrum of MCM capable assets to ensure that assault forces are able to execute their assigned missions, at an acceptable level of risk of incurring casualties, or without inordinate delay from enemy mines and obstacles.

Fleet Operating Area Support — The use of naval assets, usually organic to the battle force, to ensure that fleet units can operate in their assigned operations area and concentrate on their primary missions with an acceptable knowledge of the level of risk posed by the mine threat.

Administrative Operations — Those detailed clearance operations that are conducted to ensure that the mine threat is removed from a given ocean area. Administrative operations are most commonly performed after the cessation of hostilities and without time constraints.

Figure 3. A summary of the typical MCM missions

the theater of operations but also of the arrival rate. The operating environment affects the capabilities of the system equipments employed by Navy forces to conduct MCM operations. Because Navy forces are never really sure of the exact nature of the threat, the fundamental concept of MCM operations is based upon the precept of reducing the risk to transiting platforms to an acceptable level.

Threat. The actual mine threat faced by U.S. forces in terms of mine type and density is dictated by the adversary mine plan. Multiple mine threats will almost always be encountered. The physical characteristics of the mines are a determining factor in their detectability. It is also essential to have an understanding of the physical and operational characteristics of the sensors used by the mines to detect the presence of targets. In general, four types of mine sensors can be encountered:

- contact (mechanical)
- acoustic
- magnetic
- pressure

The location of the mine case within the water column is a major factor in determining the detectability of the mine. It should be noted that a particularly difficult problem is posed by mines that bury in the bottom—not an uncommon occurrence in certain bottom environments.

The final threat factor that must be considered is mine logic. The logic includes not only the manner in which the mine processes sensor information, but also the use of ship counts. Influence mines almost always use a combination of signature characteristics to sense and validate the presence of a target ship.

Time and Area Constraints. Invariably, certain constraints are placed upon the U.S. forces performing MCM operations. A time constraint is often encountered. This is particularly true in operations such as amphibious assault, where it is often desirable to complete MCM operations in a very limited amount of time, to prevent disclosing to defending forces the exact location of the planned assault. In addition to time constraints, area constraints are often imposed. This is particularly true when it is necessary to establish mine-free lanes through an operational area.

Theater Mine Countermeasures

Implementation of the strategy articulated in *Forward . . . From the Sea* hinges upon the Navy's ability to effectively dominate the *total* battle space. In this forward-deployed environment, it is imperative that enemy forces be denied access to the battle space to ensure freedom of action of U.S. forces both at sea and ashore. The total domination of the battle space requires that naval forces possess the ability to accomplish simultaneously the critical functions of:

- Air Warfare
- Strike Warfare
- Mine Warfare
- Surface Ship Warfare
- Submarine Warfare
- Command, Control, Communication, Computers, and Intelligence (C^4I)

These theater warfare functions are the pillars that will permit the Navy to initiate control of the total battle space—air, surface, and undersea—and to conduct maneuver warfare in the forward-deployed, littoral environment. Anything less than a complete capability across all of these functions will jeopardize the entire concept of maneuver warfare in a forward, hostile environment. Naval Expeditionary Forces form the nucleus of *the fundamental capability* that will ensure that the above pillars are achieved.

The ability to accomplish all of these functions, perhaps simultaneously, is a necessary condition to ensure the freedom of action fundamental to successful implementation of the forward-deployment strategy. Through these functions, the joint force structure will be permitted to execute all phases of expeditionary warfare, as well as protect the airlift and sea-lift portions of follow-on operations, necessary to achieve the continuous flow of critical warfighting assets.

The attributes of the *Theater Mine Countermeasures* portion of the theater warfare mosaic are delineated in Figure 4. The precept of theater mine countermeasures is based upon the synergistic use of all platforms and capabilities across the services to mitigate the threat posed by mines.

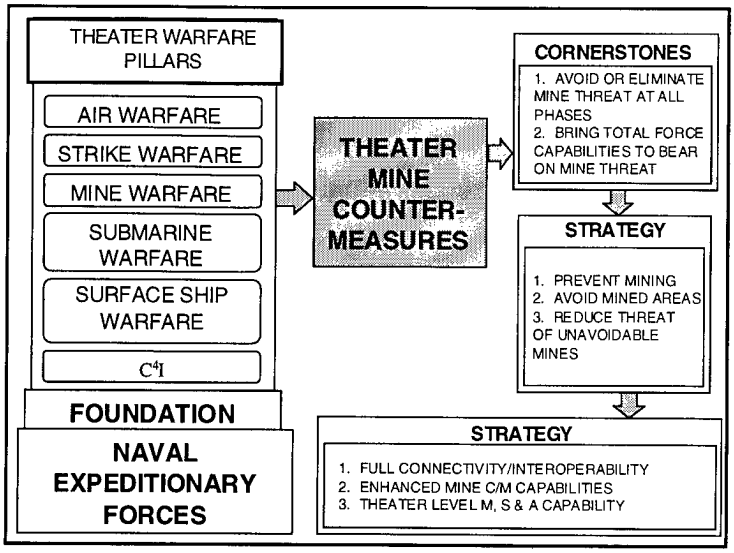

Figure 4. Attributes of theater mine countermeasures

The essence of theater mine countermeasures—illustrated pictorially in Figure 5—can be briefly articulated in terms of *cornerstones*, *strategy*, and *fundamental priorities*. Cornerstones are overarching operating principles that form the foundation of the concept. Strategy articulates the basic structure of the concept in terms of the operational objectives. Fundamental priorities identify broad categories of effort that must be pursued to ensure that the Navy possesses the wherewithal to implement the operational strategy.

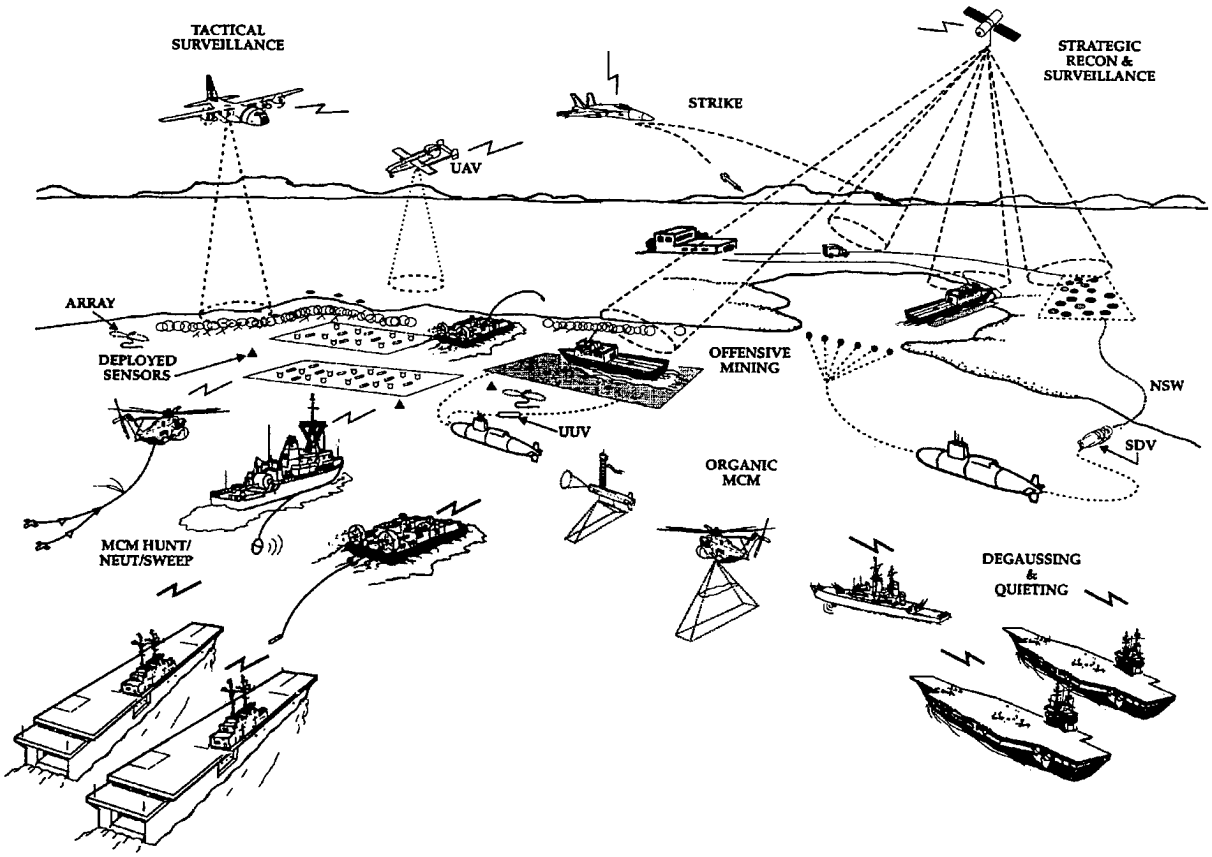

Figure 5. Theater mine countermeasures concept

Cornerstones

The theater mine countermeasures concept is based upon the precept that an effort will be undertaken to *avoid or eliminate the mine threat at all phases* of the forward-deployment process and during the movement of forces. No longer will MCM be viewed as something to be done only after the dedicated MCM platforms arrive in theater. A fundamental tenant of theater mine countermeasures is that *total force capabilities be brought to bear* on the mitigation of the mine threat. The result will be a concerted effort to counter the mine threat by the synergistic utilization of:

- Strategic surveillance and intelligence to locate enemy mine stockpiles and mine-laying activities so that strike and other forces can eliminate the mines before they are placed in the water
- Tactical surveillance and intelligence to locate mine-free areas, and to positively identify mined areas to be avoided if at all possible within the constraints of the operational objective
- Organic MCM equipments and procedures to achieve self-protection of individual combat units and task forces
- Dedicated MCM forces when the necessity arises to clear unavoidable mines, minefields, and obstacles

These cornerstones form the foundation of the theater mine countermeasures strategy.

Strategy

The theater mine countermeasures strategy consists of three parts:

Prevent Mining. To the maximum extent, take the steps necessary to prevent the enemy from planting minefields. This portion of the strategy requires the elimination of enemy mine stockpiles and mine-laying capabilities. Implementation of this element of the strategy requires the use of strike or other forces to destroy the enemy's mine warfare infrastructure. This is often a function of the Rules of Engagement imposed upon the particular conflict. However, with existing and emerging surveillance and intelligence-collection capabilities, new attention must be focused on this aspect of the MCM problem.

Avoid Mined Areas. The use of charting, survey, and geodesy assets; together with strategic and tactical surveillance and intelligence assets; complimented by the use of tactical off-board and onboard systems—both airborne and submersible—will enable naval forces to effectively avoid mine danger areas to the maximum extent. Charting, mapping, and geodesy assets must be applied on a continuous basis to produce comprehensive assessments of mineable waters. Strategic surveillance and intelligence assets can determine the extent and location of enemy mining efforts. Tactical offboard and onboard systems will be necessary to ensure that individual combat units and task forces possess a mine detection and avoidance capability during the transit phase and during on-station, battle-force operations.

Reduce the Threat of Unavoidable Mines. Operational situations will always arise requiring specialized MCM forces to deal with the threat of unavoidable mines and minefields. When these situations arise, dedicated MCM forces will be called into play to perform hunt, neutralize, and sweep actions. Because Navy operational forces will never know the exact nature of the mine threat, the fundamental concept of MCM operations is based upon the precept of reducing to an acceptable level the risk to transiting platforms. To complement the hunt, neutralize, and sweep actions, self-protection techniques such as degaussing and quieting will continue to be employed.

Fundamental Priorities

To implement this strategy, the Navy must focus on achievement of three fundamental priorities:

Full Connectivity and Interoperability. The individual ship, task force, and joint force commanders must all have at their disposal a

complete strategic and tactical picture of ongoing operations, including all aspects of theater-wide efforts. Seamless connectivity and effective interoperability are absolutely essential to the achievement of an integrated theater mine countermeasures capability. All platforms engaged in any aspect of the MCM effort must be fully integrated into the overall battle force and command authority linkages.

Enhanced MCM Capabilities. With the diminishing force structure in terms of the number of combat platforms, it is absolutely essential that Navy units and task forces be equipped with state-of-the-art combat systems that leverage all available and emerging technical advances. This is especially true of MCM elements. This thrust—to field new systems and upgrade and improve existing capabilities across the total MCM functional spectrum—is a central element of the overall theater mine countermeasures strategy. The complexity of the operating environment, coupled with the diversity of the threat, virtually guarantees that a "silver bullet" solution to the MCM problem does not exist. MCM is the prime example of a warfare area that must apply a "system of systems" approach to the solution of a complex problem.

Theater-Level MCM Modeling, Simulation, and Analysis (M, S&A) Capability. An absolutely fundamental element of MCM strategy must be the development and utilization of models, simulations, and analysis techniques that can be effectively integrated with like-capabilities in the areas of theater air defense, surface warfare, and C^{4}I. Modeling and simulation must be supported by an equally aggressive use of these tools for analysis efforts, which ultimately yield the desired information and data to produce an investment strategy and an improved acquisition decision process. Within the emerging environment, a synergistic M, S&A capability must be available not only to support acquisition decisions, but also for training; testing and evaluation; tactics evaluation and development; and mission rehearsal, reconstruction, and evaluation. The great utility of M, S&A lies in its ability to effectively assess the relative contributions of major war-fighting components to the overall Navy mission. The challenge to MCM research and development activities is to effectively combine resources to assure that an adequate M, S&A capability exists to support the needs of the MCM community.

The Concept-of-Operations Structure

Forward-deployed naval forces will be the primary U.S. force shaping the battle space within the theater of operations. To maximize the capability to shape the battle space, naval forces must be capable of unencumbered maneuver. As U.S. forces build up in-theater, the problem evolves to one of battle space dominance. This buildup of forces is attained only if U.S. ships can safely sail through sea lanes and to ports of debarkation. Depending upon the desired mission objective and the level of conflict, battle space dominance may lead to a need for power projection. In order for the Navy to successfully accomplish this war-fighting evolution, mitigation of the mine threat becomes an essential element. The key to dealing effectively with the mine threat from a total Navy war-fighting perspective requires a viable *concept of operations* for MCM. This concept of operations must be prudently broad in scope to ensure technical and operational capabilities across the spectrum of potential operations, from noncombat operations to full-scale conflict. The MCM concept of operations, illustrated in Figure 6, has been developed and promulgated by the Mine Warfare Division (N852) of the Chief of Naval Operations.[1]

MCM operations must begin during peacetime with compilation of relevant environmental data and intelligence information on mining capabilities. As tensions increase, focused surveillance operations provide updates to databases developed during peacetime. As tensions escalate further, naval forces utilizing

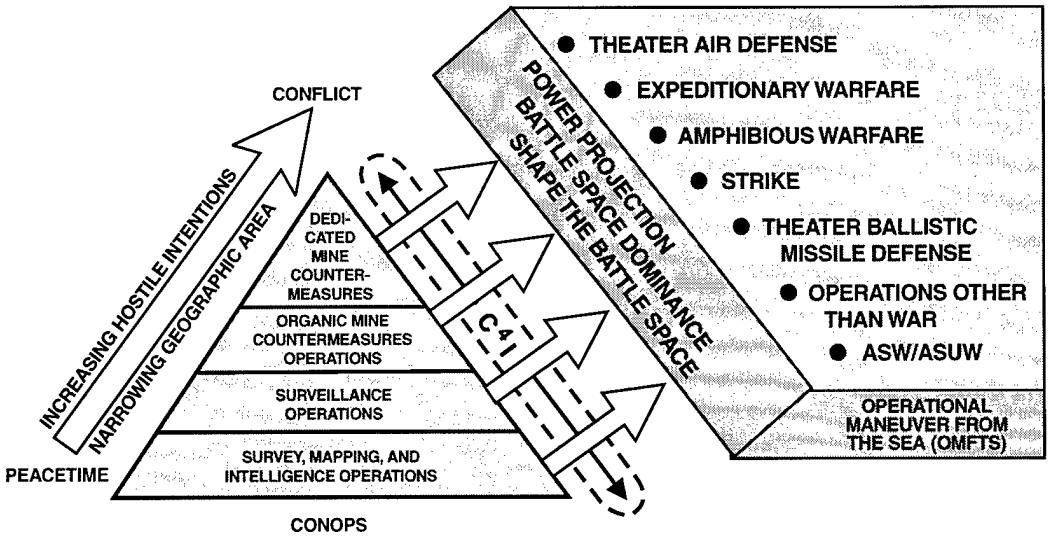

Figure 6. The top-level MCM concept of operations

organic MCM capabilities can assess the risks associated with operation in mined waters during their initial efforts to shape the battle space. Dedicated MCM forces may be required to clear enemy mines to further shape the battle space and support the projection of power from the sea.

The MCM Functions

The four levels of the concept of operations shown in Figure 6 form a logical point of departure for the development of a functional description of MCM. Each of the four top-level functions can be further decomposed into a series of supporting subfunctions. A hierarchy of MCM functions that flows from the concept of operations is shown in Figure 7. These are the functions that must be performed in order to implement the integrated MCM capability. This hierarchy is the nucleus of the MCM functional architecture.

An essential part of the decomposition is a clear definition of each of the functions. The accompanying definitions are contained in Figure 8.

Allocation of Systems Across Functions

One of the primary benefits of a viable architecture is that it shows which systems and equipments contribute to the accomplishment of the various functions. MCM system components can thus be mapped into the functions; i.e., allocated across the functions. Such an allocation of existing and developmental MCM system components is shown in Figure 9. This functional allocation clearly shows where each of the various system components contribute to overall MCM capabilities. As is evident from Figure 9, many existing and developmental system components are focused on the dedicated MCM function. This should not be surprising given that this was a primary ingredient of Cold War MCM strategy. As U.S. forces move toward the joint littoral, expeditionary warfare strategy of *Forward... From the Sea*, other MCM functions will take on added importance.

It is instructive to have an understanding of the mix of system components employed by the various platforms. In addition, certain fundamental efforts, such as tactics development, modeling and simulation, foreign mine exploitation, and organic training, do not appear in the purely functional allocation. For this reason, the depiction of MCM components shown in Figure 10 was developed. Figure 10 introduces the terminology of adjunct components and ancillary capabilities. Adjunct components are defined as

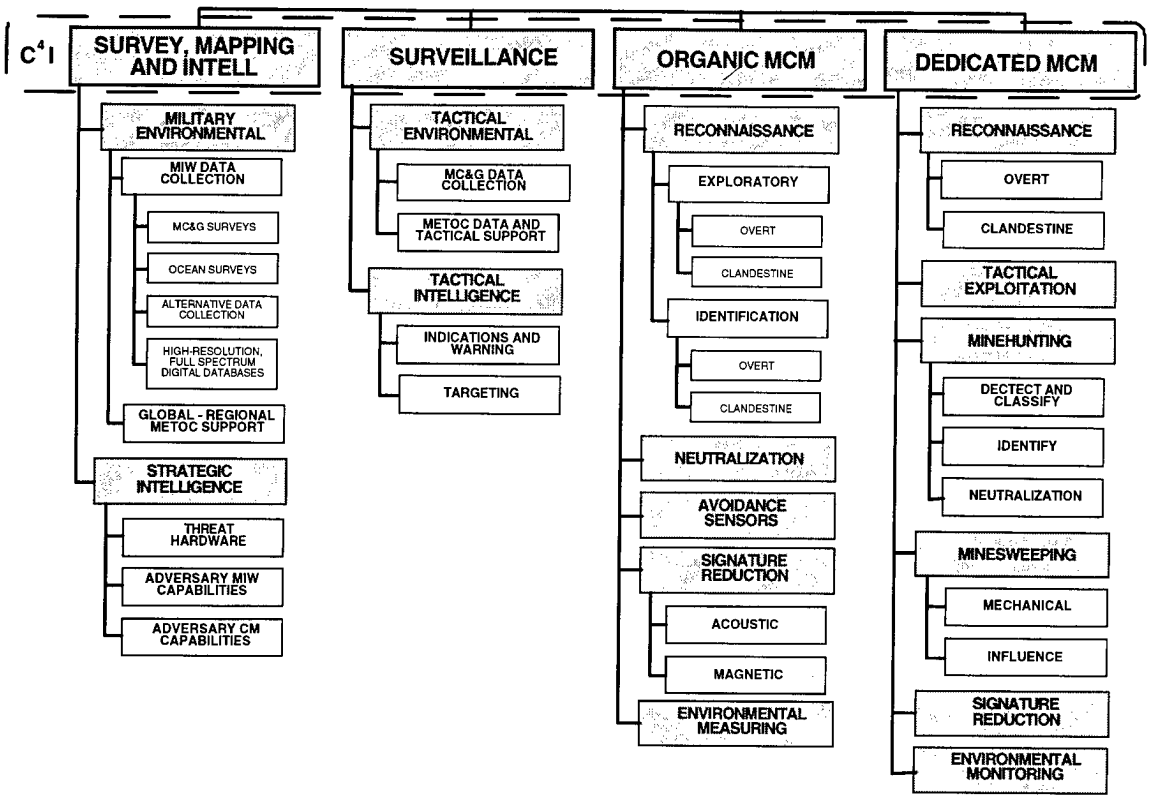

Figure 7. The MCM functions

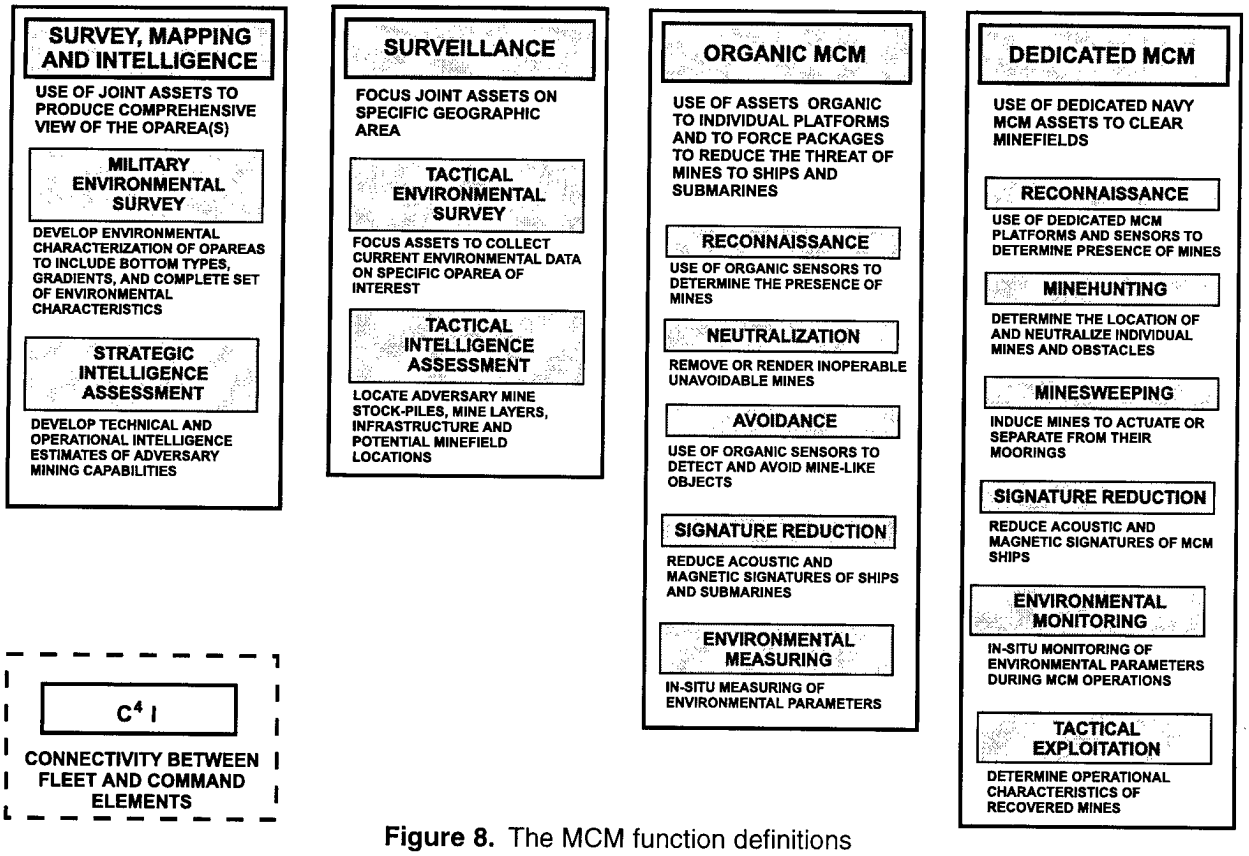

Figure 8. The MCM function definitions

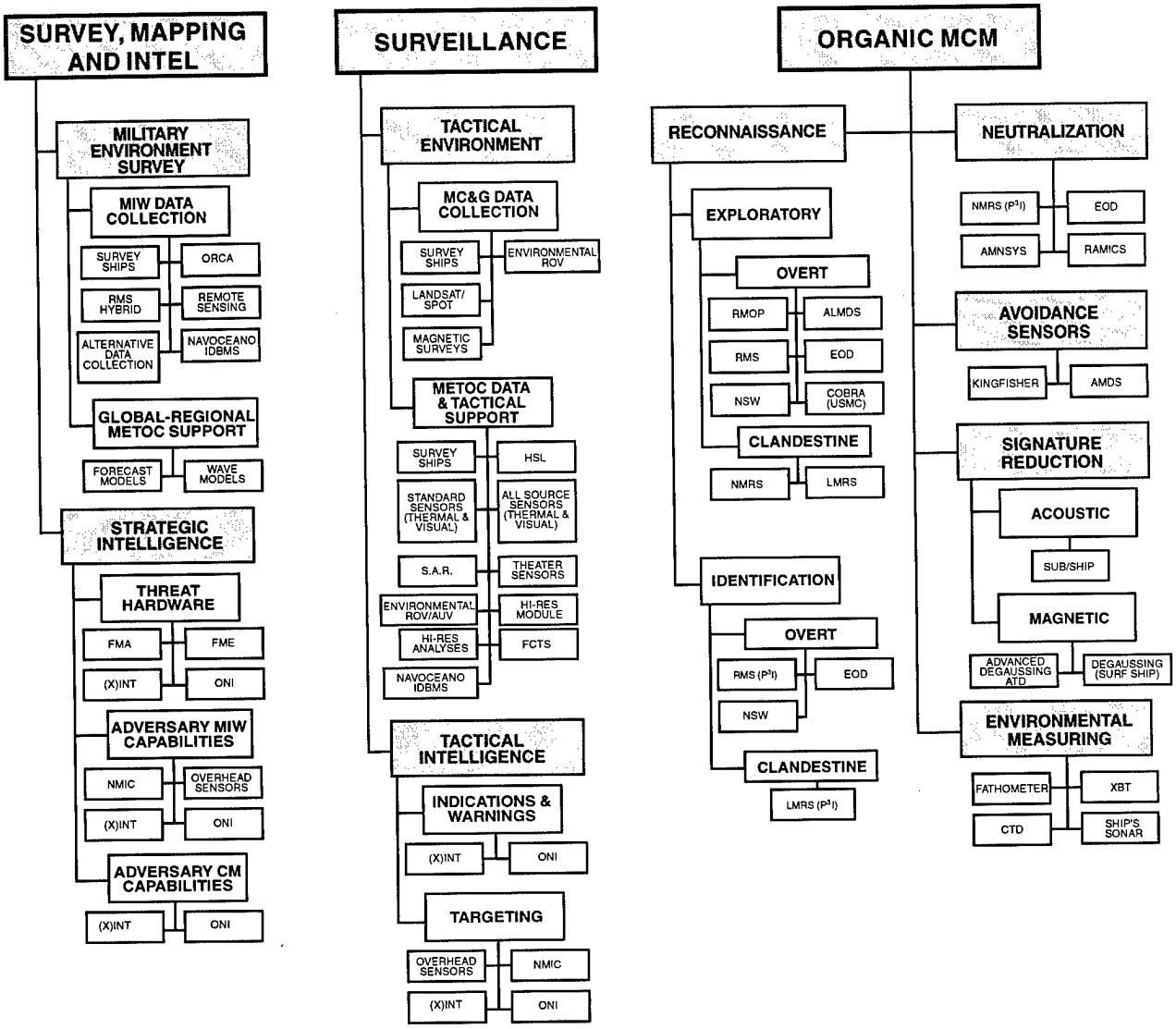

Figure 9. Allocation of MCM components and systems

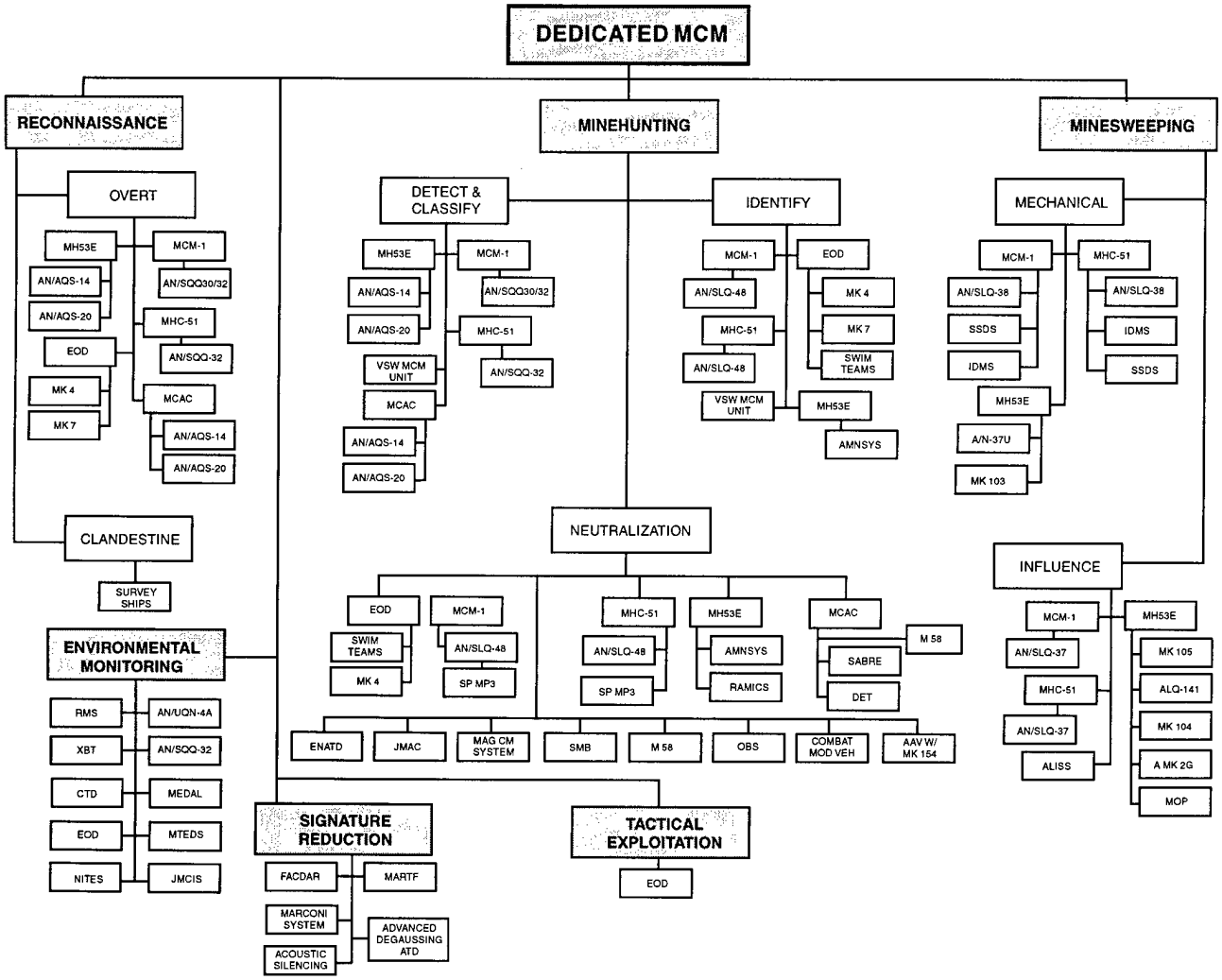

Figure 9. Allocation of MCM components and systems (continued)

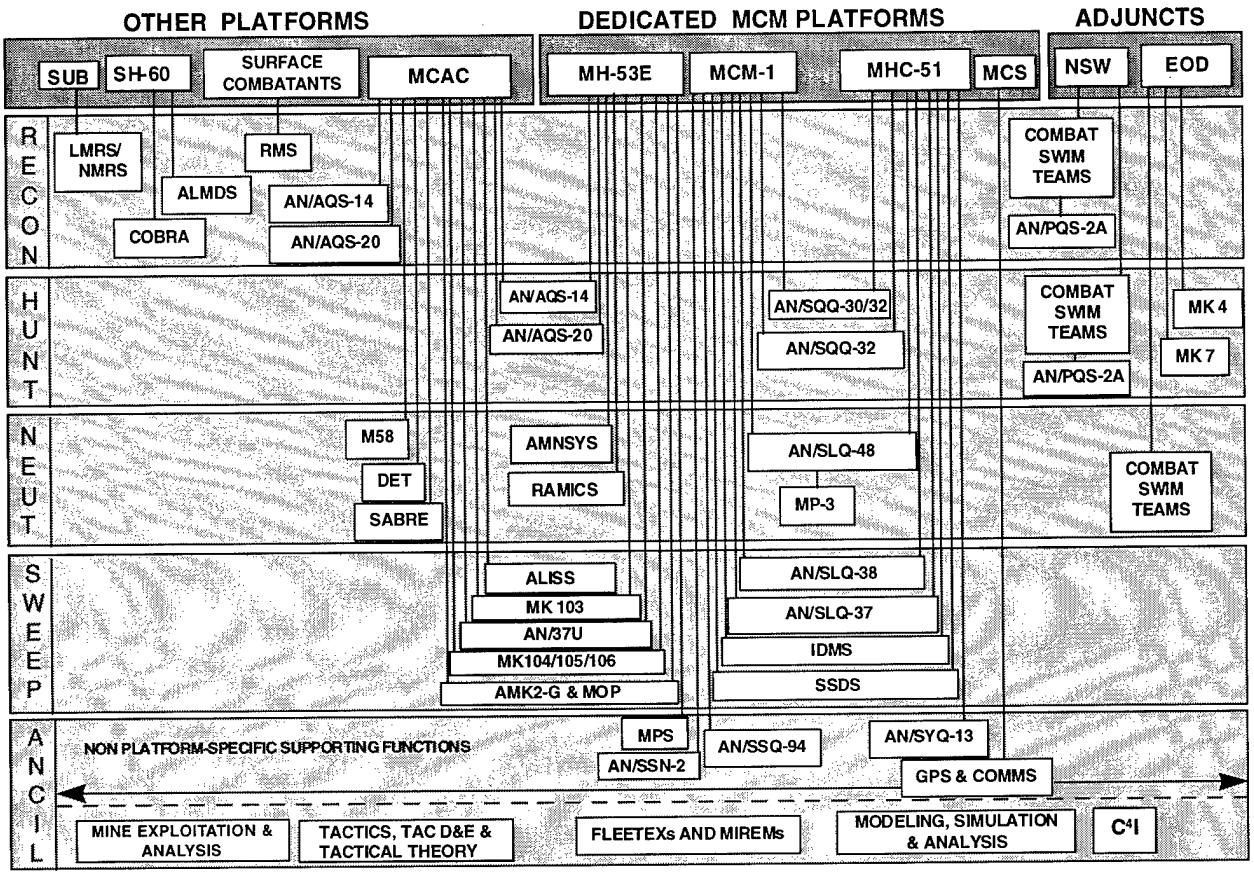

Figure 10. Relationships between platforms and MCM components

those that are necessary to the successful performance of MCM actions, but that are performed by another Navy warfare unit. Ancillary capabilities are those that are necessary for completeness of MCM capability, but that do not necessarily appear as MCM combat or system equipments.

The structure shown in Figure 10 enables one to determine at a glance the allocation of existing and developmental components across MCM platforms. This is a valuable visualization tool.

Summary and Conclusions

This article articulates a top-level, functional architecture for MCM within a theater warfare context consistent with emerging, Navy joint-littoral and expeditionary warfare thrusts. The architecture forms a single unifying structure that clearly shows the functional relationships of the various components of MCM systems in the fleet today and under development. The architecture should prove valuable in understanding the intricacies of the MCM problem and for identifying the contributions of individual systems and components. In its present form, the architecture described herein can be used as the basis for establishing a true systems engineering approach to MCM within an expeditionary warfare context.

Reference

1. *Concept of Operations For Mine Countermeasures in the 21st Century*, Chief of Naval Operations, N852, 1 Sep 1995.

The Author

Donald W. Shepherd

DONALD W. SHEPHERD earned a B.S. degree from Mississippi State University in 1963, after which he was employed as a research engineer at the Navy's Coastal Systems Station in Panama City, Florida. In 1967, he earned an M.S. degree in engineering science and mechanics from the University of Florida.

During a career that has spanned more than 30 years, Mr. Shepherd has participated in research, test, and evaluation efforts focused on countermeasures to enable U.S. ships and submarines to cope with the threats posed by torpedoes and mines. In 1982 and 1983, he served as Science Advisor to the Commander, Naval Surface Forces, U.S. Atlantic Fleet, located in Norfolk, Virginia. For a two-year period, 1985 to 1987, Mr. Shepherd was a principal technical advisor to the Naval Special Warfare Office of the Chief of Naval Operations. From 1989 to 1991, he was the U.S. Lead Scientist for the Feasibility Study portion of the surface-ship, torpedo-defense joint program with the United Kingdom. For the past three years, he has concentrated on Systematic Mine Countermeasures concepts and structures. Mr. Shepherd is currently head of the Coastal Initiatives Office at the Coastal Systems Station.

Challenges in Expeditionary Warfare: Can Simulations Help?

Elan Moritz

The new world order's impact on our maritime strategy is reflected in the Navy's white paper . . . From the Sea, *which emphasizes joint littoral warfare and joint mission areas, and in the addendum* Forward . . . From the Sea. *The Marine Corps expanded on this theme in its white paper* Operational Maneuver from the Sea, *which emphasizes the joint and seamless transition of naval operations to land combat. Recently, the Marines formulated* Sea Dragon *as the umbrella concept of concepts for flexibly addressing what might be characterized as strategic uncertainty in the 21st century. This article discusses aspects of the operational context and challenges for expeditionary warfare in the 21st century. The article also discusses some material and tactical means to address the challenges, some of the issues arising, and the potential for modeling and simulation tools to assist in exploring and solving these issues. In particular, key technologies and concepts associated with theater mine defense, naval fire support, surveillance-reconnaissance targeting and identification, and command and coordination (C^2) are reviewed and discussed in light of recent simulation exercises (SIMEXs) conducted by the Naval Surface Warfare Center, Dahlgren Division (NSWCDD).*

EW
EXPEDITIONARY
WARFARE

Naval Expeditionary Warfare: A Warfighting Paradigm for the 21st Century

In a series of capstone documents,[1-3] the Navy and Marine Corps lay a foundation and vision for a flexible and maneuver-oriented, 21st century naval force—a ready force that, in addition to traditional naval missions, will enable the United States to exert its influence globally and respond to a full spectrum of threats at a moment's notice. National commitments and interests may require naval forces to simultaneously execute peacetime operations and Operations Other Than War (OOTW), engage in military conflicts including Lesser Military Contingencies and Major Regional Contingencies, and assist in domestic emergencies. Some of the newer elements of OOTW include economic enforcement actions, and assistance in controlling and resolving diverse crises (ecological—e.g., nuclear plant radiation accidents; humanitarian—e.g., famine in third-world countries; medical—e.g., highly infectious, fatal disease pandemics).

It is clear that the 21st century will bring increasing complexity and uncertainty in all dimensions of human interactions. These will include diplomatic/political uncertainties, technological uncertainties, irrational and fanatic factors, and socioreligious uncertainties. The United States may be engaged in conflicts alongside temporary allies who may switch colors at a

moment's notice. Enemy definitions and political-military objectives may change at a moment's notice. The United States may face conflict with nations and groups who can be considered fanatic or fringe. All future conflicts are likely to have currently unpredictable technological elements; in some cases, our adversaries may possess technologies that are equal or superior to ours. Given the current rate of domestic and foreign technological progress and the ever dynamic and improving organizational structure of our own and threat forces, another pillar of the future is the *categorical revolution in military affairs*.

The defining element of the 21st century military conflict can be summarized as *strategic uncertainty*. The challenge for the U.S. Armed Forces is then the institutionalization of immediate optimal flexibility with a resulting military immediate optimal response. It currently may appear, to some, that the superiority of U.S. technological and military might will continue indefinitely. However, population growth, industrialization, and politico-religious coherences of other nations will bring several peer "contenders" into being in the coming decades. These contenders may be individual monolithic nations or federations of like-minded nations that will, in fact, have the wherewithal to pose credible conventional challenges to the interests of the United States. The focus of this article is discussion of the role of simulation and simulation-based concept generation in achieving an immediate optional response for globally distributed forces, and in particular naval forces, against credible peer contenders.

Advanced Marine Corps thinking gives significant attention to the land use of small units with unprecedented combat power. The Operational Maneuver from the Sea (OMFTS) document[3] calls on these units to be "hard to detect, fast-moving, and far-ranging" and to be "directed against an enemy center of gravity." The emerging technologies of long-range precision weapons elevate the use of sea-based (naval) fire support, in operational thinking, to the point of making reduced logistic buildup ashore a pivotal element of future operations. The combined use of Navy and Marine Corps elements to project power, prepare and shape the battlefield, and achieve battlefield dominance in near and remote littoral areas forms the functional and practical nexus of what is now termed as *Naval Expeditionary Warfare* (it must be kept in mind though, that all operations come under Joint Command; naval operations are only the most immediately flexible operations).

The nominal littoral region to be controlled by Naval Expeditionary Forces (NEFs) in a standard mission scenario is 200 miles by 200 miles, with foot-mobile units having an operational tempo measured in miles per hour, and mounted forces having a 30 or more miles per hour tempo. The mobility is to be linked with reliable and redundant C^2 to Navy command centers and Marine Air-Ground Task Force (MAGTF) engagement coordination centers (MECC). The MECCs will receive concurrent information from many teams, and sensors will make decisions on allocating fire assets to different targets. The OMFTS-based NEF-oriented concept of operation is being prepared and developed at cognizant naval activities, including the Naval Doctrine Command, Surface Warfare Development Group, Marine Corps Commandant's Warfighting Laboratory (CWL), Naval War College, and Naval Postgraduate School, and is supported by research and development activities, most notably NSWCDD. The specific future operational concept that reflects the use of this total framework is the Sea Dragon concept. Sea Dragon has at its core the concept of "dispersed, independent, and coordinated units ashore in conjunction with remote and timely fire power and logistics afloat that in total will achieve a dramatically more adaptive, effective, and less vulnerable warfighting force."[3]

The NEF/Sea Dragon concept of operation, employed to effect an immediate optimal response, is then the paradigm to address the strategic uncertainty facing U.S.

forces in the 21st century. This paradigm may be viewed as the contemporary manifestation of Liddlehart's theory of indirectness and strategic maneuver[4] (Sherman's call for placing the opponent on "the horns of a dilemma"). The NEF/Sea Dragon concept reflects new technological grand initiatives such as the Chief of Naval Operation's Arsenal Ship (see Owens' discussion of a future Navy[5]).

Sea Dragon: Specific Challenges

The CWL has identified a number of challenges requiring focus and improvement.[6,7] These, termed the Sea Dragon "long poles," are:

- Command and Coordination
  - Command decision process
  - Reliable communications on expanded battlefield
  - Distributed network communications and shared information
  - Decision support for target prioritization, asset-target allocation
  - Fires systems deconfliction
  - Integration of NEF staff (Marine and Navy)
- Fires and Targeting
  - Precision target location/designation (using Forward Observer/Forward Air Controllers or FO/FACs)
  - Multispectrum surveillance and targeting sensors
  - Sufficient combination of fires assets and precision munitions
  - Massing effects from dispersed, disparate systems
  - Target tagging/transponding
- Mobility and Maneuver
  - Deep insertion and extraction
  - Team transporter
  - Reduced load (weight/volume) on the individual Marine
  - Trailblazing
- Survivability
  - Secure, low probability of detection, identification, and jamming communications
  - Deception/stealth insertion/extraction
  - Stealth for teams on ground
  - Emergency fires/extraction
- Sustainment
  - Sustained noncontiguous maneuver elements
  - Stealthy resupply
  - "Sea-basing"
- Training, Education and Manpower
  - Systems for self-training
  - Advanced training facilities
  - Cohorts/unit stability
  - Objective aids for promotion decisions
  - Premium on intelligence in combat units

These long poles have more detailed, desired-capabilities lists that go beyond the scope of this article. NSWCDD has undertaken, under requirements sponsorship from the Navy's Director of Expeditionary Warfare (N85) and resource sponsorship from the Office of Naval Research, a simulation-based task to assist in exploring and refining relevant advanced technology initiatives. In the Joint arena, these long poles and capabilities fold into the mandatory concepts of Dominant Maneuver, Precision Engagement, Full-Dimensional Protection, and Focused Logistics that make up *Joint Vision 2010*.[8]

Naval Expeditionary Warfare SIMEXs

When one considers the enormity of the scope and span of challenges associated with 21st century expeditionary warfare, it is clear that a number of technical, material, administrative, and intellectual tools must be brought to bear to lay a foundation that assures success in combat. These must also reflect the interactive circuit connecting the leaders and national policymakers (the "worriers," or those who ask "What should we do?"), the warfighters ("warriors," who ask "How should we use what we have to win the war?"), and the acquisition managers (who ask "How much of what should we get at what price?").

In November of 1995, a series of Naval Expeditionary Warfare SIMEXs was initiated. The first Expeditionary Simulation Exercise (SIMEX I) was held at NSWCDD. There, operators and technologists representing N85, Marine Corps Combat Development Command, CWL, Surface Warfare Development Group, Naval Doctrine Command, Center for Naval Analysis, Naval Postgraduate School, Naval War College, and several Navy laboratories initiated discussions, workshops, and the first steps toward constructing illustrative simulations to advance the naval service's concepts and technologies. As part of the SIMEX process, participants were briefed by CWL on the long poles, by OPNAV's Code N00K on initiatives for naval innovations (now adopted by the Strategic Studies Group at the Naval War College), by technologists on emerging and developmental technologies, and by simulation experts on some state-of-the-art simulation and visualization tools. SIMEX I examined two of the long poles, C^2 and fire support, and set the stage for more detailed simulation and discussion to be continued in later SIMEXs.

SIMEX II was held at the Naval War College's Decision Support Center (DSC) in December of 1995. There, a more detailed simulation was presented. SIMEX I discussions were used to script a vivid visualization of an Major Regional Conflict (East) (MRC(E)) scenario employing multiple Navy and Marine assets utilizing the Sea Dragon concept of operation. (This scenario and its excursions are being continually refined by the Coastal Systems Station to reflect the detailed interactive feedback obtained as part of the SIMEX process.) Two critical capabilities were identified under the rubric of C^2:

- Maintaining reliable, secure, two-way connectivity from command elements to all individual and supporting units
- Ensuring sufficient frequency spectrum and bandwidth

The C^2 discussion generated 73 ideas grouped into the following 8 categories:

1. Access to fire support
2. Situational awareness
3. Tactical coordination
4. Logistics support/status
5. Targeting support
6. Threat analysis and bomb damage assessment
7. Direction
8. Force protection

Taking the two critical capabilities and eight categories, SIMEX II participants used the DSC tools to identify and capture (on record) desired characteristics.

A similar process was followed for the fire support long pole. The two critical fire-support capability challenges were identified as:

- Flexibility to choose and load a variety of ordnance in real time
- Reliable warhead, fire control, and weapon delivery performance, and the ability to include midcourse guidance to weapons

The fire support discussions covered a large number of targeting and weapon system considerations, including the 5-inch gun, 155mm tubes, TOMAHAWK Land Attack Missile, and NTACMS (the Navy's version of the Army's tactical missile system). The "top" 7 of 18 categories identified for consideration emerging from SIMEX II were:

1. Weapon performance (range, accuracy, lethality)
2. Pinpoint target location
3. Networked fires
4. Decision support for the engagement coordination centers
5. Reliable, secure, long-range communications
6. Rapid targeting
7. Rapid delivery of ordnance

The categories identified for C^2 and fire support provide a basis for quantitative tradeoff analysis using more detailed simulation (see Reference 9 for a detailed discussion of some specific simulations used in addressing the mine countermeasures aspect of Naval Expeditionary Warfare). The key elements that can and will be incorporated into future SIMEXs are

affordability, weapons and communication ranges, reconnaissance asset availabilities, and automatic/warfighter-in-the-loop decision-making tradeoffs.

SIMEX III is planned for Summer 1996 at NSWCDD's Coastal Systems Station. There, more detailed scenarios will be addressed with the elements identified above. Quantitative issues involving Sea Dragon teams, weapon systems, communication systems, and reconnaissance/surveillance systems will be explored as a function of ranges, quality of targeting information, and delivery times, for multiple targets and fire-support platforms. New concepts will be introduced to explore the potential and viability of robotic systems to execute detect, distract, and destroy (D^3) operations in support of amphibious/coastal warfare missions to allow Sea Dragon teams improved control of battlefield complexity and of the opponent's time lines.

Experience from SIMEXs I and II demonstrate the value of simulations. In preparing for simulations, participants are forced to articulate tactical and operational concepts in significantly more detail than is necessary for briefings and seminars. The interaction between operators and technologists accelerates clearer communication of requirements, desired capabilities, and actual system capabilities and potentials, and the intended uses and justification for use by operators. The involvement of specialists from multiple organizations and disciplines provides the opportunity for critical examination of the concepts and for the emergence of considerations unanticipated by a narrowly focused specialist. Capturing detailed scenarios and engagement evolutions in simulation provides unambiguous representation of intended courses of action, weapon and unit employments, distance and time relationships, weapon and target effects, and highly detailed visualization of the battle space.

Simulation can thus be seen as a means of letting commanders and operators train beyond training. By using simulations, it becomes possible to expand commander and operator awareness of the significance of particular actions. Through understanding and observing the results of simulations, operators develop a sense of the impact of particular orders they issue or receive. Simulations allow the individual operator and commander to develop the specific expertise required of him or her and to develop an understanding that goes beyond orders. In this way, an operator or lower level commander can understand his/her participation in the strategic picture, the element of time, the resource limitation aspects of battles, and detailed timing issues. Consequently, operators and commanders can improve information (content) flows that may, and will, answer not only the asked question, but unasked questions. Ultimately, these will combine to reduce casualties and improve operational results.

The process of preparing and executing simulations forces all participants to understand the assumptions, models, data availability, and data gaps involved in the scenario to be simulated. Along this process, technologists, operators, and commanders are then able to transform facts into data, data into information, information into knowledge, and upon reflection on the accumulated knowledge, knowledge into wisdom that can be applied in battle. As experience is gained in the use of advance simulation capabilities, operators and commanders will be able to achieve the desired optimal response to unknown situations in a rapid and ultimately immediate manner.

Conclusions

This article presented discussion of some of the elements and challenges of the emerging naval warfare paradigm for the 21st century. This paradigm calls for assuring success against strategic uncertainty through melding Navy and Marine Corps units into flexible expeditionary forces. These forces will be capable of supporting traditional naval operations and a new concept of operations highlighting operational

maneuver using small dispersed (Sea Dragon) units supported by highly capable naval fires. *The article introduces the concepts of immediate optimal response,* discusses some experiences with SIMEXs applied to NEF/Sea Dragon scenarios, *and introduces the concepts of employing robotic systems in D^3 modes* to facilitate amphibious and coastal warfare operations. The article outlines simulation as a means of providing commanders and operators the opportunity to train beyond training by using simulations to expand commander and operator awareness.

Acknowledgments

The SIMEXs and work described here were sponsored by Code 32 of the Office of Naval Research and Code N85 of the Navy Staff. SIMEXs I and II would not have occurred without the dedication, personal involvement, and interest of their participants, to whom the author is grateful. The author would like to thank in particular Mr. Robert Stiegler and his staff for supporting SIMEXs I and II; Naval War College's DSC team of directors and staff for their outstanding execution of SIMEX II; and, in particular, CAPT Brad Hayes for his tireless note taking and report preparation. The author would also like to express his thanks to the outstanding simulation execution team, headed by Mr. Kirk Dye at the Coastal Systems Station, for working tirelessly to construct and implement the computer simulations used in the SIMEXs.

References

1. . . . *From the Sea—Preparing the Naval Service for the 21st Century*, Department of the Navy, Washington, DC, Sep 1992.
2. *Forward . . . From the Sea*, Department of the Navy, Washington, DC, Nov 1994.
3. *Operational Maneuver from the Sea: A Concept for the Projection of Naval Power Ashore*, Headquarters Marine Corps, Washington, DC, 1996.
4. Liddlehart, B.H., *Strategy*, 2nd Revised Edition, Meridian, NY, 1991.
5. Owens, W.A., *High Seas*, Naval Institute Press, 1995.
6. *Technology Exploration and Exploitation Plan*, Commandant's Warfighting Laboratory, 1996.
7. *Long Poles in the Sea Dragon Tent*, Commandant's Warfighting Lab, 1996.
8. *Joint Vision 2010*, Joint Chiefs of Staff, Mar 1996.
9. Moritz, E., *"Mine Warfare Simulation," NSWC Technical Digest*, Sep 1995, pp. 194.

The Author

Elan Moritz

ELAN MORITZ, research physicist, graduated with a B.S. in physics from State University of New York at Stony Brook, and with a Ph.D. in physics from Kent State University in Ohio. Prior to joining NSWC/CSS in 1981, he was a senior engineer at EBASCO Services in New York City. As Lead Applied Physics Engineer there, he contributed to the design of the Tokomak Fusion Test Reactor (TFTR) at Princeton University and a number of commercial nuclear power plant design and safety analysis evaluations. At CSS, he headed a joint multinational development and MCM demonstration program that resulted in fielded hardware and the current international standard for detailed mine/ship/sweep encounter simulation. Later, for over five years, he directed the Navy's Exploratory Development Program for surface and submarine sonar and torpedo countermeasures. This program resulted in a number of systems and system improvements now in the Fleet. Following that, he headed the Signal and Image Processing Branch at the laboratory, leading to significant CSS capability in computer aided/automated detection and classification especially in electro-optic and sonar image understanding and processing. Dr. Moritz has served as Technical Director-Mine Warfare (OP36T and N852T). His awards include the TTCP Achievement Award and the Department of the Navy's Meritorious Civilian Service Award. He is the first Director of the Coastal Systems Station's Modeling and Simulation Office (CMSO). Dr. Moritz currently heads Dahlgren Division's Expeditionary Warfare Technologies Office and advises senior naval officials in areas associated with Mine and Expeditionary Warfare.

AN/KSQ-1 Enhances Command and Control in Amphibious Operations

Teresa L. Floore

EW
EXPEDITIONARY
WARFARE

Coordination of the amphibious assault from over the horizon has been a key challenge in implementing Operational Maneuver from the Sea[1] *(OMFTS). The Amphibious Assault Direction System, AN/KSQ-1, was developed by the Amphibious and Strategic Sealift Systems Branch of the Naval Surface Warfare Center, Dahlgren Division's (NSWCDD's) Coastal Systems Station (CSS) to allow the Commander of an Amphibious Task Force (CATF) to monitor ships and landing craft as they transit to and from the beach. The AN/KSQ-1 is a marriage of the U.S. Marine Corps' (USMC's) Position Location Reporting System (PLRS) and the Navy's Navigation Satellite Time and Ranging (NAVSTAR) Global Positioning System (GPS). The AN/KSQ-1 provides a visual display of the amphibious objective area, contributing to a more accurate tactical picture, and provides digital communication to Navy and Marine Corps assets separated by as much as 100 nautical miles. AN/KSQ-1 was a nondevelopmental acquisition that has been installed on both West and East Coast amphibious ready groups (ARGs). User consensus is that AN/KSQ-1 significantly enhances amphibious command and control (C^2). AN/KSQ-1 has additional potential for application in Naval Expeditionary Force operations, mine countermeasures, and other maneuver warfare, such as raids and noncombatant extractions.*

Key Challenge in *Operational Maneuver From the Sea*

The introduction of the Landing Craft, Air Cushion (LCAC) extended maneuver warfare by providing high-speed, over-the-horizon (OTH) power projection. Although new technology enhanced C^2 of units embarked on these and a variety of other platforms, coordination of one of the most complex and potentially confusing operations in all warfare—the amphibious assault—from over the horizon remained a key challenge. The Navy's recently fielded Amphibious Assault Direction System, the AN/KSQ-1, gives a ready means to assist commanders in directing their forces from well over the horizon to distances inland.

AN/KSQ-1 was developed by the Amphibious and Strategic Sealift Systems Branch at CSS in response to the Over-the-Horizon Amphibious Assault Command and Control (OTHAC[2]) System operational requirement (No. 242-03-91 of 7 May 1989). The AN/KSQ-1 is a marriage of the USMC-developed PLRS and the Navy's NAVSTAR GPS that allows the CATF to monitor ships and landing craft as they transit to and from the beach. AN/KSQ-1 provides a visual display that contributes to a more accurate tactical picture, and provides digital communication to Navy and Marine Corps assets separated by as much as 100 nautical miles.

System Characteristics

AN/KSQ-1 will identify, track, communicate with, and control amphibious landing craft from launch through transit, offload, and return, during the conduct of OMFTS. AN/KSQ-1 displays PLRS position location information (PLI) in the unified build environment of a Tactical Advanced Computer series (TAC-n). Originally designed to provide an OTH capability to allow the amphibious command ship to maintain safe standoff from the beach, AN/KSQ-1 has become a prime under-the-horizon C^2 system as well. It provides near-real-time position information about the tactical situation, enhancing the CATF's situational awareness and allowing communications via preformatted and short text messages when voice communications are not available. AN/KSQ-1 has already proven its usefulness in deconfliction of the near-shore area in recent amphibious operations.

Different platforms contain different AN/KSQ-1 equipment groups:

- The amphibious command group (ACG) contains the PLRS master station and receiver-transmitter, known as the basic user unit or BUU, the AN/KYK-1 workstation, and ancillary equipment. The ACG is installed on amphibious command ships (LHD and LHA).
- The primary/secondary control group (PCG/SCG) differs from the ACG in that it lacks the master station. The PCG/SCG is installed on LPD 4 and LSD 36, 41, and 49 class ships.
- User terminal groups (UTGs) will be installed on the LCAC and Landing Craft, Utility (LCU).

AN/KSQ-1 will be a part of the integrated C^2 system on the new LPD 17 class ship. Although the LPD 17 is a primary control ship, it will contain an AN/KSQ-1 ACG to provide a backup master station for ARGs.

Nondevelopmental Acquisition

AN/KSQ-1 is primarily a nondevelopmental acquisition, interfacing commercial and military equipment already in service use with new software and the Joint Maritime Command Information System (JMCIS) to display the amphibious operational area and PLRS-equipped units. The PLRS master station was originally installed in LHD 1 class ships to provide support to embarked Marines. With the advent of the LCAC (Figure 1), this resource was decided upon to disseminate PLI among the amphibious task force.

A GPS interface unit, or GPSIU, was developed by the then Naval Command, Control, and Ocean Surveillance Center, Research and Development Division, Warminster, Pennsylvania. GPSIUs are installed on all AN/KSQ-1 platforms. Onboard ships, the GPSIU transmits ownship GPS data

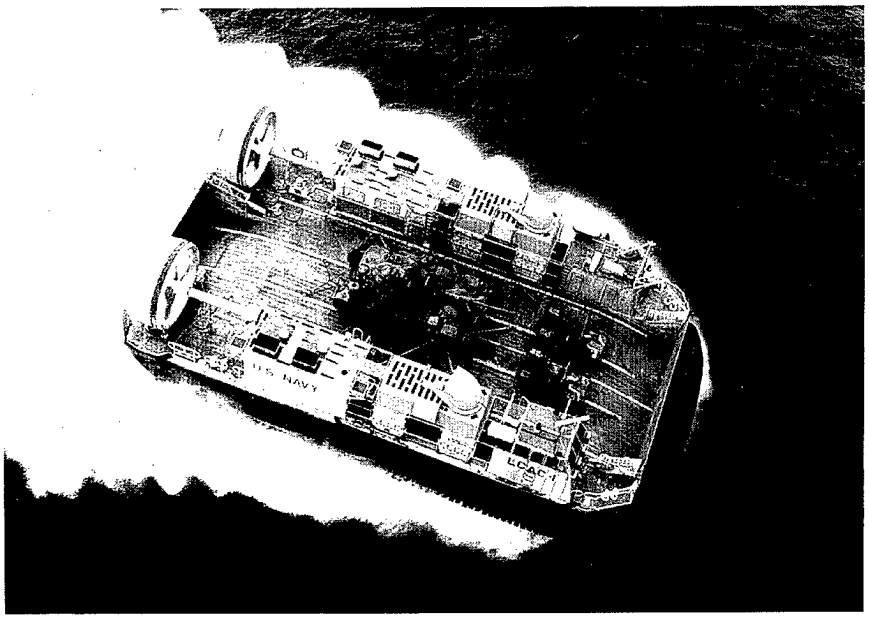

Figure 1. AN/KSQ-1 was designed to support command and control of LCAC

to the local workstation and reformats GPS position data for transmission to the PLRS master station via the BUU. The GPSIU also takes PLI from the master station (again via the BUU) and transmits it to the workstation. Onboard LCAC, the GPSIU allows nearly automatic entry of new waypoints into the craft's GPS receiver.

The new AN/KSQ-1 "GATOR" software (developed by CSS in C programming language with the aid of a Transportable Application Environment graphical user interface) operates in the workstation to deliver PLI and ownship GPS data to the JMCIS Track Database Manager for display on a JMCIS system chart. The display is updated about every 5 to 10 seconds. CSS developed GATOR software with the intention of it eventually becoming a JMCIS segment (see Figure 2). The AN/KSQ-1 Block I upgrade, planned for FY97, will integrate AN/KSQ-1 (and PLRS) with JMCIS, making PLI available to all ships in the task force.

Figure 2. The AN/KSQ-1 JMCIS software segment is appropriately named "GATOR"

Interface With PLRS

As originally developed for land use, PLRS is a line-of-sight, ultra-high frequency (UHF) system based on surveyed reference points. AN/KSQ-1 allows the use of PLRS in a naval environment by replacing the need for surveyed reference points with the interface to GPS that provides a dynamic reference capability for PLRS, enhancing system accuracy. The PLRS master station controls the network in a secure, jam-resistant environment; calculates positions based on time-of-arrival data; routes all messages and queries; and graphically displays the position of all active PLRS BUUs.

AN/KSQ-1 allows users to exploit the full capability of PLRS. It provides the CATF, the Commander of the Landing Force, and the Primary Control Officer a computer display of accurate, near-real-time information on the position and movement of AN/KSQ-1 equipped LCACs and other landing craft or ships, and any PLRS-equipped landing force elements (helicopters and ground units). Figure 3 is an example of a AN/KSQ-1 operational scenario. To extend line of sight, an airborne relay mission package is used for OTH operations.

Testing and Fleet Use

AN/KSQ-1 successfully completed operational evaluation (OPEVAL) in April 1995 in conjunction with the USS *Essex* ARG Western Pacific (WESTPAC) deployment.

- USS *Essex* (LHD 2) was outfitted with the ACG
- USS *Ogden* (LPD 5) carried the PCG
- USS *Fort Fisher* (LSD 40) and four LCAC carried UTGs
- An LCU was also equipped with a BUU but no GPSIU

The system was subsequently used during operations in Okinawa and Somalia. The first East Coast AN/KSQ-1 installation was made this year on the ships and craft of USS *Saipan* (LHA 2) ARG, intended to support operations in Bosnia.

AN/KSQ-1 hardware remained onboard the *Essex* ARG during the FY95 deployment. During the U.N.-Somalia offload, AN/KSQ-1 was used every time LCAC were in the water. PLRS data were transferred to USS *Constellation* through a temporary AN/KSQ-1 connection to the Navy Tactical Command System-Afloat (NTCS-A) local area network (LAN) onboard *Essex*. *Essex*'s tracks were then broadcast via the Office-in-Tactical-Command Information Exchange System (OTCIXS) to USS *Constellation*. The connection also allowed transferring of Joint Operational Tactical System (JOTS) overlays, position of intended movement tracks (PIMtracks), sites, and screens—reducing redundant data entry and making situation-awareness data available to other members of the battle group.

User consensus is that AN/KSQ-1 significantly enhances amphibious C[2]. USS *Essex* reported that PLRS position data remained well within advertised accuracy, further stating that "KSQ-1 is a force multiplier in command and control . . . an invaluable tool in amphibious operations."[2]

Planned Improvements

One drawback to the use of PLRS on land has been the master station's overly large footprint. PLRS was originally designed to be carried in an S-280 shelter housed on an M-923

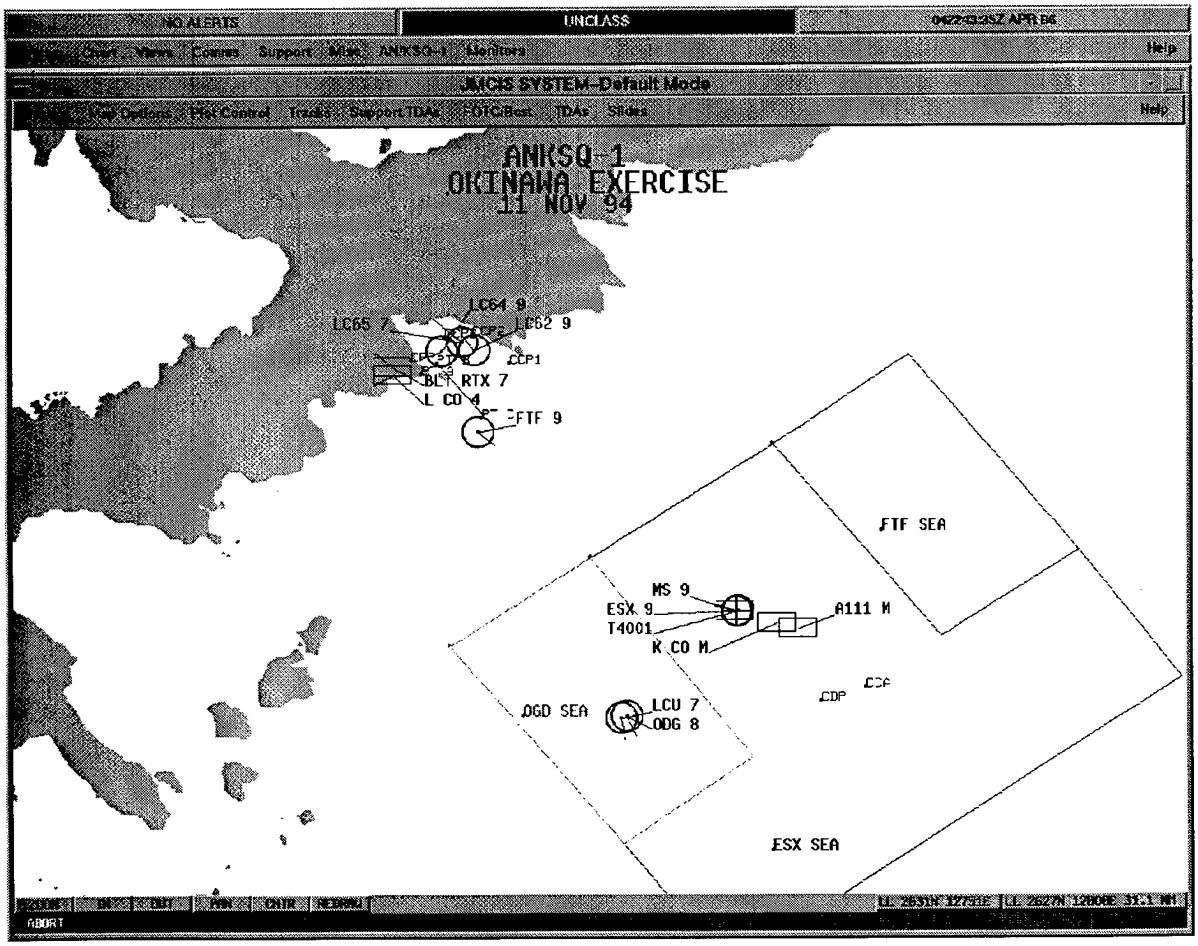

Figure 3. Sample AN/KSQ-1 operational scenario as displayed on JMCIS system chart

5-ton truck. Furthermore, many of the original master station components are no longer state-of-the-art and are not readily available. A downsizing effort is underway that will reduce the master station configuration to a suite of modern, more reliable hardware that can be transported in a Standard Integrated Command Post Shelter (SICPS) mounted on a High Mobility Multi-Purpose Multi-Wheeled Vehicle (HMMWV). A shipboard version of the downsized master station will be installed in LHD 5, 6, and 7 and LHA 1 through 5 and backfitted in LHD 1 through 4.

Use of AN/KSQ-1 is being integrated into tactics and procedures for OMFTS as they are finalized. A TACMEMO[3] is being released for the use of AN/KSQ-1 in amphibious operations. It discusses the unique features and operating requirements of the AN/KSQ-1 and PLRS systems in the naval environment. PLRS was designed to operate with many units carefully dispersed over a relatively small area (~40 km by ~40 km). A robust communications net is required to maintain system accuracy and real-time information. Deployment of Navy and Marine Corps PLRS-equipped units must be carefully and jointly planned to enhance the net and optimize the utility of the AN/KSQ-1 system, especially when it is used in small ARG operations (three to five ships, five LCAC). Close liaison between the Navy AN/KSQ-1 Employment Officer and the USMC PLRS Employment Officer is crucial to the successful operation of the system.

AN/KSQ-1 has additional potential for application in Naval Expeditionary Force operations, mine countermeasures, and other maneuver warfare, such as raids and noncombatant extractions.

References

1. FMFRP 14-21, *Operational Maneuver from the Sea* (coordinating draft), 31 Mar 1995.
2. USS ESSEX MSG 160710Z, Feb 95, Subj: AN/KSQ-1 Status Report.
3. COMSURFWARDEVGRU TACMEMO PZ0021-1-96/U.S. Marine Corps Reference Publication, MCRP 6-22.2A, Tactical Procedures for Using the AN/KSQ-1(V) Amphibious Assault Direction System, Tactics for Atlantic and Pacific Surface Forces and Fleet Marine Forces, promulgated 15 Sep 96.

The Author

Teresa L. Floore

TERESA L. FLOORE is an operational research analyst at CSS in Panama City, FL. She received a B.S. in chemistry from the University of Louisville in 1967. Ms. Floore was assigned to the AN/KSQ-1 project to provide operational research support during the early specification development period. Since then, Ms. Floore has supported AN/KSQ-1 systems engineering and integrated logistic support functions, gradually assuming responsibility for risk management, configuration management, and training. She still provides critical program management and technical support and retains much of the project's history since only the systems engineer has been on the project longer. In 1993 Ms. Floore was selected to participate in the Federal Women's Executive Leadership (WEL) Program for potential management personnel. In conjunction with that program, she spent three months at the office of the Deputy Assistant Secretary of the Navy, Expeditionary Warfare, OPNAV. In 1994, Ms. Floore accepted a long-term TDY assignment as the AN/KSQ-1 Acquisition Engineering Agent at Naval Sea Systems Command (PMS377), now PEO CLA. She has an extensive list of technical documentation to her credit, including a recent article about AN/KSQ-1 in the *Marine Corps Gazette* (January 1996) jointly authored with the previous AN/KSQ-1 acquisition manager, Col. Albert A. DeSantis, USMC. In September 1996, Ms. Floore was designated Project Engineer for AN/KSQ-1.

EW